THERMAL HISTORY OF THE GRENVILLE FRONT TECTONIC ZONE, CENTRAL ONTARIO

by

Melanie Jane Haggart

Submitted in partial fulfillment of the requirements
for the degree of Master of Science

at

Dalhousie University
Halifax, Nova Scotia
September, 1991

TABLE OF CONTENTS

LIST OF FIGURES

LIST OF TABLES

LIST OF PLATES

ABSTRACT

The Grenville Front marks the boundary between the ca. 1.2 - 1.0 Ga Grenville Province and its foreland. Abrupt increases in metamorphic grade across the Front in central Ontario, and pervasive high-strain, Front-parallel fabric in the adjacent tectonic zone (GFTZ), imply that it accommodated substantial differential uplift relative to the foreland during the Grenville orogeny. Knowledge of the timing, duration, and significance of tectono-metamorphic events at the Front is fundamental to developing models of the evolution of the orogen.

U-Pb and $^{40}Ar/^{39}Ar$ dating of a suite of minerals from a transect across the Front and GFTZ, along the north shore of Georgian Bay, provides new insight into the thermal history of the area. After metamorphism at about 1446 Ma, probably related to voluminous granitoid plutonism, the GFTZ did not undergo significant metamorphism again until about 990 Ma. The second event caused partial resetting of U-Pb systematics in titanite. All titanites from along a 15-kilometre transect perpendicular to the Front fall along a single discordia, and degree of resetting is correlated with distance from the Front. The second metamorphism was therefore a rapid event, during which temperatures exceeded those required to cause Pb diffusion in titanite, for a short time. Temperatures increased with distance from the Front toward the Grenville interior. Peak temperatures were not high enough to generate the granulite-grade mineral assemblages observed within 10 kilometres of the Front. Granulite grade metamorphism is therefore 1446 Ma, or older. Tectonism in the GFTZ accompanying the 1446 Ma event, and later tectonism related to thrust events occurring in the Grenville interior during 1160 to 1025 Ma, may have caused initial differential uplift of the GFTZ relative to the foreland.

$^{40}Ar/^{39}Ar$ dating of hornblende from the same transect confirms the trend of increasing temperature with distance from the Front, and demonstrates very rapid cooling through hornblende closure following the thermal event. $^{40}Ar/^{39}Ar$ ages from biotite and multiple diffusion domain modelling of K-feldspar provide additional evidence for rapid cooling.

Telescoping of ca. 985 Ma mineral assemblages toward the Front, documented by other workers, demonstrates that thrusting continued beyond the peak of the thermal event. The association of the temperature increase and cooling with thrusting implies that the event was the result of burial by overthrusting. The event partially reset titanite and hornblende near the Front in the GFTZ but failed to reset $^{40}Ar/^{39}Ar$ systematics in muscovite within 5 kilometres of the Front. Syntectonic erosion accompanying the thrusting event, resulting in rapid unroofing and cooling, best explains these observations.

The event post-dates the peak of metamorphism in the adjacent Britt domain of the Grenville interior by about 50 My. Metamorphism near the Front during 990 to 970 Ma, later than the peak of events in the interior, is well documented in Labrador. This implies that the event occurred on the scale of the whole orogen, and must be explained by an orogen-wide phenomenon.

The multiple diffusion domain theory of K-feldspar Ar diffusion behaviour appears to provide realistic cooling histories, which are more useful in constructing low temperature T-t paths than estimated closure temperatures assigned to plateau-like parts of apparent age spectra.

ACKNOWLEDGEMENTS

Many people have provided me with different forms of support and friendship during the course of this work. My advisors, Dr. R.A. Jamieson and Dr. P.H. Reynolds, are owed thanks for financial support and good advice. I have learned a great deal from each of them. My knowledge of the problems of the Grenville was expanded by work and discussion with Dr. N.G. Culshaw; he also helped to keep me excited about the potential results of my study when the data was slow in coming. Dr. M. Zentilli served as a member of my supervisory committee and I thank him for his encouragement.

Margaret Burke and our assistant Geoff Gallant made the fieldwork for this thesis a memorable experience. Lively discussion with Margaret aided my understanding of the rocks, while Geoff did a good job and remained dryly cheerful under sometimes difficult circumstances. Kathy Bethune introduced us to some of the problems of the Grenville Front Tectonic Zone.

Several people assisted me greatly with the technical aspects of the thesis. Keith Taylor kept the argon lab running at a high standard during the transition to a new mass spectrometer. Bob Mackay made the electron microprobe very accessible; and Jordan Mooers helped with the initial learning of mineral separation techniques. Dr. T. Krogh of the Royal Ontario Museum is thanked for the invitation to carry out U-Pb dating in his lab, and Yim-Yang (Kim) Kwok of the ROM deserves thanks for conducting the chemistry and mass spectrometry with such care.

Sandy Grist has been an invaluable source of technical information and assistance, emotional and moral support, and with his dinner-time companionship the last few months of writing, has ensured that I did not waste away entirely.

Many of my fellow students in the Dalhousie geology department, both graduate and undergraduate, have provided supportive friendship without which I would have enjoyed the experience of a graduate degree much less. In particular, my office mates John Ketchum and Mark Hendriks, and Robbie Hicks, deserve my thanks.

My parents have provided me during these three years with Sunday dinners, clean laundry, and latterly, a roof over my head. More than I ever tell them in person, I appreciate their help and encouragement.

CHAPTER I
INTRODUCTION AND GEOLOGY OF THE STUDY AREA

1.1 INTRODUCTION

Recent geological mapping of transects of the Grenville Province in Labrador, Quebec, and Ontario, combined with modern methods in geochronological, metamorphic, and structural studies, has led to the preliminary understanding of the tectonic framework of the province. It is now known to be composed of distinct lithotectonic domains which have been assembled along ductile shear zones with a consistent northwest-directed thrust sense (e.g. Davidson, 1986; Rivers and Chown, 1986). The generally high metamorphic grade and the ductile conditions under which assembly occurred imply that the province represents a cross-section of the mid- to deep roots of an orogen.

The Grenville Front marks the approximate northwestern limit of penetrative deformation and metamorphism during the ca. 1.1 Ga Grenville orogeny, the main event responsible for assembly of the province. The Front divides older structural provinces of the Shield unaffected by the Grenville orogeny from the Grenville Province proper. It is exposed for 2000 kilometres from the coast of Labrador to the north shore of Georgian Bay of Lake Huron (Fig. 1), and may continue under Paleozoic cover to Texas. The Front is recognized as a major crustal discontinuity, possibly extending to the lower crust (Green et al., 1988; Rivers et al., 1989). Some units of the Archean and early Proterozoic foreland correlate across the Front (Bethune and Davidson, 1988; Rivers and Chown, 1986), defining a "Parautochthonous Belt" (Rivers et al., 1989) up to 150 kilometres wide in places, extending the length of the orogen. This precludes its interpretation as a suture zone. However, the Front is the locus of major movement along reverse faults and thrusts, and of locally abrupt change in metamorphic grade (Owen et al., 1986; Indares and Martignole, 1989; Davidson, 1986). It is one of three fundamental boundaries recognized in the Grenville Province (Rivers et al., 1989), and knowledge of its relationships to the foreland and parautochthon which it separates is essential to the development of tectonic models for the orogen.

A deep seismic reflection profile (GLIMPCE Profile J) across the extension of the Grenville Front under Lake Huron provides an image of the deep structure of the Front at its western end. Structures in the Superior - Southern Provinces foreland are abruptly truncated by a spectacular series of east-dipping reflectors which correspond to a zone of highly strained rocks known as the Grenville Front Tectonic Zone (GFTZ). The strong reflectors die out beneath the adjacent

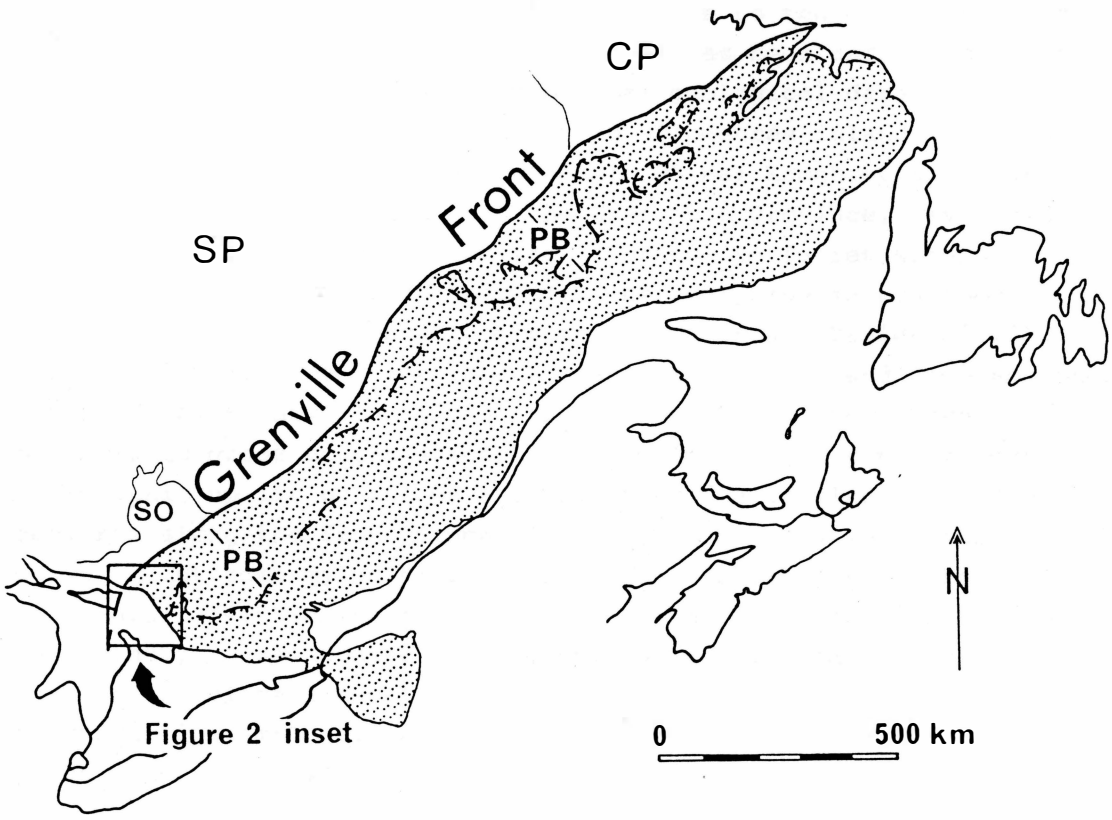

Fig. 1. The Grenville Province. The Grenville Front divides the Grenville Province (stippled) from its foreland, consisting of older structural provinces of the Canadian Shield. CP = Churchill Province; SP = Superior Province; so = Southern Province. Some units of the foreland provinces correlate across the Front, defining the Parautochthonous Belt (PB). The outline of the inset in Fig. 2 is shown.

parautochthonous Britt domain, which is characterized by subhorizontal, lozenge-shaped packages of reflectors (Green et al., 1988).

These features have been tentatively interpreted, using available pressure, temperature, and geochronological data from the GFTZ, as demonstrating northwest-directed ductile imbrication along high strain zones. High-grade metamorphism is thought to have occurred prior to strain, due to the thrusting of Britt domain over the GFTZ. Throughout these events, the foreland acted as a rigid buttress, causing deformation and relative uplift to be concentrated in the tectonic zone and at the Front. The Britt domain suffered minimal imbrication (Green et al., 1988). However, little geological information is available on the precise relationship of the Britt domain to the GFTZ, as no thorough mapping of the boundary zone between them has been undertaken. The interpretation above is based on minimal geological data.

Northeast of profile J, about 30 kilometres inland from the north shore of Georgian Bay, Sudbury dikes (1238 Ma; Krogh et al., 1987) which continue from the foreland into the Grenville Province, have been metamorphosed to upper amphibolite to granulite facies within 8 kilometres of the Front in the GFTZ. Metamorphism is presumed to have occurred during the Grenville orogeny (Bethune and Davidson, 1988; Bethune, 1989). The dikes remain essentially fresh and unmetamorphosed north of the Front. The short distance over which the change in metamorphic grade occurs suggests that considerable syn- or post-metamorphic uplift of the GFTZ relative to the foreland must have occurred along the Front since dike intrusion. However, dikes have been shown to cut some mylonite zones and gneissic fabrics in the GFTZ, particularly within the first few kilometres, and metamorphic grade in the country rocks appears to rise more abruptly adjacent to the Front than in the dikes themselves (Bethune et al., 1990). These relationships imply at least a two-stage metamorphic and deformational history for the GFTZ.

1.2 PURPOSE OF THE STUDY

Several questions arise from these observations. Firstly, what was the extent of heating of the foreland and GFTZ during the Grenville orogeny and the earlier metamorphic episode? Were the high-grade mineral assemblages observed within a few kilometres of the Front developed during the first metamorphism or the second? Secondly, subsequent to metamorphism, how quickly did exhumation and cooling of the GFTZ occur, and was it early, late, or simultaneous relative to cooling in the orogenic interior?

These questions have important implications for geodynamic and

tectonic models of the orogen. The question of the extent and time of heating of the foreland and GFTZ needs to be resolved because of the unexplained absence of a Grenvillian foreland basin. If such a basin ever existed, it has been completely eroded or otherwise removed, leaving uncertainty about how to model lithospheric behaviour (e.g. Quinlan and Beaumont, 1984; Hoffman, 1988), and also, on which side of the orogen it was located. The only way to determine if it existed northwest of the Grenville Front is to detect Grenvillian heating of "basement" rocks of the foreland, possibly a result of burial by foreland basinal sediments. Before this kind of study can be useful, controls must be provided on the timing and spatial extent of Grenvillian versus pre-Grenvillian events in the GFTZ.

Knowledge of timing and rates of cooling in the tectonic zone relative to the orogenic interior is important because these data provide the only information about exhumation available in a deeply eroded orogen like the Grenville. Exhumation rate is a fundamental control on orogenic evolution (Jamieson and Beaumont, 1989) and it must be incorporated in geodynamic and thermal models.

This study attempts to address these questions by obtaining geochronological data for relevant spatial and temperature points in the foreland and the GFTZ, by comparing this information with similar studies in other parts of the orogen, and by suggesting what tectonic models are consistent with the thermal history.

1.3 METHOD OF STUDY - THERMOCHRONOLOGY

It is generally accepted by geochronologists that the radiometric dates obtained from metamorphic minerals represent either ages of cooling or partial thermal overprinting (e.g. Zeitler, 1989). Cooling ages record the time when the daughter product of the decay scheme of interest was no longer diffusing out of the mineral. The temperature at which this occurred is known as the closure temperature, T_c. If the mineral experienced a subsequent increase in temperature, the age may have been completely or partially "reset", depending mainly on temperature but also on duration of heating, and possibly on other factors such as deformation and chemical environment.

Sufficient work has been done by geochronologists on a variety of mineral "thermochronometers" that ranges of T_c are either reasonably well known, or can be calculated. As different minerals have different closure temperatures, dating of a suite of appropriate minerals from the same locality can provide a series of temperature - time (T-t) points which together define the cooling history of the rock. This technique is a useful tool for studying the thermal histories of orogens, because

several T-t points from peak metamorphic conditions (using zircon U-Pb methods) down to about 70°C (using apatite fission tracks) can be acquired for most assemblages of rock types (e.g. DeWitt et al., 1984; Wagner et al., 1977).

In this study, thermochronometry is applied to a transect across the Grenville Front in southwestern Ontario, in an attempt to answer some of the questions discussed in the previous section. The absolute timing of metamorphic events in this area is being documented by other workers using U-Pb dating methods on zircon and monazite, which have high T_c's (see Section 1.5, Existing T-t Data) . This study uses several well-established thermochronometers in the intermediate- and low-T_c range; these are U-Pb dating of titanite, and $^{40}Ar/^{39}Ar$ dating of amphibole, mica and K-feldspar. The data are then used to construct thermal histories of the GFTZ, and are compared to similar thermochronometric studies in other parts of the orogen, in order to constrain tectonic models for this area.

1.4 GEOLOGY OF THE STUDY AREA

The area selected for this study forms a transect across the Grenville Front in the vicinity of Killarney, Ontario (Fig. 2), where nearly continuous exposure along the shores and channels of Georgian Bay provides a cross-section of the foreland, the Front, and the GFTZ.

To the northwest of the Front, the area is underlain by rocks of the Southern Province, of which the Huronian Supergroup is the main component. The mainly clastic sedimentary rocks were laid down in a basinal setting on the margin of Archean Superior Province craton, in the time period 2500 to 2200 Ma (Card, 1978). They were intruded by Nipissing diabase sills at about 2220 Ma (Corfu and Andrews, 1986), then folded about east-west trending axes and metamorphosed to greenschist to lower amphibolite grade (Card, 1978) during the Penokean orogeny (1890 - 1830 Ma, Van Schmus, 1980).

The Southern and Grenville Provinces are separated by a series of igneous complexes of two different ages. The Killarney Complex (KC), is a triangular zone of mainly felsic, high-level plutons, with intercalated volcanic rocks, dated at about 1740 Ma (van Breemen and Davidson, 1988). These rocks have been correlated with a similar terrane of the same age, the Central Plains orogen, which underlies much of the North American mid-continent. The KC and other granites of similar age along the Front to the northeast and within the Grenville Province (Krogh et al., 1971; Corrigan, 1990) may represent the eastern extension of this terrane (Davidson, 1986).

The complex is in intrusive contact with Southern Province rocks

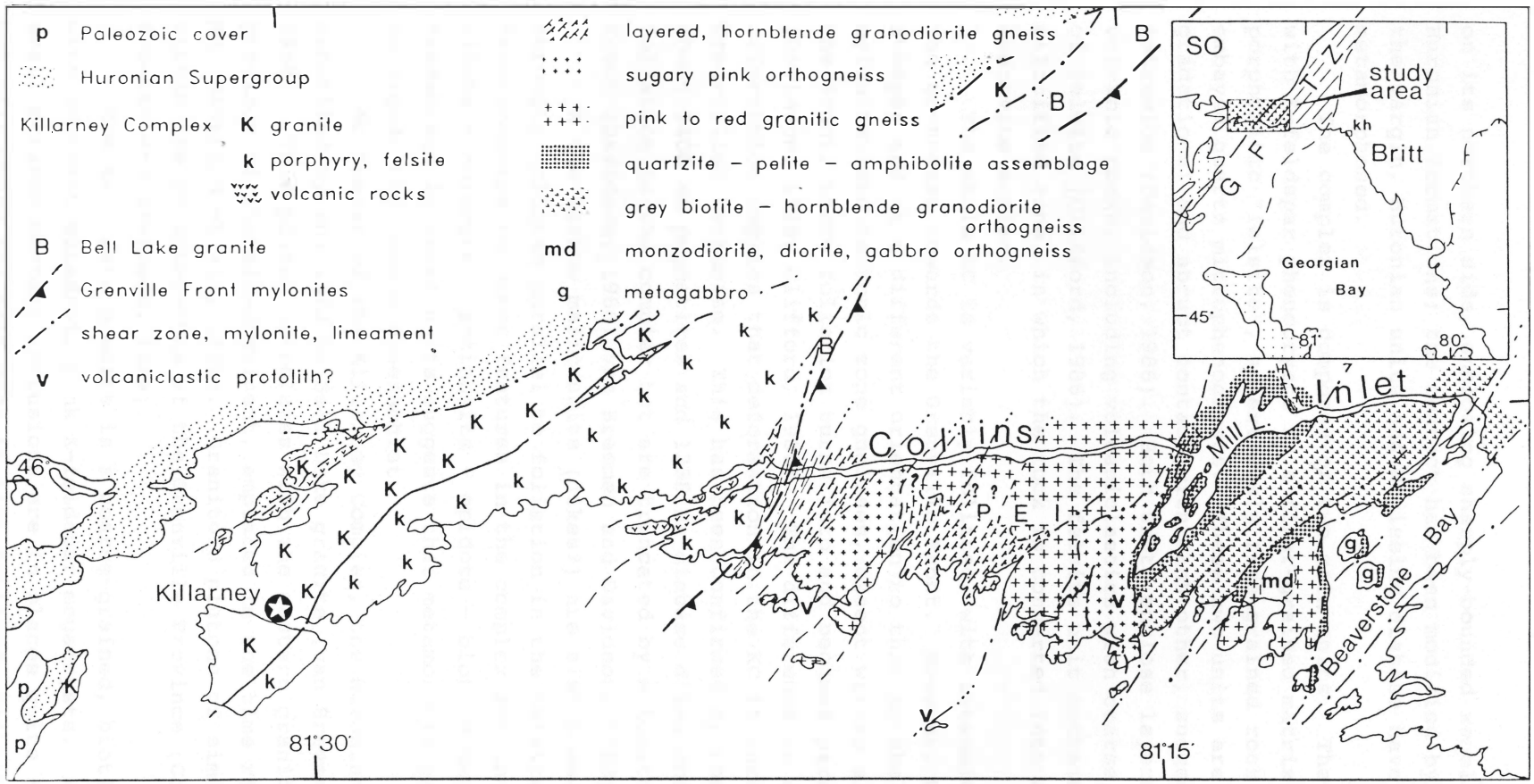

Fig. 2. Geology of the study area. Inset: The location of the study area is shown in relation to adjacent terranes. GFTZ = Grenville Front Tectonic Zone; so = Southern Province; kh = Key Harbour. Britt = Britt domain of the Central Gneiss Belt. Main figure: Generalized geological map of the study area. PEI = Philip Edward Island. The location of dikes is not shown. A ca. 600 Ma dike occupies part of the fracture defining Collins Inlet. Modified after Davidson and Bethune (1988).

on its northern side, enclosing sharply-bounded xenoliths and rafts of Huronian formations; the contact has been modified by faulting. Near the margin, Huronian units and Nipissing diabase have been thermally metamorphosed.

The complex is composed of two main units. The first is a granite with K-feldspar phenocrysts in a finer-grained matrix. The second is a porphyritic "felsite", an extremely fine-grained rock with equant, embayed quartz microphenocrysts. These two units are in both gradational and abrupt contact with each other, suggesting simultaneous intrusion (Davidson, 1986). Both units enclose layers and xenoliths of volcanic rocks, including volcaniclastics with coarse, flattened clasts of felsite (Clifford, 1986). The felsite unit contains a highly silicified zone, in which the rock is converted into a quartz - muscovite schist.

The whole KC is variably foliated, with intensity increasing to the southeast towards the Grenville Front. However, the foliation is steeper and at a different orientation to that in the adjacent Front mylonites and tectonic zone gneisses, except within a short distance of the Front, where foliation turns into and becomes parallel to the Front (Davidson, 1986; Clifford, 1986). The difference in structural orientation implies that deformation in the KC is unrelated to Grenvillian tectonism. This has been confirmed by the identification of about 1400 Ma pegmatites and 1238 Ma diabase dikes which cut the foliation in the complex but are truncated by mylonites of the Grenville Front (Davidson, 1986; van Breemen and Davidson, 1988).

A few narrow mafic units (dikes?) are also present which are strongly foliated parallel to foliation in the felsite. The age relationships to other features in the complex are uncertain, but the albite - chlorite - actinolite - epidote - biotite metamorphic assemblage in these units suggests that metamorphic grade in the KC is no higher than upper greenschist.

Northeast of the Killarney Complex, the Huronian and GFTZ are separated by the 1470 Ma Bell Lake granite (van Breemen and Davidson, 1988). This pluton correlates with the eastern granite - rhyolite province of the mid-continent, emplaced in the time range 1480 to 1450 Ma (Bickford et al., 1986). Granitoid plutons of similar age occur within the parautochthon of the Grenville Province (Corrigan, 1990; van Breemen and Davidson, 1986).

The Bell Lake granite is a coarse-grained, biotite-rich granite with abundant euhedral, pink K-feldspar megacrysts. Megacrysts and small metasedimentary inclusions are in places quite strongly aligned, but only where the host rock is also foliated, implying a secondary

rather than primary alignment (Frarey, 1985; van Breemen and Davidson, 1986). Foliation is cut by pegmatites, dated at 1430 Ma (Rb-Sr muscovite; Krogh and Davis, 1970), which are in turn cut by mylonites related to the Grenville Front (van Breemen and Davidson, 1986).

On their southeast sides, the Killarney Complex and the Bell Lake granite are truncated by mylonites of the Grenville Front. The nature of the Front varies along strike. On Philip Edward Island and Collins Inlet, the main focus of this study, the Front as defined by Davidson (1986) is represented by a single major mylonite zone, up to about 50 metres wide in places, and surrounded by protomylonites. Here the mylonites are derived from Killarney Complex felsites, pegmatites, and amphibolite dikes which have been chevron-folded and mylonitized, but retain their cross-cutting character (are not attenuated parallel to the mylonites). Farther inland near Tyson Lake, mylonites are developed in Bell Lake granite as well as probable KC equivalents. The mylonite zone apparently bifurcates and no one single fault or mylonite can be labelled the "Front"; rather several of them are responsible for progressive differential uplift of the GFTZ (Bethune and Davidson, 1988).

No detailed, up-to-date map has yet been made of the Grenville Front Tectonic Zone in the Collins Inlet area. It was last completely mapped in the 1960's at a scale of 1 to 50,000 (Frarey, 1985). In 1988, the south shore of Philip Edward Island was mapped in detail by Davidson and Bethune (1988), but units were traced inland mainly on the basis of pre-existing maps (Bethune, pers. comm., 1988) and correlations are speculative. The geology described below is thus a combination of previous work and of observations made by the author during sample collection and thin-section analysis.

Along Collins Inlet, the first nine kilometres (as far as Mill Lake) are dominated by pink, variably foliated granitic orthogneisses, some of which retain evidence of a volcaniclastic protolith (Davidson and Bethune, 1988). Krogh et al. (1971) obtained a 1730 Ma igneous zircon (U-Pb) date from similar pink granitic orthogneiss about 10 kilometres northeast of Collins Inlet, corroborating the inference that these gneisses were derived from a Killarney Complex equivalent. Minor, layered, hornblende-bearing quartzofeldspathic gneisses of uncertain parentage are also present in this part of Collins Inlet. East of Mill Lake as far as Beaverstone Bay, the gneisses are predominantly granodioritic in composition. Within Mill Lake and Beaverstone Bay, distinctive assemblages of metapelites, semi-pelites, quartzites and amphibolites have been partially weathered out, but are preserved along shores and on islands. Abundant, thin mafic dikes are present all along

the inlet (Burke, 1991). They are attenuated parallel to regional strike, but fold noses can be found which have axial planes parallel to strike. Most of the units along the inlet carry a southeast-plunging lineation, typical of the whole GFTZ.

Metamorphic grade rises abruptly from greenschist in the Killarney Complex to epidote amphibolite grade in the Front mylonites. Between the Front and Mill Lake, the granitic gneisses provide no opportunity to assess degree of metamorphism but where observed, mafic dikes have typical middle amphibolite facies assemblages of hornblende - plagioclase - biotite - quartz. Immediately southwest of Mill Lake, granitic gneisses with textures (flattened lapilli?) implying a volcaniclastic protolith were observed during fieldwork for this thesis. Within Mill Lake, metapelites bear the assemblage garnet - sillimanite - K-feldspar - biotite - quartz - plagioclase, and some mafic boudins have complex garnet - orthopyroxene - opaques (Fe-Ti oxides?) symplectic textures, with hornblende rimming orthopyroxene. These mineralogies are indicative of granulite facies metamorphism. East of Mill Lake, some mafic dikes are garnet and/or orthopyroxene - bearing, and the gneisses are slightly migmatitic. The changes in metamorphic assemblages in different rock types along the transect are summarized in Table 1.

The change from greenschist to granulite grade occurs over a distance of about nine kilometres from the Front. Several northeast-striking mylonite zones with a "top to northwest" thrust sense were mapped on Philip Edward Island by Davidson and Bethune (1988); these are probably responsible for bringing up progressively deeper crust. The juxtaposition of granitic gneisses still showing evidence of their protolith with granulite facies assemblages at Mill Lake implies that a high-strain zone on the western boundary of the metasedimentary package may be responsible for considerable relative uplift of the eastern half of the area.

The youngest rock unit exposed in the area is a set of east-west trending diabase dikes, known as the Grenville swarm. The dikes occupy an east-west fracture system which is obvious on all air photos and maps of the region as lakes and inlets off Georgian Bay. The dikes are discontinuous (Lumbers, 1975) but cut Grenville Front mylonites. They have been assigned an age of 575 Ma on the basis of K-Ar whole-rock determinations (Fahrig and West, 1986). One such dike occupies part of the fracture which defines Collins Inlet. It is locally exposed on the shores of the Inlet, but its exact extent and width are uncertain because of the deep water of the Inlet and the limited geological mapping that has been conducted in the area.

Table 1: Changes in metamorphic assemblages along transect. Abbreviations: qtz = quartz; Kfs = K-feldspar; pg = plagioclase; ab = albite; bt = biotite; musc = muscovite; ep = epidote; hb = hornblende; chl = chlorite; actin = actinolite; ti = titanite; ap = apatite; hem = hematite; zrn = zircon; opq = opaques; py = pyrite; opx = orthopyroxene; cpx = clinopyroxene; gt = garnet; sil = sillimanite; melt = leucosome (quartz, plagioclase, ±K-feldspar); (r) = retrograde or secondary phase.

approximate bulk composition	Killarney Complex	Grenville Front	Grenville Front to Mill Lake	Mill Lake to Beaverstone Bay
felsic	qtz -Kfs -pg ±musc(r) ±hem(r)	qtz -Kfs -pg -bt -ep ±ap ±ti ±chl(r)	qtz -Kfs -pg -bt ±hb ±py ±zrn ±ti ±ap ±hem(r)	qtz -Kfs -pg -bt -hb -melt ±zrn ±ap ±ti
mafic (pre-1238 Ma)	ab -qtz -chl-actin -ep -bt	hb -pg -qtz -bt -ti ±ep ±chl(r)	hb -pg -qtz -bt ±ap ±opq(r) ±hem(r) ±chl(r)	hb -pg -qtz -bt ±opx ±cpx ±gt ±melt ±ti ±ap ±opq ±chl(r)
pelitic	-	-	-	qtz -pg -gt- bt - sil -Kfs ±zrn ±ap

1.5 EXISTING T-t DATA

Few T-t data are available for this part of the Grenville Province. Bethune et al. (1990) obtained metamorphic U-Pb monazite ages of 1445 Ma from metasedimentary gneiss 3 and 7 kilometres southeast of the Grenville Front at Tyson Lake, 30 kilometres northeast of Collins Inlet. Metamorphic zircon in adjacent metadiabase (intrusion age 1238 Ma) has a U-Pb age of about 985 Ma (Bethune et al., 1991). Maximum metamorphic temperatures of ca. 720°C are indicated by the failure of the 985 Ma event to affect monazite (Bethune et al., 1990). Krogh (1989) identified a metamorphic melting event in Beaverstone Bay, at the eastern edge of the study area. U-Pb ages of zircon and titanite from leucosomes in a migmatitic gneiss define a discordia with an upper intercept of 1453 +/- 7 Ma and a lower intercept of 982 +/- 27 Ma, apparently corresponding to the same events as identified at Tyson Lake. The cause and extent of these two events are uncertain, particularly along Collins Inlet where the metamorphic grade is less telescoped than at Tyson Lake (granulite grade within 9 kilometres of the "Front" versus 3 kilometres at Tyson Lake; Davidson et al., 1990).

The only other data regarding timing of metamorphism in this part of the Grenville Province comes from about 60 kilometres southeast of the Front, in the Britt domain near Key Harbour (Fig. 2, inset). At least three phases of metamorphism have been identified: one pre-dating granite intrusion at 1684 Ma; a second post-dating this granite but pre-dating a 1442 Ma granodiorite intrusion; and a third, Grenvillian metamorphism with a peak age slightly greater than 1035 Ma, the time of closure of the U-Pb system in monazite (Corrigan, 1990).

Few reliable cooling data are available for the area. Sericite in the Killarney Complex was dated by the K-Ar system at about 1190 +/- 40 Ma (Wanless et al., 1974), and K-Ar biotite at 1180 (error unknown) (Lowdon et al., 1963) (all ages recalculated using decay constants recommended by Steiger and Jäger, 1977; recalculation by Anderson, 1988). Biotite in granitic gneiss of the GFTZ northeast of Beaverstone Bay was assigned a K-Ar age of 1000 Ma (error unknown) (Tilton et al., 1960). Three Rb-Sr muscovite ages for pegmatites cutting fabric in country rock adjacent to the Bell Lake granite (BLG) range from 1410 to 1440 Ma (Krogh and Davis, 1970). Other nearby age determinations include a K-Ar muscovite age near the BLG, of 1065 +/- 40 Ma; K-Ar biotite near the BLG, 1006 +/- 36; and K-Ar biotite from a granitic gneiss between Tyson Lake and the BLG of 897 +/- 33 (Wanless et al., 1968). K-Ar biotite ages are known to be unreliable, particularly in the vicinity of orogenic fronts (Wanless et al., 1970) and in high-grade metamorphic terranes (Foland, 1979), calling into question the validity

of these dates. Furthermore, the large error associated with the ages makes their usefulness in constraining thermal histories rather limited.

This study provides new T-t data for the 25-kilometre transect across the Grenville Front. Titanite was dated using the U-Pb method, from a suite of samples within the GFTZ (no titanite was obtained from northwest of the Front). Amphibole, biotite and K-feldspar were dated by the $^{40}Ar/^{39}Ar$ method, for suitable samples from the whole transect. These new results, combined with some of the existing data, permit construction of a complete T-t history for this part of the Grenville foreland and GFTZ.

CHAPTER II
U-Pb (TITANITE) DATING: METHODS AND RESULTS

2.1 METHODS

Uranium - lead dating of titanite was carried out in the Jack Satterley Geochronology Laboratory at the Royal Ontario Museum (ROM), Toronto. The basis of the U-Pb method has been documented by numerous workers (Faure, 1986; Parrish and Roddick, 1985). The techniques used in this study follow those outlined in Krogh (1973, 1982), and in Schärer et al. (1986). A brief description of the procedures at the ROM is given here.

2.1.1 Sample Selection

Heavy mineral separates were obtained using standard heavy liquid and magnetic separation techniques.

Grains were selected for dating one-by-one, under a binocular microscope, with the stipulations that they be:

a) crack-free, to avoid those which may have suffered late Pb-loss;

b) free of inclusions, particularly solid inclusions, which may be Pb-bearing;

c) as dark in colour as possible, indicating a high U content; this reduces uncertainties associated with the common Pb correction (see section 2.1.2).

Different generations of titanite were distinguished on the basis of size, colour, and perfection of crystal shape. For example, relict igneous grains in orthogneisses tend to be blocky and anhedral while metamorphic grains are smaller, multi-faceted subhedra to euhedra (T. Krogh, pers. comm., 1990). Possible different generations were picked into separate fractions, to be dated separately.

Some fractions were air-abraded to remove surface parts which may have suffered Pb-loss, features like leucoxene overgrowths, or to induce breakage of grains which were severely cracked. This technique was developed mainly for zircon by T. Krogh (1982), but is also suitable for titanite if done on a much shorter time scale (20 minutes per sample versus 24 hours for zircon abrasion). Because of the relative softness of titanite, abrasion is carried out without a buffer (whereas pyrite is used for zircon abrasion). After abrasion, samples were picked a final time to remove broken grains and those which still had surface irregularities or inclusions.

2.1.2 Sample Preparation and Analysis

Samples were cleaned twice by moderate heating in a solution of approximately 2M HNO_3; the second time, 2X distilled solutions were used, in acid-cleaned beakers, under positively pressured, filtered air hoods. All subsequent steps were carried out with similar standards of cleanliness. Samples were weighed, then transferred to Teflon capsules for dissolution under seal on a hot-plate, in a HF/HNO_3 solution. At this point a known amount of a mixed ^{205}Pb-^{235}U tracer was added (Krogh and Davis, 1975). Dissolution time was approximately 120 hours at 100°C. Uranium and Pb were removed from the sample using wet column HBr chemistry as described by Krogh (1973). Dried-down samples were loaded on Re single-filaments with H_3PO_4 and silica-gel, and measured on VG-30 and VG-354 thermal ionisation mass spectrometers. Analyses were corrected for a Pb blank of 8.2 picograms and a U blank of 3.8 pg, and further corrected for common Pb using the isotopic composition predicted by the Stacey and Kramers (1975) model. Linear regression and calculation of intercepts and errors (95% confidence level) was carried out using the method of Davis (1982). Blanket errors of 0.5% for the Pb/U ratio and 0.1% for the $^{207}Pb/^{206}Pb$ ratio were estimated. The error on $^{207}Pb/^{206}Pb$ may be underestimated in the case of samples with $^{206}Pb/^{204}Pb$ ratios of less than 1500 (Schärer et al., 1986), since uncertainty in the common Pb correction introduces greater error for these samples.

2.2 RESULTS

Six rock samples from the Collins Inlet transect (southeast of the Grenville Front) were prepared for dating. Three samples each yielded two fractions, possibly representing different generations of titanite; these were dated separately. As a result, nine fractions altogether were dated. Descriptions and photomicrographs of fractions are located in Appendix A; details of titanite occurrence in thin section (where observed) are described in Appendix B.

Analytical results are shown in Table 2 and plotted on a concordia diagram in Fig. 3. An inset of sample locations is included in Fig. 3. All fractions yielded discordant points with a range in $^{207}Pb/^{206}Pb$ ages between 1434.3 Ma and 1143.1 Ma. The nine fractions all fall along a single line defined by the method of Davis (1982), with a probability of fit of 4.8%. The lower intercept is 985 +21/-20 Ma, and the upper intercept is 1446 +11/-10 Ma. The fractions range in discordancy along the line from 5.7% to 78.1%.

The upper intercept age (1446 Ma) is identical within error to the upper intercept (1453 Ma) of a discordia defined by zircon and titanite

Table 2: U-Pb (Titanite) Data

Sample number*	Wt (mg)	U (ppm)	rad Pb (ppm)	$\frac{^{206}Pb}{^{204}Pb}$ (1)	$\frac{^{207}Pb}{^{206}Pb}$ (2)	$\frac{^{208}Pb}{^{206}Pb}$ (2)	$\frac{^{206}Pb}{^{238}U}$ (3)	$\frac{^{207}Pb}{^{235}U}$ (3)	$\frac{^{207}Pb}{^{206}Pb}$ age (Ma) (4)	% discord-ance
GF-32	.172	213	65	1742	.09765	.3907	.2437	3.019	1422	9.0
GF-20	.126	283	85	1783	.09804	.3495	.2467	3.075	1434	5.7
GF-19-1	.389	81	19	504	.11382	.2182	.2254	2.681	1344	30.2
GF-19-2	.127	218	56	918	.10350	.2062	.2378	2.904	1394	15.9
GF-18-1	.090	203	61	1820	.09682	.3878	.2390	2.951	1416	14.6
GF-18-2	.889	145	40	1440	.09774	.3141	.2332	2.833	1384	21.2
CI-19	.385	447	107	2215	.08962	.2655	.2077	2.386	1277	50.7
GF-35-1	.118	329	81	1937	.08722	.4068	.1934	2.137	1201	67.3
GF-35-2	.058	205	46	1376	.08734	.3632	.1841	1.976	1143	78.1

*fraction descriptions in Appendix A
1)measured ratio corrected for common Pb in the spike
2)corrected for fractionation, blank and spike
3)corrected for fractionation, blank, spike, and initial common Pb ; error estimated at 0.5% (based on lab norm)
4)corrected for fractionation, blank, spike, and initial common Pb; error estimated at 0.1% (based on lab norm)

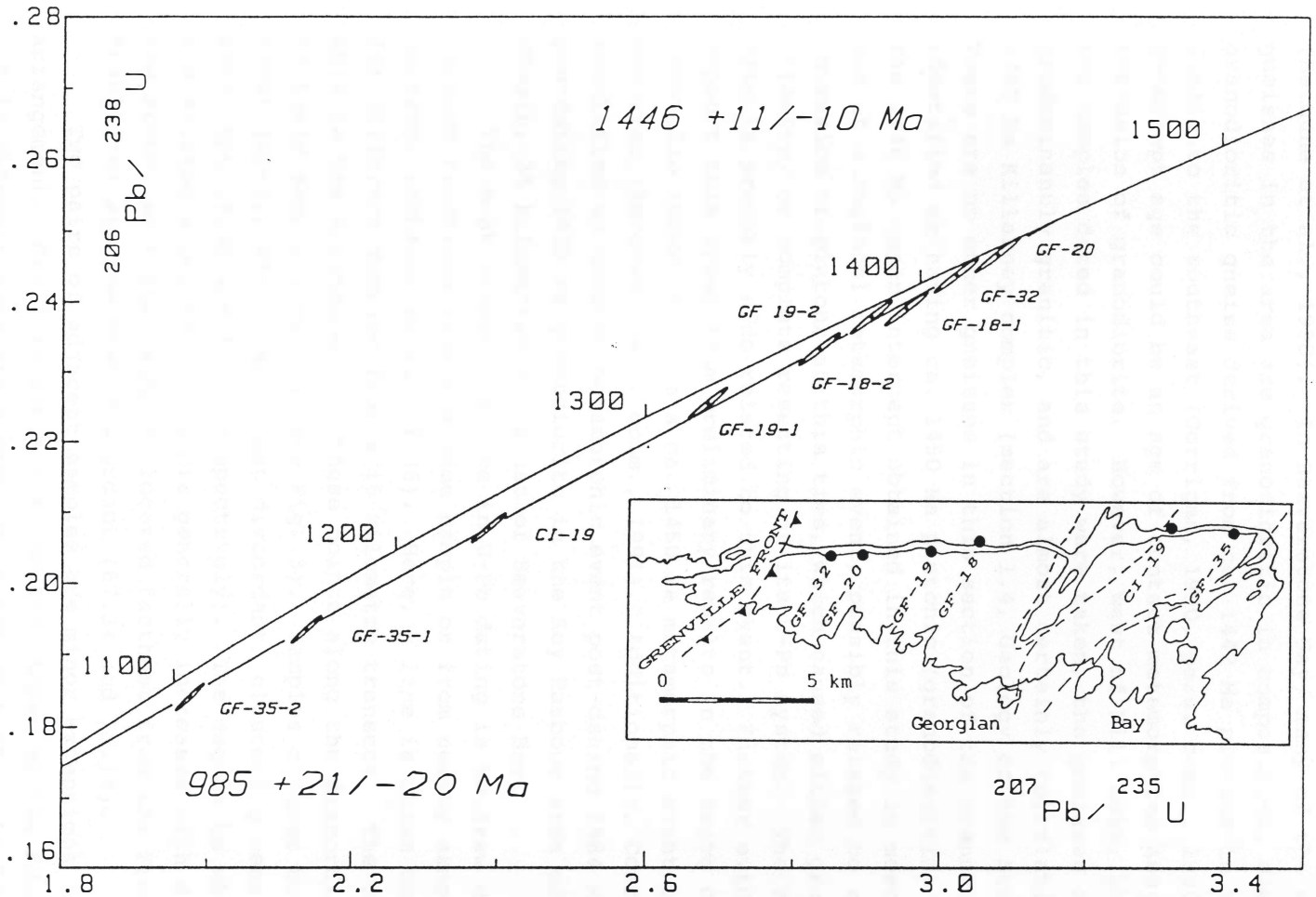

Fig. 3. Concordia diagram showing results of titanite U-Pb dating. Sample numbers correspond to sample locations shown in the inset. (-1 and -2 appended to sample number denote different titanite fractions obtained from a single rock sample).

in melt pods in Beaverstone Bay at the eastern end of this transect (Krogh, 1989). It is also identical to the age of metamorphic monazite (1445 Ma) in gneisses about 30 kilometres northeast, near Tyson Lake (Bethune et al., 1990). In Beaverstone Bay, many of the migmatitic gneisses in the area are granodioritic in composition, similar to granodioritic gneiss derived from ca. 1442 Ma plutons in the Britt domain to the southeast (Corrigan, 1990, pers. comm., 1990). The upper intercept age could be an age of contact metamorphism associated with intrusion of granodiorite. However, west of Mill Lake, where several of the samples dated in this study were taken, the gneisses are predominantly granitic, and are almost certainly correlative with the 1740 Ma Killarney complex (section 1.4, Geology of the Study Area). There are no other gneisses in this section of the transect which can be identified as having ca. 1450 Ma plutonic (granodioritic) parent rock. The 1446 Ma upper intercept obtained in this study is most probably the age of a regional metamorphic event, possibly related to voluminous intrusion of plutons at this time, which caused either growth of titanite, or complete resetting of its U-Pb system. The Krogh (1989) date is probably also related to this event. Further evidence to support this comes from preliminary results in the Britt domain of the Grenville interior where a ca. 1450 Ma metamorphic event appears to have occurred (Ketchum, pers. comm., 1991). Additionally, Corrigan (1990) identified an undated metamorphic event post-dating 1684 Ma granites and pre-dating 1442 Ma granodiorite in the Key Harbour area of the Britt domain, 35 kilometres southeast of Beaverstone Bay.

The most common practice in U-Pb dating is to draw discordia only through fractions from the same sample or from nearby samples (i.e. same outcrop) (Schärer et al., 1986). Here, a line is drawn through results for different samples from a 15 kilometre transect. The rationale for this is the arrangement of these points along the discordia in relation to their sample location (see Fig. 3). Samples closest to the Grenville Front (GF-32, GF-20) are least discordant, clustering near the upper intercept (9.0% and 5.7%, respectively). The degree to which samples are shifted along the discordia generally increases with distance from the Front, such that samples located farthest from the Front (two GF-35 fractions) are the most discordant (67.3% and 78.1%).

Two pairs of adjacent samples are minor exceptions to this arrangement. GF-32 is about 1 kilometre closer to the Front than GF-20, but is slightly more discordant (9.0% versus 5.7%). GF-18, which is about 1.5 kilometres farther from the Front than GF-19, yields a fraction of small euhedral crystals which is 14.6% discordant compared to 15.9% for similar euhedral crystals from GF-19. It also yields a

fraction of large fragments which is 21.2% discordant compared to 30.2% for fragments from GF-19.

For all other samples the pattern is consistent. This suggests that the main influence which caused the discordancy increased in importance away from the Front towards the interior of the Grenville Province.

One possible reason for the observed discordance array is mixing of two generations of titanite. Two morphologies of titanite were observed in at least four of the samples (either in thin section or in grain separates). If the picked fractions for a single sample represented more than one generation, the dates could represent mixed ages of the two generations, one formed at 1446 Ma and the second at 985 Ma.

For fraction pairs from samples GF-19 and GF-18, a distinction was made between euhedral, rounded, puck-shaped grains, all of similar small size, and anhedral, coarser, blocky fragments (see Appendix A for complete descriptions and photomicrographs). These two fractions were quite different in size and appearance, and no core/overgrowth relationship was observed between them. This is confirmed by thin-section study of GF-19, in which titanite occurs as single, rounded grains or as irregularly shaped rims on magnetite. The irregular rims are probably the source of the fragments. It is clear that in GF-19 these two types of titanite are morphologically distinct, and would have been easily identified during picking. In GF-18, titanite was only observed in thin-section as rims on zircon. Nevertheless, significant differences in size and morphology between the two picked fractions suggest that the two generations are distinct, and were successfully separated by careful picking. For GF-19 and probably GF-18, a much stronger contrast in discordancy between the two different fractions would therefore be expected if discordancy was a result only of mixing of these two generations (one fraction should be nearly concordant and the other nearly 100% discordant).

For sample GF-35, the two fractions picked were distinguished on the basis of colour, with a uniform fraction of light yellow rounded euhedra, and a mixed fraction of dark brown fragments and crystals selected. The darker fraction is more concordant, and is possibly a result of mixing of generations. However, the light yellow crystals are probably from a single generation and also fall along the discordia (78.1%). This implies that discordance of the GF-35 fractions is not due to simple mixing of the two types of titanite picked.

Only one fraction was picked from GF-32, although two types of titanite were observed in thin section. Euhedral crystals were

carefully selected and would have been easily distinguishable from the second kind, which are irregular rims on Fe-Ti oxides.

It is possible that a third generation of titanite grew at 985 Ma, but the only evidence for it is some colour variation within single grains of the GF-19-1 fraction (fragments). All other grains in all other samples appear to be homogeneous, lacking evidence of rims (as observed under the binocular microscope and in thin section). SEM images of polished grain mounts, as are sometimes made for zircons, might provide confirmation of this observation, but no such work was carried out.

However, regardless of the types and morphologies of titanite present in these samples, significant and regular enough differences in the degree of new metamorphic growth over the 15 kilometre distance are unlikely to produce the observed discordance array. Titanites were dated from several different rock types (granitic, granodioritic and amphibolitic gneisses) which obviously have different bulk compositions. Titanite-generating reactions in these different compositions in response to different conditions of metamorphism (demonstrated by results from $^{40}Ar/^{39}Ar$ dating) are unlikely to generate the regularly increasing amounts of titanite which would be required to produce the observed pattern.

The preferred interpretation of the discordance array is that titanite suffered diffusional Pb-loss at 985 +21/-20 Ma, from grains which had original ages of about 1446 Ma. Both morphologies of titanite grains in samples GF-19, GF-18, and GF-35 presumably had similar original ages, but were affected to different degrees by the 985 Ma event. The fragments dated in GF-19 and GF-18 may have contained more cracks which facilitated diffusion and resulted in greater loss of radiogenic Pb for these fractions.

The probability of fit (4.8%) of the discordia to the points is lower than normally acceptable for several fractions of titanite and zircon from the same sample (20%; L. Heaman, pers. comm. 1990). The inferior fit may be due in part to slight differences in the original age of the titanites from each sample. Also, as stated earlier, error on fractions with low $^{206}Pb/^{204}Pb$ ratios (<1500) may have been slightly underestimated (Schärer et al., 1986). If the error ellipses on samples GF-19-1, GF-19-2, GF-18-2 and GF-35-2 were expanded to incorporate 0.2% errors in $^{207}Pb/^{206}Pb$ ratios, the line fit would probably be similar but with a higher probability of fit. This was not done because it was seen as unnecessary in light of the interpretation of the results (Krogh, pers. comm. 1991), which focuses more on the nature of the discordance array and less on the error on the upper and lower intercepts. The fact

that the line fits a suite of samples from different locations and different rock units to any degree is remarkable (Krogh, pers. comm., 1991) and probably has geologic significance.

2.3 INITIAL INTERPRETATION OF TITANITE TRAVERSE

Most titanites from metamorphosed terranes yield concordant or nearly concordant dates defining either upper or lower intercepts on a discordia between "original" and "reset" ages (Schärer et al., 1986; Corfu, 1988; Corrigan, 1990). As a result, very few data are available in the literature on how to interpret a discordance array like that obtained for titanites along the Collins Inlet transect. There are, however, two exceptions, which will be described here as possible analogues for the GFTZ data.

2.3.1 Previous Work on Discordance Arrays

The first example of a discordance array is from a study conducted by Hanson et al. (1971) on titanites from a traverse across the thermal aureole of a pluton intruded 1600 My after last metamorphism. Titanites have similar morphologies along the length of the traverse, even in samples taken from beyond the thermal aureole. This implies no new titanite growth during contact metamorphism. New growth may also be precluded by the short duration of pluton-related heating, estimated at tens to hundreds of thousands of years. Titanite ages lie on or close to a chord between the original age of the country rocks in the thermal aureole and the age of the intrusion, and are more discordant as the contact is approached. The preferred interpretation of these data is that titanites have been increasingly reset to lower ages (probably due to Pb-loss), by progressively greater peak temperatures nearer the contact, during the intrusion episode (Hanson et al., 1971).

The second example of titanite U-Pb data with a thermally related discordance array is from a study of a regionally metamorphosed terrane, the Western Gneiss Region (WGR) of Norway (Tucker et al., 1987). Titanites yield an array between the time of igneous crystallization and regional metamorphism about 1250 My later. The degree of discordance generally increases with metamorphic grade, reaching 100% (complete resetting to metamorphic age) in areas where inferred metamorphic conditions were 575 to 640°C and 7.0 to 9.5 kilobars. The cause of discordance is not clearly known. However, metamorphic titanite is probably produced in lesser quantity at highest grades than at moderate grades, because at these conditions, reactions occur which are titanite-consuming (Tucker et al., 1987). This suggests that mixing of two generations would not produce the observed maximum discordance at

highest grades. Diffusional Pb-loss during metamorphism is a more plausible explanation for the observed pattern. A second important observation is that titanites from higher-strain rocks undergo more resetting than lower-strain rocks of similar metamorphic grade, implying that factors like strain state and possibly fluid availability contribute to resetting of titanite U-Pb systematics during metamorphism (Tucker et al., 1987).

The fact that a single regression line fits the data from different crustal levels of the WGR (for 41 different samples; Tucker, pers. comm., 1991) shows that the "closure" temperature of titanite must have been exceeded (in order for diffusional Pb-loss to occur) but not by enough for long enough to completely reset titanites (except at deepest crustal levels). Cooling therefore must have occurred soon after heating, and synchronously across the whole WGR, in order to define a common lower intercept for all samples. Synchronous cooling of differing crustal levels with peak metamorphic temperatures ranging from 480 to 640°C (Tucker et al., 1987) requires that cooling to titanite closure must have been rapid in the deeper levels. The duration of the heating and cooling event can be estimated from the error on the lower intercept, which defines the maximum scatter of the lower intercepts for single samples; in this case only 4 My (Tucker et al., 1987).

2.3.2 Interpretation of GFTZ Titanite Data

The data presented in this thesis for the Collins Inlet transect of the Grenville Front Tectonic Zone are analogous to both the Tucker et al. (1987) and Hanson et al. (1971) results. The ages of successive fractions are progressively shifted down the discordia with increasing distance from the Grenville Front. The regularity of this pattern and the probability that discordance is due to partial diffusive Pb-loss at about 985 Ma (as discussed in section 2.2, "Results"), demonstrate that the increasing partial resetting of titanites was a result of gradually more extreme heating during the Grenville event; either duration or temperature of heating could have been higher with distance from the Front.

The lower end of the discordia is relatively poorly constrained (to +21/-20 Ma). This is partly due to the method of line-fitting. A possible range of lines is fit to weighted data, with heavier weighting given to the data nearest the upper intercept. No data points are located beyond 78% discordancy, so the range of lower intercepts of different lines fitting the data is quite large. The problem may occur because no samples have been dated far enough from the Front, in an area where Grenvillian effects were strong enough to completely reset the

ages. Concordant titanite dates of 1001 to 1004 Ma and 963 to 980 Ma have been obtained in the Key Harbour area (Corrigan, 1990), which is about 35 kilometres farther from the Front than the most discordant samples in this study (from the north end of Beaverstone Bay). 100% discordance (concordance at the lower intercept) at ca. 985 Ma in titanites may be achieved somewhere between Beaverstone Bay and Key Harbour (but see Chapter 6).

Because of the similarity of these results to the Tucker and Hanson studies, the preferred interpretation of the data is similar their models. A period of heating, of high enough temperature to partially open the titanite to diffusion of Pb, must have occurred throughout the transect at some time before 985 Ma. Heating was more intense with increasing distance from the Front, as shown by the general trend of greater resetting with increasing distance. The probable range of temperatures reached during this time will be discussed, using all available thermochronometric data, in Section 5.2 (Integrated Interpretation of Results).

The nearest sample to the Front, GF-32, is slightly more discordant than GF-20, the next nearest sample. GF-32 probably suffered greater strain during movement on the Boundary Fault during either this or previous events, than did GF-20. This relationship is similar to that observed by Tucker et al. (1987), who found greater resetting in more deformed samples. The same phenomenon is known elsewhere (Krogh, pers. comm., 1990).

Cooling followed the thermal episode, at 985 +21/-20 Ma. The maximum duration of the event which opened and re-closed the titanite to Pb diffusion can be estimated from the error on the lower intercept, and thus is only constrained to be on the order of 40 Ma. The magnitude of this value may, however, be a function of the poor control on the lower end of the discordia (described above). The Tucker et al. (1987) and Hanson et al. (1971) models for a discordance array suggest that to produce such an array, the duration of the event must be short.

An additional, important implication of the 1446 - 985 Ma discordia is that in the intervening 460 Ma, the temperature in these rocks could not have exceeded titanite closure without causing titanite ages to shift down the discordia between 1446 Ma and the age of the event. If this were the case, the points from across the transect would not fall along the single line between 1446 Ma and 985 Ma.

Titanite results are discussed further in Chapter V (Synthesis of Results and Thermal History). The tectonic implications of this interpretation will be addressed in light of all the geochronological and geological data available in Chapter VI (Tectonic Interpretation).

CHAPTER III
$^{40}Ar/^{39}Ar$ DATING

3.1 INTRODUCTION: BASIS OF METHOD

The $^{40}Ar/^{39}Ar$ dating method is based on the radioactive decay of ^{40}K to ^{40}Ar over geologic time. ^{39}K in the sample being dated (usually a monomineralic volume of a K-bearing phase) is converted to ^{39}Ar by irradiation with fast neutrons in a nuclear reactor. Argon is extracted from the sample by heating in a vacuum furnace. The isotopic ratio of ^{40}Ar to ^{39}Ar is then measured in a mass spectrometer, corrected for interfering isotopes and atmospheric Ar components, and used in the calculation of the age of the sample.

The amount of ^{39}K converted to ^{39}Ar during irradiation is dependent on the irradiation parameters (specifically, the neutron flux density and the energy distribution of the neutrons), which are difficult to measure directly. For this reason, standard flux monitors with a known age are included with the unknowns in a "package" during irradiation. The isotopic ratios in the standards are measured, and a term describing the irradiation parameters is calculated. This term is known as the J-value.

The mathematical development of the age equation and the J-value calculation are detailed in Mitchell (1968), McDougall and Harrison (1988, pp. 17 - 19), and Grist (1989).

The standard procedure for carrying out $^{40}Ar/^{39}Ar$ dating is to extract gas in sequential temperature steps, and to measure isotope ratios for each step. The apparent age of each step is plotted against the percentage of total ^{39}Ar released which each step represents. The result is an age spectrum. The larger the step (in gas volume), the more weight its apparent age carries in the determination of the age of the sample.

The value of the step-heating experiment (versus a conventional K-Ar date or total gas date) is that steps which have irregularities in the isotopic ratio, due to various experimental and natural artifacts, may be recognized, and can be eliminated from the age determination. For example, the first few percent of gas released may give impossibly high ages, due to reactor-induced recoil of ^{39}Ar from the near-surface regions of grains (Harrison, 1983). If a sample has experienced a late thermal episode, the first gas released may have young ages. The later steps may still record the original age of the sample. In either case, a K-Ar age or total gas age would incorporate these artifacts in the age calculation, possibly giving a geologically meaningless result.

Many different forms of age spectra may arise. The meaning of

those obtained in this study will be considered in Section 3.3.1 (Introduction to Interpretation of $^{40}Ar/^{39}Ar$ Age Spectra).

The age obtained by $^{40}Ar/^{39}Ar$ dating of a metamorphic mineral is normally considered to correspond to the temperature at which radiogenically produced Ar ceased to diffuse out of the mineral, termed the "closure temperature". Diffusion is a thermally activated process which can be described by an Arrhenius relationship. Based on this, Dodson (1973) derived an expression which describes closure of diffusional processes in minerals:

$$T_c = \frac{(E_a/R)}{\ln\left[\frac{A\,R\,T_c^2(D_0/a^2)}{E_a\,(dT/dt)}\right]} \qquad (1)$$

where T_c is closure temperature, E_a is activation energy, R is the gas constant, A is a geometrical constant, a is effective diffusion length, D_0 is frequency factor (diffusivity when $T = \infty$), and dT/dt is cooling rate. The expression permits calculation of closure temperature for given diffusion parameters and geometry of diffusion domains, and assumes a single diffusion domain size, and slow cooling as a linear increase in 1/T. The development of Dodson's theory is completely explained in McDougall and Harrison (1988) and Grist (1989).

Berger and York (1981) proposed a method for extracting the diffusion parameters directly from step-heating experiments. The method assumes that the diffusional processes operating during step-heating are the same as those operating in nature when the mineral closes to Ar diffusion. For this assumption to be valid, only one mineral phase must be present, and the phase must remain stable throughout the experiment. Hydrous phases like micas and amphiboles have been shown to undergo structural breakdown during <u>in vacuo</u> heating (Gaber et al., 1988). Diffusion experiments are only valid for these minerals if they are conducted under hydrothermal, oxygen buffered conditions (McDougall and Harrison, 1988). Closure temperatures for conventional $^{40}Ar/^{39}Ar$ dates on amphiboles and micas must therefore be assumed rather than calculated.

K-feldspars appear to conform to the requirements for using the Berger and York method, permitting calculation of closure temperature for each sample dated.

3.2 METHODS

The standard techniques used in $^{40}Ar/^{39}Ar$ dating are well known

because the method has been in common use since the late 1960's. A full and relatively up-to-date discussion of technical considerations is available in McDougall and Harrison (1988). A brief outline of methods used in this study, especially where these are specific to the laboratory, is given below.

3.2.1 Sample Selection

Samples used for $^{40}Ar/^{39}Ar$ dating were selected on the basis of their appearance in thin section. Brief field descriptions and thin section descriptions are presented in Appendix B.

Minerals appropriate for dating by the $^{40}Ar/^{39}Ar$ method (hornblende, biotite and K-feldspar) were examined with the following criteria in mind:

a) Intergrown phases should be avoided if possible. This is particularly important when the mineral of interest has a relatively low K-content, and is intergrown with a high-K phase, since even a small amount of the high-K phase may produce enough radiogenic Ar during outgassing to obscure that produced by the phase for which dating is intended.

b) Samples should be fresh and unaltered to avoid grains which have suffered K-loss or gain during weathering or late reaction, for example partial chloritization of biotite or development of sericite in K-feldspar grains.

c) Multiple generations of a particular mineral group should be recognized so that they can be segregated if possible during separation, or at least acknowledged during interpretation of spectra. The relative timing of mineral growth, deformation, and episodes of heating (metamorphism?) should be determined if possible, so that the dates obtained can be assigned to the correct event.

d) The range of grain size of the particular phase to be dated should be noted so that during sample preparation an appropriate grain size fraction is selected (ideally, 1/2 to 1/4 of the average grain size; McDougall and Harrison, 1988). If the selected fraction is too coarse, much of the mineral phase being sought will be present as part of polymineralic grains, which should not be used for dating because age spectrum interpretation will be difficult. If it is too small, the separate will consist of unrepresentative fragments of the original grains, which may cause the effective diffusion radius of the sample to be reduced below that which operated in nature.

3.2.2 Sample Separation

Mineral fractions were extracted from crushed and sieved bulk rock

samples using standard magnetic, heavy liquid and paper-panning techniques. Relatively clean separates were then picked by hand under a binocular microscope to increase purity.

Two batches of samples were processed. The first was prepared for analysis with a modified MS10 mass spectrometer, requiring large sample volumes to obtain measurable gas volumes. As grain sizes in almost all samples used in this study were relatively small (125 to 180 microns diameter in most), large numbers of grains were required to make up the sample volume. This precluded selection of individual grains, so that samples were likely to have at least some degree of contamination by other phases. Hornblende samples are the most likely to exhibit problems arising from contamination, due to the relatively low K-content (hence large volume requirement), and difficulty of distinguishing intergrown biotite except on very close examination of each individual grain.

The second batch was prepared for analysis by a new VG3600 mass spectrometer, which has sufficient sensitivity to permit step-heating analyses on much smaller sample volumes. This allowed individual selection from an initial volume of separated grains, increasing the proportional purity of the samples dated, and greatly reducing the time required for purification.

The system used to date each sample is noted in the sample descriptions in Appendix B and on their data summary sheets in Appendix C.

3.2.3 Sample Analysis

All $^{40}Ar/^{39}Ar$ data acquired for samples dated in this study using the methods below are summarized in Appendix C.

Samples dated using the MS10 system were analysed according to the procedures outlined in Muecke et al. (1988), except as noted here.

The flux monitor used in this study was MM-Hb hornblende, with a standard K-Ar age of 519 ±3 Ma (Alexander et al., 1978). Standards were placed at regular intervals throughout the irradiation cannister. J-values were measured for each standard, then plotted with errors versus position in the cannister. A line was fitted to these points using the York (1969) method, then J-values for the interspersed samples were determined by interpolation along the line. This permitted determination of J to within ±1% (1σ) or better, depending on the goodness of fit of the line. The values of individual errors in J (1σ) are quoted with the J-values for each sample on their data summary sheets in Appendix C.

Hornblende and biotite samples were heated to a maximum of 1150°C

in an external Lindberg furnace, with step-heating schedules varying according to the gas volumes derived. (Size of steps was cut down in temperature ranges which produced large gas volumes, in order to maximize the resolution of the age spectrum). K-feldspar samples were heated in uniform, timed steps to a maximum of 1150°C in this system. Some were then transferred for complete outgassing to a higher temperature furnace attached to the VG3600 mass spectrometer, as described below. Time steps for K-feldspar outgassing are precise to ±1 minute. Temperature is accurate to ±1% in the range used, with about 1°C fluctuation during the heating step, for the Lindberg furnace.

All remaining samples were analysed on the new VG3600 mass spectrometer, which for the present study was coupled to a double-vacuum tantalum resistance furnace built at Dalhousie University by K. Taylor. Packaging and irradiation procedures, and the standard used, were the same as those for the MS10 system, except that packages were much smaller. Samples were loaded into a circular loading port system designed and built by K. Taylor, which permits simultaneous loading to the vacuum line of up to 12 samples. After loading, the line was "roughed out" by a mechanical pump-backed sorption pump. High vacuum was then achieved by a 25 litre per second ion pump. Prior to individual sample loading to furnace, the furnace was outgassed at maximum temperature (about 1300°C) for about 1 hour; this was repeated until measured blank was sufficiently low.

Temperature in the sample chamber was measured by a platinum - rhodium thermocouple, which was previously calibrated using a second, external thermocouple inserted into the hot zone. Temperatures were found to be offset by a value of 70°C (K. Taylor, pers. comm., 1991), consistent over the temperature-range capability of the furnace. All temperatures quoted for steps have been corrected for this offset. A control is also provided on the high temperature calibration of the furnace by outgassing of pure K-feldspar, which melts incongruently to leucite and liquid at 1150 ±20°C (Deer et al., 1966), and in the process often liberates a large volume of Ar. Very large steps were obtained for several samples within temperature steps which crossed this temperature range. Only one sample (CI-14K) released a large amount of Ar outside this temperature range (at 40°C or more lower than expected). This may be due to Na in the alkali feldspar, exhibited by the presence of albite exsolution lamellae. The melting temperature of K-feldspar is reduced from the pure K-end-member temperature of 1150°C to a minimum of 1063°C for about 65% Na-feldspar (Bowen and Tuttle, 1950). Assuming the calibration provided by K-feldspar melting in several other samples, temperature is known to ±20°C; fluctuation during a single step is about

5°C once the furnace has reached temperature.

Hornblende and biotite samples were maintained at temperature for about 30 minutes. Approximately 20-minute heating steps for K-feldspar were carefully timed, starting when the furnace reached temperature and ending when the furnace was turned down; these times are precise to ±1 minute. The duration of each heating step is noted on the data summary sheets for K-feldspars in Appendix C.

During extraction, gas was cleaned by constant exposure to a GP50 Al-Zr alloy getter, run at room temperature. After admission to the mass spectrometer, an automated data acquisition system provided by VG Isotopes measured the abundance of each Ar isotope 15 times. The size of the ^{40}Ar peaks necessitated measurement of the $^{40}Ar/^{39}Ar$ ratio using the Faraday detector first; then $^{36}Ar/^{39}Ar$ and $^{37}Ar/^{39}Ar$ ratios were measured using the electron multiplier. (The initial version of operating software provided by VG Isotopes and used in this study did not permit switching between the Faraday and the multiplier during the 15 measurements). Measured ratios were then extrapolated back to zero time (the time of initial admission of gas to the mass spectrometer) using linear regression. Treatment of data beyond this stage was the same as for the MS-10 system, described in Muecke et al. (1988), using software written at Dalhousie University. Age spectra were obtained for all samples; in addition, Arrhenius plots were calculated for some K-feldspars, again using Dalhousie University software.

3.2.4 Error Analysis

Error in J is the major source of error in the final age assigned to the sample. J is the same for each individual step in a single sample, so is not considered in the error quoted on steps nor when comparing ages of steps. Error on individual steps (quoted at 1σ in Appendix C) is mainly a function of the uncertainty in the correction for atmospheric argon, which arises as a result of the small size of the ^{36}Ar peak which must be measured to make the correction. Step errors also depend on uncertainties in measurement of ^{40}Ar and ^{39}Ar peaks, in mass discrimination corrections, and in interfering isotope corrections. Error on J-values (quoted at 1σ in Appendix C) was determined by using the York (1969) method to fit lines to the J-value versus position data for the standards. Error quoted is the error in the intercept on the J-value (y-) axis, which is thus a maximum error for the package; actual errors may be less for samples in the middle of the package.

Errors on final ages were calculated using a standard sum of squares calculation on the steps which were considered to have representative ages (plateaux for some samples; see section 3.3.1

(Introduction to Interpretation of $^{40}Ar/^{39}Ar$ Age Spectra). The final error calculation incorporates error in J and is quoted at 2σ.

$^{37}Ar/^{39}Ar$ ratios were measured for all amphiboles. Apparent Ca/K ratios were calculated for each step using the relationship: Ca/K = ((1.82 ±.17) x ($^{37}Ar/^{39}Ar$)), in which the coefficient is that quoted by Onstott and Peacock (1987) for the 5C site of the McMaster University nuclear reactor in Hamilton, Ontario. The coefficient is consistent within error with values of 1.83 reported by Hanes et al. (1985) and 1.9 obtained by the Dalhousie laboratory (P.H. Reynolds, pers. comm., 1991), for the McMaster 5C site, which was also used in this study. Errors quoted on calculated Ca/K ratios (2σ) are a combination of the 9.3% error (2σ) in this value and a typical error of 1% (2σ) in the $^{37}Ar/^{39}Ar$ ratio.

3.3 HORNBLENDE AND BIOTITE RESULTS

K-feldspar, biotite and hornblende separates were all dated using the $^{40}Ar/^{39}Ar$ method in this study. The interpretation of K-feldspar results is more complex than for hornblende and biotite, and will be addressed in a separate chapter. The following introduction to interpretation of $^{40}Ar/^{39}Ar$ results therefore deals only with K-feldspar regarding the points of interpretation which it has in common with biotite and hornblende.

3.3.1 Introduction to Interpretation of $^{40}Ar/^{39}Ar$ Age Spectra

The original theory of Ar diffusion used by the earliest workers for $^{40}Ar/^{39}Ar$ age interpretation, was the single-site, volume diffusion model of Turner (1968). This model predicts that samples cooled quickly through their closure temperature, and not subsequently disturbed, will yield perfectly flat age spectra (plateaux) corresponding to the time of closure to diffusion. Thermally disturbed samples are predicted to exhibit age gradients, with the original age reduced to some degree, depending on the intensity of the episode.

Experience with the $^{40}Ar/^{39}Ar$ method has shown that considerable deviation from the theoretical model occurs in the spectra produced by real samples, probably due to violation of one or more of the assumptions of the model. Disturbed samples often record their original closure age in higher temperature extraction steps (Berger and York, 1981), permitting application of the method in thermally complex terranes. Disturbed samples also often yield several low-temperature increments contributing to a significant volume of gas release, which sometimes record the age of a thermal disturbance.

These observations, made in light of the prediction of plateaux by

the Turner theory, led to the establishment of arbitrary criteria for spectrum interpretation, which required the existence of a "plateau" in an age spectrum for the determination of a geologically meaningful age. The definition of a plateau varies between different workers, but generally requires that several contiguous steps, making up a significant proportion of the total gas released, have the same age within the error. For reasons discussed later the absence of a plateau is no longer considered a valid criterion for outright rejection of an analysis, particularly for K-feldspars. Likewise, the presence of a plateau is no longer sufficient to validate an age. However, the tradition of describing a sample as having or lacking a plateau persists.

The amphiboles and biotites dated in this study have been tested for the presence of a plateau in their spectra using the criteria of Fleck et al. (1977). The requirements are as follows: that contiguous gas fractions representing more than 50% of total ^{39}Ar released have no age difference between any two fractions at the 95% confidence level. This requirement is tested using the Critical Value test, in which apparent age differences between steps can be no greater than the Critical Value:

$$C.V. = 1.96(\sigma_1^2+\sigma_2^2)^{\frac{1}{2}} \qquad (2)$$

where σ_1, σ_2 are the standard deviations of the ages. Steps containing less than 3% of gas release are ignored in the determination of a plateau. An example of a $^{40}Ar/^{39}Ar$ apparent age spectrum with a plateau is illustrated in Fig. 4a.

Age spectra often have irregular shapes, either failing to yield a plateau, or having a plateau but otherwise disturbed, due to both experimental and geological effects. The interpretation of spectra is not always straightforward, but the accumulated experience of workers using the method has produced a degree of understanding of irregular spectra which permits at least partial interpretation. The considerations of interpretation which have arisen in this study are discussed below.

Impurities in the separate may release components of radiogenic Ar which are different in age from the bulk of the separate. This is a particular problem for relatively low-K phases like amphibole since the total gas produced is low and thus more easily swamped if a high-K impurity is also outgassing. Clearly, careful sample selection and purification are essential, but when a sample is variably altered or

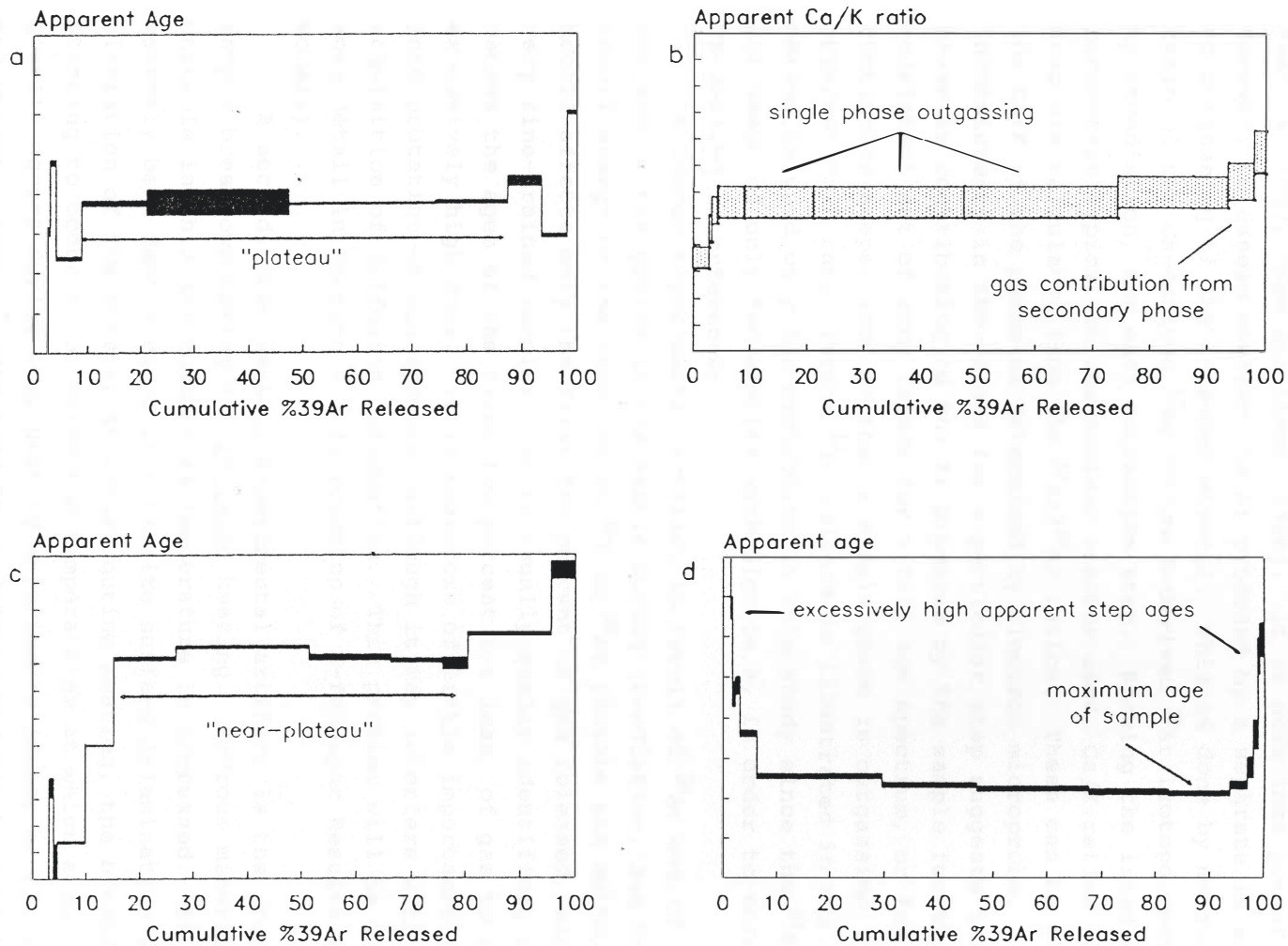

Fig. 4. Example $^{40}Ar/^{39}Ar$ apparent age spectra and Ca/K ratio plots. a) A plateau, according to the criteria stated in text. b) Ca/K ratio plot. c) A near-plateau. d) A U-shaped spectrum caused by excess Ar. See text for explanation.

intergrown, and when a large sample is required, sample purity is not always certain. Contribution of gas from a secondary alteration phase or exsolution lamellae is a commonly observed effect (Onstott and Peacock, 1987; Ross and Sharp, 1988). It is sometimes possible, however, to assess whether the Ar produced by a separate is actually due to outgassing of the intended mineral. This is done by measuring the ratio of the Ca-derived ^{37}Ar to the K-derived ^{39}Ar isotope, both produced by irradiation, for each extraction step. Knowing the irradiation parameters typical of the nuclear reactor used, Ca/K ratios for each step are calculated from the $^{37}Ar/^{39}Ar$ ratios. These can be compared to the Ca/K of the phase as determined by electron microprobe. Inconsistency in the values for a particular step suggests that another phase is contributing to the Ar produced by the sample for that step. A consistent set of step values for a full age spectrum, or for several contiguous steps, implies that a single phase is outgassing. A plot of apparent Ca/K ratio versus ^{39}Ar release is illustrated in Fig. 4b. This method is used only for amphiboles in this study since the ^{37}Ar isotope was measured only for samples with high Ca/K, in order to correct for Ca-derived interferences.

A common experimental artifact is recoil of ^{39}Ar out of the near-surface of the grains in the sample during irradiation, due to the recoil energy of the reaction of ^{39}K to ^{39}Ar (Huneke and Smith, 1976). Recoil affects only the first few percent of gas released, except for very fine-grained samples. It is usually easily identified, because it causes the ages of the first few percent (or less) of gas to have excessively high ages. It is therefore of little importance in the interpretation of age spectra, although it may interfere with the acquisition of diffusion information. This problem will be discussed in more detail in Section 4.3 (Discussion of K-feldspar Results and Models).

A second, more serious experimental artifact is the problem of sample breakdown during dry <u>in vacuo</u> heating. Hydrous minerals become unstable in this environment as temperature is increased. It has recently been demonstrated that biotite suffers delamination and alteration of the crystal structure during heating, the breakdown starting to occur at or below the temperatures at which argon release usually occurs during step-heating experiments (Gaber et al. 1988; Lo and Onstott, 1989). This results in drastic modification of the mechanism of argon release relative to the way it happens in nature, calling into question models of the significance of plateaux or gradients. The existence of a plateau for biotite may be nothing more than a result of re-homogenization of the distribution of ^{40}Ar and ^{39}Ar

during heating. The age of the plateau may thus be a geologically meaningless number if it has been partly disturbed, for example by a thermal event or by the incorporation of excess Ar (see below for discussion of excess Ar). A further consequence of biotite breakdown is that diffusion experiments are not valid for this phase unless conducted under isothermal, hydrothermal, oxygen-buffered conditions, which are beyond the capability of most laboratories conducting routine $^{40}Ar/^{39}Ar$ analysis.

Amphiboles seem to suffer only minor structural change during dry heating (Gaber et al., 1988) and plateaux obtained from amphiboles are usually still interpreted with reasonable assurance. A recent study, however, has shown that amphiboles can also yield plateaux in certain cases where they demonstrably contain excess Ar or have been partially reset, possibly due to isotope re-homogenization during sample breakdown (Maboko et al., 1991). This illustrates that requiring a plateau for amphibole may also be an artificial constraint on interpretation, since consistency in step ages and between samples may be more significant than a rigorous plateau requirement. Some workers have begun to attach significance to ages of relatively flat spectra which do not contain plateaux because they yield reasonable ages ("near-plateau ages") consistent with nearby samples or known thermal histories (Schermer et al., 1990). This method of spectrum interpretation is probably preferable to establishing strict but arbitrary rules requiring plateaux (Harrison, 1990). An apparent age spectrum containing a "near-plateau" is illustrated in Fig. 4c.

K-feldspars, being anhydrous, do not appear to break down during step heating (Foland, 1974), although structural changes have been invoked in the past to explain irregularities in the Arrhenius plots produced for certain samples. K-feldspars usually fail to yield plateau ages, an observation which led early workers to reject K-feldspar as a thermochronometer, on the grounds that it is intrinsically "leaky". However, it is now understood that the age gradients or stepped spectra typical of K-feldspars are a result of slow cooling or partial resetting in response to a thermal event, and that geologically meaningful ages can be acquired for such spectra (Harrison, 1990). The means by which this is done is discussed in detail in section 4.1, the Introduction to K-feldspar interpretation.

The occurrence of "excess argon" is the most problematic of the possible difficulties with $^{40}Ar/^{39}Ar$ age spectrum interpretation. Excess Ar is ^{40}Ar not produced by <u>in situ</u> decay of ^{40}K. It is distinct from inherited Ar, which results from retention of old <u>in situ</u> radiogenic Ar during a thermal event. Excess Ar has been identified in various

minerals from different geologic environments, in particular in biotite and from orogenic fronts like the present study area (Wanless et al., 1970; Dallmeyer, 1987; Owen et al., 1988). It is thought to be a result of localized argon overpressure during mineral crystallization or recrystallization, causing Ar of non-atmospheric composition (with an excess ^{40}Ar component) to enter the structure at temperatures at which diffusion is not fast enough to expel it again (Harrison and McDougall, 1981). Because it is non-atmospheric, the normal correction using the atmospheric $^{36}Ar/^{40}Ar$ ratio does not fully remove the excess ^{40}Ar from the age calculation.

"U-shaped" age spectra are characteristic of some samples containing excess Ar, and the recognition of these permits partial interpretation of the spectrum without further data manipulation. The U-shaped spectrum (Fig. 4d) typically has very high ages at both low and high amounts of gas release, with a low point in the middle. The low point is often a geologically reasonable age and at worst defines a maximum age for the sample (Harrison and McDougall, 1981).

More irregular forms of age spectra caused by excess Ar can also potentially be interpreted. This is based on the observation that different non-radiogenic components (if present) are sometimes released in different temperature ranges. On an "inverse isochron" plot, in which $^{36}Ar/^{40}Ar$ is plotted against $^{39}Ar/^{40}Ar$ for each step, one or more components of non-atmospheric Ar may be revealed if several contiguous steps define a line (Roddick et al., 1980; Heizler and Harrison, 1988). The $^{36}Ar/^{40}Ar$ ratio defined by the Y-intercept of the line is used instead of the atmospheric ratio to correct for non-radiogenic ^{40}Ar in these steps. Ages are re-calculated and may redefine the shape of the age spectrum from discordance to relative concordance if several non-radiogenic components are identified (Heizler and Harrison, 1988). For a single non-radiogenic component, the age of the steps can be calculated using the $^{40}Ar/^{39}Ar$ ratio defined by the X-intercept. The method alternatively provides confirmation that the atmospheric assumption is correct (note that the steps making up a plateau will always plot as a straight line intersecting the $^{36}Ar/^{40}Ar$ axis at the atmospheric value; P.H. Reynolds, pers. comm., 1991).

An important prerequisite for using this method is that the sample line blank is known for the dating system, and is corrected for before the data are plotted on the isochron plot (Roddick, 1978). If the sample line blank is poorly known, the method cannot be used. In this study, samples were dated using two different extraction systems and mass spectrometers (described in Section 3.2.3, Sample Analysis). The error in the blank measurement on the MS10 system is of the same

magnitude as the total measurement of the $^{36}Ar/^{40}Ar$ ratio. Thus the y-axis co-ordinates of many points on the inverse isochron plot cannot be distinguished from one another nor from zero, and the inverse isochron method cannot be applied to the samples dated on this system.

At the time samples were dated on the VG3600 system, sample line blank was poorly known, because the system was new (K. Taylor, pers. comm., 1991). As a result the inverse isochron method cannot be applied to this second group of samples.

Interpretation of $^{40}Ar/^{39}Ar$ age spectra can be a subjective process, particularly if tests like the inverse isochron method cannot be used. This makes the validity of single ages somewhat questionable. However, by dating closely spaced samples of the same mineral, and by dating suites of minerals with different closure temperatures, this problem can be resolved to a significant degree. Consistent ages and patterns of ages are the best assurance that the dates interpreted from age spectra are valid.

Where possible in this study, closely spaced samples and/or different phases from the same rock were dated. The results of the individual hornblende and biotite samples are described below, divided into sections by mineral phase. (K-feldspar interpretation is more complex and the results will be addressed separately in Chapter 4). Most samples exhibit recoil effects and other minor irregularities in steps which contribute <3% of total gas; these are ignored in the descriptions unless they are part of a larger trend. Complete data sheets on all step-heating experiments are presented in Appendix C. Electron microprobe data and calculated Ca/K ratios for hornblendes are given in Appendix D.

Within each section, samples are addressed in order of sample location, starting with samples in the Southern province foreland, and progressing into the Grenville Front Tectonic Zone. Sample locations are shown in Fig. 5. The significance of the dates are described with reference to all the available data in Chapter 5.

3.3.2 Hornblende $^{40}Ar/^{39}Ar$ Results

Sample GF-44H (Fig. 6a) yields a disturbed, U-shaped spectrum. Steps have unreasonably high ages for the first 20% of gas release (older than the probable igneous age of 2220 Ma). Apparent ages drop to a minimum, then rise again and level off. This form of spectrum is normally attributed to the presence of excess Ar, and the apparent age minimum is normally taken as a maximum for the age of the sample (Harrison and McDougall, 1981). However, in this sample the apparent Ca/K ratios are also highly irregular, varying from 3.6 to about 43.5

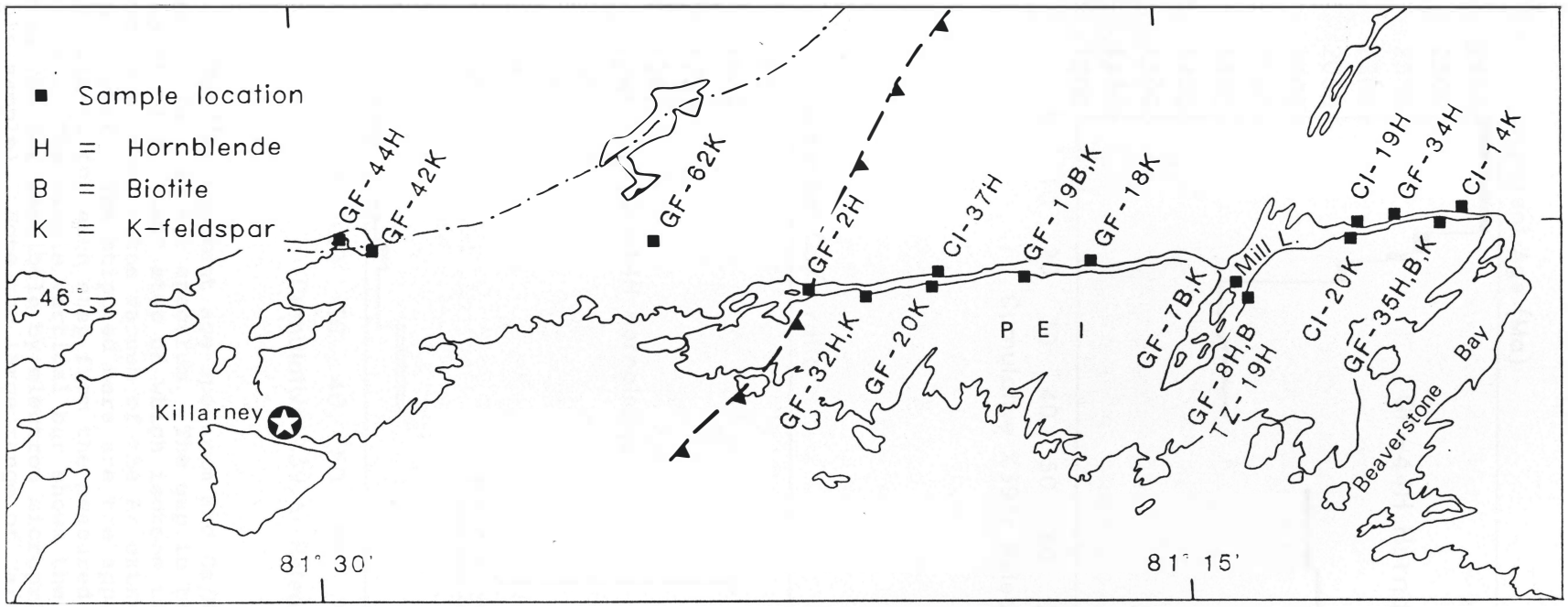

Fig. 5. $^{40}Ar/^{39}Ar$ sample location map. More than one mineral phase was dated in several samples. The sample numbers are the same for separates from the same rock but are appended by different letters denoting the mineral. Sample numbers are also the same for titanite from the same rocks (Fig. 3 inset).

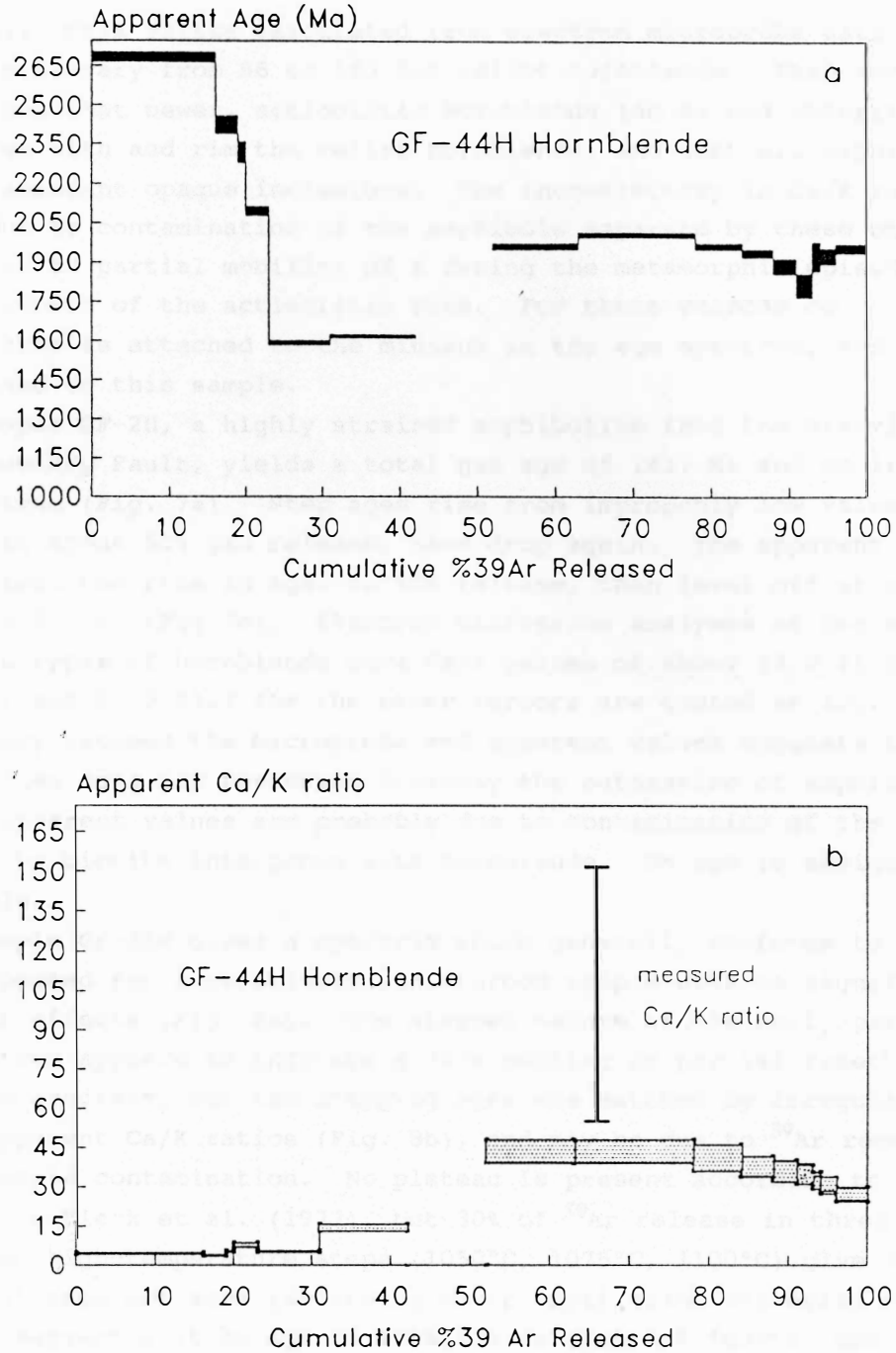

Fig. 6. $^{40}Ar/^{39}Ar$ apparent age spectrum and Ca/K ratio plot for GF-44H amphibole. a) Age spectrum. The gap in the spectrum is the result of a "lost" step on which isotope ratios were not measured due to a leak in the vacuum of the Ar extraction system. b) Ca/K ratio plot. The stippled bars are the apparent Ca/K ratios calculated for each step from the measured $^{37}Ar/^{39}Ar$ ratios, with 2σ errors. The single vertical bar shows the range of Ca/K ratios measured for amphibole by electron microprobe (not an error bar in this sample). Note the large range of Ca/K step ratios.

(Fig. 6b). Ca/K ratios calculated from electron microprobe data (Appendix E) vary from 56 to 153 for relict hornblende. Thin section study shows that newer, actinolitic hornblende (no K) and chlorite are intergrown with and rim the relict hornblende, and that all amphiboles contain abundant opaque inclusions. The inconsistency in Ca/K ratios may be due to contamination of the amphibole separate by these other phases, or to partial mobility of K during the metamorphic episode causing growth of the actinolitic rims. For these reasons no significance is attached to the minimum in the age spectrum, and no age is assigned to this sample.

Sample GF-2H, a highly strained amphibolite from the Grenville Front Boundary Fault, yields a total gas age of 1417 Ma and an irregular age spectrum (Fig. 7a). Step ages rise from improbably low values to a maximum at about 50% gas release, then drop again. The apparent Ca/K ratios mimic the rise in ages to 50% release, then level off at a value of 9.5 ±1.0 (2σ) (Fig 7b). Electron microprobe analyses of two slightly different types of hornblende give Ca/K values of about 13.0 ±1.3 for one type, and 13.3 ±1.3 for the other (errors are quoted at 2σ). The discrepancy between the microprobe and apparent values suggests that the gas obtained does not represent strictly the outgassing of amphibole. The low apparent values are probably due to contamination of the separate by biotite intergrown with hornblende. No age is assigned to the sample.

Sample GF-32H gives a spectrum which generally conforms to the shape expected for a relatively undisturbed sample with no significant excess Ar effects (Fig. 8a). The stepped nature of the early part of the spectrum appears to indicate a slow cooling or partial resetting diffusion gradient, but the stepping ages are matched by irregularities in the apparent Ca/K ratios (Fig. 8b), and may be due to ^{39}Ar recoil or slight sample contamination. No plateau is present according to the criteria of Fleck et al. (1977), but 30% of ^{39}Ar release in three contiguous high-temperature steps (1050°C, 1075°C, 1100°C) give mutually consistent apparent ages (according to critical value criteria) which define a segment with an age of 1206 ±18 Ma (2σ). A fourth, non-contiguous step (1000°C), gives the same age for another 12% of gas, while the 1025°C step, which contributes 25% of total gas, has a slightly higher age of 1230 Ma. All these steps have Ca/K ratios of 6.6 to 7.1 ±0.7, roughly consistent with the measured value of 7.7 ±0.8. Together they define an approximate "near-plateau" age of 1215 ±18 Ma (2σ), which is the preferred date for the sample.

CI-37H yields an irregular spectrum which is at best consistent for two steps contributing 23% of the gas (Fig. 9a). Ca/K ratios (Fig.

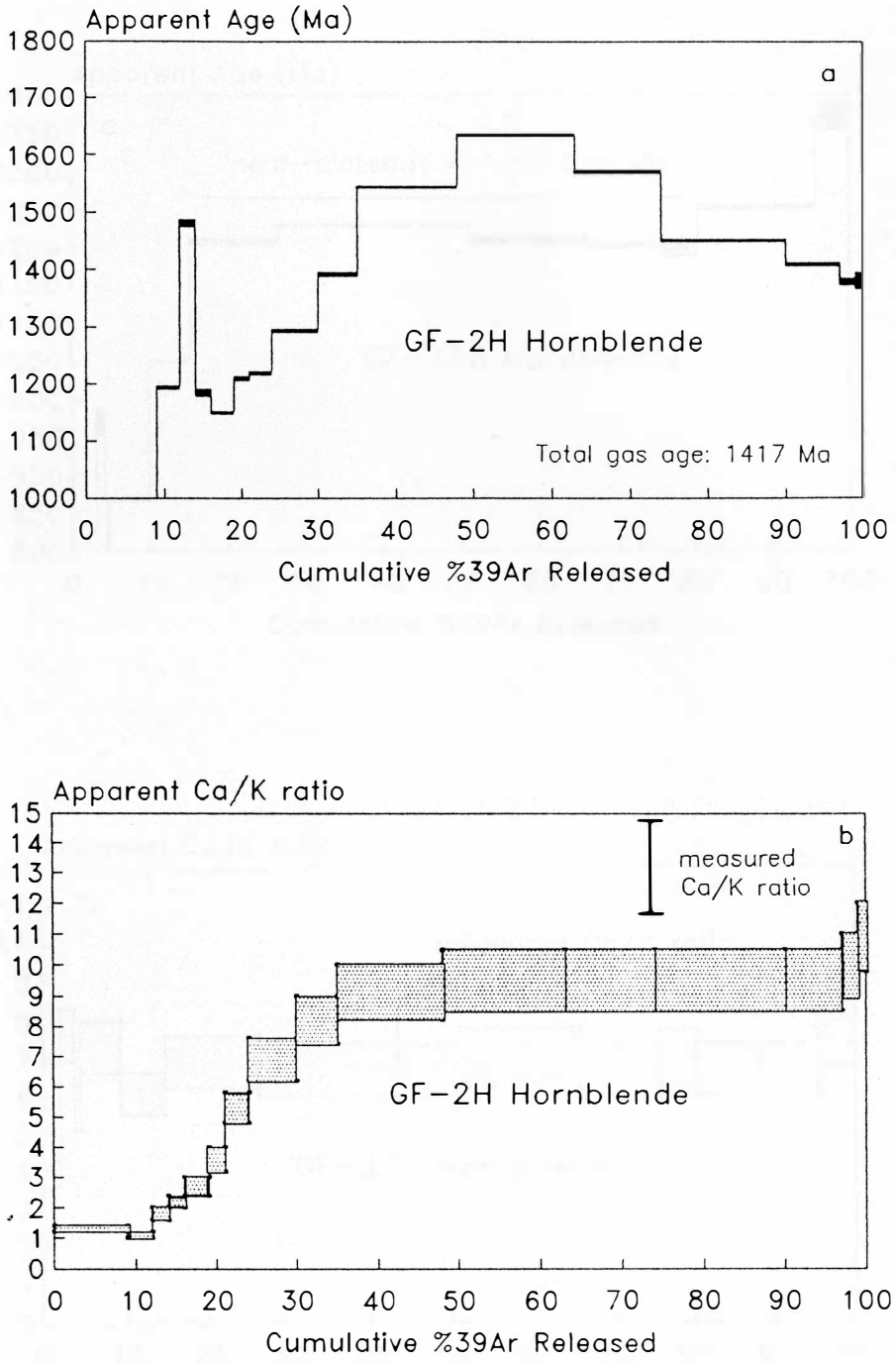

Fig. 7. $^{40}Ar/^{39}Ar$ apparent age spectrum and Ca/K ratio plot for GF-2H hornblende. a) Age spectrum. b) Ca/K ratio plot. The increase in apparent Ca/K ratios (stippled bars; 2σ errors) over the first 50% of cumulative gas released corresponds to an increase in step ages in the age spectrum. The last 50% of gas released has a consistent Ca/K ratio but is lower than the Ca/K ratio measured by electron microprobe (error bar; 2σ errors). This indicates contamination of the outgassed sample by a higher K or lower Ca phase, probably biotite.

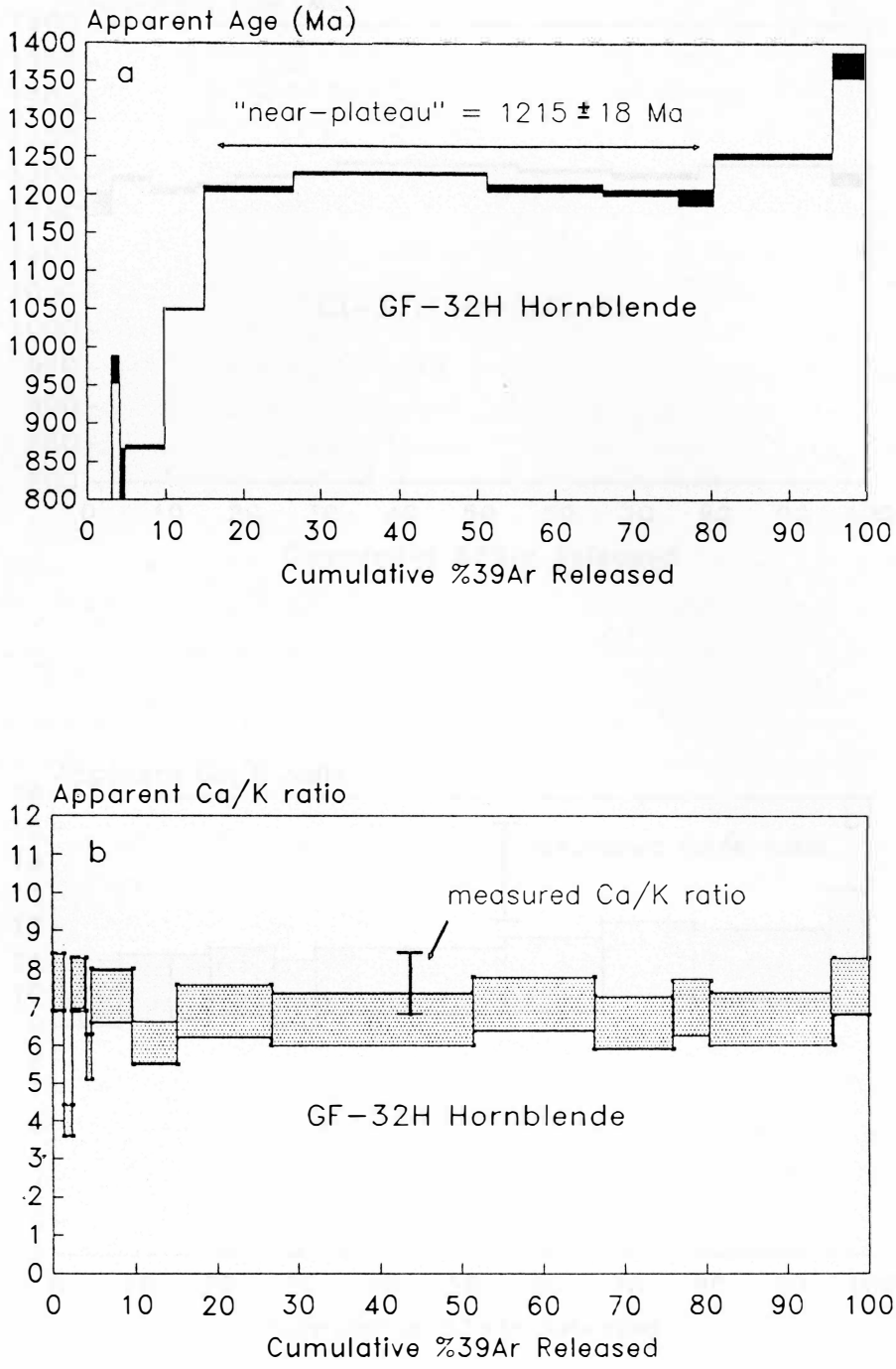

Fig. 8. $^{40}Ar/^{39}Ar$ apparent age spectrum and Ca/K ratio plot for GF-32H hornblende. a) Age spectrum. Five steps with fairly consistent apparent ages define a near-plateau. b) Ca/K ratio plot. The near-plateau in the age spectrum corresponds to consistent Ca/K step ratios which agree within error with the measured value. The first 17% of gas released has irregular Ca/K ratios, corresponding to irregular step ages.

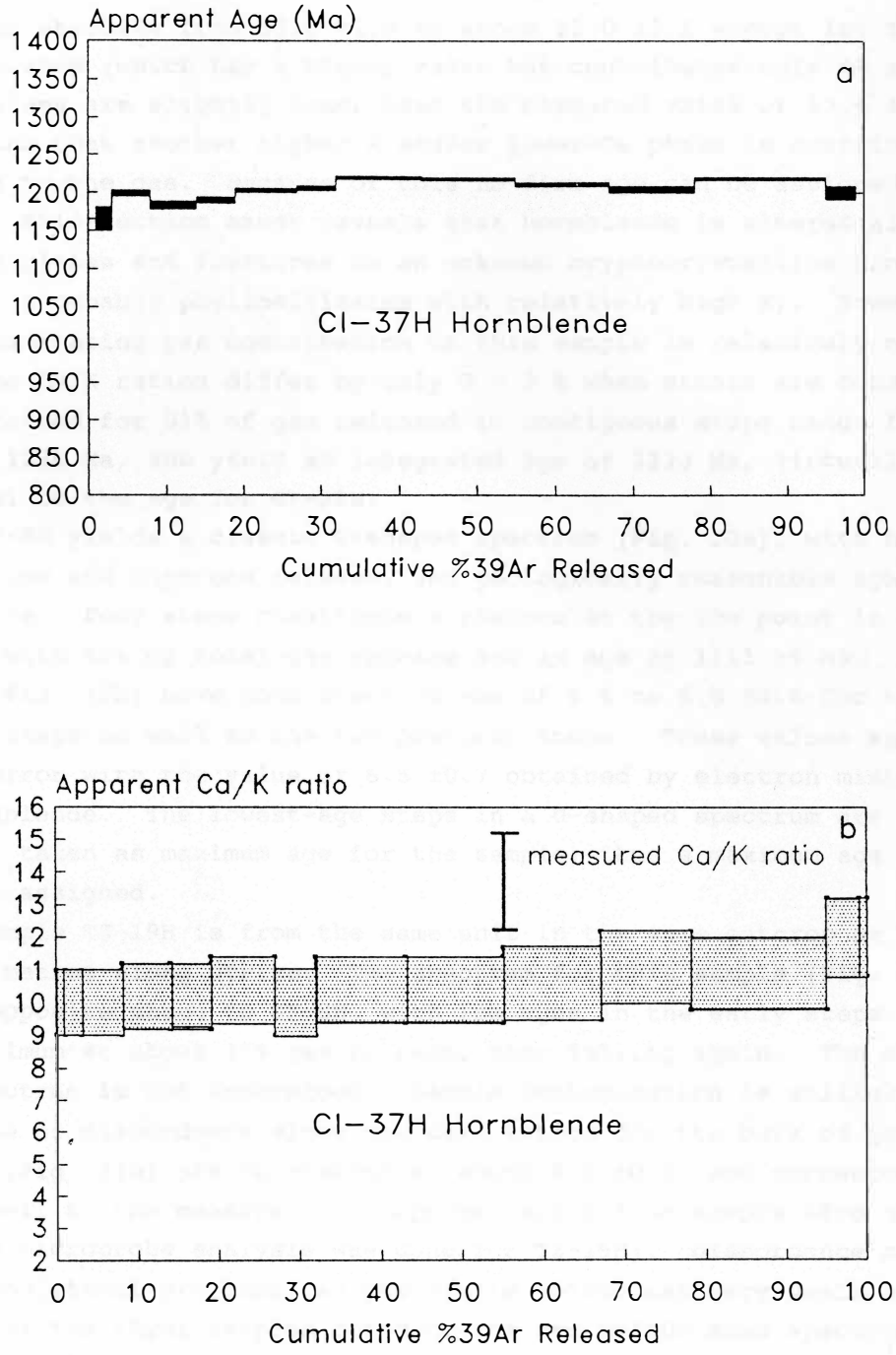

Fig. 9. $^{40}Ar/^{39}Ar$ apparent age spectrum and Ca/K ratio plots for CI-37H hornblende. a) Age spectrum. Step ages are very consistent, but fail to define a plateau. No age is assigned. b) Ca/K ratio plot. Ca/K step ratios are also consistent, but do not agree within 2σ error with the Ca/K ratio measured by electron microprobe. The difference is small, suggesting only slight contribution of gas from the contaminating phase.

9b) climb steadily from 10.0 ±1.0 to about 11.0 ±1.1 except for the last measured step (which has a higher value but contributes only 4% of gas). These values are slightly lower than the measured value of 13.6 ±1.4, indicating that another higher-K and/or lower-Ca phase is contributing slightly to the gas. Because of this no firm age can be assigned to the sample. Thin-section study reveals that hornblende is altered along cleavage planes and fractures to an unknown cryptocrystalline brown material (probably phyllosilicates with relatively high K). However, the contaminating gas contribution in this sample is relatively minor, since the Ca/K ratios differ by only 2 - 3 % when errors are considered. Ages obtained for 81% of gas released in contiguous steps range from 1200 to 1220 Ma, and yield an integrated age of 1213 Ma, virtually identical to the age for GF-32H.

GF-8H yields a classic U-shaped spectrum (Fig. 10a), with high ages at low and high gas release, and geologically reasonable ages in the centre. Four steps constitute a plateau at the low point in the saddle, with 50% of total gas release and an age of 1111 ±9 Ma. Ca/K ratios (Fig. 10b) have consistent values of 5.6 to 5.8 ±0.6 for the four plateau steps as well as the two previous steps. These values agree within error with the value of 6.5 ±0.7 obtained by electron microprobe for hornblende. The lowest-age steps in a U-shaped spectrum are normally taken as maximum age for the sample; thus a maximum age of 1111 ±9 Ma is assigned.

Sample TZ-19H is from the same unit in the same outcrop as GF-8H, about 7 metres along strike. The spectrum for this sample (Fig. 11a) is of the opposite shape to GF-8H, with low ages in the early steps, rising to a maximum at about 15% gas release, then falling again. The shape of this spectrum is not understood. Sample contamination is unlikely to be the cause of discordance since the Ca/K ratios for the bulk of gas release (Fig. 11b) are consistent at about 8.0 ±0.8, and correspond fairly well to the measured (microprobe) value from sample GF-8 of 6.5 ±0.7 (no microprobe analysis was done for TZ-19H). Discordance may be due to analytical problems, as the sample volume was very small and it was one of the first samples dated on the new VG3600 mass spectrometer when sample line blanks were virtually unknown. Alternatively, the drop in ages at high temperature may have a geological explanation such as post-closure deformation inducing partial outgassing of sites which are retentive of Ar under laboratory conditions (e.g. Maluski 1978). The sample is highly strained (see Appendix B) but the timing of this relative to last metamorphism is not certain. The maximum age of 956 ±6.2 Ma and the age of the largest step of 888 Ma are both unreasonable when compared to other nearby samples (CI-19H, GF-34H, GF-35H,

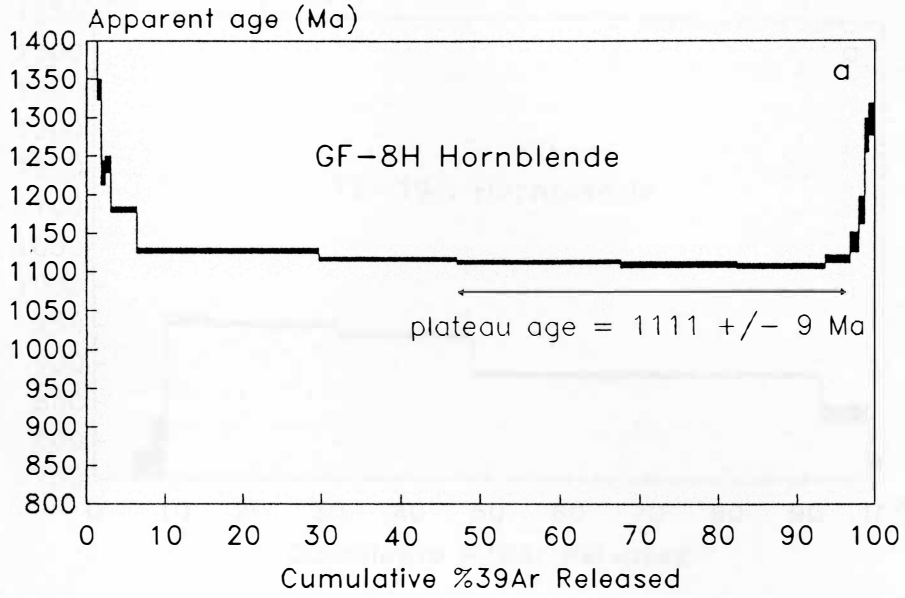

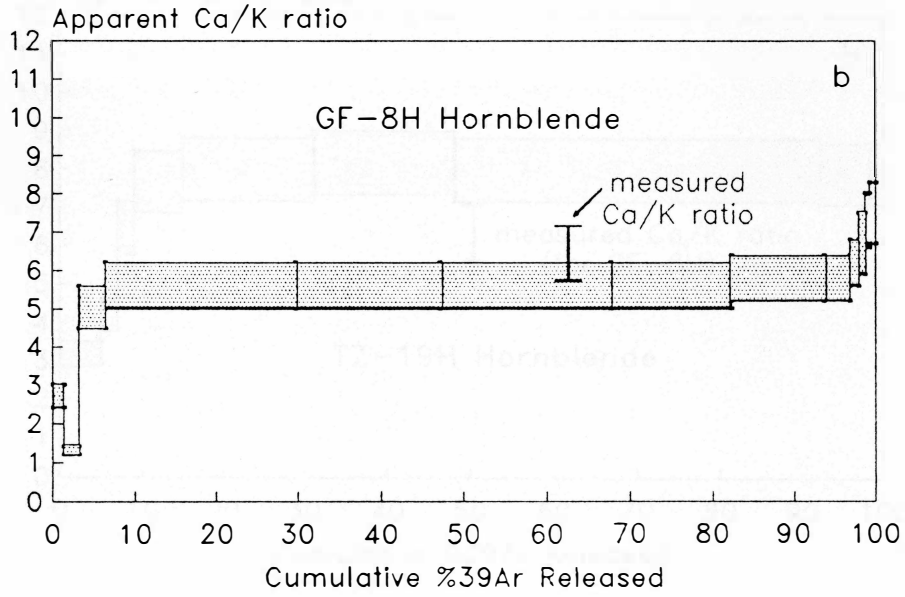

Fig. 10. $^{40}Ar/^{39}Ar$ apparent age spectrum and Ca/K ratio plot for GF-8H hornblende. a) Age spectrum. The spectrum has a classic U-shape, demonstrating contamination by excess Ar. The four lowest-age steps constitute a plateau, which defines the maximum age of the sample. b) Ca/K ratio plot. The step ratios are mutually consistent, and are consistent with the measured value within 2σ error.

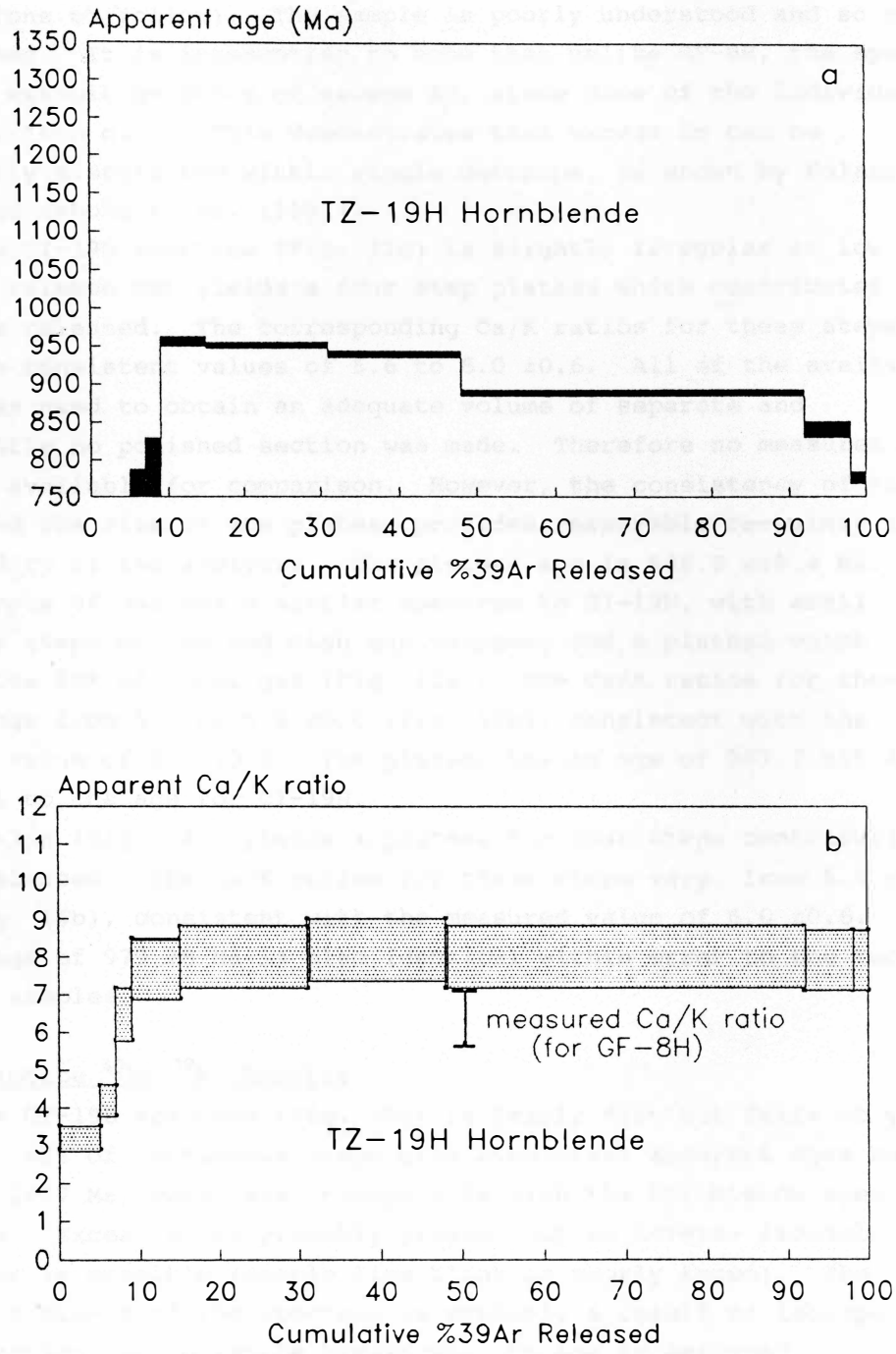

Fig. 11. $^{40}Ar/^{39}Ar$ apparent age spectrum and Ca/K ratio plot for TZ-19H hornblende. a) Age spectrum. The spectrum is complex and is poorly understood. No age is assigned. b) Ca/K ratio plot. The step values are consistent and are roughly consistent with the measured Ca/K ratio for GF-8H, which was taken from the same outcrop. Sample contamination is probably not the cause of the discordant age spectrum.

descriptions to follow). The sample is poorly understood and so no age is assigned. It is interesting to note that unlike GF-8H, the spectrum does not exhibit evidence of excess Ar, since none of the individual steps are "too old". This demonstrates that excess Ar can be irregularly distributed within single outcrops, as shown by Foland (1979) and Maboko et al. (1991).

The CI-19H spectrum (Fig. 12a) is slightly irregular at low and high gas release but yields a four step plateau which contributes 78% of total gas released. The corresponding Ca/K ratios for these steps (Fig. 12b) give consistent values of 5.6 to 6.0 ±0.6. All of the available sample was used to obtain an adequate volume of separate and consequently no polished section was made. Therefore no measured Ca/K value is available for comparison. However, the consistency of the ratios and the size of the plateau provides reasonable certainty about the validity of the analysis. The plateau age is 988.0 ±18.4 Ma.

Sample GF-34H has a similar spectrum to CI-19H, with small, irregular steps at low and high gas volumes, and a plateau which contributes 58% of total gas (Fig. 13a). The Ca/K ratios for these steps range from 5.6 to 5.8 ±0.6 (Fig. 13b), consistent with the measured value of 6.3 ±0.6. The plateau has an age of 987.7 ±15.4 Ma, identical to the age for CI-19H.

GF-35H (Fig. 14a) yields a plateau for four steps contributing 92% of gas released. The Ca/K ratios for these steps vary from 5.5 to 5.6 ±0.6 (Fig. 14b), consistent with the measured value of 6.0 ±0.6. The plateau age of 979 ±8 Ma is also identical within error to the two previous samples.

3.3.3 Biotite $^{40}Ar/^{39}Ar$ Results

The GF-19B spectrum (Fig. 15a) is fairly flat but fails to yield a plateau. 62% of contiguous steps give consistent apparent ages between 1246 and 1257 Ma, which are incompatible with the hornblende ages from this area. Excess Ar is probably present but no inverse isochron correction is possible (sample line blank is poorly known). The relative flatness of the spectrum is probably a result of isotope homogenization due to sample breakdown. No age is assigned.

GF-7B has a relatively flat spectrum (Fig. 15b) with apparent ages in the range 1020 - 1035 Ma, but fails to yield a plateau. One step in the middle has an anomalously high age relative to other steps. This form of spectrum has been observed by other workers and is attributed to the presence of minute alteration zones of chlorite along cleavage planes in biotite (Hess and Lippolt, 1986; Lo and Onstott, 1989). These have not been observed in this sample, but may be cryptocrystalline and

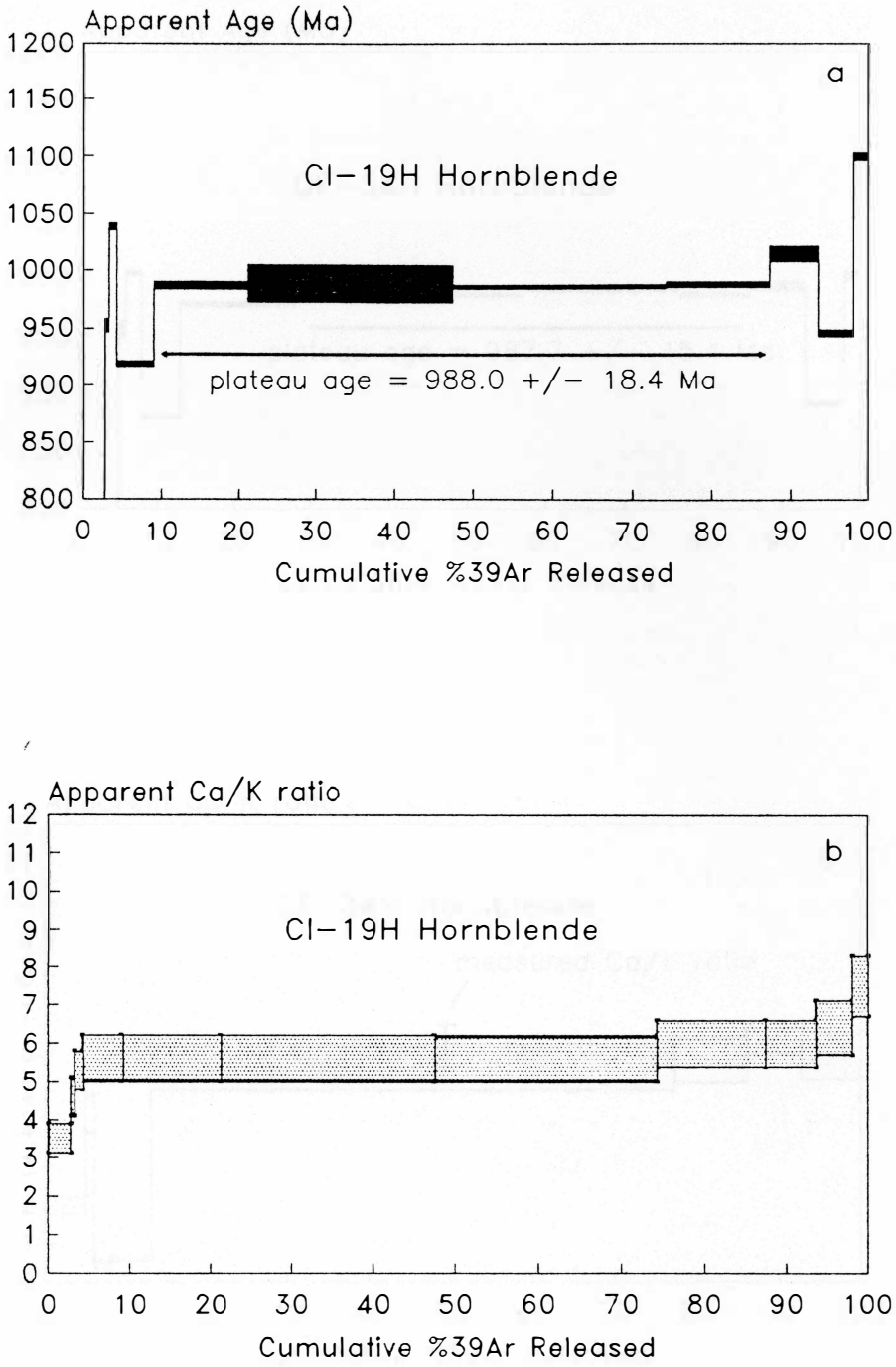

Fig. 12. $^{40}Ar/^{39}Ar$ apparent age spectrum and Ca/K ratio plot for CI-19H hornblende. a) Age spectrum. The spectrum yields a 4-step plateau contributing 78% of total gas. b) Ca/K ratio plot. Step ages are consistent over the range of the plateau in the spectrum. Ca/K ratio was not measured by electron microprobe for this sample.

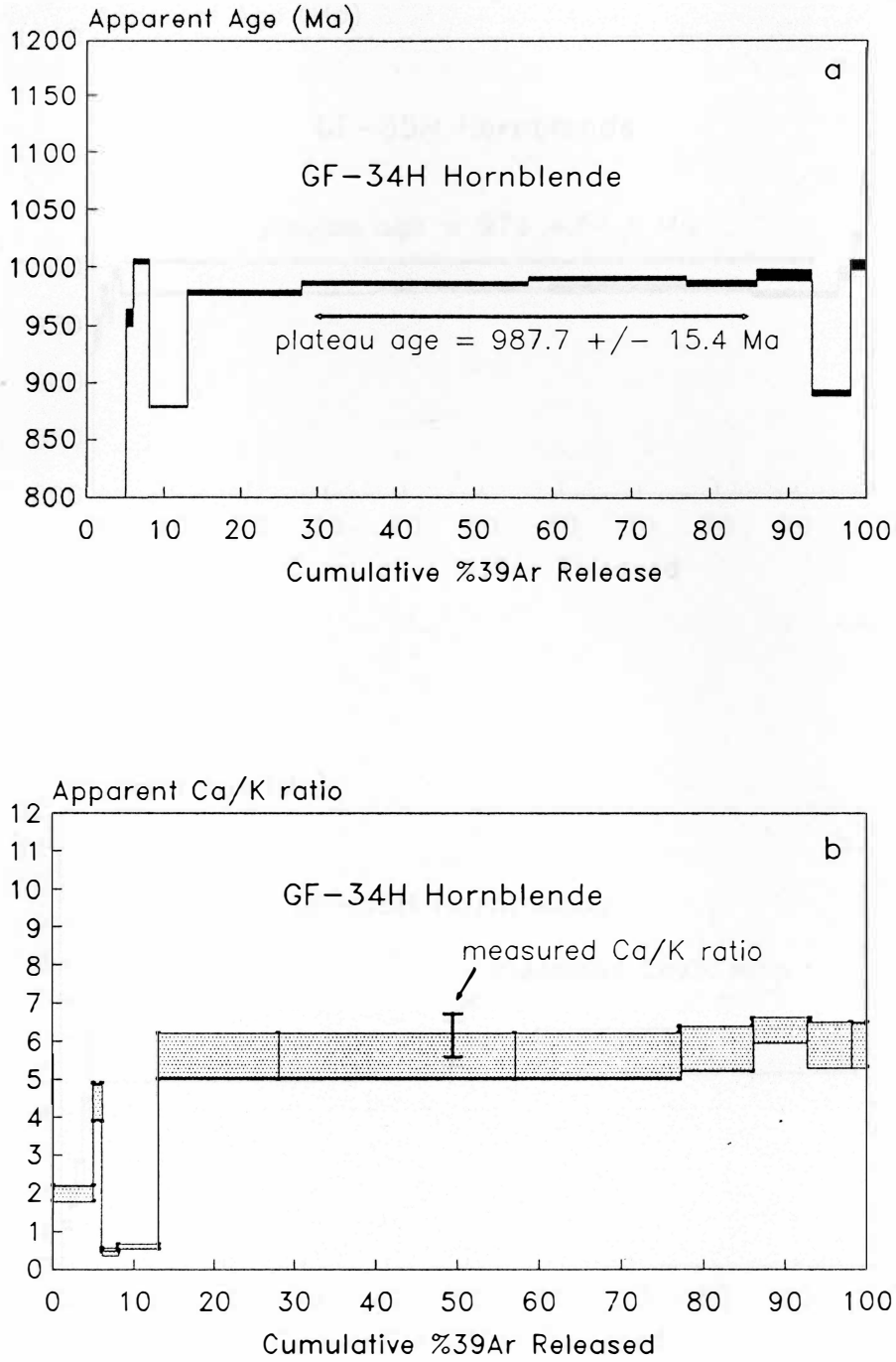

Fig. 13. $^{40}Ar/^{39}Ar$ apparent age spectrum and Ca/K ratio plot for GF-34H hornblende. a) Age spectrum. Three steps make up a plateau contributing 58% of total gas. Note the nearly identical age of this plateau with that of CI-19H (Fig. 12a). b) Ca/K ratio plot. The steps which constitute the age plateau have mutually consistent Ca/K ratios and are consistent with the measured value.

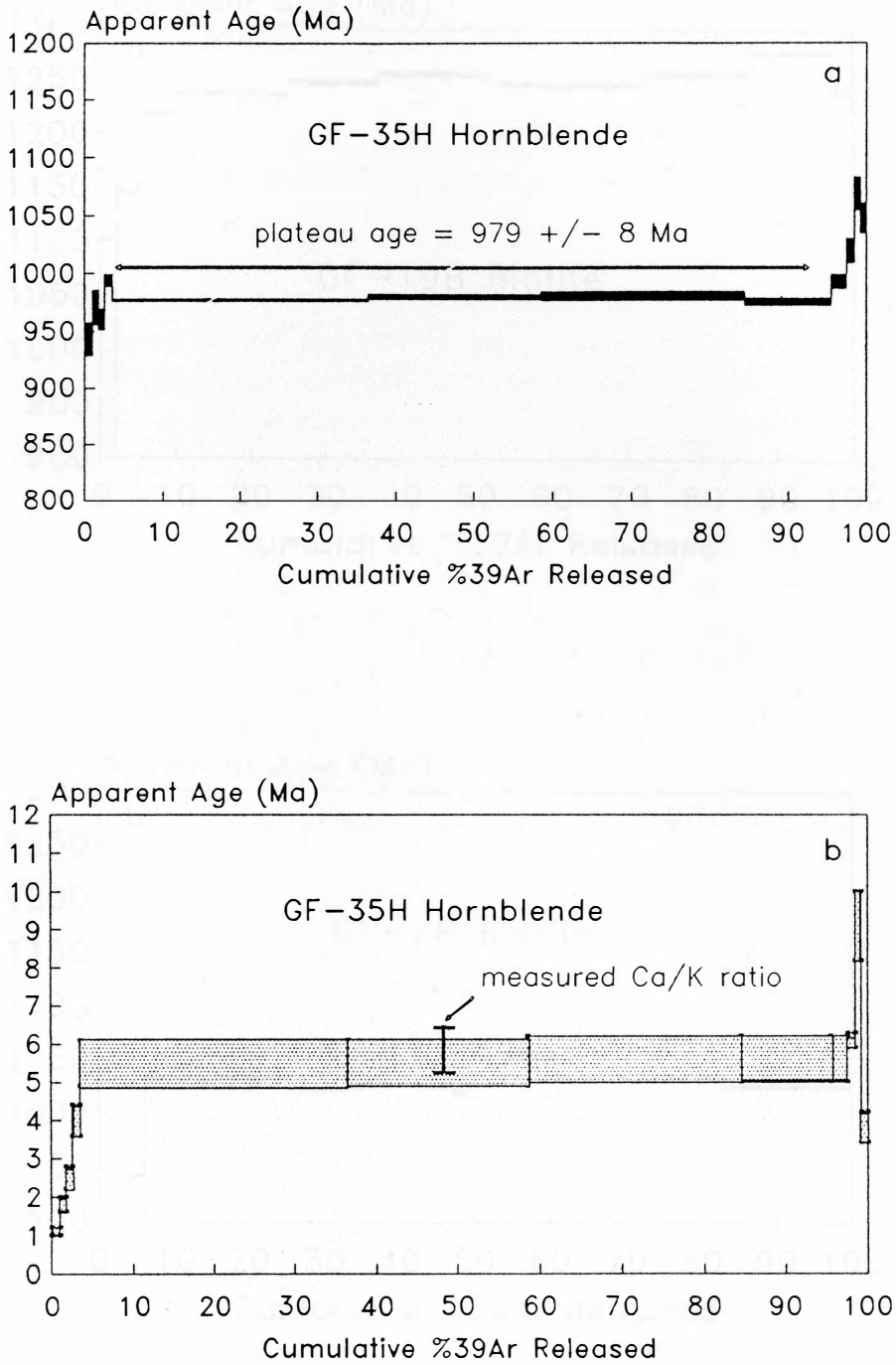

Fig. 14. $^{40}Ar/^{39}Ar$ apparent age spectrum and Ca/K ratio plot for GF-35H hornblende. a) Age spectrum. Four steps define a plateau which contributes 92% of total gas. b) Ca/K ratio plot. The same four steps have mutually consistent Ca/K ratios which are consistent with the measured value.

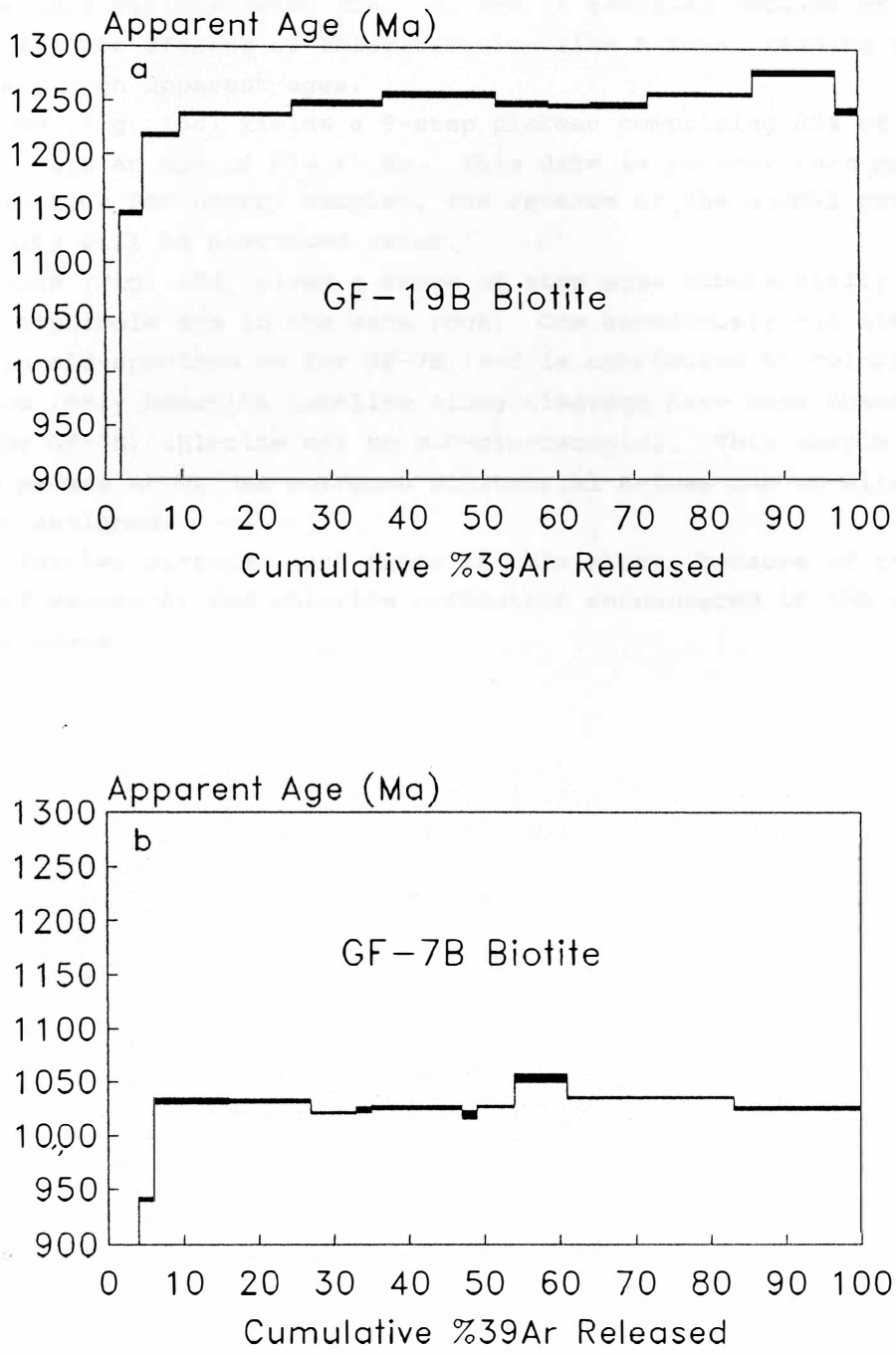

Fig. 15. $^{40}Ar/^{39}Ar$ apparent age spectra for biotites. a) GF-19B age spectrum. The spectrum is irregular and the step ages are older than for nearby hornblende. Excess Ar is present. b) GF-7B age spectrum. No plateau is defined but step ages are roughly consistent at about 1030 to 1040 Ma. The single older step at about 55 to 60% gas release suggests the biotite is altered slightly to chlorite. See text for explanation.

therefore only visible using TEM. No age is assigned because of possible further effects of chloritization like K-loss, leading to excessively high apparent ages.

GF-8B (Fig. 15c) yields a 9-step plateau comprising 83% of gas released, with an age of 954 ±7 Ma. This date is younger than maximum K-feldspar ages for nearby samples, the reverse of the normal pattern. Its validity will be discussed later.

GF-35B (Fig. 15d) gives a range of step ages substantially older than the amphibole age in the same rock. One anomalously old step is present in mid-spectrum as for GF-7B, and is attributed to chlorite alteration (only hematite lamellae along cleavage have been observed, but as for GF-7B, chlorite may be sub-microscopic). This sample either contains excess Ar or has suffered substantial K-loss due to alteration; no age is assigned.

No further biotites were dated in this study, because of the problem of excess Ar and chlorite alteration encountered in the samples described above.

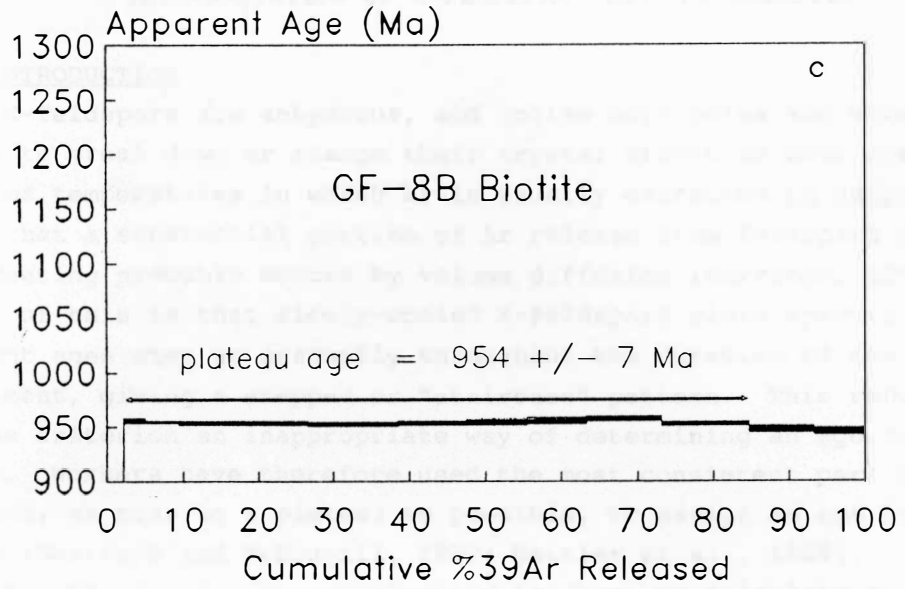

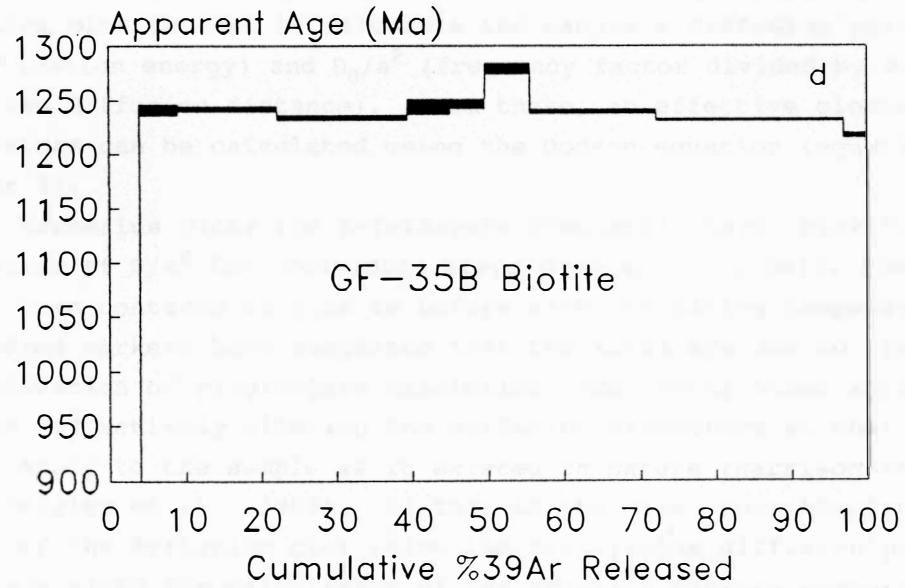

Fig. 15 cont'd. c) GF-8B biotite $^{40}Ar/^{39}Ar$ apparent age spectrum. A 9-step plateau is present contributing 83% of gas released. d) GF-35B biotite. The step ages are about 270 m.y. older than hornblende in the same rock. Chlorite alteration (K-loss) may be indicated by the single, higher-age step at about 50 to 55% cumulative gas released; excess Ar is probably present.

CHAPTER IV
INTERPRETATION OF K-FELDSPAR $^{40}Ar/^{39}Ar$ RESULTS

4.1 INTRODUCTION

K-feldspars are anhydrous, and unlike amphiboles and micas, do not appear to break down or change their crystal structure over most of the range of temperatures in which Ar is usually extracted in vacuo. This means that a substantial portion of Ar release from feldspars during step-heating probably occurs by volume diffusion (Harrison, 1990). One result of this is that slowly-cooled K-feldspars yield spectra in which apparent ages step up gradually throughout the duration of the experiment, giving a stepped or "staircase" pattern. This renders the plateau criterion an inappropriate way of determining an age for the sample. Workers have therefore used the most consistent part of the spectrum, as near to a plateau as possible, to assign an age to the sample (Harrison and McDougall, 1982; Heizler et al., 1988).

For these ages, recent practice has been to calculate a closure temperature based on diffusion information available in step-heating experiments, using the method advanced by Berger and York (1981) (see Appendix E, part 1). Arrhenius plots are constructed based on the step-heating data for ^{39}Ar. The line ideally defined by data on the Arrhenius plot is used to calculate the sample's diffusion parameters, E_a (activation energy) and D_0/a^2 (frequency factor divided by square of effective diffusion distance). From these, an effective closure temperature can be calculated using the Dodson equation (equation (1), Chapter 3).

Arrhenius plots for K-feldspars frequently have "kinks", at which the values of D/a^2 for individual steps drop abruptly below the previous trend, then continue to rise as before with increasing temperature (Fig. 16). Some workers have suggested that the kinks are due to the re-homogenization of plagioclase exsolution lamellae or other structural changes, effectively altering the diffusion parameters so that they no longer apply to the sample as it existed in nature (Harrison et al., 1986; Heizler et al., 1988). If this is the case, only the linear, low-T part of the Arrhenius plot below the kink yields diffusion parameters which are valid for calculation of the sample's closure temperature (Harrison and McDougall, 1982; Zeitler, 1988b). Closure temperatures calculated in the past using this assumption are in the range of 125°C to 185°C for microcline and up to 315°C for orthoclase (Harrison and McDougall, 1982; Heizler et al., 1988).

More recent work suggests that the kinks need not necessarily be explained by exsolution lamellae re-homogenization. Inconsistencies are

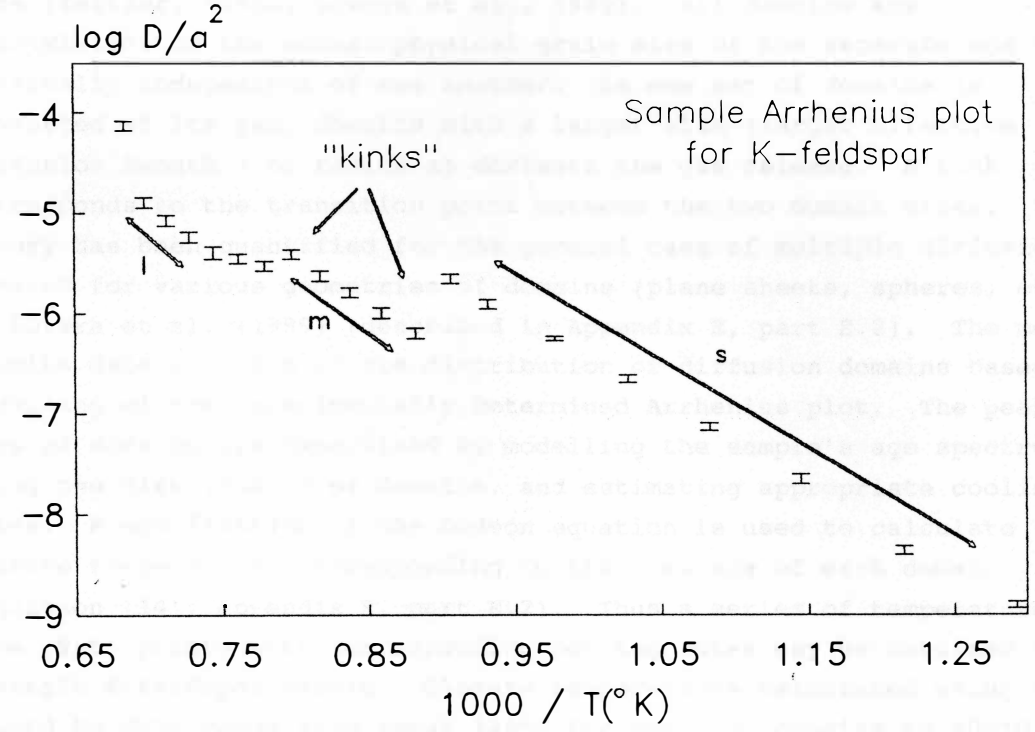

Fig. 16. Typical Arrhenius plot for K-feldspar (error bars). The slope of the segment marked s, to the right of the first "kink", can be used to determine E_a, the activation energy of diffusion of Ar; the y-intercept of this segment has been used by some workers to define D_0/a^2, the frequency factor divided by the square of the effective diffusion radius, for the whole sample. This is based on the premise that a "kink" corresponds to a breakdown of the sample's structure once furnace temperature is high enough, so that only the first segment describes the true diffusion behaviour of the sample. New work suggests that kinks may be due to the existence of more than one effective diffusion domain size, a. The three segments marked s, m, and l then correspond to temperature ranges in which gas derived from small, medium and large domains dominate the gas release. In this case, determination of D_0/a^2 requires modelling of the domain distribution.

found between cooling rates calculated using only the low-T segment of the Arrhenius plot to determine T_c, and the (mathematically predictable) shape of age spectra expected for such rates (Lovera et al., 1989). An alternate explanation for kinks which appears to provide internally consistent cooling histories is to assume that the sample is made up of "diffusion domains" of several different sizes, rather than a single size (Zeitler, 1988a; Lovera et al., 1989). All domains are subdivisions of the actual physical grain size of the separate and are physically independent of one another. As one set of domains is exhausted of its gas, domains with a larger size (larger effective diffusion length l or radius a) dominate the gas release. A kink corresponds to the transition point between the two domain sizes. This theory has been quantified for the general case of multiple diffusion domains for various geometries of domains (plane sheets, spheres, etc.), by Lovera et al. (1989) (described in Appendix E, part E.2). The method permits determination of the distribution of diffusion domains based on modelling of the experimentally determined Arrhenius plot. The peak ages of domains are determined by modelling the sample's age spectrum using the distribution of domains, and estimating appropriate cooling rates. A modification of the Dodson equation is used to calculate closure temperatures corresponding to the peak age of each domain (equation (14), Appendix E, part E.2). Thus a series of temperature-time (T-t) points with corresponding cooling rates may be obtained from a single K-feldspar sample. Closure temperatures calculated using this method to date range from about 125°C for smallest domains to 400°C for the largest domains, depending on cooling rates (Harrison, 1990; Foster et al., 1990).

Whether this theory correctly describes Ar diffusion in K-feldspars is still a matter of debate. Some authors insist that changes occur in K-feldspars at low-T conditions in nature, such as development of micropores (Parsons et al., 1988, 1991) or other sub-solidus reactions, which cause activation energy (E_a) of argon release during low temperatures of step-heating to be unrelated to the diffusive behaviour of argon during the sample's cooling history (Villa 1988, 1991). These arguments are countered by evidence that the "small" domains do not change their physical structure on normal step-heating (Lovera et al., 1991a), and by the contention that samples which have such characteristics are specific examples of non-ideal K-feldspars and are not typical of all samples (Harrison, 1990). However, the best test of the validity of the multiple diffusion domain theory is to determine if consistent results are obtained by applying it, and some success has been achieved to date (Lovera et al., 1989; Richter et al., 1991;

Schärer et al., 1990; Harrison, 1990).

All K-feldspars dated in this study have had diffusion experiments conducted on them, the results of which are presented below in conjunction with their spectra. Where possible, Arrhenius plots and age spectra have been modelled to determine apparent diffusion domain size distributions and thereby to calculate several T-t points.

Two points should be made here regarding the modelling. First, some workers have established the practice of modelling orthoclase using a spherical geometry to describe domains, and microcline using a plane-sheet geometry. This is based on the observation that in microcline, experimentally calculated effective diffusion distances are often on the order of the spacing between nearly ubiquitous albite exsolution lamellae. Orthoclase is more often non-perthitic and spherical geometry is seen as better describing its diffusion behaviour (Harrison and McDougall, 1982; Heizler et al., 1988; Lovera et al., 1989). However, mineralogists insist that exsolution lamellae boundaries are largely coherent and are therefore not likely to act as routes for escape of Ar (Parsons et al., 1988, 1991). No convincing evidence has yet been presented to demonstrate that any particular geometry accurately describes the reservoirs out of which argon diffuses. As using different geometries to model different kinds of K-feldspars may introduce an unjustifiable bias between samples in the calculated diffusion parameters, a single geometry was used in this study regardless of the presence or absence of optically visible exsolution lamellae. A spherical geometry was selected for modelling. Where evidence is available that a different geometry would be more appropriate, it has been noted.

Secondly, the step-heating schedules used in this study were in some cases not ideal for determining Arrhenius parameters. Samples dated on the MS-10 system could only be heated to a maximum of 1150°C, and a few were heated only to lower temperatures. In other samples, substantial volumes of gas were obtained above 1150°C. The D/a^2 value for each individual step is a direct function of the fraction of total gas it represents (see Appendix E, equation (11)). If the total gas is underdetermined because the sample is not fully outgassed, the apparent D/a^2 terms and consequently the D_0/a^2 for each domain will be overestimated, yielding artificially low T_c's. Thus the data obtained for samples that were not fully outgassed cannot be used to reliably determine closure temperatures.

Some of the samples initially dated on the MS10 system were transferred for complete outgassing to the high-temperature furnace attached to the VG3600. No comparison of voltage recorded on the mass

spectrometer analysis system versus actual volume of gas is available between the two systems, so comparing measured voltages is not a satisfactory way to determine relative volume of steps. An approximation of percent of total gas released in each step has been made in the Data Summary Tables in Appendix C, based on release patterns for samples which were completely outgassed on the VG3600 system. These data are used to plot the age spectra, but the estimation is insufficiently precise for production of reliable Arrhenius plots.

Finally, those samples which were completely outgassed in the high-temperature furnace were heated with relatively coarse schedules. This was done because they were among the first samples dated on the new VG3600 mass spectrometer and heating steps were made large in order to ensure adequate gas volume. As a result, limited numbers of points define the slope of segments of the Arrhenius plots, leading to uncertainty in the calculated activation energy, E_a. However, the plots are well-enough defined to permit complete modelling of several samples and to make a "first-pass" attempt at defining cooling histories. The question of whether this process is more satisfactory than using estimated closure temperatures, or assigning T_c's for "plateau" ages based on the low-T gas release, will be addressed later in the context of the results from this study. The results as they were acquired are described below. Errors quoted on model closure temperatures consider only the uncertainty in the activation energy defined by the Arrhenius plot; errors on both T_c and E_a are quoted at 2σ. Errors quoted (2σ) on model ages consider errors in J only.

4.2 K-FELDSPAR $^{40}Ar/^{39}Ar$ RESULTS

GF-42K (Fig. 17a) is a highly perthitic microcline from the Killarney Complex. It was step-heated only to 900°C, which is insufficient to fully outgas the sample. (The sample was discarded accidentally before outgassing was completed on the high-temperature furnace). Based on the release pattern of sample GF-62K, a similar perthitic microcline outgassed with the same heating schedule (described below), the gas obtained by 900°C represents less than 56% of the total gas available in the sample. The calculation of the Arrhenius plot depends on the total gas present, so a reliable set of parameters cannot be determined. The age spectrum is also of little use since the characteristic pattern of increases in step age continues well beyond 900°C outgassing for most K-feldspars. However, this characteristic permits assignation of a <u>minimum</u> age of 886 ±26 Ma. A corresponding closure temperature of 200 ±75°C is realistic considering typical values obtained in other studies for perthitic microcline (Lovera et al.,

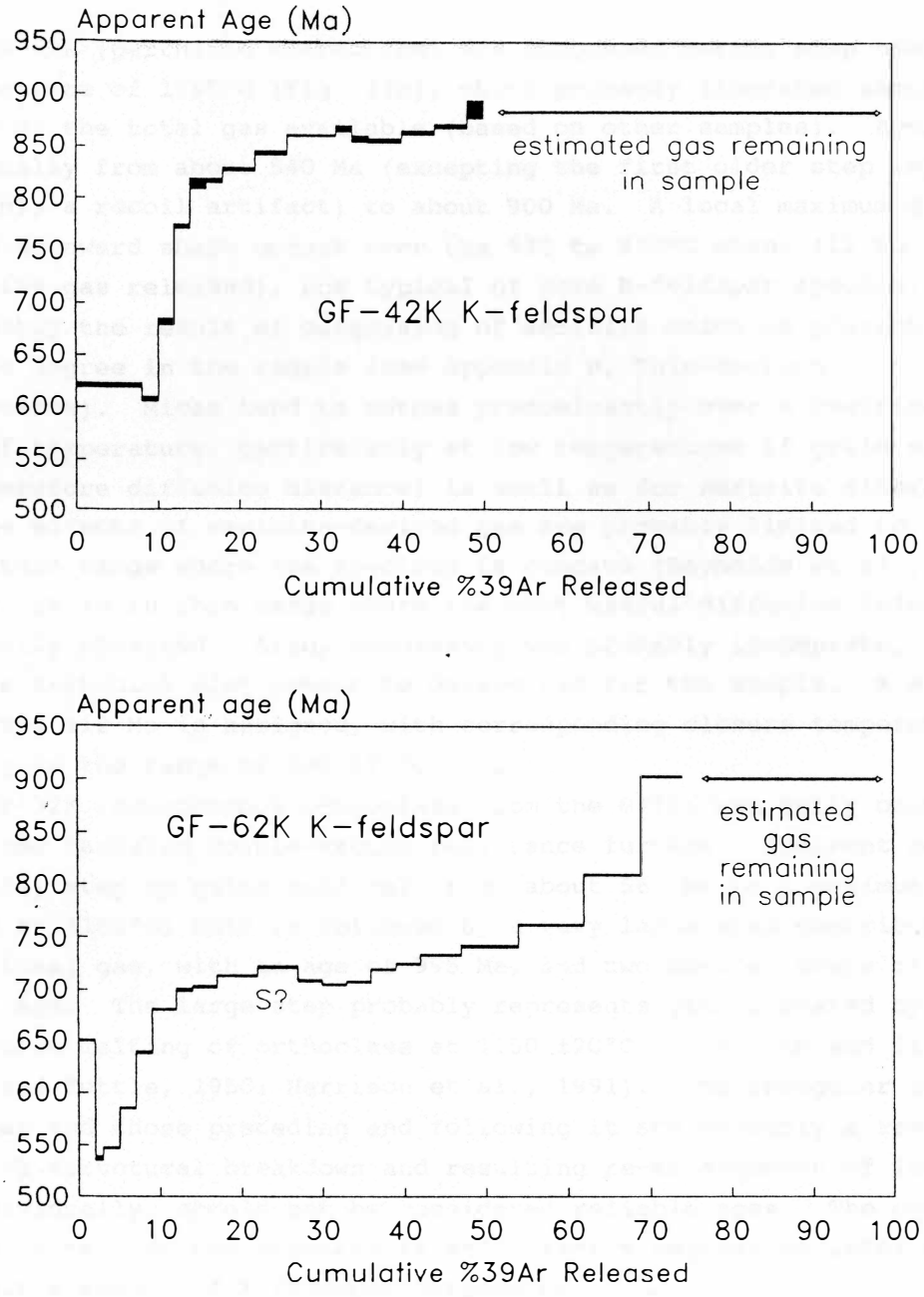

Fig. 17. Approximate $^{40}Ar/^{39}Ar$ apparent age spectra for GF-42K and GF-62K K-feldspar. a) GF-42K age spectrum. The sample was heated only to 900°C which is insufficient to fully outgas K-feldspar. The amount of gas remaining has been estimated to plot the spectrum. b) GF-62K age spectrum. The sample was heated to 1150°C which may be insufficient to fully outgas it. The remaining gas has been estimated to plot the spectrum. The concave-downward shape over 12 to 33% cumulative gas release (denoted S?) may be a result of outgassing of sericite.

1989).

GF-62K (perthitic microcline) was outgassed during step heating to a temperature of 1150°C (Fig. 17b), which probably liberated about 75% or more of the total gas available (based on other samples). Ages step up gradually from about 540 Ma (excepting the first older step which is presumably a recoil artifact) to about 900 Ma. A local maximum giving a concave-downward shape occurs over the 630 to 810°C steps (12 to 33% of cumulative gas released), not typical of pure K-feldspar spectra. This is probably the result of outgassing of sericite which is present to a moderate degree in the sample (see Appendix B, Thin-Section Descriptions). Micas tend to outgas predominantly over a restricted range of temperature, particularly at low temperatures if grain size (and therefore diffusion distance) is small as for sericite alteration. Thus the effects of sericite-derived gas are probably limited to the temperature range where the spectrum is concave (Reynolds et al., 1987). However, it is in this range where the most useful diffusion information is normally obtained. Also, outgassing was probably incomplete, so a reliable Arrhenius plot cannot be determined for the sample. A minimum age of 903 ±12 Ma is assigned, with corresponding closure temperature probably in the range of 200 ±75°C.

GF-32K (homogeneous orthoclase from the GFTZ) was fully outgassed in the new tantalum double-vacuum resistance furnace. Apparent ages (Fig. 18a) step up quite uniformly from about 560 Ma to a maximum of 1057 Ma at 1160°C; this is followed by a very large step contributing 26% of total gas, with an age of 995 Ma, and two smaller steps of similar age. The large step probably represents gas liberated by the incongruent melting of orthoclase at 1150 ±20°C to leucite and liquid (Bowen and Tuttle, 1950; Harrison et al., 1991). The irregular ages of this step and those preceding and following it are probably a result of incipient structural breakdown and resulting re-arrangement of isotopes, and individually, should not be considered reliable ages. The overall stepped pattern of the spectrum is sufficiently regular to infer that it is purely a result of K-feldspar outgassing.

The low-temperature-release part of the age spectrum shows a trend towards an age of about 600 Ma, observed in several other K-feldspar samples from this study as well. In GF-32K only a small volume of gas gives this age, with the 650°C and 700°C steps, representing 5% of gas, having a mean age of 598 Ma. This is probably due to slight radiogenic gas loss from the feldspar due to intrusion of the Grenville dike along Collins Inlet (section 1.4, Geology of the Study Area). The age of Grenville dikes has been estimated at 575 Ma (Fahrig and West, 1986), based on K-Ar whole-rock determinations. The predominance in the early

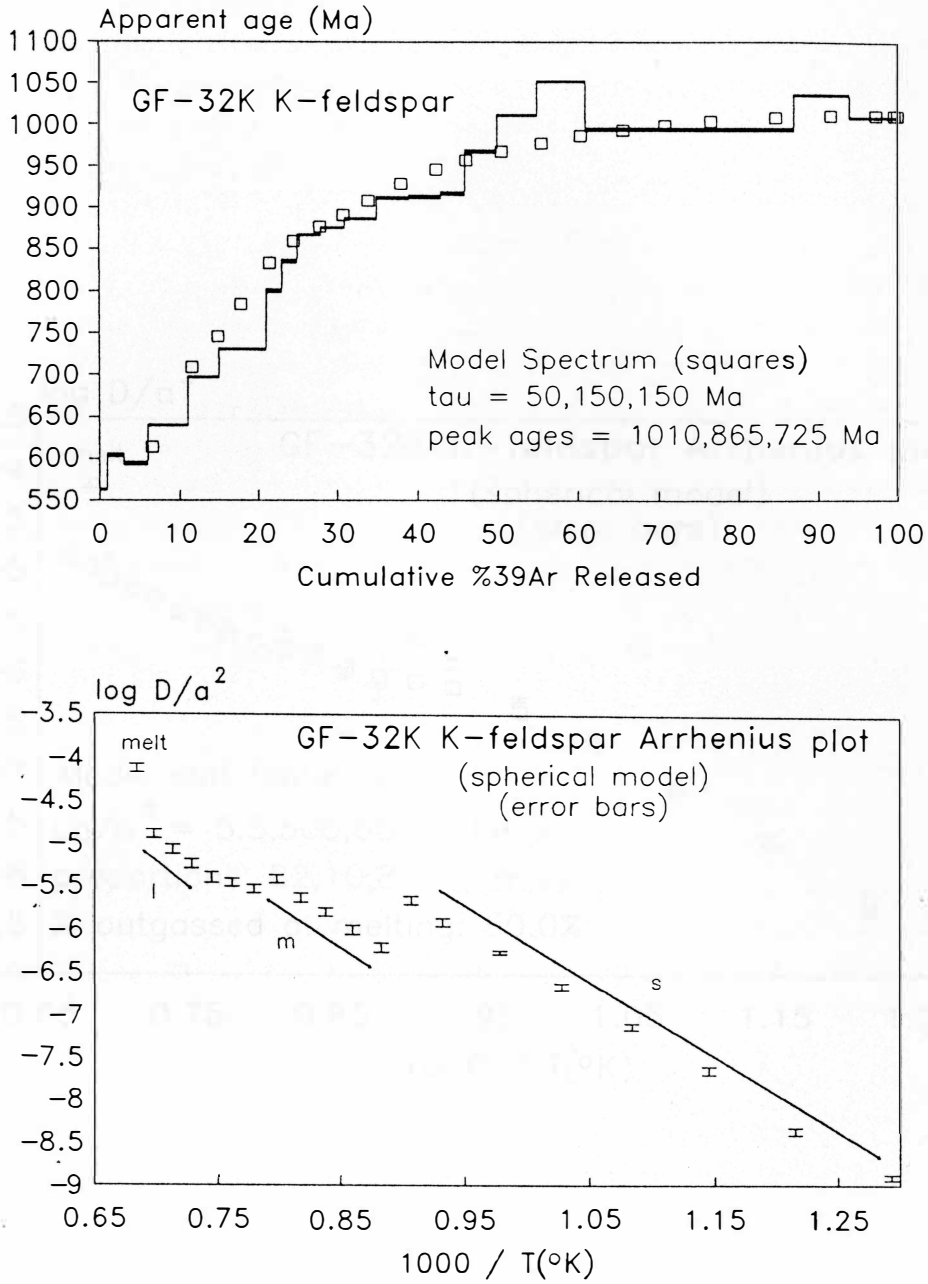

Fig. 18. GF-32K K-feldspar $^{40}Ar/^{39}Ar$ apparent age spectrum and Arrhenius plot, with models. a) Observed age spectrum (bars) and model age spectrum (squares). The large single step at 61 to 87% cumulative gas released is due to incongruent melting of the sample. Parameters used in the model, tau (τ) and the model peak ages, are noted. The model fails to fit the observed spectrum at 22 to 25% and 37 to 47% cumulative gas released. See text for description and explanation. b) Observed Arrhenius plot. The approximate ranges where small (s), medium (m) and large (l) domains appear to dominate gas release are noted, as is the point resulting from incongruent melting.

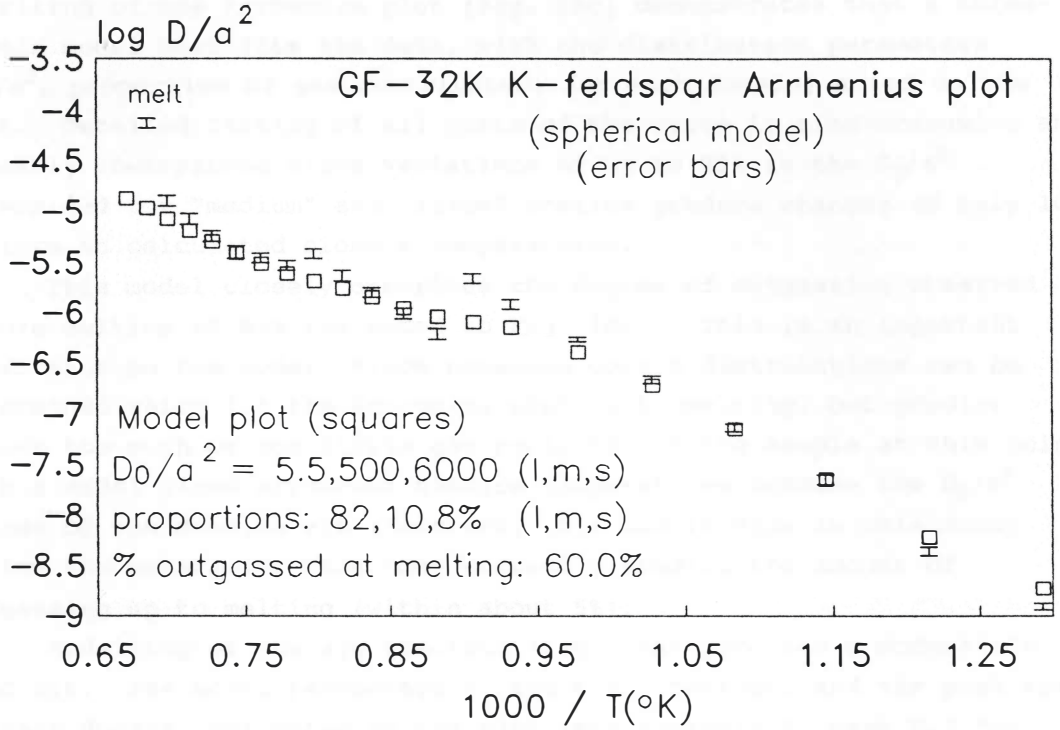

Fig. 18, cont'd. c) Observed Arrhenius plot (error bars) with model (squares) superimposed, for GF-32K K-feldspar. The model fits "small" domains well but does not match the kinks or the slope of the medium and large domain segments. This probably causes the divergence between the observed and model age spectrum in the corresponding ranges of cumulative gas release as noted in a).

release parts of these K-feldspar age spectra (see results below) of plateau-like features at a mean age of about 600 Ma suggests the previous estimate is slightly too young. A few small steps in GF-32K at lower release temperatures, with younger ages, may represent post-intrusion cooling ages or recoil effects.

The Arrhenius plot (Fig. 18b) is very regular, with three well-defined, sub-parallel segments. Linear regression using the method of York (1969) defines a well-constrained line (SUMS / n-2 = .081) through eight points of the lower segment, giving an E_a of 38.6 ±1.0 kcal/mol. Modelling of the Arrhenius plot (Fig. 18c) demonstrates that a three-domain model best fits the data, with the distribution parameters (D_0/a^2, proportion of gas contributed, for each domain) noted on the plot. Detailed fitting of all parts of the curve is time-consuming and probably unwarranted since variations of up to 25% in the D_0/a^2 determined for "medium" and "large" domains produce changes of only 10°C or less in calculated closure temperatures.

This model closely describes the degree of outgassing observed before melting of 61% (as noted in Fig. 18c). This is an important constraint on the model, since numerous domain distributions can be determined which fit the Arrhenius plot up to melting, but predict either too much or too little gas remaining in the sample at this point. Such a model gives erroneous closure temperatures because the D_0/a^2 values of the domains are incorrect. All models made in this study follow the constraint that they correctly predict the amount of outgassing up to melting (within about 5%).

Modelling of the age spectrum (Fig. 18a) produces a moderately good fit. The model parameters τ, the time constant, and the peak age of each domain, are noted on the plot (see Appendix E, part E.2 for description of the modelling procedure). The "large" domain, high-temperature end of the spectrum can only be approximated because of the large melting step and the erratic nature of the step ages on each side of the big step. It is assumed that at melting, the remaining gas is disturbed and isotopes are homogenized. The age of gas remaining in any domain is averaged out in the observed ages of the melting step and the preceding (initial breakdown?) and subsequent (gas release from leucite plus melt?) steps. The model cannot describe melting, so in the model, the average age of the model steps above melting temperatures approximates the average age of the observed melting steps.

The model fails to reproduce the curve at 22 to 25% and at 37 to 47% outgassing. This is an expected result as it is in these ranges that the kinks in the Arrhenius plot occur, which the model also fails to describe. Finally, the age spectrum model does not consider the

partial resetting of small domains during dike intrusion at 600 Ma, which appears to be minimal and probably affects only the small domains to any significant degree. This is necessary because the model's mathematical description of diffusion applies to slow cooling only and does not correctly describe resetting episodes. The following T-t points are defined by "large" and "medium" domains: 232 ±14°C at 1010 ±20 Ma; 168 ±12°C at 865 ±18 Ma.

Sample GF-20K is microcline with no perthite exsolution visible in thin-section. The age spectrum (Fig. 19a) initially has less than 3% of gas in very young steps which are probably affected by recoil and have large atmospheric components; the spectrum then steps up quite regularly from two steps which contribute 7% of gas and have a mean age of 598 Ma; again this is probably due to partial resetting by Grenville dike intrusion. This sample has no obvious (large) melting step, so it is assumed that melting occurred at 1150°C. Instead, steps are of quite uniform size except in the range 870 - 990°C, where a slightly concave downward shape suggests slight sericite contamination. The sample was only outgassed to 1170°C; after this substantial gas, probably most of what was available, was obtained in repeated steps at 1170°C and 1150°C.

The Arrhenius plot for GF-20K (Fig. 19b) has three well-defined, linear segments. From the segment below the first "kink", an activation energy of 36.9 ±5.8 kcal/mol was calculated using the method of York (1969) (SUMS / n-2 = .289). Modelling of the Arrhenius plot using data up to the last 1170°C step gives a three-domain model with parameters as noted on the plot (Fig. 19c). Precise modelling of the age spectrum is difficult in this sample (Fig. 19a). The model can be made to fit in the 15 - 35% outgassing range and again above about 60% outgassing until melting. Because the sample probably melted at 1150°C, the model is fit to the mean age of the gas obtained above this temperature, which ranges from 1047 Ma to 1084 Ma. The zone in which the model departs significantly from the observed spectrum occurs over the 870 - 1080°C steps. It is also in this range that the model fails to describe the subtleties of the Arrhenius plot. The fitting problems may be due to false assumptions in the multiple diffusion domain model, or violations of the slow cooling requirement (see Section 4.3, Discussion of K-feldspar Results and Models). Alternatively, the poor fit over 870 - 990°C may be a result of contamination by sericite. Lastly, the choice of a spherical model may be inappropriate considering that the feldspar is microcline and could well be cryptoperthitic. Nevertheless, the distribution of domains in this sample ensures that the model appears to describe both "large" and "medium" domains fairly well, as the fit above 65% outgassing is a result of subequal gas contribution from both domain

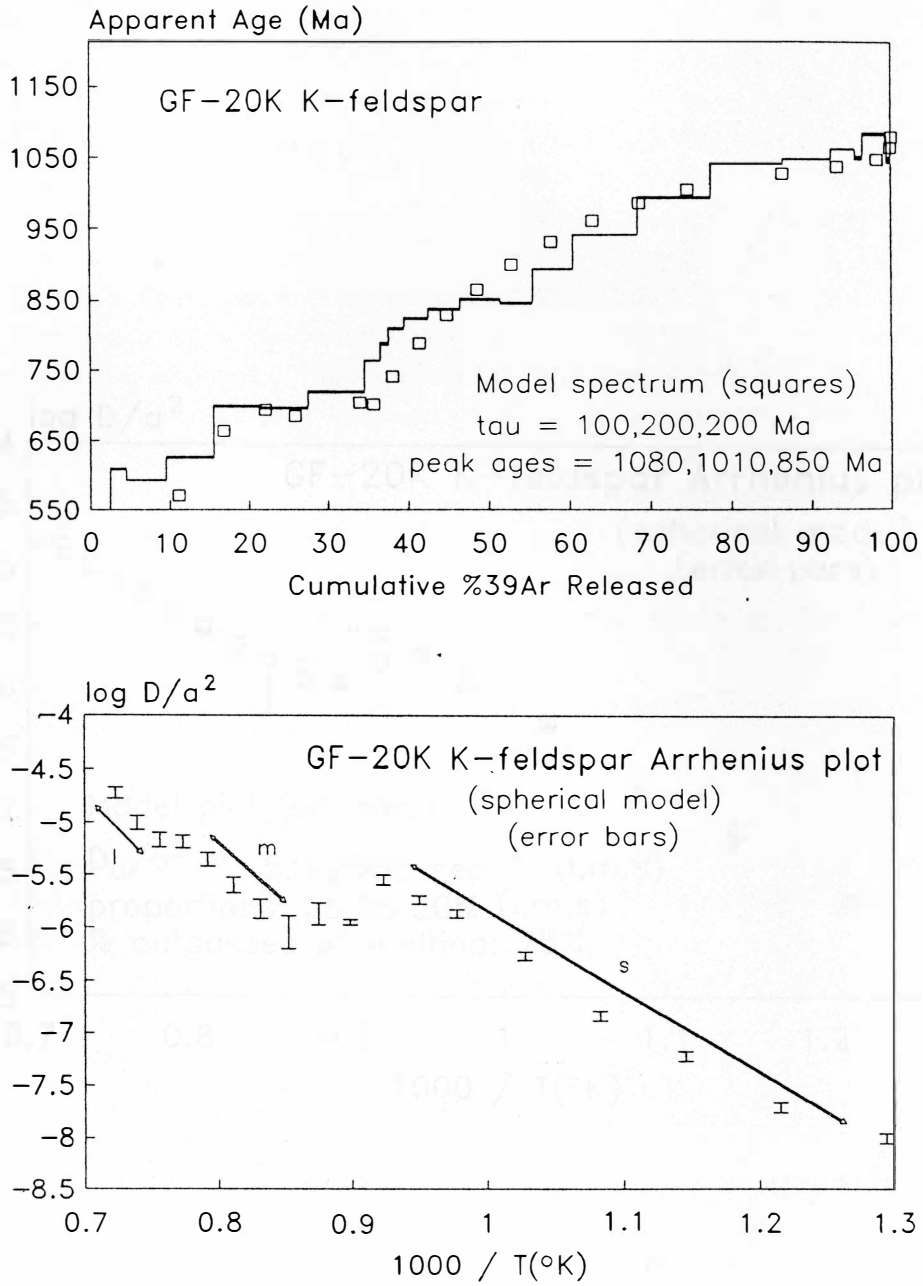

Fig. 19. GF-20K K-feldspar $^{40}Ar/^{39}Ar$ apparent age spectrum and Arrhenius plot, with models. a) Observed (bars) and model (squares) age spectrum. See text for complete description. b) Observed Arrhenius plot. Segments apparently caused by dominance of gas release by small (s), medium (m) and large (l) domains are noted.

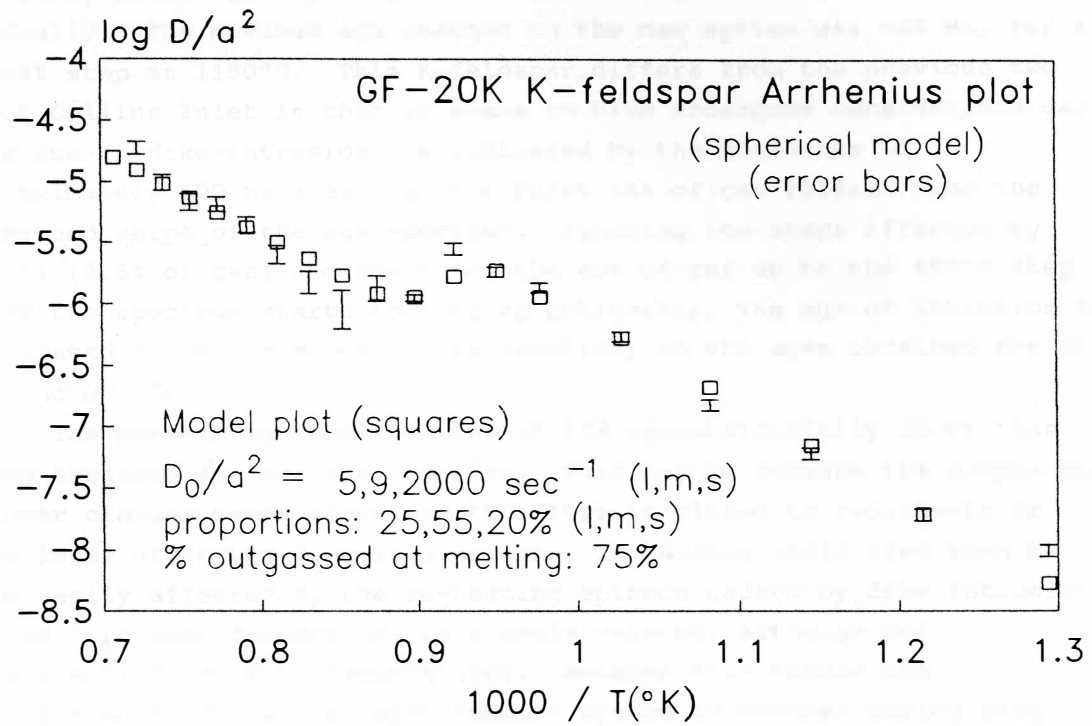

Fig. 19 cont'd. c) Observed Arrhenius plot (error bars) with model (squares) superimposed, for GF-20K K-feldspar. The divergence in the two plots over the .92 to .76 range on the x-axis corresponds to the mismatch in the 35 to 60% cumulative gas released range between the observed and model spectrum in a).

sizes. Small domains are again not considered due to probable effects from resetting at 600 Ma. Two poorly defined T-t points are obtained: 203 ±74°C, 1080 ±10 Ma; 185 ±72°C, 1010 ±10 Ma.

Sample GF-19K is a microcline which is optically homogeneous (no exsolution lamellae). The sample was initially outgassed to 1050°C on the MS10 system, then transferred for final outgassing to the VG3600 system. By comparing the percentage of gas normally obtained by 1050°C for fully outgassed samples of similar nature, GF-20K and GF-18K, an approximate age spectrum can be plotted (Fig. 20). After two initial small steps which have probably been affected by recoil, ages are initially almost identical for more than 10% gas release, then step up gradually. The maximum age reached on the new system was 888 Ma, for a repeat step at 1150°C. This K-feldspar differs from the previous two along Collins Inlet in that it seems to have undergone considerable gas loss due to dike intrusion, as indicated by the dominance of approximately 600 Ma ages over the first 14% of gas release, and the flattened shape of the age spectrum. Ignoring the steps affected by recoil (2.5% of gas) and averaging the age of gas up to the 690°C step where the spectrum starts to step up noticeably, the age of intrusion is calculated to be 598 Ma, which is identical to the ages obtained for GF-32K and GF-20K.

The maximum age obtained for GF-19K is substantially lower than those obtained for previous samples. This may be because the sample had a lower closure temperature and therefore it closed to radiogenic Ar loss later after the Grenville orogeny; the sample would also then be more easily affected by the re-heating episode caused by dike intrusion (since "opening" temperature is closely related, although not equivalent, to closure temperature). Because this sample was transferred from one mass spectrometer system to another during step heating, and because of the significant resetting at ca. 600 Ma, the hypothesis of low closure temperature cannot be tested by modelling. However, the sample was obtained within about 500 metres of an observed outcropping of the Grenville dike on Collins Inlet, unlike the previous samples which are from a section of the Inlet where the dike (known to be discontinuous) has not been observed (Davidson and Bethune, 1988). Consequently, the sample was probably heated to higher temperatures by dike intrusion, and suffered considerably more gas loss than other samples, resulting in maximum ages which are partially reset and therefore meaningless.

Sample GF-18K, a microperthitic orthoclase which has partly ordered to microcline, yields an enigmatic age spectrum (Fig. 21a). The lowest age obtained for the low temperature, initial gas release part of

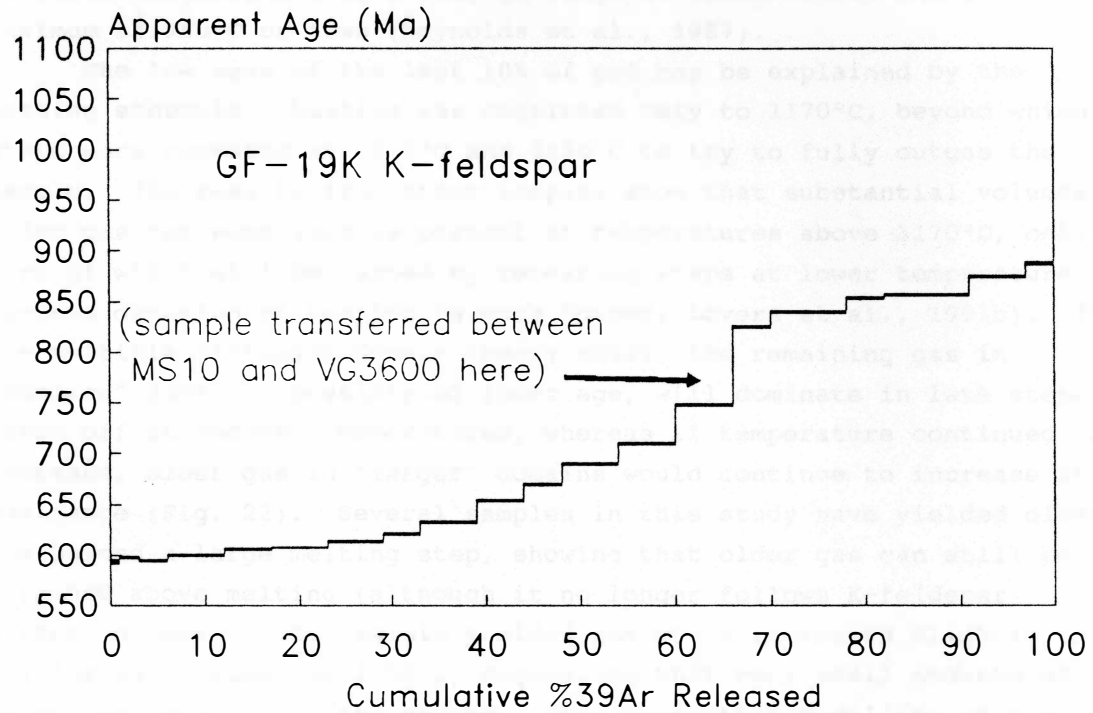

Fig. 20. Approximate $^{40}Ar/^{39}Ar$ apparent age spectrum for GF-19K K-feldspar. See text for description.

the spectrum is 691 Ma, and the first step containing more than 2% of gas has an age of 725 Ma, despite its location about 200 metres across Collins Inlet from an outcrop of 598 Ma Grenville dike. Apparent ages then step up to a maximum of 918 Ma at about 60% outgassing, and decrease again to a constant value of about 890 Ma. The humped shape of this spectrum is not characteristic of feldspars except those containing excess Ar (Foster et al., 1990), which is unlikely in this case because the ages are too young rather than too old compared to nearby feldspars. Contamination by sericite can be ruled out because of the persistence of the apparent age maximum to 1040°C, contradicting the normal pattern of sericite outgassing over a limited range of temperature, and to a maximum of 950°C or less (Reynolds et al., 1987).

The low ages of the last 10% of gas may be explained by the heating schedule. Heating was continued only to 1170°C, beyond which steps were repeated at 1170°C and 1150°C to try to fully outgas the sample. The results from other samples show that substantial volumes of older gas can sometimes be present at temperatures above 1170°C, only part of which will be tapped by repeating steps at lower temperatures (unless duration of heating is much longer; Lovera et al., 1991b). If the multiple diffusion domain theory holds, the remaining gas in "smaller" domains, possibly of lower age, will dominate in late steps taken off at reduced temperatures, whereas if temperature continued to increase, older gas in "larger" domains would continue to increase in dominance (Fig. 22). Several samples in this study have yielded older gas beyond a large melting step, showing that older gas can still be obtained above melting (although it no longer follows K-feldspar diffusion laws). This sample yielded gas which increased slightly in age for each repeat at 1150°C, suggesting that very small amounts of older gas remained in the sample. This means that modelling of the Arrhenius plot and spectrum will yield a close approximation of the true closure temperature of the sample (if the other assumptions of the method are valid).

However, the age decrease in the 60 to 90% outgassing range is not as easily explained, since furnace temperature was increasing in this section. One possible explanation is the partially ordered structural state of the sample, causing complications not present in other samples. The microcline could be behaving differently from the orthoclase due to differences in activation energy or their domainal structure. A second possible explanation is the failure of the present model to fully describe domainal behaviour. It is worth noting that the drop in ages in this sample corresponds to a kink in the Arrhenius plot (kink 2, between m and l segments; see Figs. 21a and 21b). This subject will be

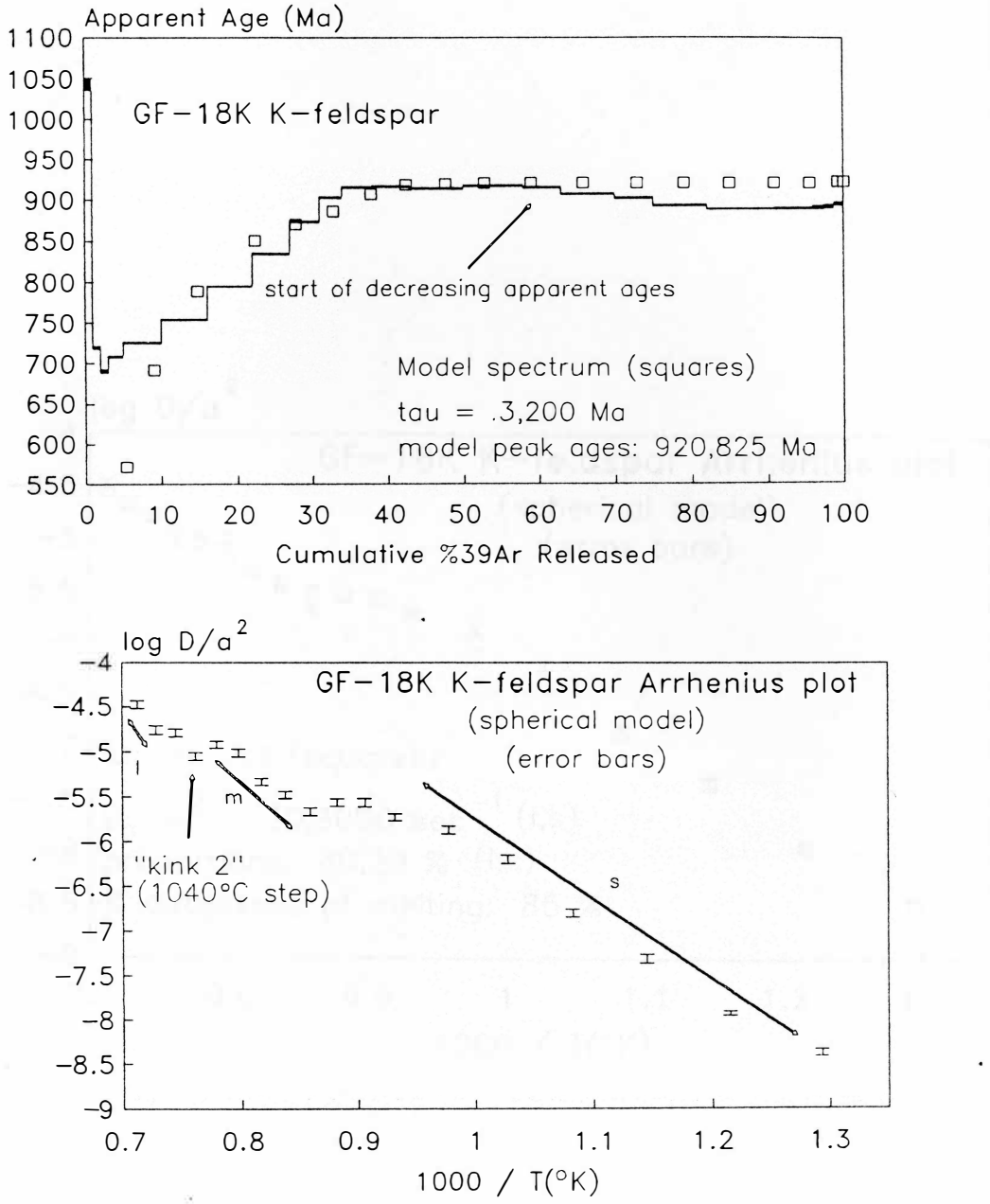

Fig. 21. GF-18K K-feldspar $^{40}Ar/^{39}Ar$ apparent age spectrum and Arrhenius plot, with models. a) Observed (bars) and model (squares) age spectrum. The observed spectrum exhibits a decrease in step ages starting at about 60% cumulative gas released. This corresponds to the 1040°C step. The model spectrum assumes a peak age of 920 Ma for gas released after this point because the model cannot describe the decrease in apparent ages. b) Observed Arrhenius plot. There is evidence for three domains (s = small, m = medium, l = large) although the large domain segment is poorly defined. The location of the second kink (kink 2) corresponds to the 1040°C step, where the decrease in apparent ages occurs.

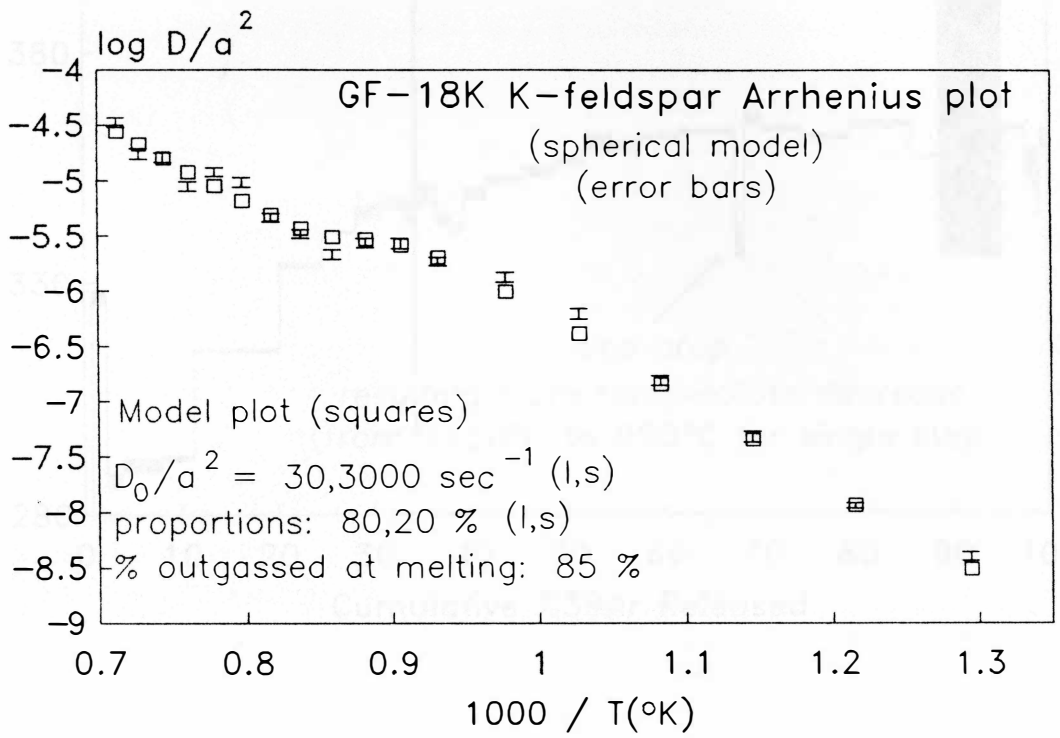

Fig. 21 cont'd. c) GF-18K observed Arrhenius plot (error bars) with two-domain model (squares) superimposed. See text for explanation.

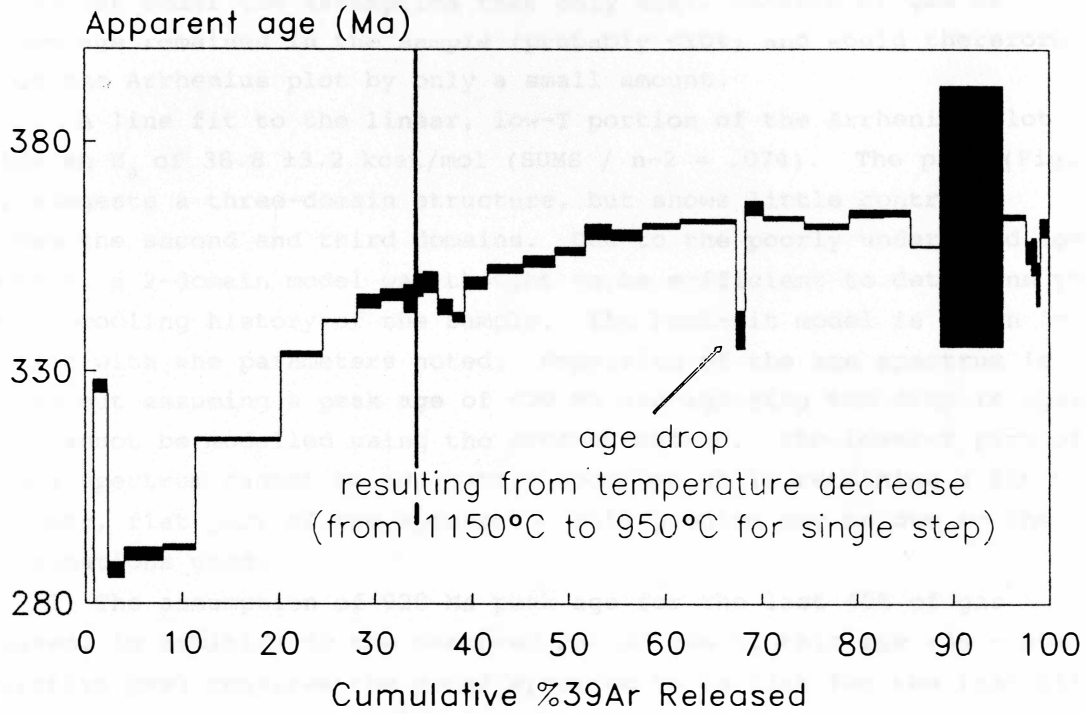

Fig. 22. Example of a K-feldspar $^{40}Ar/^{39}Ar$ apparent age spectrum illustrating effect of reducing furnace temperature. The downward spike caused by a low step age at about 70% cumulative gas released is due to a reduction in furnace temperature. Temperature was reduced to 950°C from 1150°C for this one step. The disturbance in the spectrum at about 35% gas released is also caused by several reduced temperature steps but the size of the steps is very small (0.1% of total gas released) and the calculated ages are not reliable. The remainder of the experiment was conducted using monotonically increasing or stable furnace temperature. The drop in apparent age is probably because older gas in larger domains is not tapped when the temperature is reduced. Plotted using data of Lovera et al. (1991) (sample MH.10.cf).

considered more fully in Section 4.3 (Discussion of K-feldspar Results and Models).

Because of the lack of evidence for excess Ar, the peak age of 918 Ma must be treated as a "real" feldspar age. The possibility that older gas might have been present in the sample had it been outgassed to higher temperatures suggests that this could be a minimum age. This is supported by evidence obtained during the modelling procedure, which is carried out under the assumption that only small amounts of gas of unknown age remained in the sample (probably <10%) and would therefore change the Arrhenius plot by only a small amount.

A line fit to the linear, low-T portion of the Arrhenius plot yields an E_a of 38.8 ±3.2 kcal/mol (SUMS / n-2 = .074). The plot (Fig. 21b) suggests a three-domain structure, but shows little contrast between the second and third domains. Due to the poorly understood age spectrum, a 2-domain model was thought to be sufficient to determine the general cooling history of the sample. The best-fit model is shown in Fig. 21c with the parameters noted. Modelling of the age spectrum is carried out assuming a peak age of 920 Ma and ignoring the drop in ages, which cannot be modelled using the present method. The lower-T part of the age spectrum cannot be adequately modelled while retaining a fit to the upper, flat part of the spectrum. This problem may be due to the approximations used:

1) The assumption of 920 Ma peak age for the last 40% of gas released, in addition to the observed 25% of gas of this age (35 - 60% cumulative gas) requires the model spectrum to be flat for the last 65% of outgassing, necessitating rapid cooling in the input parameters. As there is no other evidence available for rapid cooling at 920 Ma it is probably not real. A higher peak age would allow better description of the shape of the curve below 35% outgassing. Additionally, more, older gas would have the effect of "shrinking" the size of the flat portion of the spectrum, allowing modelling with more realistic cooling rates. This evidence supports the suggestion that 920 Ma is only a minimum, and implies that the model cooling rate is too high.

The corresponding T_c calculated for the larger domains is probably a maximum for the 920 Ma age, because the slower cooling rate needed to fit a more complete spectrum would lead to a lower T_c. However, the possible failure to outgas the sample fully introduces a competing effect on the estimated T_c. Underestimating total gas leads to overestimation of all D_0/a^2 values in the sample and thereby to erroneously low calculated closure temperatures; these would probably apply to slightly older ages. Which of these two effects would dominate is difficult to assess with the present data. The estimated cooling

rate differs in this sample by two orders of magnitude from other calculated rates (see Table 2), but two or more orders of magnitude change in D_0/a^2 could be caused by addition of a single, large melting step like that observed in GF-32K. The two effects may therefore cancel one another (see equation (14), Appendix E, part E.2). This subject, as well as other possible influences on modelled closure temperatures, will be addressed more fully in Section 4.3 (Discussion of K-feldspar Results and Models).

2) A second possible false assumption may be the use of spherical geometry. The effect of using a plane-sheet geometry in the models instead, would be to allow a flatter age spectrum without requiring such a rapid cooling rate.

The sample does not appear to be affected by intrusion of the Grenville dike at 600 Ma, despite its proximity to a known outcrop of the dike (and the relatively low calculated closure temperature for small domains). The reason for this is not known; it may be that here the dike is narrow and therefore affected its country rock less than in other sections. The dike has not been thoroughly mapped and this cannot be tested. An alternative explanation is that the age spectrum has been affected by an experimental problem such as massive recoil or homogenization of the ^{40}Ar isotope during heating. The former theory is preferred, as modelling of the Arrhenius plot and age spectrum produced reasonable if not definitive and complete results. Additionally, the 725 Ma minimum age of gas in the sample (for a reliably large step) is similar to the minimum for other samples also unaffected by the dike, and presumably represents final closure of the K-feldspar to diffusive loss of argon. Because of the lack of resetting, the smallest domains can be used to define the cooling history. The two-domain model produces two T-t points as follows: 285 ±44°C, 920 ±10 Ma; 150 ±34°C, 825 ±8 Ma.

Sample GF-7K (Fig. 23) is microperthitic orthoclase from mylonitic, granulite grade metasediments. After a few percent of gas affected by recoil, ages step up steeply from 726 Ma to a local peak at 1200 Ma, drop abruptly and step up gradually to 1066 Ma, before melting at 1150°C, which is expressed as a very large step of age 1043 Ma. Dating was started on the old MS-10 system and transferred for complete outgassing to the VG3600 after the 900°C step, which was repeated on the new system. Exact matching of the two halves of the spectrum is difficult so its shape over the transition point is uncertain; this includes the steps surrounding the local maximum. However, it is clear that there is a major abnormality in the spectrum in this region. The best explanation is again sericite outgassing over a limited T-range,

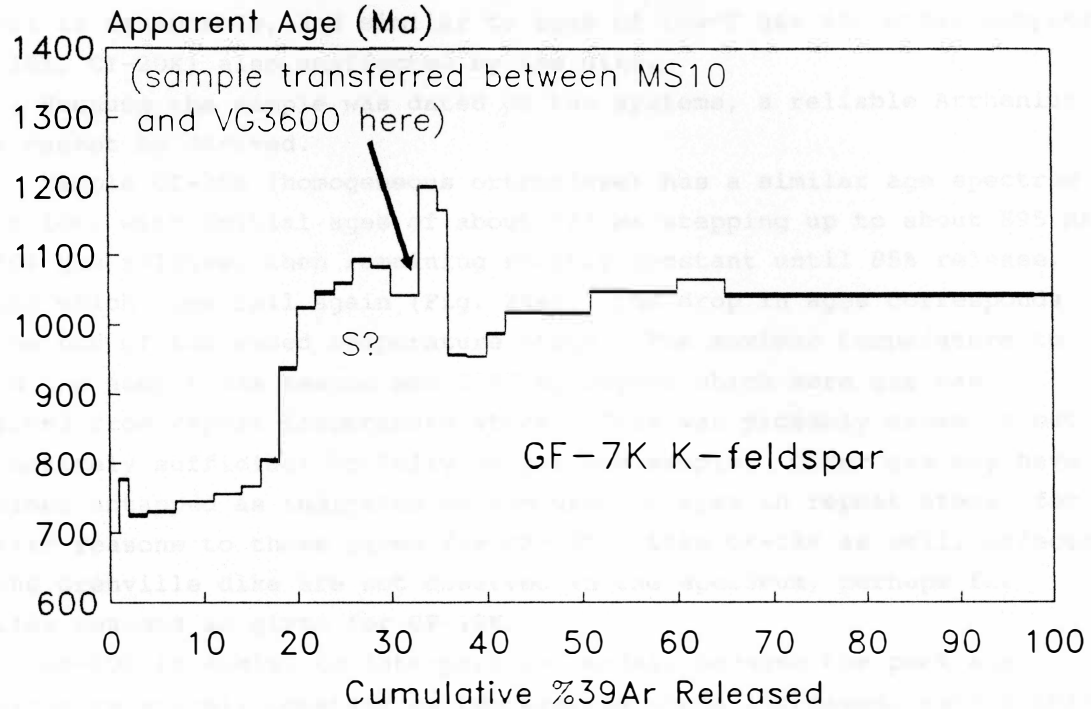

Fig. 23. Approximate $^{40}Ar/^{39}Ar$ apparent age spectrum for GF-7K K-feldspar. The concave downward part of the spectrum, denoted S?, is probably a result of outgassing of sericite.

because as for samples GF-62K and GF-20K, the spectrum returns to a "normal" curve once the spike has dropped off.

The peak ages of the strictly K-feldspar part of the spectrum, including the melting step, are similar to those obtained for sample GF-32K and GF-20K at high furnace temperatures. The sample is south of Collins Inlet and is not expected to show the effects of Grenville dike intrusion. Rather, the minimum age should represent final closure of the sample to escape of radiogenic argon following the last event in the area. The age of about 726 - 731 Ma of the first gas not affected by recoil is reasonable, and similar to ages of low-T gas for other samples (GF-18K, CI-20K) also unaffected by the dike.

Because the sample was dated on two systems, a reliable Arrhenius plot cannot be derived.

Sample CI-20K (homogeneous orthoclase) has a similar age spectrum to GF-18K, with initial ages of about 725 Ma stepping up to about 895 Ma at 50% gas release, then remaining roughly constant until 85% release, beyond which ages fall again (Fig. 24a). The drop in ages corresponds to the end of increased temperature steps. The maximum temperature to which the sample was heated was 1150°C, beyond which more gas was obtained from repeat temperature steps. This was probably close to but not entirely sufficient to fully outgas the sample. Older gas may have remained untapped as indicated by the drop in ages in repeat steps, for similar reasons to those given for GF-18K. Like GF-18K as well, effects of the Grenville dike are not observed in the spectrum, perhaps for similar reasons as given for GF-18K.

CI-20K is easier to interpret and model, because the peak age remained relatively constant as temperature steps increased, rather than falling as for GF-18K. This provides assurance that strictly K-feldspar is outgassing, and permits satisfactory modelling of the observed spectrum. A three-domain model best fits the Arrhenius plot (Figs. 24b and 24c), with an E_a of 32.8 ±2.0 kcal/mol derived from a line fit to the first seven points (SUMS / n-2 = .068). The contrast in D_0/a^2 and the distribution of the three domains is such that when modelling the age spectrum (Fig. 24a) the large domains have little effect on the outgassing up to melting temperature; thus the peak age (910 Ma) of large domains is only a guess, and is probably a minimum given the failure to outgas the sample above 1150°C. The corresponding cooling rate for large domains is then a maximum, as it describes very rapid cooling in order to mimic the horizontal nature of the spectrum observed for medium domains; this is an artificial constraint. The fast cooling rate results in a relatively high model closure temperature. This effect competes with probable failure to fully outgas the sample, as

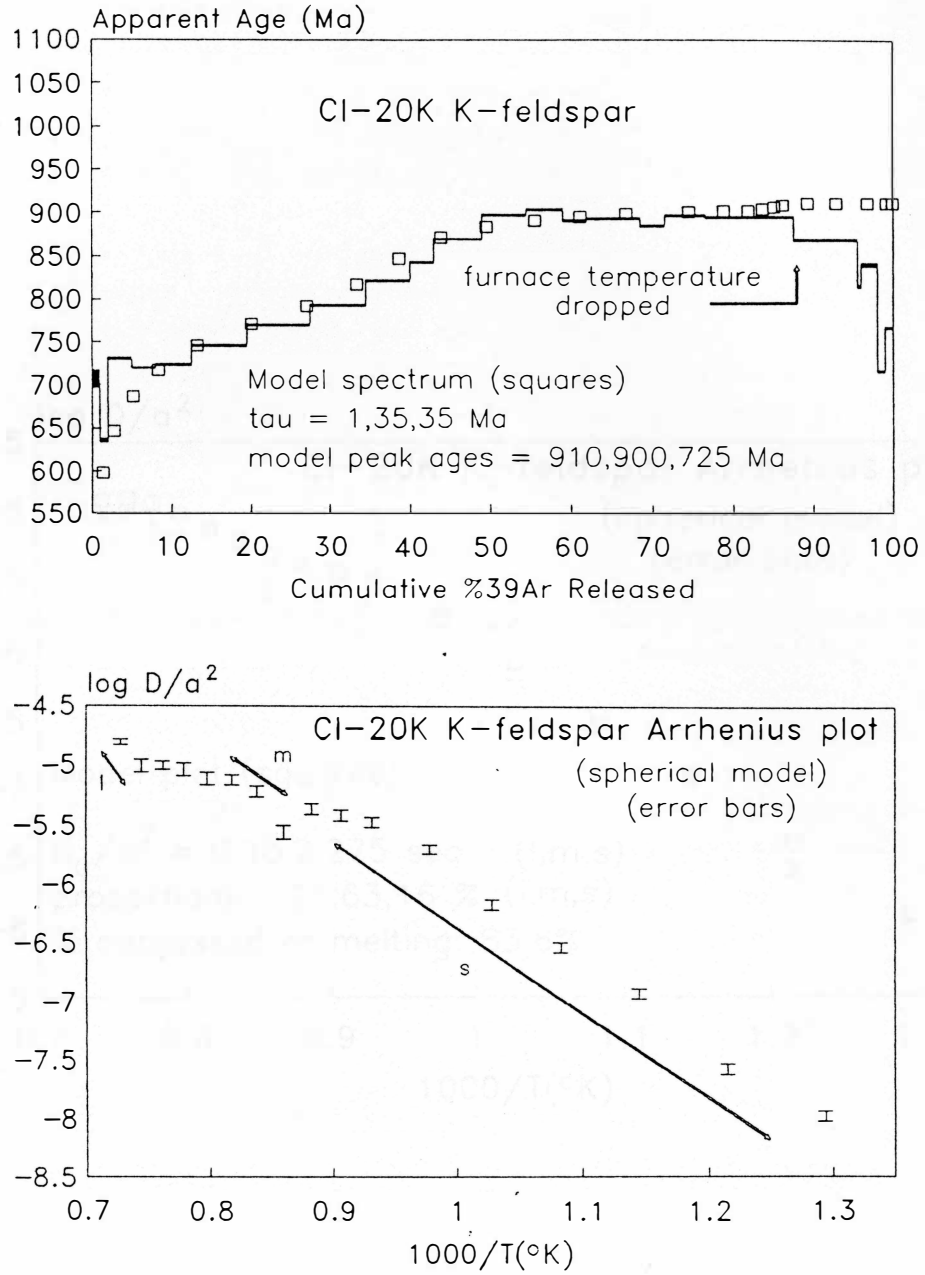

Fig. 24. CI-20K K-feldspar $^{40}Ar/^{39}Ar$ apparent age spectrum and Arrhenius plot, with models. a) Observed (bars) and model (squares) age spectrum. The drop in ages over the last 10% of gas released corresponds to a decrease in furnace temperature. The spectrum was modelled assuming a small amount of older gas remained in the sample, hence the departure of the model from the observed spectrum. Refer to text for detailed explanation. b) Observed Arrhenius plot. Approximate ranges of gas dominated by small (s), medium (m) and large (l) domains are shown.

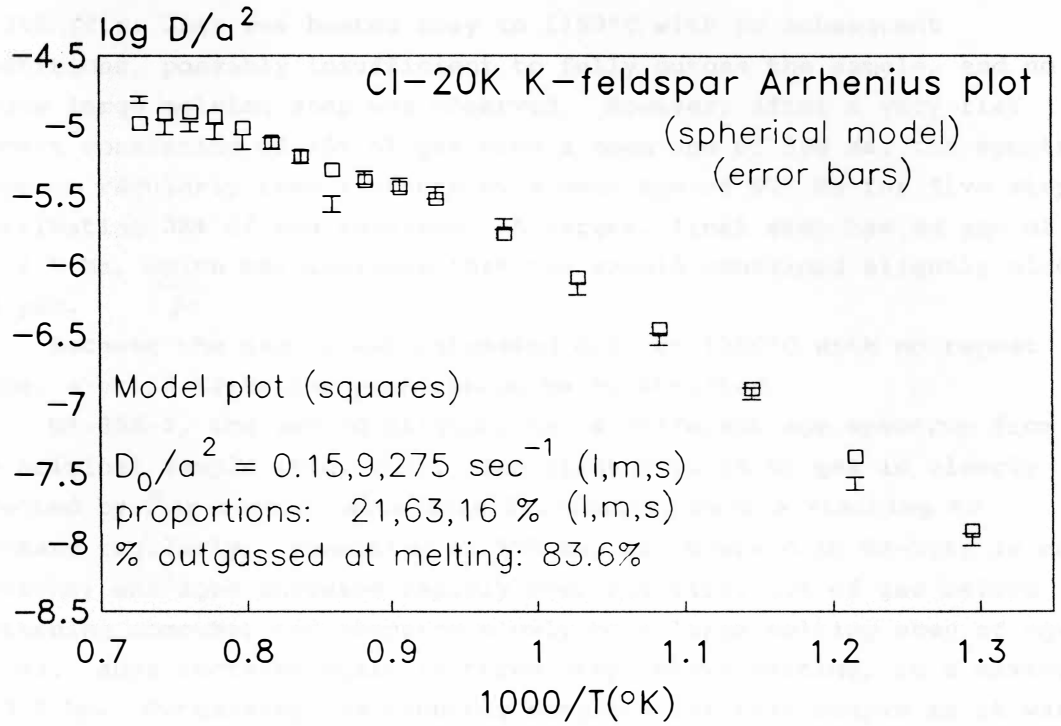

Fig. 24 cont'd. c) CI-20K observed (error bars) and model (squares) Arrhenius plot. See text for explanation.

described for GF-18K, leading to underestimation of T_c for all domains. Again, this subject is addressed more fully in Section 4.3 (Discussion of K-feldspar Results and Models).

Medium and small domains are well constrained, with an excellent fit to the Arrhenius plot and the age spectrum. The following T-t points are defined by the model: 261 ±34°C, >910 ±18 Ma; 170 ±28°C, 900 ±18 Ma; 101 ±24°C, 725 ±14 Ma.

The next sample, a homogeneous orthoclase, was run in two different aliquots. The first, denoted GF-35K, was a large separate prepared for the MS10 system, and the second, GF-35K-2, was a much smaller separate picked very carefully and dated on the VG3600 system. GF-35K (Fig. 25a) was heated only to 1150°C with no subsequent repetitions, possibly insufficient to fully outgas the sample, and no single large melting step was observed. However, after a very flat segment consisting of 16% of gas with a mean age of 598 Ma, the spectrum steps up regularly then flattens at a mean age of 977 Ma for five steps contributing 38% of gas released. A larger, final step has an age of 990 ± 9 Ma, which may indicate that the sample contained slightly older gas yet.

Because the sample was outgassed only to 1150°C with no repeat steps, a valid Arrhenius plot cannot be constructed.

GF-35K-2, the second aliquot, has a different age spectrum from the original sample (Fig. 25b). The first 3 to 5% of gas is clearly affected by ^{39}Ar recoil, with ages fluctuating before starting to increase regularly. Resetting at 598 Ma, as observed in GF-35K, is not apparent, and ages increase rapidly over the first 30% of gas before flattening somewhat and stepping slowly to a large melting step of age 935 Ma. Ages increase again in three steps above melting, to a maximum of 975 Ma. Outgassing was probably complete for this sample as it was heated to 1210°C and the last two steps were extremely small.

The Arrhenius plot (Fig. 25c) is quite regular at high temperatures but the low-T segment is non-linear. The first three or four of the seven steps defining this part of the curve are affected by ^{39}Ar recoil, which may partly explain the irregular shape (since the Arrhenius plot is based on ^{39}Ar release). The apparent "medium" domains define a very linear segment which is clearly much steeper than the lower segment. The drastic difference in slope of these two segments invalidates the assumption of equivalent activation energy used in the models constructed in this study. Therefore no attempt has been made to model the Arrhenius plot.

The difference in the results yielded by these two aliquots requires further discussion before an age can be assigned. They will be

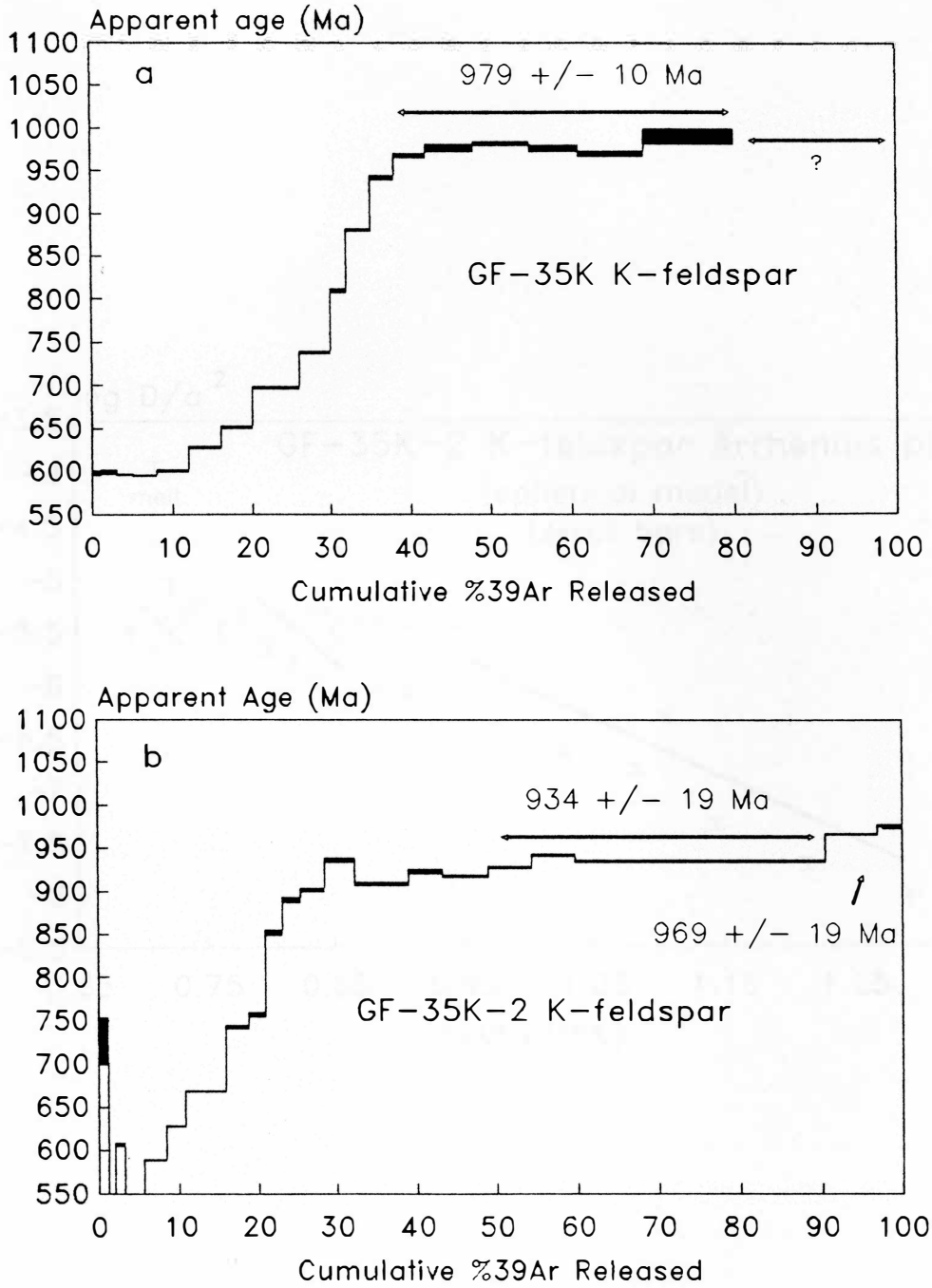

Fig. 25. GF-35K K-feldspar $^{40}Ar/^{39}Ar$ apparent age spectrum, and GF-35K-2 spectrum and Arrhenius plot. a) Approximate age spectrum for GF-35K. The sample may not be fully outgassed. See text for description. b) Apparent age spectrum for GF-35K-2. The large single step from about 60 to 90% gas release results from incongruent melting. Note the contrast between this spectrum and the GF-35K spectrum above. The ages of steps at low gas release (below 10%), and in the flat parts of the spectra above 35% release, are quite different. See text for description.

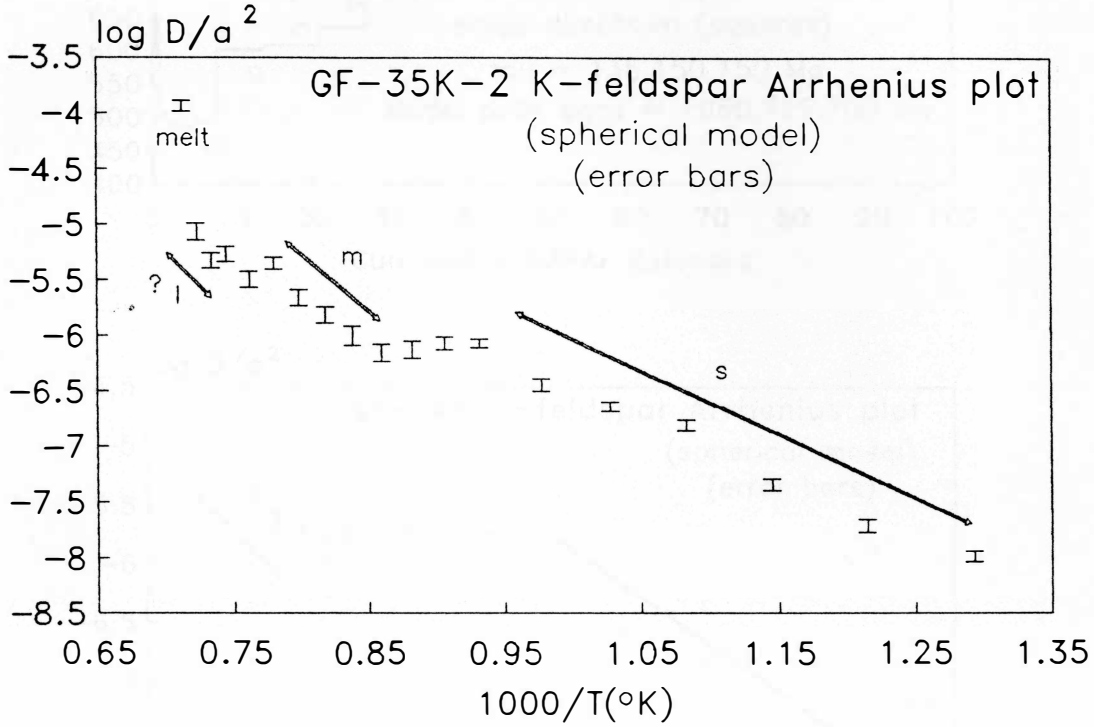

Fig. 25 cont'd. c) GF-35K-2 K-feldspar Arrhenius plot. Note the difference in slope between the low-temperature segment, s, and the upper two segments, m and l. The uppermost segment, l, is poorly defined.

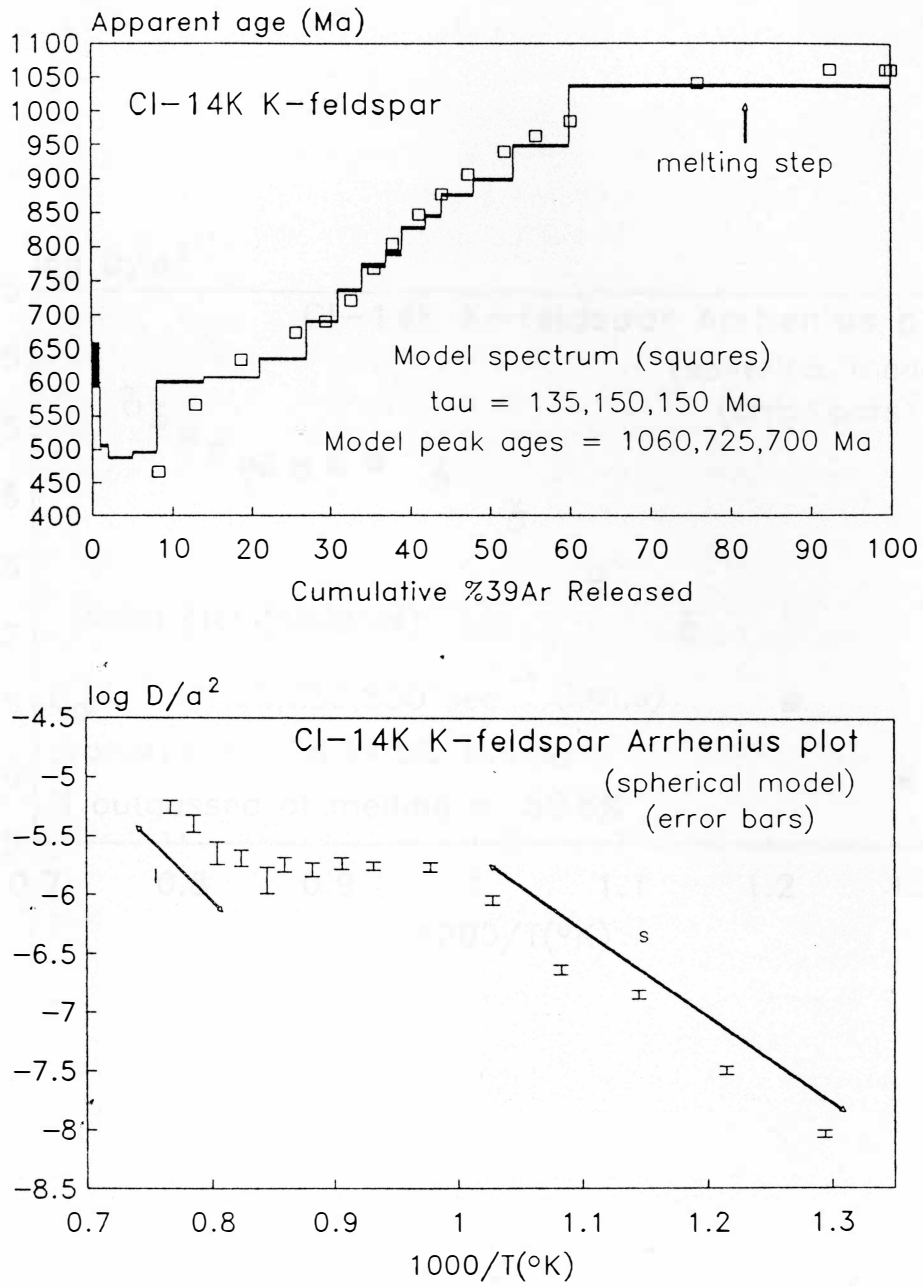

Fig. 26. CI-14K K-feldspar $^{40}Ar/^{39}Ar$ apparent age spectrum and Arrhenius plot, and models. a) Observed (bars) and model (squares) age spectrum. The last 40% of gas released was obtained in a single step, probably resulting from incongruent melting of the sample. b) Observed Arrhenius plot. The plot suggests a two-domain structure (small, s, and large, l) with a high degree of overlap in their range of gas release.

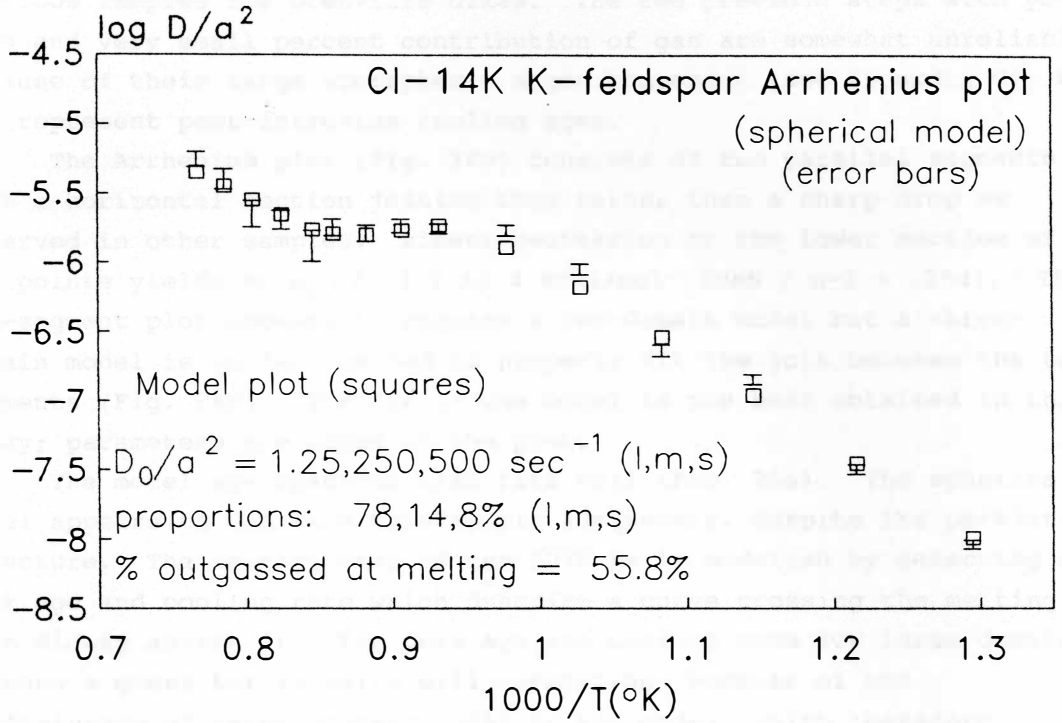

Fig. 26 cont'd. c) CI-14K observed (error bars) Arrhenius plot, with model (squares) superimposed. A three domain model is required to satisfactorily fit the data, with a low contrast in D_0/a^2 between small (s) and medium (m) domains.

assessed in detail in section 4.3 (Discussion of K-feldspar Results and Models).

Sample CI-14K, perthitic orthoclase, yields a very regular age spectrum (Fig. 26a), which steps up from about 490 Ma to a peak age, for a large melting step, of 1038 Ma. Two large steps early in release give a flat, apparently reset segment with an average age of 605 Ma (±6 Ma when J is considered), almost identical to the age determined in previous samples for Grenville dikes. The two previous steps with young ages and very small percent contribution of gas are somewhat unreliable because of their large atmospheric argon component (see Appendix C), but may represent post-intrusion cooling ages.

The Arrhenius plot (Fig. 26b) consists of two parallel segments with a horizontal section joining them rather than a sharp drop as observed in other samples. Linear regression of the lower section of six points yields an E_a of 33.2 ±3.4 kcal/mol (SUMS / n-2 = .254). The two-segment plot appears to require a two-domain model but a three-domain model is in fact needed to properly fit the join between the two segments (Fig. 26c). The fit of the model is the best obtained in this study; parameters are shown on the plot.

The model age spectrum also fits well (Fig. 26a). The spherical model appears to describe this sample adequately, despite its perthitic structure. The melting step of age 1038 Ma is modelled by selecting a peak age and cooling rate which describe a curve crossing the melting step midway across it. The peak age and cooling rate for large domains is thus a guess but is quite well constrained because of the predominance of large domains (78%) in the model, which therefore dictate the shape of the spectrum above about 30% gas release. Both medium and small domains appear to be affected by resetting so no significance is attached to the model results for these domains. Thus only one T-t point is obtained for sample CI-14K: 166 ±44°C, 1060 ±22 Ma.

4.3 DISCUSSION OF K-FELDSPAR RESULTS AND MODELS

The modelled Arrhenius plots and age spectra do not fit the observed data in detail in almost all examples. One possible reason for this is that the multiple diffusion domain theory may be wrong. However, some results, including those for unmodelled samples, are better explained using the theory than the old single-site diffusion model. Non-ideal data may explain many of the fitting problems. Additionally, some of the assumptions made have been demonstrated recently to be inadequate for certain K-feldspars. The data are discussed and interpreted below in light of the most recent developments

of the multiple diffusion domain theory, in order to clarify the results of this study.

4.3.1 Discussion of Data

One of the critical assumptions used in the modelling is that each domain size has equivalent activation energy. For normal heating schedules the low-temperature segment of the Arrhenius plot, resulting mainly from outgassing of the smallest domains, is defined by the greatest number of points on the Arrhenius plot. Therefore this segment was used here to define the slope of all the segments, and thus the activation energy for the whole sample. The heating schedules used for all modelled samples were relatively coarse because of uncertainty about whether samples would produce measurable gas volumes for the new VG3600 mass spectrometer. By the first kink, which in these samples occurred at 800°C or higher, only seven or eight points defined the line used to determine activation energy. The line-fit method of York (1969) established errors of 6 to 16% (2σ) on the slopes of these lines, introducing errors of the same magnitude on calculated activation energy, and hence to closure temperatures applicable to all domains. Ideally, to better define activation energy, many more steps of shorter duration should be used, resulting in a line fit to a greater number of points. This is made more important because the early steps are often affected by ^{39}Ar recoil, as was the case for up to four points in some modelled samples. Gas volumes may not reflect simple volume diffusion in these steps. Harrison et al. (1991) have shown that depending on whether the size of small domains is larger or smaller than the characteristic recoil length, recoil can affect either the estimate of E_a, or the D_0/a^2 value.

Furthermore, recent work has shown that the assumption of equivalent activation energy may not necessarily be correct. Some workers have started to used "cycled" step-heating experiments, in which temperature is not monotonically increased but rather increased and then decreased and held at low temperatures for long time spans (Lovera et al., 1989; Lovera et al., 1990). The information obtained from this comes at the expense of the age spectrum, which will have an erratic pattern; but the result is to yield better defined arrays of points on the Arrhenius plot for all domains. Such a plot is illustrated in Figure 27. Experiments using cycled temperatures have demonstrated that different diffusion domains in a single sample can have activation energies which vary by as much as 8 kcal/mol (Harrison et al., 1991). There is some evidence in the samples modelled in this study that different diffusion domains have different E_a; sample GF-20K in

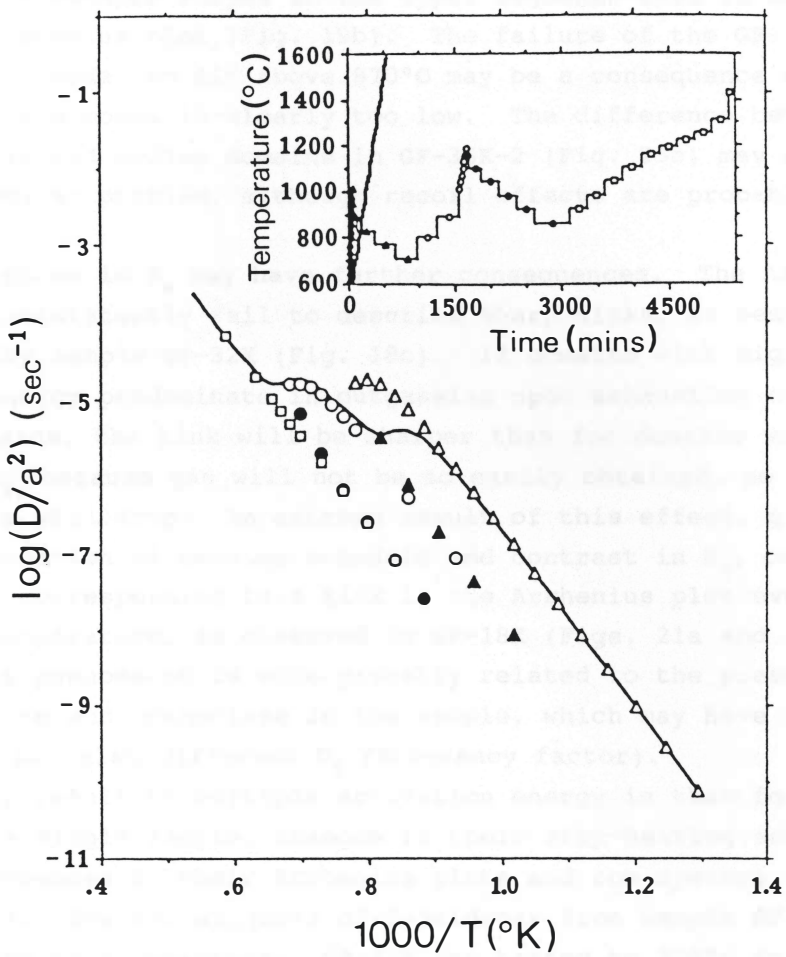

Fig. 27. Computed (model) Arrhenius plots contrasting conventional and cycled heating schedules. The inset illustrates the two heating schedules used. The nearly straight line with a high slope corresponds to monotonically increasing temperature steps. The line with symbols shows the cycled schedule. Equivalent symbols are used in the Arrhenius plots. The solid line is the plot resulting from the monotonic schedule and is similar to the plots obtained in the present study. The symbols demarcate the result of the cycled experiment. Initially temperature is increased (open triangles) using short time steps. Melting is avoided. Temperature is then reduced (closed triangles), then cycled up and down again (open circles, closed circles), then finally raised until the sample is fully outgassed. Note that in a real sample melting would occur once 1150°C was exceeded, so that the points obtained after this temperature was first reached would not be valid for determination of Arrhenius parameters. To avoid this, all heating should be conducted below this temperature, using long duration steps to ensure adequate gas volumes. The result of the cycling procedure is better definition of the lines corresponding to all domains, so that activation energy and D_0/a^2 of each domain can be better defined. (After Lovera et al., 1991).

particular has steeper slopes in the upper segments than in the lower one on its Arrhenius plot (Fig. 19b). The failure of the GF-20K Arrhenius plot model to fit above 870°C may be a consequence of this, as the slope of the model is clearly too low. The difference between the slope of small and medium domains in GF-35K-2 (Fig. 25c) may be due in part to a similar problem, although recoil effects are probably also responsible.

Differences in E_a may have further consequences. The Arrhenius plot models consistently fail to describe sharp kinks, as best illustrated by sample GF-32K (Fig. 18c). If domains with higher activation energy predominate in outgassing upon exhaustion of small, lower E_a domains, the kink will be sharper than for domains with equivalent E_a, because gas will not be so easily obtained, so diffusivities will drop. An extreme result of this effect, given the correct combination of heating schedule and contrast in E_a, could be a drop in ages corresponding to a kink in the Arrhenius plot even upon increasing temperature, as observed in GF-18K (Figs. 21a and 21b); however, this phenomenon is more probably related to the presence of both microcline and orthoclase in the sample, which may have not only different E_a but also different D_0 (frequency factor).

Another result of multiple activation energy is that for different aliquots of a single sample, changes in their step-heating schedule will lead to differences in their Arrhenius plots and age spectra (Harrison et al., 1991). The two aliquots of K-feldspar from sample GF-35 may have exhibited this behaviour. GF-35K was heated to 900°C in fifteen 30° steps, while 35K-2 was heated to 890°C in only 10 steps, seven of 50° and three of 30°. Lovera et al. (1989) have shown that the shorter the duration of heating over a fixed range of temperature in the heating schedule, the less gas will come out of the domains, particularly the larger ones, before melting. Ages will therefore be younger before melting. This behaviour is observed in the two aliquots of GF-35K (Figs. 25a and 25b), but the differences in heating schedule are probably not drastic enough to fully explain the differences in the spectra.

However, the further differences in the age spectra of these two aliquots can also be explained using an extension of the multiple diffusion domain theory. The thoroughness of the purification procedure during sample preparation is for practical reasons a function of the size of the aliquot. The sample prepared for the VG3600 system was picked more carefully because of the much smaller time involved in picking a 5 mg versus a 100 mg sample. Larger grains, being more easily observed under the binocular microscope, may have been preferentially

removed because of this. The resultant aliquot (GF-35K-2), with a greater percentage of small grains and possibly of small domains, would have suffered a greater percentage effect of reactor-induced recoil, causing the differences in the low-T part of the age spectrum. The loss of larger grains may have skewed the domain size distribution by preferentially removing grains which contained the largest domains, hence less "old" gas was present to influence step ages, in particular of that of the melting step. Evidence that some older gas was present in the sample comes from the approximately 969 Ma age of the last 9% of gas released (Fig. 25b), but the overall contribution of this age of gas to the age spectrum is clearly reduced from the GF-35K spectrum (Fig. 25a). This argument is strengthened by experimental evidence that by sieving separates to very small grain sizes, the volume fraction of small domains can be increased substantially (Lovera et al., 1991a).

Both of these explanations for the differences between the two aliquots of K-feldspar from sample GF-35 require multiple diffusion domain sizes to adequately explain the observations. This is some of the best evidence available in this study that the model is at least in part correct.

There is therefore considerable evidence in the samples dated in this study that the multiple diffusion domain theory describes the outgassing behaviour well, and that many of the failures of the models are due to underestimation of the activation energy of larger domains. The consequence of underestimating activation energy is that closure temperatures will be underestimated, since the closure temperature calculation is a direct function of activation energy (see equation (14), Appendix E, part E.2), and depends much less directly on D_0/a^2. Harrison et al. (1991) have demonstrated this point by carrying out modelling of an Arrhenius plot using the equivalent activation energy assumption for one model, and multiple activation energies in a second (Figs. 28a and 28b). After determining diffusion parameters, they can achieve virtually identical fits to the age spectrum using either method, but the calculated cooling histories differ by as much as 30°C for a given age (Fig. 28c).

For all samples modelled in this study except perhaps CI-20K, slopes in Arrhenius plots for medium and large domains are greater than those for small domains. Calculated closure temperatures for medium and large domains must therefore be considered minima. Harrison et al. (1991) suggest a value of up to 30°C increase in modelled T_c for a 5 kcal/mol increase in E_a of larger domains over the small domain E_a.

A second problem introduced by the heating schedules used in this study is that for many samples, substantial amounts of gas remained in

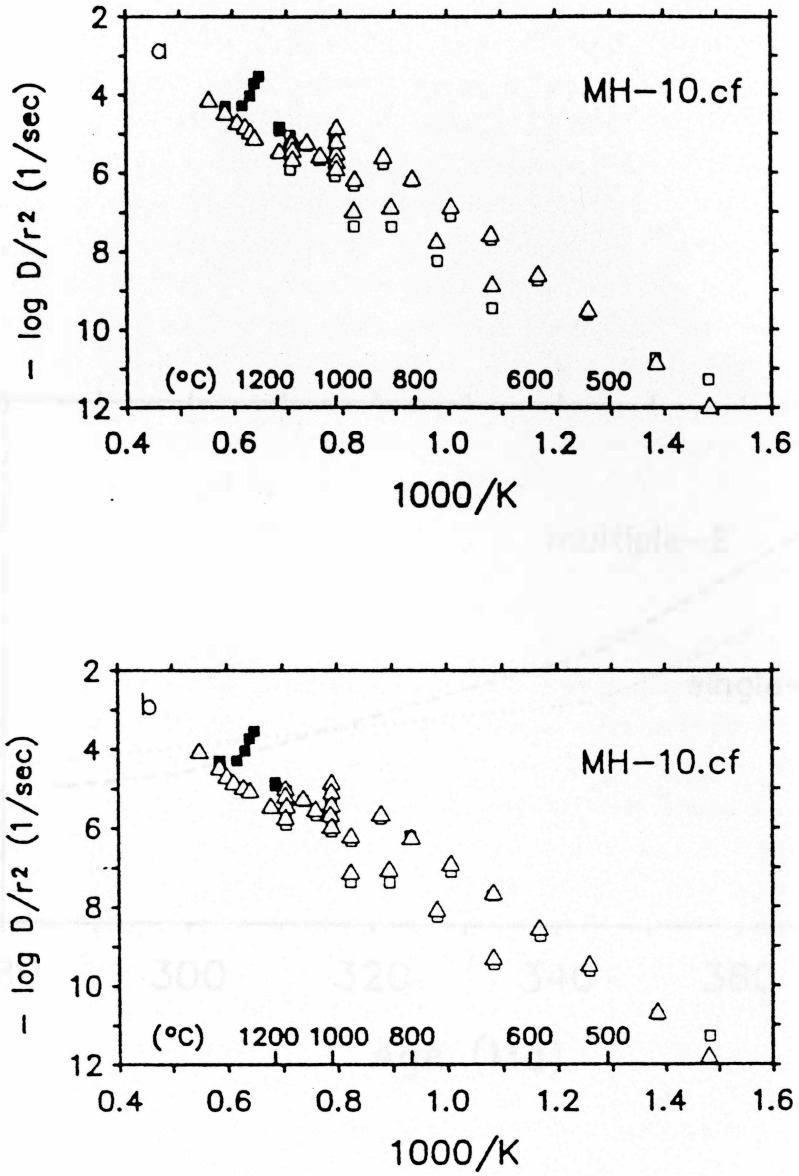

Fig. 28. Effect on computed thermal history of assuming equivalent activation energy for all domains. a) Model Arrhenius plot (triangles) versus observed Arrhenius plot (squares) obtained by cycling temperature. The model plot is calculated assuming equivalent activation energy for all domains. It fails to reproduce the observed plot for steps cycled to low temperature. b) New model (triangles) versus the same observed plot (squares) as in a). This model uses activation energy of 8 kcal/mol higher for medium and large domains than that calculated for small domains and applied to all domains in a). Note the better fit at lowered-T cycled steps. (After Harrison et al., 1991).

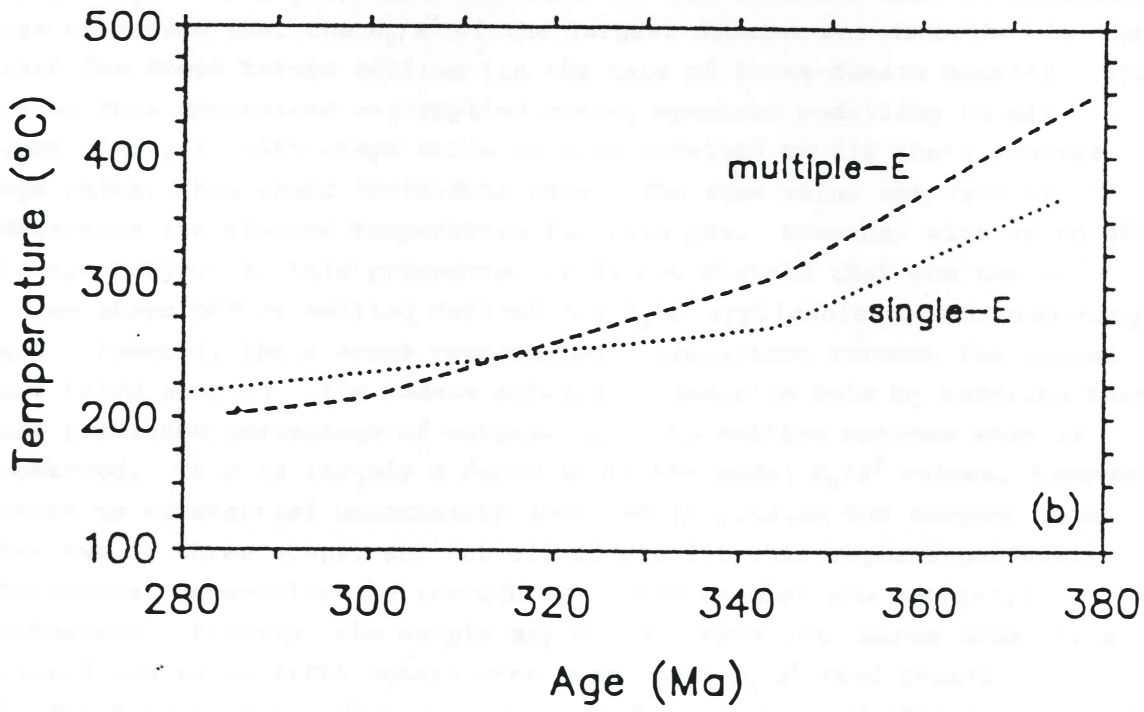

Fig. 28 cont'd. c) Temperature histories defined by the two different models. Essentially identical fits to the age spectrum were obtained for the different models, but the resulting thermal histories differ by as much as 30°C. The multiple E_a model yields much higher temperatures at equivalent times for the medium and large domains in the sample. (After Harrison et al., 1991).

the samples at incongruent melting at 1150°C or less. This is an avoidable problem if all heating steps are kept very short in duration, especially at lower temperatures, and if temperatures are increased in small increments during heating. The most extreme cases of this problem are samples GF-32K (Fig. 18a), GF-7K (Fig. 23), GF-35K-2 (Fig. 25b), and CI-14K (Fig. 26a), which yielded 26%, 40%, 31% and 40% of total gas, respectively, in single steps. Sample breakdown causes the Ar to escape by some mechanism other than by which it occurred in nature (and probably not volume diffusion), and invalidates the mathematical description of diffusion used in the modelling procedure. The ^{40}Ar is probably re-distributed during melting, and thus the ages of individual steps beyond this point are meaningless. The solution used in modelling was to assume that the D_0/a^2 of the largest domains was described by the last few steps before melting (in the case of three-domain models). The value thus determined was applied during spectrum modelling to all remaining gas, with steps above melting modelled to fit their average age rather than their individual ages. The same value was used to determine the closure temperature for this gas. However, with up to 40% of gas subject to this procedure, it is not certain that the two or three steps before melting defined the D_0/a^2 applicable to all remaining gas. Possibly these steps represented a transition between the second and third domains. The models attempt to describe this by ensuring that the predicted percentage of outgassing up to melting matches what is observed. This is largely a function of the model D_0/a^2 values; however there is substantial uncertainty involved in finding the correct value for two or three steps, and not all models fit this segment perfectly. Additional uncertainty is introduced if the samples are not fully outgassed. Finally, the sample may contain more than three domains: a fourth and maybe fifth domain with even lower D_0/a^2 (and therefore higher T_c) may exist (Foster et al., 1990). Because of this the closure temperatures calculated from the present models must again be considered minima, especially for the modelled samples GF-32K and CI-14K which had large melting steps.

The correct cooling rate to assign to the large domains is also uncertain when the sample melts, since the model spectrum uses an arbitrary peak age and cooling rate. The only constraint on their selection is that the total gas age of this section is approximately equivalent to the total gas age of the melting steps. If too low a peak age is selected, the cooling rate will be too high, and vice-versa. For the models of samples with large melting steps, the cooling rates may not be valid for large domains.

The heating schedules used here were responsible for a final

degree of uncertainty; since some samples yielded up to 13% of their gas in steps beyond melting, it is possible that some samples were not fully outgassed even if taken to the melting temperature. GF-20K, GF-18K and CI-20K are subject to this uncertainty, since they were heated to maximum temperatures of 1170 (±20)°C for the first two and 1150 (±20)°C for the last, with no observed melting step. The heating was conducted following coarse heating schedules, identical to schedules which left substantial gas at melting and beyond in other samples. For all three samples additional gas was obtained in short repeat steps at equal and lower temperatures, but as temperature is the main controlling influence on outgassing during step-heating, it is possible that not all gas was obtained. The net result of failure to fully outgas samples is that D_0/a^2 values are too high, and lead to underestimated closure temperatures.

Uncertainty in D_0/a^2 is of much less importance in the calculation of T_c than the E_a term, which is directly proportional to T_c. However, for these three samples, it is possible that closure temperatures are additionally underestimated due to this problem.

4.3.2 Summary of Results

The results of this study are admittedly only a first-pass attempt at determining multiple T-t points from K-feldspars, because of the difficulties described above. However, several conclusions can be reached about the samples considering the points just addressed.

In samples GF-32K and CI-14K, T_c may be slightly underestimated for the oldest gas in the sample because of large melting steps, and the associated cooling rates may be erroneous. For GF-20K, GF-18K and CI-20K, incomplete outgassing may have reduced the T_c estimate. Underestimation of activation energy may dominate these other effects in large and medium domains; therefore for most samples, model T_c's for large and medium domains could be underestimated to some degree, probably less than 30°C (Harrison et al., 1991). In GF-18K and CI-20K, however, the effect is probably offset, and possibly overcompensated, by overestimation of cooling rates for larger domains. Cooling rates obtained by modelling will also not be strictly valid for samples with multiple E_a. For small domains in GF-18K and CI-20K, not affected by dike intrusion, the estimated activation energy and cooling rates should be correct, but the possible failure to fully outgas the samples may lead to slight underestimation of T_c in these domains as well. They should also be treated as minima.

The two different spectra from samples GF-35K and GF-35K-2, although unmodelled, can now potentially be interpreted, given that the

multiple diffusion domain theory explains their differences. The heating schedule for GF-35K was relatively fine compared to others in this study, with more steps taken at smaller temperature intervals below 900°C than for other samples (see Appendix C, $^{40}Ar/^{39}Ar$ Data Summary Sheets). At 1150°C no large melting step was observed, and the peak ages of gas obtained from the sample were consistent with the oldest gas in GF-35K-2, which was heated to 1210°C. These observations suggest that GF-35K may in fact have been nearly fully outgassed at 1150°C. The peak "plateau" age of 979 Ma is therefore taken as the maximum age of the K-feldspar in this sample. This probably corresponds to a minimum closure temperature of 200 - 250°C, based on the results for other samples in this study. The plateau-like feature in GF-35K-2 at 935 Ma may correspond to the peak age of "medium" domains but without modelling it is difficult to pinpoint an exact age, since the contribution of gas from larger domains to these steps is uncertain.

A summary of all K-feldspar T-t data with their interpreted significance is given in Table 3.

4.3.3 Comment on Multiple Diffusion Domain Theory

The "old" method of determining K-feldspar T-t points, of assigning estimated closure temperatures to flat portions of spectra, is a limiting procedure. The variability of peak ages obtained in this study and the existence of stepped age spectra demonstrates that K-feldspars close at a range of closure temperatures, probably in the range of 125 to over 300°C. Assigning an assumed temperature covering this range to a single age would lead to a large swath, rather than a controlled curve, on a T-t diagram.

The question of whether kinks in Arrhenius plots demonstrate sample breakdown, and therefore invalidate calculated diffusion parameters, has yet to be answered. However, despite the complications introduced by the non-ideal data modelled in this study, a reasonable set of T-t points has been obtained using the multiple diffusion domain theory. Additionally, several observations can only be explained by the theory. It seems likely that this theory correctly describes Ar diffusion in K-feldspar, at least in general terms. The T-t points obtained here are therefore considered to be reasonable constraints on the low-temperature cooling history of the Grenville Front Tectonic Zone. Further assessment of their validity follows in Chapter V (Synthesis of Results and Cooling History).

Table 3: Summary of K-feldspar Modelling Results

Sample Number	E_a kcal/mol	D_0/a^2 sec^{-1}	$\frac{dT}{dt}$* °C/My	T_c °C	Age Ma	Comments
GF-42K	-	-	-	200±75	886±26	Ages are minima;
GF-62K	-	-	-	200±75	903±12	T_c's are estimated.
GF-32K	38.6 ±1.0	5.5	0.26	232±14	1010±20	T_c is a minimum@.
		500	0.07	168±12	865±18	T_c is a minimum@.
		6000	-	-	-	Reset by dike.
GF-20K	36.9 ±5.8	5	0.12	203±74	1080±10	T_c is a minimum@.
		9	0.06	185±72	1010±10	T_c is a minimum@.
		2000	-	-	-	Reset by dike.
GF-19K	-	-	-	-	-	Strongly reset by dike
GF-18K	38.8 ±3.2	30	53.2	285±44	920±10	Cooling rate too high; T_c uncertain.
		3000	0.05	150±34	825±8	T_c is a minimum@.
GF-7K	-	-	-	200±75	1045±10	T_c is estimated.
CI-20K	32.8 ±2.0	0.15	17.3	261±34	910±18	Cooling rate too high; T_c uncertain.
		9	0.34	170±28	900±18	T_c a minimum@.
		275	0.24	101±24	725±14	T_c a minimum@.
GF-35K	-	-	-	250±50	979±10	T_c estimated;
GF-35K-2	-	-	-			peak age is for both aliquots
CI-14K	33.2 ±3.4	1.25	0.09	166±44	1060±22	T_c a minimum@.
		250	-	-	-	Reset by dike.
		250	-	-	-	Reset by dike.

* All cooling rates are uncertain because of uncertainty in T_c.
@ T_c may be underestimated in these samples by up to 30°C.

CHAPTER V
SYNTHESIS OF RESULTS AND THERMAL HISTORY

5.1 CLOSURE TEMPERATURES AND RESETTING

In order to interpret thermochronologic data, appropriate closure temperatures must be assumed. Closure temperatures are only applicable to samples which have undergone simple cooling histories. If rocks have suffered a subsequent thermal episode which partially resets their isotopic systems, the date obtained may no longer represent cooling through a fixed temperature. All dates obtained in a study of this kind must be assessed with this in mind before they are interpreted as ages and used in construction of cooling paths.

The closure temperatures applicable to different domains in K-feldspar have been determined experimentally as described in Chapter 4. For titanite, hornblende, and biotite, T_c must be assumed; the rationale for closure temperatures assigned in this study is described below.

5.1.1 Closure Temperature in the Titanite U-Pb System

Titanite closure temperature is often cited as being in the range 600 - 650°C (Ghent et al., 1988), but as for the $^{40}Ar/^{39}Ar$ system, closure temperature is a function of cooling rate and effective diffusion distance as well as activation energy. Some geochronologists now quote titanite closure as being in the range of 500 - 670°C, depending on grain size, which is thought to describe effective diffusion distance (Mezger et al., 1991). By comparison with estimated conditions of metamorphism, Tucker et al. (1987) found that titanite could lose significant radiogenic Pb at temperatures as low as 480 - 540°C, implying that Pb diffuses in titanite in the range of 500°C. Based on evidence to follow from other isotopic systems, titanite in the GFTZ underwent partial resetting at temperatures which in some places probably did not exceed 500 - 550°C. Normally, for simple post-metamorphic or post-intrusion cooling, titanite yields cooling ages older than hornblende (e.g. Corrigan, 1990; DeWitt et al., 1984). It will be assumed here that the lower intercept obtained on a concordia diagram represents cooling of titanite through a closure temperature of 500°C or higher, as compared to the lower T_c of hornblende, described below.

5.1.2 Closure Temperature in the Hornblende $^{40}Ar/^{39}Ar$ System

Substantial work has been undertaken on hornblende in recent years to try to better determine its closure behaviour. Hydrothermal diffusion experiments and empirical field studies have been conducted by

various workers (Harrison, 1981; Harrison and McDougall, 1980; Onstott and Peacock, 1987; Baldwin et al., 1990). Relatively consistent values of activation energy have been obtained by these studies (60 - 65 kcal/mol), but it is becoming apparent that as for K-feldspar, effective diffusion distances for Ar are not necessarily dictated by the physical grain size of the separate, but by some other sub-grain size structures. Candidates for these structures are phyllosilicate intergrowths or alteration, and exsolution lamellae (Baldwin et al., 1990; Onstott and Peacock, 1987), which may subdivide the hornblende into domains ranging down to 10μ in size. The effect of these is to lower the retentivity of the hornblende, and thus to lower the closure temperature. Calculated closure temperatures using the best available diffusion parameters and the effective diffusion radii defined by such features are as low as 360 to 450°C in some samples for slow cooling of 5°C/Ma (Baldwin et al., 1990; Onstott and Peacock, 1987). For more homogeneous hornblendes, assuming effective radii closer to the physical grain size of the separate yields closure temperatures on the order of 500°C. Homogeneous igneous hornblendes cooled rapidly may close as high as 580°C (Harrison, 1981).

Proper characterization of microstructure and textures using TEM and SEM is needed in order to define the possible sizes of effective diffusion radii. This is beyond the scope of this study, but observations in thin-section reveal the presence of brown cryptocrystalline alteration products, probably phyllosilicates, along cleavage planes in most hornblende samples dated here. The timing of these features is uncertain and they may post-date cooling after the Grenville orogeny, but given the long history of the GFTZ (e.g. at least one metamorphism by 1450 Ma), they or similar features may have been present and acted as diffusion pathways for Ar during the ca. 1.0 Ga Grenvillian episode in the area. This uncertainty requires that a fairly large possible range of T_c be assigned; about 450 ±50°C is considered appropriate.

5.1.3 Closure Temperature in the Biotite $^{40}Ar/^{39}Ar$ System

Experimental work has also been carried out on biotite but much of it has been invalidated due to failure to keep the sample stable throughout the experiment (McDougall and Harrison, 1988). The few remaining experiments yield varying results, possibly because of compositional dependence of diffusion parameters in biotite (Harrison et al., 1985). The best estimates of closure temperature in biotite require assignment of substantial uncertainty to the value, in order to incorporate this possibility as well as the dependence on cooling rates

inherent in all T_c determinations. Based on experimental work as well as comparison of results from field studies, a T_c of 300 ±50°C is considered realistic for biotite.

5.1.4 Resetting of Radioactive Isotopic Systems

The systematics of U-Pb in titanite and K-Ar in hornblende and biotite are poorly understood for increasing temperature. Closure temperature (T_c) is not necessarily equivalent to "opening" temperature (T_o), which is the temperature at which an isotopic system is fully reset during re-heating. T_c and T_o may be different because of differences in heating/ cooling rates or in kinetic behaviour during heating versus cooling (Cliff, 1985). A general, "very rough rule of thumb" given in a review paper by Zeitler (1989) is that heating to closure temperature (as defined for cooling rates of 10°C/Ma) requires 10 Ma to induce 99% resetting, and for a duration of only 1 Ma, overstepping of 50 - 100°C above T_c would be required for 99% resetting. Additionally, the kinetic differences between the behaviour of Pb in titanite, which is part of the crystal structure, and Ar, which is inert and occupies voids, are not understood. Therefore for conditions of increasing temperature, the degree of resetting of one system may be quite different from the degree of resetting of another, despite having similar closure temperatures. However, it can be stated qualitatively that partial resetting may occur at temperatures as low as closure, but complete resetting will require overstepping of T_c by some amount depending on the duration of the event.

Additionally, studies of the effect of strain on resetting K-Ar isotopic ages show that although temperature is the main control on diffusive loss of Ar, recrystallization due to strain accompanying a temperature increase can facilitate resetting (Desmons et al., 1982; Berry and McDougall, 1986) since creation of new, smaller grains will speed diffusive argon loss (Dempster, 1986). The Tucker et al. (1987) study also demonstrated the facilitating effect of strain on resetting of the U-Pb system in titanite. Temperature is the dominant factor, so that minimum closure temperature must be reached to reset ages. However, the overstepping of T_c required during a short thermal event accompanied by strain is probably less than for a short, purely thermal event.

5.2 INTEGRATED INTERPRETATION OF RESULTS

The best way to interpret the $^{40}Ar/^{39}Ar$ results obtained in this study is by comparison, both between nearby samples, and with the titanite results. As described in section 2.3 (Discussion of Titanite

Results), titanite records a thermal event causing partial resetting at 985 +21/-20 Ma which affected the transect to a greater degree with increasing distance from the Grenville Front. The upper intercept age of ca. 1450 Ma is apparently the age of a granulite grade metamorphic event in the parautochthon of the southwestern Grenville Province. The single discordia between the upper and lower intercept which fits all data suggests that no significant thermal episode occurred in this region in the intervening 450 Ma. Because titanite results are from the GFTZ, this region will be addressed before the foreland results are discussed.

5.2.1 Grenville Front Tectonic Zone

The variability of the $^{40}Ar/^{39}Ar$ dates from the GFTZ presented in Chapters 3 and 4 clearly demonstrates the importance of dating multiple samples in a small area when studying a region of complex metamorphic and structural history. Only a few samples in this study have provided unequivocal, easily interpreted spectra. Howevever, most samples dated provide some information about Grenvillian or earlier events when interpreted in light of all available data, from several phases in the same sample or from nearby outcrops. The results will be discussed in these groupings, starting with samples nearest the Grenville Front and moving eastward into the GFTZ.

Grenville Front to Mill Lake

Hornblende from a thin, mylonitic amphibolite dikelet on the Grenville Front Boundary Fault ("the Front") failed to yield a useable age, because of contamination of the separate despite careful picking. Although the age spectrum is extremely complex, the total gas age of the sample is 1417 Ma, which seems a reasonable age for cooling following a high-temperature 1450 Ma event. It is tempting to interpret the complex spectrum as a result of re-distribution of Ar, without loss or gain, due to subsequent deformation on the Grenville Front (e.g. Maluski, 1978). The difference in apparent versus measured Ca/K ratios clearly demonstrates that a higher-K phase, probably biotite, is contributing significantly to the gas obtained from the sample. Thus the total gas age is at best some average of hornblende and biotite ages, and given the propensity of biotite to contain excess Ar, may not represent a mixture of cooling ages, but rather, a meaningless number. This sample shows the value of calculating apparent compositional data from the isotope ratios and comparing it to electron microprobe data in order to assess sample purity.

Sample GF-32H is from a hornblende-bearing quartzofeldspathic

gneiss, about 1.5 kilometres into the GFTZ. It has no plateau but yields a fairly flat spectrum with a near-plateau age of 1215 ± 18 Ma. A titanite fraction dated from the same rock gave a 9.7% discordant point on the 1446 - 985 Ma discordia. Titanite is generally considered to have a higher closure temperature than hornblende (500°C or more versus 450 ± 50°C for metamorphic hornblende), meaning that during cooling it closes to diffusive loss of radiogenic Pb before hornblende closes to loss of radiogenic Ar. However, the systematics of U-Pb in titanite and K-Ar in hornblende are much less well understood for increasing temperature, as described above. Titanite and hornblende in the same rock experiencing the same temperature increase may thus respond quite differently. Also, there is some evidence that in this sample, partial resetting of titanite may have been facilitated by strain accompanying the thermal event at ca. 985 Ma.

The 1215 Ma date obtained for GF-32H hornblende may therefore represent very slow cooling following the 1446 Ma event with no effects from the 985 Ma episode. Alternatively, it may be a result of an event not recorded in titanite, such as intrusion of the Sudbury dike swarm at 1238 Ma (Krogh et al., 1987). The outcrop from which sample GF-32 was taken is not near any known Sudbury dike so thermal effects from intrusion of a dike are unlikely. However, intrusion of the dike swarm could also have caused, or been the result of, a regional uplift event which induced exhumation and cooling through the closure temperature for hornblende, having passed through the temperature for U-Pb titanite closure 240 Ma before. Little other evidence is available from data obtained in this study to support this theory (excepting CI-37H, discussion to follow), but several K-Ar dates on biotite and muscovite in the Killarney Complex about 5 to 10 kilometres west yield consistent values of 1180 to 1190 Ma (± 40 Ma) (Wanless et al., 1974; Lowdon et al., 1963). 20 to 35 kilometres farther northeast in the Southern Province, the only other two K-Ar muscovites dated from north of the Grenville Front in this region give ages of 1224 ±45 Ma (2σ) and 1224 ± 40 Ma (2σ) (Wanless et al., 1974; ages recalculated using the decay constants of Steiger and Jäger (1977) by Anderson (1988)). The mutual consistency of these dates at about 1200 Ma suggests they may represent a real event. As closure temperatures of micas are generally lower than those for hornblende, these dates might demonstrate further cooling of the whole area.

The 1215 Ma date for GF-32H could also indicate the presence of excess Ar, but as it does not exceed the age of titanite, this cannot be confirmed.

Given the evidence of partial resetting of titanite at about 985

Ma, the best interpretation of the 1215 Ma date is that it represents partial resetting of the K-Ar system in hornblende during the same event. The relative flatness of the age spectrum may be a result of homogenization of isotopes due to sample breakdown during <u>in vacuo</u> heating (Maboko et al., 1990; Lee et al., 1991), eliminating any ^{40}Ar gradients induced by partial resetting. The latter interpretation precludes use of this date in a T-t history of the area as it does not represent the true age of any event or of cooling. However, some speculation is possible using the Zeitler (1989) "rule of thumb". Temperatures during the thermal event at ca. 985 Ma could have reached but not exceeded hornblende closure for less than ten million years, without complete resetting, or about 50°C higher for one million years. The duration of the thermal episode is uncertain but assuming a maximum T_c for hornblende of 500°C, maximum temperatures of 550°C are implicated for the event, assuming it lasted 1 Ma or more. The small degree of resetting of the titanite suggests that this value could be even lower, but could not be less than 500°C without leaving the titanite undisturbed. Strain could also have facilitated resetting in the hornblende (e.g. Desmons et al., 1982; Deutsch and Steiger, 1985), as it may have done for titanite.

A K-feldspar was also dated from this sample. GF-32K yielded a regularly stepping age spectrum which had a modelled peak age of about 1010 Ma, corresponding to a minimum T_c of 232 ±14°C. Error cannot be mathematically calculated for a model but considering the error in J-value only, of ±2% (2σ) for this sample, a <u>minimum</u> error of ±20 Ma can be assigned to the model age, which is of course based on the step-heating data. The 1010 ±20 Ma peak age is then consistent (at about 990 Ma) with the 985 +21/-20 Ma age of partial resetting of titanite, implying that the K-feldspar in this sample could have been completely reset at the same time. Evidence to follow demonstrates that farther east along the transect, cooling to a similar temperature range occurred slightly later; this suggests diachronous cooling in the two parts of the transect. Alternatively, this K-feldspar could contain excess Ar. The preferred interpretation is that this is a real cooling age, partly because the spectrum has a 995 (±20 Ma) melting step. The model age is 1010 ±20 Ma mainly because of the effect of apparently older gas obtained after melting, for which Ar systematics are not understood. Assuming the age is a cooling age, the virtually identical peak age of the feldspar and the titanite lower intercept implies rapid cooling, in agreement with the interpretation of the titanite discordia discussed in Chapter 2. Cooling must have slowed soon afterwards, as the sample did not cool below about 170°C before 865 Ma.

Sample CI-37H was obtained from a thin, isoclinally folded amphibolite unit from about 3 kilometres east of the "Front". This unit is one of a series of very thin, dike-like units which are abundant along Collins Inlet (Burke, 1991) and is probably compositionally equivalent to GF-2H which was taken from a similar unit. In this area, these metabasic rocks have the mineral assemblage hornblende - plagioclase - biotite - quartz, indicative of middle amphibolite grade metamorphism (of uncertain age). The separate yields a fairly flat spectrum, but as for GF-2H, Ca/K ratio analysis indicates contribution of gas from a higher K and/or lower Ca phase. The discrepancy in Ca/K ratios is small in this sample, suggesting that the contribution is relatively minor. The best date for the sample is about 1213 Ma, in close agreement with the date of 1215 Ma obtained for GF-32H. This may further support the argument of an event at about this time not recorded in titanite, possibly slight exhumation and cooling following Sudbury dike intrusion. Unfortunately, no further evidence is available to test this hypothesis, and the evidence presented here is at best tenuous. Given the lack of further data, the interpretation that this too is a partially reset hornblende, which has undergone isotope homogenization to eliminate age gradients, must be preferred, and again no T-t point assigned.

A K-feldspar, GF-20K, was dated from a nearby outcrop of granitic gneiss, about 250 metres across Collins Inlet from CI-37H. A model peak age of 1080 Ma is obtained for the sample, to describe gas released above the melting temperature. Given the evidence presented so far that there was a thermal event at ca. 990 - 985 Ma, the age spectrum for this sample may be the complex result of substantial but not complete resetting. However, temperatures in this area must have reached 500°C or more, which for all K-feldspars known to date (Harrison, 1990) would be sufficient to fully reset the K-Ar system. Therefore it must be assumed that the K-feldspar contains excess Ar. According to either interpretation, the T-t points calculated by modelling are meaningless.

Titanite was also dated from this sample and produced a 5.7% discordant point on the discordia, the least discordant of all titanite dated in this study, despite being from about 1.5 kilometres further into the GFTZ than GF-32. A possible interpretation, as noted in section 2.3 (Discussion of Titanite Results), is that GF-32 has undergone more strain due to its proximity to the Grenville Front Boundary Fault, and its titanite is therefore more susceptible to diffusive loss of lead than in GF-20.

No further hornblende was dated in the next 6.5 kilometres of perpendicular distance from the Front. Two K-feldspars from granitic

gneisses were dated in this stretch and give results which provide limited information about post-Grenvillian cooling and other events. The first, GF-19K, was strongly affected by gas loss due to intrusion of a Grenville dike along Collins Inlet. This and other samples provide a re-definition of the age of these dikes as 598 ±6 Ma, previously thought to be about 575 Ma (Fahrig and West, 1986). Because GF-19K suffered considerable gas loss at this time, it is uncertain whether its peak age of 888 Ma is a cooling age or a result of partial resetting during the Grenville and/or the dike intrusion episode. Also, it was only heated to 1150°C during step-heating, possibly inadequate to fully outgas it. Biotite from this rock (GF-19B) yielded meaningless results due to excess Ar.

The second sample, GF-18K, gave somewhat equivocal results because of an unusually shaped age spectrum and possible failure to fully outgas the sample. However results are adequate to attempt modelling and yielded two approximate points on the post-Grenvillian cooling curve. The age of the oldest step is 918 Ma, implying complete resetting of the sample during the ca. 990 - 985 Ma event. This age may be a minimum since there is evidence that older gas may have been left in the sample during step-heating. Modelling of the age spectrum further justifies this interpretation, which causes uncertainty in the T-t points obtained. Cooling through a closure temperature of about 285 ±44°C at 920 Ma or earlier can be inferred from the data; subsequent cooling to as low as 150°C by 850 Ma followed. This is in close agreement with data from GF-32K, which defined cooling to as low as 170°C by 865 Ma.

Summarizing all data available for this section of Collins Inlet (Grenville Front to Mill Lake), at about 985 +21/-20 Ma the area underwent a temperature increase which resulted in variable resetting of different isotopic systems. Based on hornblende $^{40}Ar/^{39}Ar$ data, temperatures did not exceed about 550°C but must have reached 500°C for a brief time in order to partially reset titanite. Strain on the Grenville Front may have accompanied this thermal event, facilitating resetting of isotopic systems in nearby rocks. Extremely rapid cooling followed until 990 Ma or later. Subsequent cooling must have slowed drastically as the area was still at 150 - 170°C or more at 850 - 865 Ma.

Mill Lake

The next set of data comes from samples taken on the shores and islands of Mill Lake. This section of the transect is underlain by interlayered metasediments and metabasites, providing the best opportunity to assess metamorphic grade along the transect. Assemblages

of garnet - sillimanite - K-feldspar - plagioclase - quartz in metapelites and garnet - orthopyroxene - plagioclase - quartz - Fe-Ti oxides - (hornblende) in some metabasites demonstrate that these rocks have been metamorphosed at granulite grade. Hornblende rims orthopyroxene, indicating subsequent retrogression. Not all metabasites contain orthopyroxene or garnet; whether this is due to differences in bulk composition or to complete retrogression is not clear. However, southeast of this area units are migmatitic in places (Davidson and Bethune, 1988), suggesting that east of Mill Lake metamorphic grade is higher than the middle amphibolite facies described by the metabasites west of Mill Lake. All rocks in Mill Lake have undergone substantial strain, demonstrated by quartz ribbons in pelites and elongate, fractured garnet in amphibolite. The times of metamorphism and strain are uncertain.

Dated samples from the area yield complex results. A biotite (GF-7B) separated from a metapelitic outcrop on an island in the lake yielded a fairly flat spectrum but shows evidence of slight alteration to chlorite. K-feldspar from the same sample (GF-7K) could not be modelled but gave peak ages in the range of 1045 Ma (excluding contribution from sericite). The maximum ages of both these minerals are not unreasonable given the timing of events occurring in the nearby Britt domain of the interior Grenville Province. However, the K-feldspar was heated during analysis only to 1150°C with no repeat steps, and may have contained older gas yet, as do other samples heated above 1150°C in this study. Also, there is abundant evidence already presented that even closer to the Grenville Front, temperatures reached between 500°C and 550°C during the thermal event at ca. 990 - 985 Ma, and that the intensity of this event increased to the southeast. Both K-feldspar and biotite would have suffered complete loss of Ar under these conditions, making the two samples suspect of having incorporated excess Ar. They therefore cannot be used to define T-t points to constrain the cooling history of the area.

Two hornblende samples were dated from an outcrop southeast of GF-7. The samples were taken about 7 metres apart in the same boudinaged amphibolite unit. A bulk sample (GF-8H) of about 300 milligrams dated on the MS-10 system gave a classic U-shaped excess Ar spectrum, defining a maximum age of 1111 Ma. A 1.9 milligram separate (TZ-19H) dated on the VG3600 system yielded a poorly understood concave downward age spectrum. This may be due to experimental artifacts, or an unrecognized geological explanation such as very late strain. However, all apparent ages are too young for the sample to contain excess Ar. Neither of these results provide much information on the Grenvillian history of the

area except to show that it was affected more by reheating at some point later than 1450 Ma than were hornblendes nearer the Front, since its maximum age is 1111 Ma. Nevertheless, they demonstrate that excess Ar is not necessarily a ubiquitous phenomenon even on the scale of a single outcrop, and must therefore be proven before it is used as an explanation for unexpected results.

Biotite dated from the same sample as the hornblende with excess argon yielded a plateau age of 954 ± 7 Ma, which is geologically reasonable, and has clearly been completely reset. Due to the propensity of biotite to contain excess Ar, this age must be considered a maximum; evidence to follow suggests it is probably a valid cooling age. Biotite closure temperatures are generally accepted to be in the range of 300 ±50°C, depending on cooling rates. For probable cooling rates at 30 Ma after the thermal event of 10°C/Ma or less, the actual closure temperature for biotite in this transect is probably at the low end of the estimated range, less than 300°C.

In summary, most data available from the group of samples in Mill Lake are subject to problems of excess Ar. This may be a result of the high strain state of the rocks in this area, which may have facilitated movement of fluids, including ^{40}Ar, from deeper crustal levels during the ca. 990 Ma thermal event. The biotite GF-8B, however, provides a T-t point on the cooling curve which helps constrain the K-feldspar results in nearby samples.

Mill Lake to Beaverstone Bay

The remaining part of the transect east of Mill Lake gave consistent results for all phases dated and will be considered together here. Three hornblende separates from different rock types yielded mutually consistent ages of 988.0 ±14 Ma, 987.7 ±15.4 Ma, and 979±8 Ma (CI-19H, GF-34H, and GF-35H, respectively; 2σ errors). These ages are indistinguishable from the 985 +21/-20 Ma age of the titanite lower intercept, demonstrating that in this part of the GFTZ, the thermal episode causing partial resetting of titanite succeeded in completely resetting hornblende. Hornblende closure temperatures were probably about 450 ±50°C, so temperatures of resetting must have reached well above 500°C in this area. The virtually identical age of the titanite lower intercept and hornblende, as well as further evidence available from feldspars and from other studies, suggests that this episode may have been brief, requiring overstepping of closure temperatures in order to accelerate resetting; if this is the case, temperatures may have been as high as 600 - 650°. It is unlikely that temperatures reached higher than this because if so, titanite would have been fully reset. The

possible T-range of this event, of 500 - 650°C, is not hot enough to have produced the granulite grade metamorphic assemblages preserved in the rocks in Mill Lake; however, it could have induced retrogression of orthopyroxene to hornblende. The first metamorphic episode recorded in the rock must therefore pre-date the 990 Ma thermal event. Likewise, maximum temperatures of 600 - 650°C probably would not cause generation of migmatitic melts in the gneisses east of Mill Lake (Turner, 1981), suggesting that this metamorphic event also pre-dates the 990 Ma event. The continuous discordia between 1446 Ma and 985 Ma in titanites across this transect shows that no other metamorphism at temperatures higher than about 500°C could have occurred in the intervening 460 Ma. The granulite grade metamorphism must be 1450 Ma or older.

A biotite from sample GF-35 (GF-35B) yields a nearly concordant spectrum. The age spectrum clearly gives excessive ages since they exceed the consistent hornblende ages by about 250 Ma. Either incorporation of excess Ar or loss of K may be responsible for this.

Three K-feldspars were dated from this area, one in duplicate. The first (CI-20K) is from an outcrop 300 metres across Collins Inlet from the outcrop where hornblende and titanite in sample CI-19 were obtained. It has a relatively flat age spectrum like GF-18K and may not have been fully outgassed during the step-heating experiment since it was heated to a maximum of 1150°C. Maximum ages of steps were about 900 Ma, and may have been slightly higher in the remaining (untapped) gas, as is the normal pattern of feldspars heated with a similar schedule. The sample was clearly entirely reset by the 990 Ma thermal event, and cooled through a poorly defined modelled temperature of 261 ±34°C at about 910 Ma or earlier. The lower temperature part of the spectrum yielded better constrained T-t points implying cooling to 170°C by 900 Ma, and to 101°C by 725 Ma.

Two K-feldspar separates were obtained from sample GF-35, in which titanite, hornblende, and biotite were also dated. They were picked independently and dated on two different systems following different heating schedules (see Appendix C). The spectra obtained are dissimilar, an explainable result as addressed in Section 4.3 (Discussion of K-feldspar Results and Models). Both samples have evidence of gas of maximum age of 979 ±10 Ma, indicating that the sample was fully reset by the 990 Ma event. The virtually identical age of the K-feldspar, hornblende, and titanite lower intercept in this one rock sample (GF-35) suggests extremely rapid cooling to their closure temperatures following heating. Neither K-feldspar aliquot was modelled, so their closure temperature is uncertain, but work by others on modelling K-feldspar using the multiple diffusion domain theory has

yielded maximum temperatures on the order of 400°C for extreme cooling rates of 200°C/Ma (Foster et al., 1990). This is the maximum possible T_c for these samples. A minimum T_c of 250°C is implied by modelling of CI-20K, and if biotite in Mill Lake is considered, T_c must be above 250°C. A range of 300 ±50°C is assigned to the GF-35K peak age, for cooling rates observed here.

A final K-feldspar from slightly east of GF-35 has a maximum (melting) step age of 1038 Ma. Even considering errors, this age is too old to be consistent with all other data from the area. Partial resetting is not a reasonable explanation since several consistent hornblende dates demonstrate that temperatures reached in this area at 990 Ma must have exceeded 500°C, high enough to reset any K-feldspar regardless of structural state. The only rational explanation for this sample is that it contains excess Ar.

Using all data available from this section of the transect, east of Mill Lake, the following conclusions can be reached. The thermal event at about 990 - 985 Ma was of sufficient intensity to fully reset the K-Ar system in amphibole but only affected titanite in part. Temperatures must therefore have exceeded 500°C by a substantial amount, but were probably no higher than 650°C. Based on this well-constrained temperature range, the partial melting and granulite-grade metamorphism which affected the rocks as far west as Mill Lake must be 1446 Ma in age or older. After the thermal event at ca. 990 Ma, cooling occurred very quickly since initial closure of largest domains in K-feldspar, at T's between 250 and 350°C, happened within 5 - 10 m.y. of closure in hornblende; hornblende dates cooling through ca. 450°C at a time indistinguishable from final closure in titanite.

5.2.2 Grenville Foreland

Having constrained the thermal history of the GFTZ near the Front, the foreland results can now be better interpreted.

An amphibole sample (GF-44H) from 11 kilometres northwest of the Front (as identified by Davidson, 1986) yields complicated results which reflect contamination of the sample with secondary phases and/or mobility of potassium. The sample is from an amphibolite pod which may be equivalent to 2220 Ma Nipissing diabase (Card, 1978; Frarey, 1985). If so, this pod, which is adjacent to the northern margin of the Killarney granite, has suffered contact metamorphism at 1740 Ma in addition to greenschist to amphibolite grade metamorphism during the Penokean Orogeny at about 1890 - 1830 Ma (Bickford et al., 1986). A complicated mineralogy and disturbed amphibole age spectrum are probably the result of these multiple, relatively low temperature events. Any

subsequent Grenvillian heating causing complete or partial resetting of the K-Ar system cannot be ruled out using the spectrum of this individual sample. However, given the fact that Grenvillian metamorphism failed to reset titanite or to completely reset hornblende in the GFTZ, approximately 12 kilometres away perpendicular to the Front, sufficient heating of this area to reset amphibole is unlikely. Other evidence from lower closure temperature systems confirms this.

The two K-feldspar samples (GF-42K, GF-62K) from northwest of the Front also give equivocal results because of the failure to fully outgas the samples. Minimum ages of 886 Ma and 900 Ma imply that final closure to Ar could have occurred subsequent to the ca. 1000 Ma Grenville orogeny, but whether this represents cooling following a thermal episode or simply slow cooling due to final erosional unroofing cannot be resolved by this data.

However, the K-Ar muscovite dates of 1180 - 1190 Ma obtained by Wanless et al. (1974), described in section 5.2.1 (GFTZ), are from locations relatively close to the two K-feldspars, about 5 to 10 kilometres northwest of the Boundary fault. Although these K-Ar dates may disguise very complicated thermal histories, the fact that they are older than 990 Ma demonstrates that they were not fully reset at this time and that temperatures in this area could not have exceeded about 350°C since about 1180 Ma. For muscovite, excess Ar is a rare problem (Parrish and Roddick, 1983; Anderson, 1988; McDougall and Harrison, 1988; Culshaw et al., in press). The mutual consistency of the ages from different locations strengthens the argument that these dates are, at worst, partially reset, and may possibly represent ages of cooling or of growth of muscovite.

The poor quality of data obtained in this study for the Grenville foreland precludes determination of its low-temperature thermal history during the Grenville event. Clearly, more work must be conducted in this area before questions related to the possible existence of a foreland basin can be resolved.

5.2.3 Summary of Results

The two extreme ends of the GFTZ part of the transect, near the Grenville Front, and east of Mill Lake, have provided the most useful T-t information of the study. Both areas demonstrate partial resetting of titanite at 985 +21/-20 Ma, which suggests that temperatures exceeded 500°C for a short time. Near the Front, however, hornblende has been only partially reset, in contrast with the eastern end of the transect where hornblendes record post - 990 Ma cooling. This implies that temperatures were not more than 550°C near the Front. East of this,

temperatures may have reached 650°C for a brief time without resetting titanite, and were definitely well above the complete "opening" temperature for hornblende, probably of 500 - 600°C depending on duration of heating. The higher temperatures reached in the eastern part of the transect, as predicted by the titanite discordance array, are therefore confirmed and additionally constrained by hornblende data.

The higher temperature thermal history of the middle part of the transect is not so well constrained, partly because of the absence of hornblende samples over much of Collins Inlet, and partly because of excess argon and other (experimental?) problems. However, titanites from this segment (GF-18, GF-19) fall along the discordia midway between those from the two ends of the transect, thereby implying temperatures midway between the two end ranges of 500 - 550°C and 500 - 650°C.

K-feldspars from each end of the transect have been fully reset by the thermal event, and certain samples preserve a record of very rapid cooling following this event. Near the Front, a "large domain" model cooling age of 1010 ±20 Ma implies cooling through a minimum T_c of 232 ±14°C (could be up to 30°C higher) by no later than about 990 Ma, suggesting that the ca. 985 Ma event in titanite is slightly older, possibly up to its maximum age, within error, of 1006 Ma. Assuming that in Mill Lake the biotite age of 954 ±7 Ma which dates cooling through no lower than 250°C also applies nearer the Front, the true closure temperature of large domains in GF-32K K-feldspar must exceed 250°C. Also assuming that the K-feldspar between this region and Mill Lake records part of the same thermal history, the curve is restricted to cooling through a minimum of 285 ±44°C by 920 Ma or earlier, and to 150 ±34°C by 825 Ma. These points constrain the cooling curve of the Grenville Front to Mill Lake segment of the transect quite well, as shown in Figure 29 (curve A). The maximum temperature reached in this area is used as a starting point for the curve.

At the eastern end of the transect, hornblende and K-feldspar both record rapid cooling after resetting. Two hornblende ages are compatible with cooling as early as 1002 Ma, but a third date is better constrained and gives a maximum age of 987 Ma, probably corresponding to temperatures in the range of 450°C. Cooling to 400°C or lower by about 979 ±10 Ma is defined by K-feldspar, and to about 170°C by 900 Ma. The cooling history is also constrained by the biotite in Mill Lake, presuming it had a similar thermal history. The similarities between the two ends of the transect suggest this is a valid interpretation. Cooling to 300 ±50°C at 954 ±7 Ma is defined. The curve for this segment of the transect is shown in Figure 29 (curve B), again using the maximum temperatures reached as a starting point.

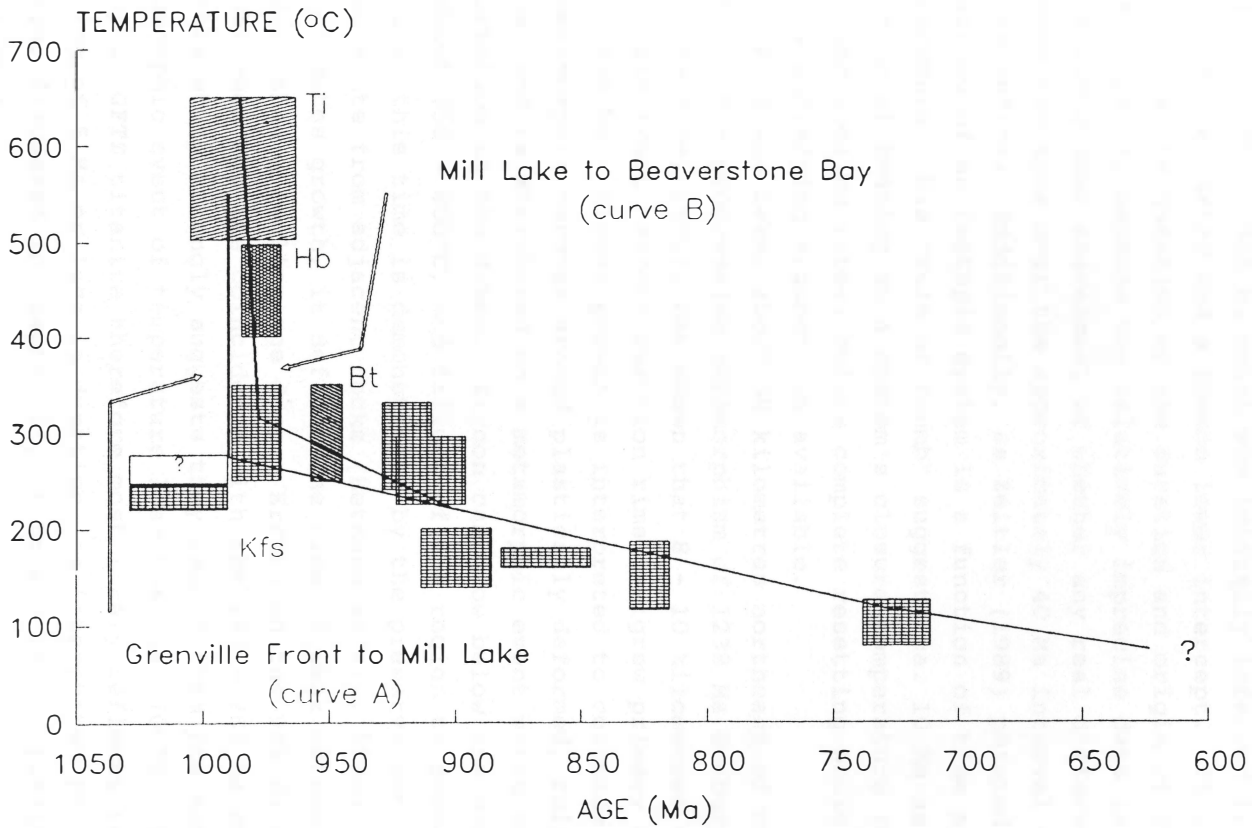

Fig. 29. Cooling history of the Grenville Front Tectonic Zone. Age data are plotted as error boxes. Only cooling data are shown. GF-35H is the only hornblende plotted as its age is identical to others but has the lowest associated error. All valid modelled K-feldspar ages are plotted. The oldest K-feldspar, GF-32K, may have a higher T_c than the calculated model value. The possible range for its T_c is denoted with a blank box containing the small ? symbol. Curve A applies to the Grenville Front to Mill Lake section of the transect, and curve B applies to Mill Lake to Beaverstone Bay. The latter is better constrained. See text for further description.

5.3 DISCUSSION

Both ends of the GFTZ segment of the transect have very similar T-t histories, the main difference being the maximum temperatures reached by the rocks at about 990 Ma. The $^{40}Ar/^{39}Ar$ data confirm the rapid cooling at 990 - 985 Ma which was initially inferred from the fact that all titanites dated had a common lower intercept. It is more difficult to address the question of the duration and origin of the thermal event. This is partly because the relatively imprecise data in this study do not allow closer assessment of whether any real differences exist between the ages over the approximately 40 Ma interval which their errors define. Additionally, as Zeitler (1989) pointed out, degree of resetting of an isotopic system is a function of time as well as temperature. His "rule of thumb" suggests ca. 10 Ma as a maximum duration of heating at a system's closure temperature (as defined for moderate cooling rates) before complete resetting would occur. However, a more satisfying argument is available.

At Tyson Lake, about 30 kilometres northeast of Collins Inlet, a study of the progressive metamorphism of 1238 Ma Sudbury dikes in the GFTZ (Bethune, 1991), has shown that 8 - 10 kilometres southeast of the Grenville Front, zircon reaction rims overgrew primary baddelyite at about 985 Ma. Zircon growth is interpreted to coincide with formation of metamorphic coronas around plastically deformed, relict plagioclase laths, and is attributed to a metamorphic event which outlasted deformation in the dikes. Zircon can grow below its closure temperature of about 750 - 800°C, and failure of the region to reach more than ca. 720°C at this time is demonstrated by the preservation of 1445 Ma ages in monazite from adjacent rocks (Bethune et al., 1990). Because this zircon dates growth, it defines the time of peak metamorphism more closely than a cooling age does. Errors on the 985 Ma date are as yet unpublished but its coincidence with the 990 - 985 Ma cooling identified in this study strongly suggests they result from the same, short-lived metamorphic event of temperature less than ca. 700°C. The discordance array in GFTZ titanite therefore most likely reflects rapid heating and cooling of 5 Ma or less in duration, as interpreted for the similar arrays, discussed in Chapter II, of Hanson et al. (1971) and Tucker et al. (1987).

The cooling ages obtained from $^{40}Ar/^{39}Ar$ dating suggest this metamorphism took place between about 990 and 985 Ma, and was then followed by decreasing cooling rates. Using 990 Ma as the maximum age of peak temperatures, minimum cooling rates for the eastern part of the transect, where the data are better constrained, are on the order of 10°C / Ma, and could be as high as 50°C / Ma, during this time interval.

Cooling then slowed to about 10°C / Ma until closure of diffusion in K-feldspar, then slowed again to rates of about 2 - 6°C / Ma by about 950 Ma. The significance of these conclusions is discussed in Chapter VI.

CHAPTER VI
TECTONIC INTERPRETATION

6.1 THERMAL HISTORY OF THE BRITT DOMAIN

The tectonic relationship of the Grenville Front Tectonic Zone to the orogenic interior is not yet well known, because of a paucity of reliable dates as well as limited geological mapping involving detailed structural and metamorphic analysis. The present study area suffers from both of these problems and therefore lacks a strong tectono-metamorphic database to which the T-t data can be linked. However, by comparing the results of this study with work carried out at other locations along the Grenville Front and in the Britt domain to the southeast, some speculations about the tectonic development of the GFTZ can be made.

Corrigan (1990) and Culshaw et al. (in press) have elucidated the thermal history of the Britt domain of the Central Gneiss Belt, which is the tectonic division of the Grenville province to the southeast of the GFTZ in Ontario. The area underwent metamorphism and deformation at least once before intrusion of granitic bodies at about 1680 Ma. This was followed by a metamorphic episode of unknown age which predated granodiorite with an intrusion age of 1442 Ma. The northern part of the Britt domain (near Key Harbour; see Fig. 2, inset) underwent peak Grenvillian metamorphism at ca. 1035 Ma (slightly discordant U-Pb in monazite). Metamorphic conditions at this time reached 700 - 800°C and 8 - 10 kilobars (Corrigan, 1990). U-Pb data from titanite in the area yield bimodal results, with one group giving ages of 963 - 980 Ma, and a second group, 1001 - 1004 Ma. The older ages are interpreted to represent cooling of the area through titanite closure temperatures of <600°C, while the younger are considered to have remained open to Pb diffusion for longer, or to represent a second generation of growth. Finally, U-Pb zircon dates on a post-tectonic pegmatite dike give precise ages of 990 Ma, and date the time of emplacement of the dikes into warm, ductile, but generally static crust (Corrigan, 1990). Cooling through the closure temperature of hornblende followed at ca. 964 to 974 Ma, both at Key Harbour and throughout the Britt domain to the south (Culshaw et al., in press).

These data illustrate that Grenvillian deformation and metamorphism in northern Britt domain occurred over a much longer time span than the late events in the western part of the GFTZ, identified by this study. The pattern of titanite discordance in the GFTZ rules out metamorphism at temperatures of ≥500°C between about 990 Ma and 1450 Ma. This means that the event causing upper amphibolite grade metamorphism

at ca. 1035 Ma at Key Harbour did not affect rocks of the present transect, 35 kilometres northwest toward the Front.

Additionally, the fact that ca. 990 Ma pegmatite post-dates the major deformation in Britt domain implies that the bulk of Grenvillian thrust-related deformation had ceased by 990 Ma.

Cooling of the Britt domain following these events took much longer than in the GFTZ. Culshaw et al. (in press) have used the U-Pb data of Corrigan (1990) described above in conjunction with $^{40}Ar/^{39}Ar$ dating to derive the cooling history shown in Fig. 30. The curve indicates that the whole Britt domain was still at temperatures of ca. 300°C at 900 Ma, in contrast with the GFTZ, which had cooled to ≤300°C by as early as 954 ±7 Ma, and was at about 200°C at 900 Ma. There is some suggestion in the Culshaw et al. data that cooling was not uniform over the whole area; there appears to be a decrease in cooling ages toward the south, which is supported by data from other workers in the more central part of the Grenville Province (Cosca et al., submitted). The shape of the Culshaw et al. cooling curve hinges strongly on the consistency of muscovite $^{40}Ar/^{39}Ar$ age plateaux at 924 - 904 Ma to which they have assigned a closure temperature of 350 ±25°C. This T_c may be too high, as some workers have demonstrated that muscovite can close as low as 280°C (Snee, 1982; quoted by Zeitler, 1989) and that a value of 320 ±40°C may be more appropriate. For the northern part of the Britt domain, maximum cooling rates from titanite closure at 1000 Ma to hornblende closure at ca. 970 Ma are 5°C / Ma, and for hornblende to muscovite, also 5°C / Ma, although Culshaw et al. predicted slightly lower rates of 2-4°C for this time period.

Unfortunately, no muscovite data are available for the GFTZ, but cooling over the temperature range of 350°C to 250°C is moderately well constrained by the biotite and K-feldspar data from this study; cooling rates during the 990 - 980 Ma time interval were definitely much higher than in Britt domain (minimum rates of 10°C / Ma, but more probably up to 50°C / Ma), although cooling slowed soon afterwards to rates similar to those in the Britt.

6.2 TECTONIC INTERPRETATION

Because the Grenville Front is one of only three recognized fundamental boundaries of the Grenville Province (Rivers et al., 1989), understanding its significance is of great importance in developing tectonic models of the orogen. The data produced by this study shed some light on the problem of the tectonic history of the Front and the adjacent GFTZ.

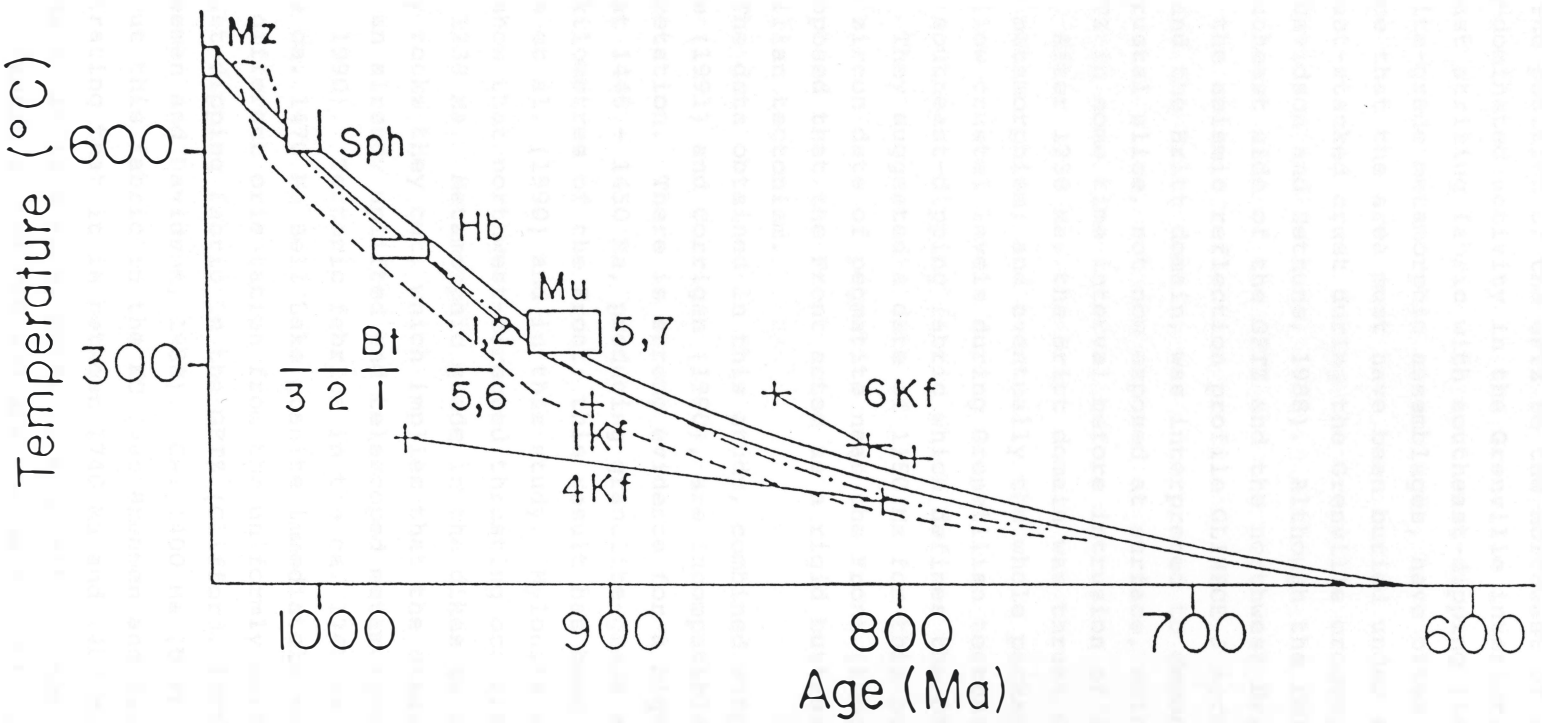

Fig. 30. Cooling history of the Britt domain. Curves shown are possible cooling histories constrained by one-dimensional thermal modelling. Mz = monazite, Sph = titanite (U-Pb dates); Hb = hornblende, Mu = muscovite, Bt = biotite, Kf = K-feldspar (all $^{40}Ar/^{39}Ar$ dates). The biotite and K-feldspar dates which fall below the curves have been attributed to excess Ar. Crosses joined by lines are T-t points obtained for single K-feldspar samples by multiple diffusion domain modelling. Note that at 990 Ma, the Britt domain is undergoing cooling through about 550°C. At 900 Ma, the area is still at temperatures of about 300°C. After Culshaw et al. (in press).

6.2.1 Old Models

The position of the GFTZ to the northwest of northwest-directed, thrust-dominated activity in the Grenville interior, its pervasive northeast striking fabric with southeast-dipping lineations, and its granulite-grade metamorphic assemblages, have often been cited as evidence that the area must have been buried under a considerable depth of thrust-stacked crust during the Grenville orogeny (Green et al., 1988; Davidson and Bethune, 1988). Although the relationship between the southeast side of the GFTZ and the northwest Britt domain is poorly known, the seismic reflection profile GLIMPCE J across the Front, the GFTZ, and the Britt domain, was interpreted to demonstrate the presence of a crustal slice, not now exposed at surface, which was thrust over the GFTZ in some time interval before intrusion of 1238 Ma Sudbury dikes. After 1238 Ma, the Britt domain was thrust over this, causing a second metamorphism; and eventually the whole package was thrust back up to shallow crustal levels during Grenvillian tectonism, generating the strong southeast-dipping fabric which defines the GFTZ (Green et al., 1988). They suggested a date of 1150 Ma for this burial event, based on a U-Pb zircon date of pegmatite near the Front (Krogh and Wardle, 1984), and proposed that the Front acted as a rigid buttress throughout Grenvillian tectonism.

The data obtained in this study, combined with the results of Bethune (1991) and Corrigan (1990), are incompatible with much of this interpretation. There is strong evidence for a high-grade metamorphic event at 1445 - 1450 Ma, producing granulite-grade assemblages within 3 - 9 kilometres of the Front; this result has been obtained both by Bethune et al. (1990) and in this study. Mylonite zones cut by Sudbury dikes show that northwest-directed thrusting occurred along the Front before 1238 Ma. Metamorphic grade in the dikes is lower than in the country rocks they cut, which implies that the dikes were emplaced across an already uplifted and telescoped metamorphic gradient (Bethune et al., 1990). Tectonic fabrics in the ca. 1740 Ma Killarney Complex and the ca. 1470 Ma Bell Lake granite immediately northwest of the Front have a different orientation from the uniformly northeast-striking, southeast-dipping fabric in the GFTZ (Clifford, 1986; Davidson, 1986; van Breemen and Davidson, 1988). Ca. 1400 Ma (U-Pb zircon) pegmatite dikes cut this fabric in the KC (van Breemen and Davidson, 1988), demonstrating that it is between 1740 Ma and 1400 Ma in age. Pegmatite dikes dated at 1430 Ma by Rb-Sr on muscovite (Krogh and Davis, 1970) cut tectonic fabric in the BLG and are themselves cut by 1238 Ma dikes (van Breemen and Davidson, 1988). This fabric must therefore be between 1470 Ma and about 1430 Ma in age. The obvious candidate for the cause of

this is tectonism related to metamorphism at ca. 1445 Ma, which may also have been responsible for initial uplift of granulite grade rocks relative to the foreland in this area. If significant topography was generated by this event, it was probably eroded away by about 200 - 400 My later. However, the voluminous intrusion of granitoids during this interval (1470 Ma Bell Lake granite; 1457 Ma Britt pluton, van Breemen et al., 1986; 1442 Ma Mann Island granodiorite, Corrigan 1990; possibly other granodiorites now with gneissic fabric in the GFTZ and Central Gneiss Belt, van Breemen and Davidson, 1988) suggests that crustal growth and granulite grade metamorphism were primarily related to plutonism. Additionally, not all of these plutons bear the imprint of a tectonic event and metamorphism at this time. The Mann Island granodiorite and Britt pluton are apparently "single-cycle"; that is, affected by only one tectono-metamorphic event, the ca. 1035 Ma Grenville orogeny (Corrigan, 1990). Possibly the peak of deformation and metamorphism at ca. 1450 Ma was outlasted by plutonism, or as van Breemen and Davidson (1988) point out, magmatism and tectonism were not necessarily coeval in different places. These points all argue against burial by an invisible crustal slice to explain pre-1238 Ma metamorphism, as proposed by Green et al. (1988). Whatever the cause and extent of the 1450 Ma activity, it seems probable that at least some of the relative uplift of what became the GFTZ, relative to the Southern Province and Front granites, occurred at this time. This explains in part the juxtapositioning of rocks nearly unaffected by Grenvillian metamorphism with granulite-grade rocks, without invoking 20 kilometres of differential uplift of the GFTZ during Grenville tectonism alone.

In the Collins Inlet transect, granulite-grade metamorphism, of probable 1450 Ma age, is observed in the rocks of the islands of Mill Lake. These are juxtaposed with granitic gneisses containing relict volcaniclastic textures at the southwest end of the lake. The evidence that both west and east of Mill Lake, temperatures at ca. 990 Ma reached relatively similar ranges (maximum 100 - 150°C hotter in the east), suggests that the high-strain zone between the two areas probably accommodated a significant amount of movement well before 990 Ma. Although much of the GFTZ consists of high-strain gneisses and multiple mylonite zones, the position of this zone at the bottom of a package of metasediments surrounded by fairly homogeneous granitoid gneisses, seems a logical location for concentration of strain.

Work along the Grenville Front about 100 kilometres to the northeast, near Sudbury, has demonstrated activity along the Front at about 1150 Ma, possibly related to Grenvillian thrust events of similar age along major boundaries in the interior of the orogen (e.g. van

Breemen et al., 1986). Pegmatoids near the Front contain zircons of 1150 Ma in age (Krogh and Wardle, 1984), implying that minor activity was occurring during this interval. In the present study area at least, no metamorphism of this age is apparent. However, at this time, relative uplift of the GFTZ may have occurred along older mylonite zones reactivated by the compressional activity in the interior of the orogen. Reactivation of older structures during collisional tectonics is a common phenomenon, observed, for example, in the Himalayan orogen, even along structures thousands of kilometres north of the main mountain range (Molnar and Tapponnier, 1975). Further detailed dating of syntectonic pegmatites in the various shear zones of the GFTZ would help to resolve this possibility. Again, this could explain additional uplift of high-grade rocks relative to the foreland.

Certainly, by the later stages of the Grenville orogeny at ca. 1 Ga, the tectonic zone had already undergone differential uplift relative to the foreland. The titanite U-Pb system was closed by 1445 Ma, implying that the area had already cooled through about 500°C since granulite grade metamorphism. Further cooling may or may not have occurred after this; the effect of the late Grenvillian thermal event has obliterated this information, at least from the samples in the present study. The fact that 35 kilometres southeast of the present transect the Britt domain underwent peak metamorphism at 1035 Ma suggests that the GFTZ must have had some activity at this time. The titanite data do not rule out weak heating during this time frame, but temperatures could not have exceeded about 500°C.

The data from this study demonstrate that the GFTZ near the Front did not undergo significant metamorphism again until about 990 Ma. The Britt domain has clearly undergone quite a different T-t history, as described above. The question that arises is this: If the 990 - 985 Ma thermal event and subsequent rapid cooling is unrelated to the peak of tectono-metamorphic activity in the Britt domain, what is it related to?

6.2.2 New Model

The work of Bethune (1991) on the Sudbury dikes illustrates that the peak of the 990 Ma metamorphism outlasted plastic deformation of plagioclase in the dikes, since these are rimmed by metamorphic coronas corresponding to the 985 Ma zircon rims. The age or cause of the plagioclase deformation is not available from the information presently published, but it must be between 1238 Ma and 985 Ma. However, Bethune (1991) has also noted that late, high-temperature ductile shear zones caused recrystallization of the 985 Ma overgrowths, showing that deformation was still underway in the GFTZ after the metamorphic event.

It is apparent, then, that any tectonic model for the late evolution of the GFTZ must involve both a source of heat, probably burial, and a thrusting event, to explain the observations. In this regard, the general model of Green et al. (1988) has some merit, although it is probable that much of the deformation, and generation of reflective shear zones in the GFTZ, which they assign to the last events in the Front's history, had already occurred well before 1.0 Ga.

The data of Corrigan (1990) demonstrate that by 990 Ma, the Britt domain had ceased to undergo pervasive deformation and was starting to cool. Major metamorphism and deformation within other parts of the southwestern Grenville Province had also finished; in some parts of the Central Gneiss Belt (CGB), cooling to hornblende closure temperature of about 450°C occurred as early as 1000 Ma (Cosca et al., submitted). Major thrusting apparently migrated from northwest to southeast in the CGB, and the latest tectonism in this region, dated by syn-tectonic pegmatites in thrusts, occurred at 1027 Ma (Nadeau, 1990). Burial, uplift and cooling of a segment of the Grenville Front Tectonic Zone as late as 990 Ma is unexpected given the patterns of peak activity in the interior of the orogen. The explanation for this event may therefore be related to cooling of the interior.

During the late stages of collisional orogenesis, horizontal driving forces diminish, and gravity may induce extensional faulting of the overthickened crust unless the horizontal confining stress is sufficient (Molnar and Lyon-Caen, 1988; Dewey, 1988). Late extensional shear on a large scale has been demonstrated in the interior of the Grenville Province (van der Pluijm and Carlson, 1989) and has also been observed in the southern Britt domain (Ketchum, Ph.D. thesis in progress; Culshaw et al., in press), along re-activated thrusts. The timing of these events is not yet known, although they post-date thrusting. Possibly, extension played some role in the rapid cooling of the GFTZ after 990 Ma, due to rapid unroofing by extensional faulting at higher crustal levels. However, as yet, no evidence for extensional movement has been noted on any of the mylonite zones which occur in the GFTZ or along the Front. This may be due in part to a simple lack of detailed structural analysis of the area, although the work of Davidson and Bethune (1988) failed to reveal any "top-side down" kinematic indicators in the mylonites they mapped. Nevertheless, it is difficult to envision a scenario of extensional movement along re-activated thrusts which would explain burial and heating, and then subsequent rapid cooling, of an area to the north-west of southeast-dipping structures. Rather, to explain this kind of episode, a burial event related to overthrusting, with subsequent rapid unroofing, is more

plausible.

A cooling collisional orogen undergoes stiffening, an opposite response to the weakening due to thermal relaxation after thrusting which is now a well-known phenomenon (England and Thompson, 1982). This is because ductility is a function of temperature, so that simply, as the rocks cool they become stronger. Additionally, during metamorphism, water is produced by prograde reactions, which contributes to weakening of the crust; once metamorphism has peaked, the rocks are relatively stronger.

Various workers have shown that orogenic crust is capable of transmitting horizontal forces across it for very long distances. For example, crustal shortening is occurring at the margins of the Tibetan plateau while the plateau itself is undergoing only high-level extension and apparently, no internal deformation; the horizontal compressional forces of the Himalayan orogen thought to be responsible (Molnar and Tapponnier, 1975; Molnar and Lyon-Caen, 1988).

Although the Grenville orogen underwent substantial internal deformation during the period 1160 - 1025 Ma, as shown by thrust events and metamorphism during this interval, its behaviour must have changed as it cooled. The additional strength of the deeper crust gained by cooling may have permitted transmission of forces across the orogen in its late stages. Possibly, the last increment of compressional stress occurred shortly before 990 Ma, having been active in stages for nearly 150 My previously; this could be due, for example, to accretion of another fragment of crust to the southeast margin of the unknown continent which caused the Grenville orogeny to occur. The area between the Britt domain, which had cooled to about 550°C or less by this point, and the old, cold Superior cratonic margin, was already the locus of deformation and thrusting along mylonite zones from events as far back as 1450 Ma. Some of these thrusts may also have been active at temperatures less than 450°C during the 1160 to 1025 Ma activity in the Grenville interior. This area, wedged between the buttressing Superior Province and the stiffening Grenville Province, was therefore an ideal place to accomodate the final crustal shortening of the Grenville event.

Some burial must have been involved, at least for the 15 kilometre segment of the GFTZ studied here, in order to cause the temperature increase required to partially reset titanite, and to induce metamorphism in the Sudbury dikes. Whether the northern margin of the Britt domain was thrust over the whole GFTZ, or whether segments of the 35 kilometre wedge of the GFTZ between the study area and the Britt domain buried the segments nearest the Front, cannot be determined from the present data. Further dating of the area between Beaverstone Bay

and Key Harbour, as well as structural and metamorphic studies, would help resolve this question.

The rapid cooling for 5 to 10 My following burial is probably too rapid to have occurred simply due to unroofing during isostatic rebound and erosion, although later this process probably occurred. Bethune's (1991) Sudbury dike study demonstrates that 8 to 10 kilometres southeast of the Front, some shear zones post-date the 985 Ma metamorphic event. Also, progressively deeper levels of metamorphism of the dikes are exposed with increasing distance into the GFTZ, until about 20 kilometres from the Front. The results of the titanite dating in this study suggest that strain accompanied partial resetting of titanite near the Grenville Front on Collins Inlet. Rapid exhumation by erosion, removing material fed to surface by tectonically driven differential uplift (Jamieson and Beaumont, 1989) would explain these observations, as well as the short period of very rapid cooling after 990 Ma. The failure of the rocks to reach peak temperature conditions for more than a few million years is demonstrated by the complete resetting of the titanite in the GFTZ transect. Rapid unroofing would also help to explain the abrupt fall-off in peak temperatures northwest of the Grenville Front, where K-Ar muscovite ages 5 kilometres beyond the Front have not been reset, and temperatures therefore must have remained at 350 - 400°C or less. Syntectonic unroofing accompanying the thermal event implies that after burial, thermal equilibrium may not have been reached, since peak metamorphism is often attained after a significant time lag (Fowler and Nisbet, 1988; e.g. Corrigan, 1990). The thickness of the crust causing burial may therefore have been higher than that predicted for a normal geothermal gradient. Metamorphic assemblages in the area do not show evidence for this, but at other localities along the Front to the northeast, for example near Val d'Or, Quebec, kyanite is found locally in the parautochthon (Indares and Martignole, 1989).

The rapid cooling phase did not last long, and by about 955 Ma at the latest, cooling rates were more analagous to rates in the Britt domain as determined by Culshaw et al. (in press). This could signal the end of compressional forces at the margins of the Grenville Province, and the onset of cooling controlled by unroofing due to isostatic rebound and erosion.

The main points of the new tectonic model suggested above are summarized and contrasted with the model of Green et al. (1988) in Table 4.

Table 4: Summary of contrasts between Green et al. (1988) and new tectonic models.

Main observations	Green et al. (1988)	This study
pre-1238 Ma high-grade metamorphism	burial by (now) invisible crustal slice in early stages of Grenvillian orogeny	metamorphism at 1446 Ma related to granitoid intrusion with accompanying tectonism
post-1238 Ma metamorphism and deformation	burial by Britt domain during activity in Grenville interior (ca. 1150 Ma??)	partial unroofing of granulites by continuing reverse movement along Front during peak tectonometamorphic activity in Grenville interior (1238 Ma to 1025 Ma); no significant metamorphism during this time burial by southeastern GFTZ or northern Britt domain at ca. 990 Ma while interior of Province cooling (thermally stiffening)
exposure	thrusting of GFTZ to surface / development of fabric in GFTZ during Grenvillian tectonism (ca. 1150 - 1025 Ma?)	ca. 990 - 985 Ma thrusting along pre-existing, reactivated shear zones accompanied by rapid unroofing (erosion?)/ cooling

6.2.3 Supporting Evidence

This interpretation suggests that the 990 - 985 Ma metamorphism was a regional, rather than local, event. If stresses were being transmitted across the orogen from some unknown collisional events to the southeast, it is unlikely that the section of the Grenville Front being studied here was the only area to experience these effects.

In the western Quebec segment of the Grenville Front, detailed structural and metamorphic analysis of an area between the Front and 30 kilometres southeast was carried out in order to separate the effects of early, Kenoran (Archean) metamorphism from Grenvillian effects (Indares and Martignole, 1989) (this area did not experience 1450 Ma metamorphism). Results suggest that the Grenville orogeny was responsible for a low temperature, high pressure metamorphism in the region, which was then thrust-imbricated. This was superimposed on a Kenoran-age, already telescoped, metamorphic terrane. A short duration of heating related to the Grenvillian event is implied by the observations, as well as subsequent rapid cooling, based on the failure of garnet compositions to re-equilibrate despite temperature conditions of ≥600°C. K-Ar ages of biotite demonstrate cooling to ca. 300°C by 950 Ma (Indares and Martignole, 1989; Snelling, 1962). Although the times of these events are as yet unconstrained, the qualitative similarities with the western end of the Grenville Front are noteworthy.

In different parts of Labrador, there is similar evidence for a late metamorphic event near the Front. East of the Labrador Trough, in an area up to 100 kilometres south of the Grenville Front, Krogh and Wardle (1984) found a mixing line defined by U-Pb dating of titanite, monazite and zircon, with a lower intercept of 993 Ma, similar to the titanite discordia obtained in this study. New zircon which grew during this episode formed at 992 Ma.

In eastern Labrador, Schärer et al. (1986) dated new growth of titanite and zircon in two tectono-metamorphic terranes adjacent to the Grenville Front, at times of about 978 - 970 Ma. In terranes farther south, more distant from the Front, titanite and monazite yielded ages of about 1038 to 1026 Ma, dating Grenvillian metamorphism in these areas. Their interpretation of the results is that the more northern terranes nearer the Front underwent Grenvillian metamorphism about 60 My later than the Southern parts, and attribute this to exposure of different crustal levels separated by a major fault. They do not speculate on the cause of this event. The widespread nature of their sample localities precludes observation of any progressive trends in partial resetting of phases possibly preserved by a rapid metamorphic event, which is crucial to the interpretation proposed here of a short-

lived, late thermal event along the northern margin of the Grenville Province. However, their observation of the late peak of metamorphism in the area, combined with Krogh and Wardle's mixing lines to the west, suggests again a strong analogy with the area studied in this thesis.

In conclusion, evidence along various different parts of the ca. 2000 kilometre long Grenville Front may point to a late metamorphic event, involving burial and rapid uplift, at a time when more southerly parts of the orogen had already passed through their metamorphic peak and were cooling. Thermal stiffening may have permitted late transmission of stress across the orogen which had formerly accomodated compressional stresses with internal strain. In the late stages of the orogenic event, stress was accomodated instead by the rocks of the GFTZ, pushed against the strong, cold buttress of the various foreland provinces. Probably, this effect would occur at different times in different places along the orogen, depending on the geometry and rheology of the foreland, the nature of the cooling crust to the southeast, and the time of concentration of the compressional forces from the far southeast. However, testing this theory will need considerably more work on intergrating structural and metamorphic studies with the results of detailed geochronology over small areas, since changes in results critical to interpretation can occur over relatively short distances on the scale of the orogen.

CHAPTER VII
CONCLUSIONS

7.1 SUMMARY OF CONCLUSIONS

The GFTZ underwent granulite grade metamorphism at 1446 Ma, part of a regional event affecting the Parautochthonous Belt in central Ontario. Temperatures in the GFTZ did not exceed titanite closure again until about 990 Ma, even during metamorphism of the Britt domain at 1035 Ma. At 990 to 985 Ma, the GFTZ underwent a brief thermal event, which opened titanite to diffusion of Pb but failed to completely reset the U-Pb system. Temperatures during the event were greater to the southeast, away from the Grenville Front, probably due to increasing depth of burial by crustal blocks overthrust from the southeast. Rapid cooling followed, preserving identical lower intercept ages in all titanites along a 15 kilometre transect perpendicular to the Front.

Hornblende $^{40}Ar/^{39}Ar$ dating confirms that temperatures were higher to the southeast. Failure of the ca. 990 event to reset hornblende ages near the Front restricts the peak temperature of the event to ≤550°C. About 10 kilometres farther southeast, hornblende was completely reset and records cooling ages of 979 ±8 Ma, which are almost identical to the titanite lower intercept. This confirms rapid cooling immediately post-dating the thermal event.

Biotite and K-feldspar $^{40}Ar/^{39}Ar$ dating, and multiple diffusion domain modelling of K-feldspar, additionally demonstrate rapid cooling until 979±10 Ma, and an abrupt decrease in cooling rates following this.

The initial rapid cooling rates, evidence for deformation continuing after the metamorphic peak, and an abrupt drop across the Grenville Front in temperatures reached at 990 Ma, are best explained by rapid exhumation by erosion during differential uplift of the GFTZ relative to the foreland.

This thesis establishes for the first time that Grenvillian tectonism in the GFTZ post-dated all major tectonothermal activity in the Grenville interior at the southwestern end of the Province. A similar sequence of events has previously been recognized in Labrador.

The age of Grenville dikes is about 598 ±6 Ma, not 575 Ma as previously reported (Fahrig and West, 1986).

K-feldspar multiple diffusion domain modelling yields fairly consistent results despite the non-ideal data in this study. If the theory is correct, it can provide considerable control on thermal histories for temperatures ≤350°C.

7.2 FUTURE WORK

Future work in this part of the Grenville Province should concentrate on resolving the relationships between the GFTZ and the Britt domain. Metamorphic, structural, and geochronologic studies of the area between the present transect and Key Harbour are needed. The location and nature of the transition between rocks affected by the short ca. 990 Ma event, and cooled rapidly, and rocks which underwent peak metamorphism at 1035 Ma must be resolved before an understanding of the geodynamic evolution of the GFTZ can be achieved.

APPENDIX A
TITANITE FRACTION DESCRIPTIONS

GF-32: - non-magnetic at 1.0 amps; magnetic at 1.7 amps
- rounded, euhedral clear light to medium brown crystals
- grain size 60 - 120 μm
- abraded.

GF-20: - magnetic at 1.0 and 1.7 amps
- rounded to flattish light honey-brown euhedral crystals; some cracks and inclusions
- grain size 60 - 120 μm
- abraded.

GF-19-1: - magnetic at 1.0 and 1.7 amps
- large anhedral fragments; light to medium brown with variation in colour within grains
- grain size 110 - 230 μm
- abraded.

GF-19-2: - magnetic at 1.0 and 1.7 amps
- small euhedral rounded to flat crystals, dark to medium brown
- grain size 60 - 120 μm
- slightly abraded.

GF-18-1: - magnetic at 1.0 amps
- small rounded euhedral light to medium brown crystals; some with reddish material clinging
- grain size 90 - 120 μm
- abraded.

GF-18-2: - magnetic at 1.7 amps
- large red-brown to light honey-brown fragments
- grain size 170 - 290 μm
- abraded.

CI-19: - magnetic at 1.0 and 1.7 amps
- light brown to dark red-brown, rounded to flat euhedral crystals
- grain size 30 - 110 μm
- unabraded.

GF-35-1: - magnetic at 1.0 and 1.7 amps
- dark brown, fragments and rounded euhedral to subhedral crystals; some inclusions
- grain size 60 - 120 μm
- abraded.

GF-35-2: - magnetic at 1.0 and 1.7 amps
- light yellow, rounded euhedral crystals; some cracks and minor red-brown coating
- grain size 60 - 140 μm
- abraded.

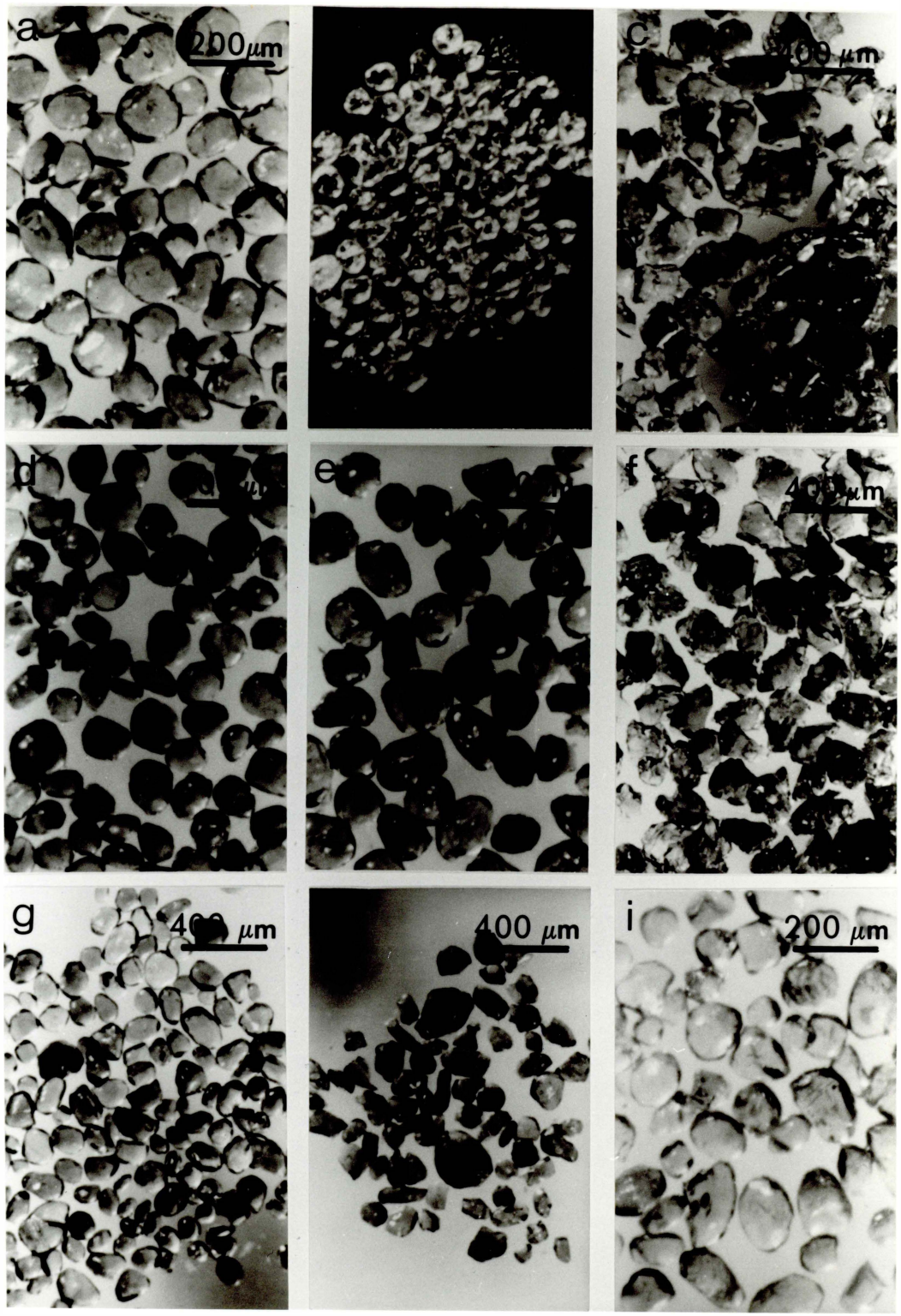

Plate 1: Titanite fractions prior to abrasion. Grains with cracks and inclusions which remained after abrasion were removed. a) GF-32. b) GF-20. c) GF-19-1. d) GF-19-2. e) GF-18-1. f) GF-18-2. g) CI-19. h) GF-35-1. i) GF-35-2.

APPENDIX B
SAMPLE DESCRIPTIONS

Samples described below are ordered with respect to their position along the study transect, from northwest (foreland) to southeast (GFTZ). "MS10" and "VG3600" denotes the mass spectrometer and corresponding gas extraction system used to date the sample.

GF-44:
In outcrop: a pitted, rough-weathering, grey-black metadiabase with disseminated pyrite; possibly Nipissing metadiabase.
In thin section: Strongly sausseritized plagioclase laths define a relict sub-oophitic texture. Relict hornblende grains are severely, patchily replaced by ragged actinolitic hornblende, a colourless amphibole, chlorite, and opaque grains (chalcopyrite?). Patches of talc surround coarse opaque grains.
Dated phase(s): amphibole; grain size 250 μm to 1 mm; MS10

GF-42:
In outcrop: a massive, fine-grained pinkish-red granite enclosing sharply-bounded rafts of Huronian siltstones (Killarney Complex/ Southern Province contact).
In thin section: A porphyritic granite with a fine-grained groundmass of equant, interlocking quartz and feldspar grains, with rational grain boundaries. Phenocrysts are about 1 mm diameter, coarsely perthitic microcline, split into angular subgrains by strips of recrystallized grains. Phenocryst grain boundaries are embayed by groundmass-size feldspar. Some phenocryst grain margins and occasionally cores, have zones and patches of secondary fine-grained muscovite; all phenocrysts are turbid due to a cryptocrystalline, reddish brown alteration phase (hematite?).
Dated phase: microcline; grain size .5 to 1.5 mm (phenocrysts); 15 to 60 μm (matrix); MS10

GF-62:
In outcrop: Reddish-pink weathering, medium-grained weakly foliated granite.
In thin section: Rock is slightly cataclased. Quartz has a range of grain sizes and is strained into subgrains with sutured grain boundaries. Feldspars have a strongly bimodal distribution; large grains are blocky and have recrystallized to very fine-grained aggregates along grain margins and in fractures. Plagioclase is antiperthitic, and some grains have twins offset along fractures.

antiperthitic, and some grains have twins offset along fractures. Microcline is coarsely perthitic and has myrmekitic rims. The section is cut by fractures along which opaques, fine-grained muscovite, chloritized biotite and titanite are concentrated; zones of reddish-brown hematite dust cause turbidity in feldspars adjacent to fractures.
Dated phase: microcline; grain size 250 μm to 1.25 mm (coarse)
5 to 60 μm(recrystallized); MS10

GF-2:
In outcrop: a thin, mylonitic amphibolite dike, chevron-folded with fold axes parallel to lineation in granitic mylonite host.
In thin section: Very fine-grained. Hornblende laths are strongly aligned, with ragged, finely recrystallized grain boundaries. Minor amounts of biotite are intergrown with hornblende. Plagioclase and minor quartz are uniformly fine-grained and equant, have irregular, recrystallized grain boundaries, and are evenly interspersed with hornblende. Plagioclase is moderately sericitic. Titanite is present as tiny (<50 μm), abundant, euhedral to rounded grains in clumps, strings and as single grains, most of which are subparallel to foliation.
Dated phase: hornblende; grain size 100 to 250 μm; MS10.

GF-32:
In outcrop: a layered, straight, hornblende granodiorite gneiss.
In thin section: section has a protomylonitic texture, with medium-sized, equant grains of the major constituents surrounded by finely recrystallized grains. Quartz, plagioclase and orthoclase have scalloped and sutured grain boundaries, and undulatory extinction or subgrains. Orthoclase is not visibly perthitic. Feldspars are variably sericitized. Hornblende is poikiloblastic, with inclusions of quartz, feldspars, titanite and apatite, and is altered along cleavage to a brown, cryptocrystalline material. Greenish biotite with hematite lamellae is concentrated in fine-grained recrystallized layers; these define an anastomosing foliation. Titanite occurs singly or in clumps of rounded to pear-shaped grains, as inclusions in hornblende and feldspars or between grains, especially in the recrystallized zones; and as irregularly-shaped rims on opaque grains.
Dated phases: hornblende - grain size 100 - 500 μm; VG3600.
orthoclase - grain size 15 μm - 1.1 mm; VG3600.
titanite

CI-37:
In outcrop: nose of isoclinally folded, cross-cutting amphibolite dike, with very strong southeast-dipping lineation. (Sample obtained from M. Burke).
In thin section: Strongly aligned, green-brown hornblende laths dominate the section; these are interspersed with equant plagioclase, and minor quartz and biotite. Hornblende is altered along cleavage planes and fractures to cryptocrystalline brown material; most grains have opaque inclusions. Hornblende grain margins are irregular and surrounded by finely recrystallized grains. In some places hornblende and biotite are severely intergrown but this is volumetrically insignificant. Plagioclase is moderately sericitized. Tiny (25 μm) apatite is dispersed throughout the section. A few annealed fractures are present along which fine-grained biotite, opaques, hematite and sericite are concentrated.
Dated phase: hornblende - grain size 100 μm - 1.25 mm; MS10.

GF-20:
In outcrop: a well-foliated pink biotite granite gneiss with variable grain size.
In thin section: a protomylonitic texture, with about 50% equant, finely recrystallized groundmass, and 50% coarse porphyroclasts of quartz, plagioclase and microcline. Most coarse feldspars have a core and mantle structure, surrounded first by subgrains and then by recrystallized secondary grains. Quartz and feldspars have undulatory extinction and scalloped grain boundaries, except in some zones of recrystallized grains which have polygonal grain boundaries. Some myrmekite is present on rims of microcline; no perthite lamellae are apparent. Feldspars are moderately sericitized. Chloritized, irregular laths of biotite with enclosed hematite lamellae are distributed throughout the section; some are associated with annealed fractures defined by concentrations of opaques (pyrite), hematite, apatite, chlorite, zircon, rutile(?), and an unknown yellowish cryptocrystalline alteration phase. Titanite is not present in the section.
Dated phases: microcline - grain size - 10 μm to 1 mm; VG3600.
titanite

GF-19:
In outcrop: a medium-grained, weakly foliated grey to pink orthogneiss.
In thin section: Mainly medium-grained, granoblastic texture. Most of main constituents (quartz, feldspar, biotite) are subhedral to anhedral, with rational grain boundaries. In some zones, quartz and feldspar

grains have scalloped grain boundaries, undulose extinction and/or subgrains, and strips of finely recrystallized grains are present. Microcline has dense tartan twinning, and myrmekite is developed on grain margins; minor sericite is present. No perthite exsolution is visible. Biotite is greenish and some grains have minor development of hematite lamellae, but laths are euhedral to subhedral and appear to be in textural equilibrium. Section contains coarse (1 - 2 mm) grains of magnetite defining a weak foliation; these are partly rimmed by elongate blebs of titanite and rounded apatite grains. Titanite, rutile and apatite are also present as rounded grains associated with biotite or as individual, interstitial grains.

Dated phases: microcline - grain size - 15 to 500 μm; MS10 and VG3600
biotite - grain size - 10 to 350 μm; MS10.
titanite (2 kinds?)

GF-18

In outcrop: a foliated, red granite orthogneiss.

In thin section: A biotite-bearing, granitic protomylonite; quartz and feldspars are partly recrystallized, with about 50% original grains; these have sutured grain boundaries. Some plagioclases have bent twins. Most K-feldspar is orthoclase but minor cross-hatch twinning is present in some grains, and grains are microperthitic. Some grains have myrmekitic subgrains or recrystallized grains surrounding or enclosed by them; a few exhibit core- and - mantle structure. Biotite contains hematite lamellae. In places it is associated with pyrite and large zircon grains which are partly converted to several unknown alteration phases. Titanite is present only in trace amounts, as rims on zircon. Biotite and zones of recrystallized grains define an anastomosing foliation.

Dated phases: orthoclase (?) - grain size 10 μm to 1.25 mm; VG3600.
titanite (2 kinds?)

GF-7:

In outcrop: a pink, moderately foliated gneiss, interlayered with mixed paragneisses.

In thin-section: A pelitic protomylonite with assemblage qtz-pg-Kfs-gt-bt-sil-zrn-ap. Quartz occurs as ribbons with only moderate recrystallization and defines a strong preferred orientation. Orthoclase is microperthitic and plagioclase is antiperthitic; many grains are quite blocky and have undulatory extinction or in some grains, sharply bent twins. Feldspars have not recrystallized, and some grains are moderately to strongly sericitic. Minor myrmekite is

developed at grain margins. Biotite is quite pristine except for numerous pleochroic haloes surrounding small zircon grains. Garnet contains inclusions of sillimanite, biotite, and quartz, and is strongly embayed. Sillimanite needles and small rhombs occur in clusters and layers which cut across garnet and quartz grain boundaries. Biotite, sillimanite and garnet are concentrated in layers which with quartz ribbons define a foliation; this has been folded but timing of mineral growth relative to this is unclear.
Dated phases: orthoclase - grain size: 25 μm to 1 mm; MS10 and VG3600
biotite - grain size: 10 to 500 μm; MS10

GF-8:
In outcrop: A garnet amphibolite boudin, from a mafic layer (dike?) in layered semi-pelitic to pelitic metasediments.
In thin-section: A moderately foliated, biotite-garnet amphibolitic gneiss. Hornblende and biotite define the foliation; these are substantially intergrown. Hornblende is altered to a brownish cryptocrystalline substance along cleavage. Quartz and plagioclase are equant and have rational grain boundaries; plagioclase is slightly sericitic. Garnet is fractured and embayed, and is elongated parallel to foliation; it contains inclusions of biotite, apatite, and an opaque phase (Fe-Ti oxides?).
Dated phases: hornblende - grain size: 10 to 500 μm; MS10
biotite - grain size: 10 to 250 μm; MS10.

TZ-19:
In outcrop: Another boudin from same layer as GF-8. (Sample obtained from M. Burke).
In thin-section: see GF-8.
Dated phase: hornblende - grain size 10 to 500 μm; VG3600

CI-20:
In outcrop: not observed (sample obtained from M. Burke); a biotite granodiorite orthogneiss.
In thin-section: Feldspars and quartz are in layers of equant, unrecrystallized grains with rational grain boundaries, alternating with strips of very finely recrystallized grains. Biotite is coarse and fresh but contains lamellae of hematite; it occurs in the coarse qtz - feldspar layers associated with severely altered relict hornblende. Biotite is also concentrated as finer grains in the recrystallized strips. Orthoclase and plagioclase are moderately sericitic, and have minor myrmekite between them. Relict hornblende is almost completely

replaced by an unknown cryptocrystalline substance. Zircon and apatite are present in trace amounts.
Dated phase: orthoclase - grain size: 25 μm to 1.25 mm; VG3600.

CI-19:
In outcrop: not observed (sample obtained from M. Burke); amphibolitic gneiss.
In thin-section: A fairly granoblastic amphibolite with a slight preferred orientation. Clinopyroxene, plagioclase, hornblende and minor quartz occur in equant, anhedral grains with rational grain boundaries except for slight recrystallization around the margins of some plagioclase and quartz. Hornblende and clinopyroxene are slightly altered along fractures and cleavage. Severely chloritized biotite is present in minor amounts; some grains are intergrown with hornblende. Titanite occurs as isolated, rounded small grains. Trace apatite is present.
Dated phases: hornblende - grain size: 50 to 750 μm; VG3600.
titanite

GF-34:
In outcrop: a migmatitic amphibolite pod in a migmatitic granodioritic gneiss.
In thin-section: Equant hornblende, plagioclase and quartz grains with rational to ragged grain boundaries define a granoblastic texture. Hornblende is altered along fractures and cleavage to a brown cryptocrystalline material, and rarely is intergrown with minor biotite. Quartz and plagioclase are slightly recrystallized along grain margins and some myrmekite is developed between them; plagioclase is slightly sericitic. Trace apatite and opaques are present.
Dated phase: hornblende - grain size: 25 to 500 μm; VG3600.

GF-35:
In outcrop: a migmatitic biotite-hornblende granodioritic gneiss.
In thin section: Anhedral, equant grains of quartz, feldspar, biotite, and hornblende, with rational to scalloped grain boundaries, sit in a recrystallized matrix. Recrystallized zones define a weak preferred orientation. Quartz has undulatory extinction. Plagioclase and orthoclase are variably sericitic; some are severely altered and some only slightly. Orthoclase is homogeneous (no visible perthite exsolution). Hornblende contains apatite and zircon inclusions, and lamellae of an opaque phase; it is locally intergrown with biotite, which has hematite along cleavage planes. Minor apatite and opaques,

and trace zircon, are present. Titanite is not present in the section.
Dated phases: hornblende - grain size: 100 to 750 μm; MS10
biotite - grain size: 100 to 750 μm; MS10
orthoclase - grain size: 50 μm to 1 mm; MS10 and VG3600 (two different aliquots)
titanite (two kinds?)

CI-14:
In outcrop: not observed (sample obtained from M. Burke) - a biotite - hornblende granodioritic gneiss.
In thin-section: Section has a protomylonitic texture, with irregular, equant grains of quartz and feldspars surrounded by unrecrystallized quartz ribbons and fine-grained feldspar. Porphyroclasts of feldspar have undulatory extinction and sub-grains developed; some plagioclase twins are gently bent. Anastomosing layers of recrystallized grains define a moderate preferred orientation. Orthoclase and plagioclase have moderate amounts of sericite alteration, and orthoclase is microperthitic. Red-brown biotite has minor hematite along cleavage. Hornblende is locally severely altered along fractures and cleavage to chlorite and cryptocrystalline material. Trace zircon, apatite and opaques are present.
Dated phase: orthoclase - grain size: 10 μm to 3 mm; VG3600

APPENDIX C

$^{40}Ar/^{39}Ar$ STEP-HEATING EXPERIMENT DATA SUMMARY SHEETS

For all samples: error estimates at one sigma level; $^{37}Ar/^{39}Ar$ (37/39), $^{40}Ar/^{36}Ar$ (40/36), and $^{39}Ar/^{36}Ar$ (39/36) ratios are corrected for interfering isotopes. %IIC = interfering isotopes correction.

GF-44H HORNBLENDE (MS10)

°C	mV39	%39	AGE(Ma)	%atmos	37/39	40/36	39/36	%IIC
650	10	16	2685±18	6	2.4	5349	3.6	<1
700	2	3	2427±34	7	2.0	4328	3.5	<1
750	<1	1	2320±40	9	2.8	3417	2.9	<1
800	2	3	2096±17	7	4.2	4059	4.2	<1
850	5	8	1592±7	7	2.8	4406	7.2	<1
900	7	11	1615±7	5	7.8	6545	10.7	1
925	6	10	-	-	-	-	-	-
950	7	11	1962±13	7	23.9	4416	5.2	2
975	9	15	2005±8	6	23.9	4743	5.4	2
995	4	6	1962±13	8	22.5	3608	4.1	2
1015	3	4	1937±15	16	20.6	1843	1.9	2
1035	2	3	1886±28	29	19.8	1022	0.9	1
1055	1	2	1813±44	31	19.0	949	0.9	1
1075	<1	1	1923±53	34	17.8	869	0.7	1
1100	1	2	1924±31	29	16.7	1003	0.9	1
1150	2	4	1951±17	21	14.9	1436	1.4	1

$J = 2.49 \times 10^{-3} \pm 0.5\%$

GF-2H HORNBLENDE (MS10)

°C	mV39	%39	AGE(Ma)	%atmos	37/39	40/36	39/36	%IIC
650	21	9	871±2	17	0.7	1771	5.7	<1
700	6	3	1194±3	9	0.6	3171	7.4	<1
750	5	2	1482±6	10	1.0	2936	5.0	<1
800	5	2	1186±6	10	1.2	2939	6.9	<1
850	6	3	1150±2	9	1.5	3270	8.1	<1
875	5	2	1210±3	10	2.0	3064	7.0	<1
900	7	3	1220±3	9	2.9	3120	7.1	<1
925	15	6	1293±2	5	3.8	5568	12.2	<1
940	13	5	1394±4	6	4.5	5239	10.3	<1
955	32	13	1546±2	3	5.0	10963	19.1	<1
970	36	15	1637±2	2	5.2	12168	19.5	<1
985	26	11	1573±3	3	5.2	11483	19.5	<1
1000	38	16	1452±2	3	5.2	11071	21.2	<1
1015	18	7	1410±4	4	5.2	6654	13.0	<1
1030	5	2	1379±6	16	5.5	1892	3.3	<1
1045	3	1	1379±16	34	6.0	865	1.2	<1

$J = 2.435 \times 10^{-3} \pm 0.5\%$

CI-37 HORNBLENDE (MS10)

°C	mV39	%39	AGE(Ma)	%atmos	37/39	40/36	39/36	%IIC
800	2	1	-	-	-	-	-	-
900	4	2	1166±15	68	5.5	433	0.3	<1
915	8	5	1199±4	38	5.5	777	1.2	<1
925	9	6	1184±5	32	5.6	934	1.6	<1
935	7	5	1190±4	24	5.6	1208	2.3	<1
945	12	8	1203±3	24	5.7	1206	2.3	<1
960	8	5	1206±3	20	5.5	1491	3.0	<1
975	18	11	1220±2	18	5.7	1649	3.4	<1
990	19	12	1219±2	16	5.7	1801	3.7	<1
1005	18	12	1212±3	19	5.8	1581	3.2	<1
1020	16	11	1205±4	24	6.1	1211	2.3	1
1050	27	17	1219±2	16	6.0	1799	3.7	1
1080	7	4	1200±9	43	6.6	690	1.0	1
1130	1	<1	-	-	-	-	-	-

$J = 2.43 \times 10^{-3} \pm 0.5\%$

GF-32H HORNBLENDE (VG3600)

°C	mV39	%39	AGE(Ma)	%atmos	37/39	40/36	39/36	%IIC
650	1	<1	1218±43	1	-	29408	67.0	-
700	3	<1	524±9	57	4.2	518	1.5	<1
750	3	<1	559±209	51	2.2	576	1.7	<1
800	2	<1	1026±376	??	-	14558	41.3	-
850	3	1	971±18	35	4.2	845	1.7	<1
900	2	<1	821±46	38	3.1	773	1.8	<1
950	15	5	869±2	7	4.0	4107	13.7	<1
975	16	5	1051±1	4	3.3	7148	19.2	<1
1000	35	12	1208±4	1	3.8	20186	46.3	<1
1025	75	25	1230±2	<1	3.7	41371	93.3	<1
1050	45	15	1211±6	<1	3.9	33684	77.5	<1
1075	29	10	1204±4	3	3.6	10937	24.9	<1
1100	14	5	1199±11	3	3.8	9683	22.1	<1
1150	46	15	1253±4	1	3.7	22738	49.7	<1
1200	13	4	1372±17	4	4.1	7092	13.2	<1

$J = 2.22 \times 10^{-3} \pm 1.0\%$

GF-8H HORNBLENDE (MS10)

°C	mV39	%39	AGE(Ma)	%atmos	37/39	40/36	39/36	%IIC
650	5	1	1827±11	11	1.5	2801	3.5	<1
700	2	<1	1336±14	11	0.7	2601	5.2	<1
800	2	<1	1229±15	14	0.7	2157	4.7	<1
850	3	<1	1240±11	15	-	1978	4.2	-
900	12	3	1181±4	4	2.8	7579	19.5	<1
930	87	23	1128±3	2	3.1	17112	48.1	<1
950	65	18	1117±3	2	3.1	17011	48.4	<1
965	76	21	1113±3	1	3.1	20102	57.6	<1
980	55	15	1109±4	2	3.1	13115	37.4	<1
995	42	11	1107±3	3	3.2	8472	23.9	<1
1010	12	3	1117±5	12	3.2	2424	6.1	<1
1020	4	1	1139±13	27	3.4	1086	2.2	<1
1040	3	<1	1180±18	35	3.7	851	1.4	<1
1070	2	<1	1276±22	37	4.0	802	1.2	<1
1100	3	<1	1297±21	46	4.1	642	0.8	<1

$J = 2.485 \times 10^{-3} \pm 0.5\%$

TZ-19H HORNBLENDE (VG3600)

°C	mV39	%39	AGE(Ma)	%atmos	37/39	40/36	39/36	%IIC
900	3	5	628±18	53	1.8	555	1.4	<1
950	1	2	729±59	83	2.3	358	0.3	<1
975	<1	2	744±85	86	3.6	342	0.2	<1
1000	3	6	957±6	10	4.2	2908	8.6	<1
1025	8	16	951±4	6	4.4	4801	15.0	<1
1050	9	17	940±5	8	4.5	3922	12.2	<1
1075	22	44	888±4	4	4.4	7471	26.0	<1
1100	2	4	840±11	29	4.3	1012	2.8	<1
1125	1	2	781±13	41	4.3	715	1.8	<1

$J = 2.305 \times 10^{-3} \pm 0.5\%$

CI-19H HORNBLENDE (VG3600)

°C	mV39	%39	AGE(Ma)	%atmos	37/39	40/36	39/36	%IIC
850	10	3	737±6	47	1.87	634	1.5	<1
900	2	<1	953±6	19	2.46	1574	4.1	<1
950	4	1	1039±4	12	2.87	2389	6.0	<1
975	18	5	919±3	5	3.14	6452	20.6	<1
1000	45	12	988±4	2	3.15	18852	56.5	<1
1025	98	26	989±16	<1	3.12	33412	100.6	<1
1050	100	27	987±1	<1	3.15	52947	160.5	<1
1085	49	13	988±3	2	3.26	17544	52.5	<1
1120	23	6	1015±7	3	3.31	10082	28.8	<1
1150	17	5	956±3	10	3.54	3047	8.9	<1
1200	7	2	1100±3	7	4.09	4196	10.3	<1

$J = 2.22 \times 10^{-3} \pm 1.0\%$

GF-34H HORNBLENDE (VG3600)

°C	mV39	%39	AGE(Ma)	%atmos	37/39	40/36	39/36	%IIC
850	24	5	625±2	37	1.09	796	2.7	<1
900	2	<1	957±8	22	2.43	1345	3.3	<1
950	10	2	1005±2	<1	0.27	40796	120.5	<1
975	23	5	880±1	3	0.31	9011	30.8	<1
1000	71	15	978±2	<1	3.05	35799	109.5	<1
1025	134	29	986±2	<1	3.08	58686	178.1	<1
1050	91	20	991±2	<1	3.14	44674	134.6	<1
1075	42	9	987±2	2	3.20	16049	48.0	<1
1100	30	7	994±5	3	3.29	10768	31.6	<1
1150	25	5	892±2	8	3.26	3660	11.7	<1
1200	9	2	1003±4	16	3.23	1871	4.7	<1

$J = 2.22 \times 10^{-3} \pm 1.0\%$

GF-35H HORNBLENDE (MS10)

°C	mV39	%39	AGE(Ma)	%atmos	37/39	40/36	39/36	%IIC
750	2	1	943±14	33	0.6	909	2.2	<1
800	1	<1	971±15	10	1.0	2906	9.1	<1
850	2	<1	960±9	13	1.4	2363	7.3	<1
900	3	1	994±5	7	2.2	4386	13.8	<1
950	75	33	977±1	1	3.0	24122	82.5	<1
980	49	22	980±2	1	3.0	28405	96.9	<1
1000	58	26	981±4	1	3.1	25781	87.8	<1
1020	24	11	976±3	3	3.1	8760	29.3	<1
1040	5	2	993±6	8	3.1	3676	11.4	<1
1060	2	1	1020±10	20	3.6	1450	3.7	<1
1100	2	<1	1069±14	33	5.0	885	1.8	<1
1150	2	<1	1048±13	38	2.1	772	1.5	<1

$J = 2.49 \times 10^{-3} \pm 0.5\%$

GF-19B BIOTITE (MS10)

°C	mV39	%39	AGE(Ma)	%atmos	40/36	39/36
500	10	2	714±3	20	1476	5.9
550	14	3	1145±2	5	6002	15.6
600	29	5	1218±2	2	12810	31.6
650	79	15	1237±2	2	17290	42.0
700	63	12	1248±3	2	17813	42.7
750	80	15	1256±3	2	14111	33.4
800	39	7	1248±3	5	5508	12.7
850	30	6	1246±2	8	3549	7.9
900	40	8	1247±3	8	3607	8.0
950	74	14	1257±2	6	5242	11.9
1000	60	11	1278±3	10	2841	6.0
1050	14	3	1242±3	45	661	0.8
1100	2	<1	-	-	-	-

$J = 2.435 \times 10^{-3} \pm 0.5\%$

GF-7B BIOTITE (MS10)

°C	mV39	%39	AGE(Ma)	%atmos	40/36	39/36
500	20	4	521±2	45	656	2.6
550	11	2	941±2	2	12441	44.0
600	50	10	1032±3	<1	42366	135.4
650	52	11	1032±2	<1	44992	143.8
700	32	6	1021±1	<1	42529	137.9
750	9	2	1024±3	<1	40476	130.6
800	59	12	1026±2	2	17690	56.3
850	9	2	1019±4	5	6031	18.7
900	24	5	1027±1	6	5358	16.3
950	36	7	1053±4	4	7487	22.5
1000	106	22	1035±1	2	14476	45.4
1050	85	17	1025±2	4	7911	24.7

$J = 2.485 \times 10^{-3} \pm 0.5\%$

GF-8B BIOTITE (MS10)

°C	mV39	%39	AGE(Ma)	%atmos	40/36	39/36
500	5	1	397±6	51	580	2.8
550	6	1	837±4	10	2910	11.0
600	15	3	956±2	2	12223	42.6
650	22	4	955±1	2	16940	59.5
700	88	17	954±2	<1	34510	122.6
750	61	12	953±2	<1	40813	145.5
800	46	9	954±2	1	29438	104.5
850	41	8	955±3	2	19042	67.1
900	40	8	956±3	3	8769	30.2
950	50	10	958±2	3	10433	36.1
1000	59	12	953±2	4	7818	27.0
1050	44	9	948±3	9	3430	11.3
1150	34	7	946±3	14	2126	6.6

$J = 2.5 \times 10^{-3} \pm 0.5\%$

GF-35B BIOTITE (MS10)

°C	mV39	%39	AGE(Ma)	%atmos	40/36	39/36
600	25	4	-	-	-	-
650	31	5	1241±5	5	6435	15.2
700	83	13	1242±2	3	10873	26.6
750	107	17	1234±2	3	11410	28.2
800	35	6	1244±7	5	5865	13.9
850	29	5	1247±4	7	4414	10.3
900	37	6	1279±5	8	3846	8.5
950	103	17	1240±2	4	7917	19.2
1000	155	25	1232±1	2	16749	41.8
1050	19	3	1218±2	15	1974	4.3

$J = 2.495 \times 10^{-3} \pm 0.5\%$

GF-42K K-FELDSPAR (MS10)

°C	mV39	%39	AGE(Ma)	%atmos	40/36	39/36	TIME (sec)
480	42	4	621±2	6	5216	29.7	1200
510	18	1	608±2	2	17843	108.6	1200
540	17	1	682±3	1	27235	145.6	1200
570	18	1	773±2	<1	30445	140.0	1380
600	15	1	814±5	<1	30023	129.4	1200
630	16	1	817±2	1	22323	95.5	1200
660	19	2	828±2	<1	32147	135.8	1200
690	28	2	844±2	1	30614	126.3	1200
720	35	3	861±1	1	28400	114.2	1380
750	8	<1	867±3	2	17079	67.5	1200
780	13	1	858±3	1	25079	101.1	1200
810	26	2	856±2	1	23489	94.9	1260
840	27	2	864±2	1	25548	102.1	1200
870	20	2	870±2	1	24529	97.1	1200
900	8	<1	886±9	1	29528	114.5	1200

$J = 2.485 \times 10^{-3} \pm 0.5\%$

GF-62K K-FELDSPAR (MS10)

°C	mV39	%39	AGE(Ma)	%atmos	40/36	39/36	TIME (sec)
480	17	2	651±1	15	1975	9.4	1200
510	13	1	537±2	4	8255	55.9	1320
540	16	2	547±1	3	11363	76.0	1200
570	21	2	585±1	2	16063	100.2	1200
600	20	2	639±1	2	14953	84.0	1200
630	25	3	681±1	1	22290	116.7	1320
660	23	2	700±2	1	24464	124.1	1200
690	30	3	703±1	4	7178	35.1	1200
720	47	5	714±1	<1	35024	174.1	1200
750	47	5	722±1	<1	30555	149.6	1260
780	30	3	709±1	2	16611	82.4	1200
810	27	3	705±1	2	13884	69.1	1200
840	23	3	708±1	3	11040	54.3	1200
870	28	3	720±1	7	4401	20.3	1200
900	26	3	725±1	7	4282	19.6	1200
950	46	5	734±1	3	11761	55.5	1380
1000	60	7	742±1	3	11207	52.1	1200
1050	70	8	762±1	6	4665	20.2	1200
1100	66	7	810±1	5	5498	22.3	1380
1150	45	5	903±1	9	3330	11.3	1200

$J = 2.435 \times 10^{-3} \pm 0.5\%$

GF-32K K-FELDSPAR (VG3600)

°C	mV39	%39	AGE(Ma)	%atmos	40/36	39/36	TIME (sec)
500	17	<1	755±3	20	1509	5.2	1560
550	16	<1	560±3	6	5164	29.7	1200
600	37	1	563±1	4	7205	41.9	1200
650	47	2	604±2	1	21547	118.7	1320
700	79	3	594±2	6	4663	24.8	1380
750	148	5	640±1	2	16313	83.4	2100
800	117	4	697±1	2	15122	69.8	1200
830	160	6	731±1	1	21586	94.5	1200
860	45	2	801±2	5	6498	24.6	1680
890	50	2	836±2	4	8137	29.5	1380
920	82	3	867±1	2	12924	45.5	1380
950	94	3	876±1	1	22238	78.0	1200
980	115	4	887±1	2	16562	56.8	1200
1010	98	4	912±2	2	18284	60.7	1500
1040	105	4	914±2	<1	54459	182.3	1560
1070	81	3	918±2	<1	82129	273.9	1200
1100	111	4	969±2	<1	100996	314.1	1260
1130	132	5	1012±1	<1	91916	270.4	1200
1160	161	6	1052±1	<1	73585	205.4	1200
1190	716	26	995±2	<1	59323	178.0	1200
1220	204	7	1036±1	<1	43187	122.8	1140
1250	165	6	1009±1	<1	37080	109.0	1320

$J = 2.22 \times 10^{-3} \pm 1.0\%$

GF-20K K-FELDSPAR (VG3600)

°C	mV39	%39	AGE(Ma)	%atmos	40/36	39/36	TIME (sec)
500	6	1	433±3	45	661	3.0	1200
550	5	<1	480±2	31	949	4.9	1440
600	8	1	436±6	20	1462	9.8	1320
650	12	2	609±1	5	5401	29.4	1380
700	25	5	593±1	2	11967	69.4	1380
750	35	6	626±1	1	21784	120.0	1380
780	32	6	699±1	1	27625	133.6	1440
810	30	6	696±1	1	28179	137.1	1200
840	37	7	719±1	4	7060	32.0	4980
870	9	2	763±1	3	10309	44.0	1200
900	6	1	788±2	7	4013	15.7	1260
930	11	2	810±1	4	6930	27.0	1500
960	15	3	824±1	3	10780	41.9	1320
990	21	4	838±1	2	13141	50.2	1200
1020	26	5	852±1	2	18664	70.4	1200
1050	23	4	847±1	2	14674	55.5	1200
1080	28	5	895±1	2	17534	62.1	1200
1110	43	8	942±1	1	22639	75.4	1260
1140	51	9	994±1	1	24608	76.5	1260
1170	50	9	1042±1	1	22574	66.0	1200
1170b	30	6	1048±1	2	18637	53.8	r
1170c	16	3	1062±1	3	9674	27.0	r
1150d	6	1	1050±3	4	6702	18.7	r
1170e	15	3	1084±2	<1	75639	211.7	r
1150f	4	<1	1047±4	9	3210	8.5	r

$J = 2.315 \times 10^{-3} \pm 0.5\%$

r = repeated temperature step to attempt to fully outgas sample

GF-19K K-FELDSPAR (MS10)

°C	mV39	%39*	AGE(Ma)	%atmos	40/36	39/36	TIME (sec)
480	4	<1	811±5	14	2051	7.5	1200
510	3	<1	627±6	5	6278	34.9	1200
540	5	<1	581±3	5	5443	32.9	1140
570	10	1	588±2	2	13153	81.0	1200
600	15	1	594±2	1	21342	131.0	1200
630	24	2	598±1	1	22480	137.2	1200
660	28	2	595±1	1	24849	152.7	1200
690	62	5	600±1	<1	32740	199.8	1560
720	52	4	606±1	<1	37769	227.9	1200
750	60	5	608±1	<1	37022	222.8	1200
780	65	5	614±1	1	21094	124.5	1200
810	45	4	621±1	<1	34194	200.3	1320
840	66	5	633±1	1	27002	154.1	1200
870	58	5	654±1	2	12570	68.2	1260
900	47	4	670±1	2	18164	96.4	1200
950	65	5	690±1	2	17157	87.9	1200
1000	65	5	710±1	3	11646	57.2	1200
1050	65	5	748±1	5	6447	29.0	2220

GF-19K K-FELDSPAR (cont'd) (VG3600)

°C	mV39	%39*	AGE(Ma)	%atmos	40/36	39/36	TIME (sec)
1000	66	2	771±5	9	335	13.85	1200?
1025	62	2	798±6	11	2739	10.67	1380
1050	75	2	816±2	9	3183	12.27	1320
1075	132	4	825±1	7	4457	17.45	1500
1100	283	8	840±1	4	8137	32.15	1200
1125	153	4	854±1	6	5195	19.67	1200
1150	338	9	857±1	3	8639	33.32	2280
1175	222	6	875±1	3	9409	35.46	1320
1150b	108	3	888±2	7	3991	14.12	r

$J = 2.43 \times 10^{-3} \pm 0.5\%$

* estimated $\%^{39}Ar$ release, due to two mass spectrometer analysis, based on pattern for GF-18 and GF-20

r = repeated temperature step to attempt to fully outgas sample

GF-18K K-FELDSPAR (VG3600)

°C	mV39	%39	AGE(Ma)	%atmos	40/36	39/36	TIME (sec)
500	49	<1	1043±7	22	1347	3.1	1320
550	66	1	720±2	15	2010	8.0	2100
600	82	1	691±2	9	3445	15.6	1200
650	151	2	709±1	3	8473	39.2	1200
700	314	5	726±1	2	12853	58.6	1200
750	410	6	754±1	2	16307	71.4	1320
800	394	6	795±1	1	23163	95.5	1440
830	349	5	835±1	1	20408	79.1	1200
860	282	4	874±1	2	17437	63.6	1200
890	224	3	903±1	2	15173	53.0	1440
920	271	4	916±1	2	18089	62.2	1320
950	329	5	917±1	2	19521	67.1	1380
980	480	7	915±1	1	26881	93.1	1200
1010	490	8	918±1	1	25688	88.6	1320
1040	303	5	916±1	2	17517	60.2	1380
1070	434	7	908±1	1	21603	75.3	1380
1100	314	5	902±1	1	20470	71.9	1200
1130	436	7	893±1	1	27177	97.1	1200
1170	573	9	888±1	1	24449	87.9	1260
1170b	310	5	889±1	2	14208	50.5	r
1150c	95	1	890±1	5	5707	19.6	r
1150d	70	1	891±2	7	4049	13.6	r
1150e	78	1	894±2	6	4752	16.0	r

$J = 2.315 \times 10^{-3} \pm 0.5\%$
r = repeated temperature step to attempt to fully outgas sample

GF-7K K-FELDSPAR (MS10)

°C	mV39	%39*	AGE(Ma)	%atmos	40/36	39/36	TIME (sec)
480	10	1	-	-	-	-	-
510	9	1	777±2	2	18795	83.2	1200
540	13	2	726±2	1	21868	105.6	1200
570	21	3	731±1	<1	31985	153.7	1200
600	26	4	746±1	<1	44514	209.1	1200
630	21	3	757±1	1	27067	124.3	1200
660	17	2	767±1	2	12079	53.9	1260
690	15	2	804±2	4	7123	29.4	1200
720	17	2	938±2	1	25826	90.7	1260
750	17	2	1025±2	1	20174	62.9	1200
780	12	2	1047±3	1	22357	67.9	1200
810	11	2	1060±2	2	14094	41.8	2580
840	13	2	1093±2	3	10043	28.3	1200
870	17	2	1083±2	2	12189	35.0	1200
900	21	3	1042±1	2	12539	37.9	1200

GF-7K K-FELDSPAR (cont'd) (VG3600)

°C	mV39	%39*	AGE(Ma)	%atmos	40/36	39/36	TIME (sec)
900	21	2	1200±1	6	5055	12.22	1440
925	15	1	1166±1	4	6719	17.15	1200
950	22	2	957±1	4	7129	23.67	1380
975	29	2	955±1	5	6368	21.09	1500
1000	28	2	988±1	4	8386	26.91	1200
1025	49	4	1020±1	3	10716	33.22	1680
1050	65	5	1017±1	2	13572	42.52	1320
1075	54	4	1050±1	2	16039	48.32	1440
1100	69	5	1048±1	2	13576	40.88	?
1125	74	5	1066±1	<1	29715	88.58	1200
1150	452	33	1043±3	1	23185	70.87	1860

$J = 2.425 \times 10^{-3} \pm 0.5\%$

* estimated $\%^{39}Ar$ release, due to two mass-spectrometer analysis; based on GF-20K and GF-18K
? = step not timed

CI-20K K-FELDSPAR (VG3600)

°C	mV39	%39	AGE(Ma)	%atmos	40/36	39/36	TIME (sec)
500	49	1	707±10	13	2296	9.2	1260
550	41	1	636±2	7	4295	21.0	1200
600	96	3	731±1	2	14334	62.4	1320
650	91	3	720±1	2	16409	73.0	1200
700	161	4	724±1	5	6382	27.4	1260
750	242	7	746±1	2	18496	78.9	1380
800	288	8	770±1	1	21925	90.1	1200
830	242	7	793±1	1	25957	103.1	1260
860	196	5	822±1	2	19520	74.0	1200
890	104	3	843±1	2	14072	51.3	1200
920	213	6	870±1	1	23174	81.9	1260
950	197	5	898±1	3	9249	30.8	1320
980	158	4	904±1	1	20973	70.6	1200
1010	111	3	892±1	2	19383	66.2	1200
1040	231	6	894±1	<1	36971	127.0	1980
1070	115	3	885±1	2	18724	64.6	1500
1100	190	5	897±1	<1	33042	113.0	1500
1150	388	11	895±1	<1	40131	137.7	1200
1180	295	8	868±1	1	27941	99.3	r
1180b	17	<1	815±2	8	3659	13.1	r
1150c	78	2	840±2	7	4388	15.3	r
1150d	49	1	715±1	6	4871	20.9	r
1150e	33	<1	766±1	8	3657	14.1	r

$J = 2.22 \times 10^{-3}$ ±1.0%
r = repeated temperature step to attempt to fully outgas sample

GF-35K K-FELDSPAR (MS10)

°C	mV39	%39	AGE(Ma)	%atmos	40/36	39/36	TIME (sec)
480	7.2	<1	734±3	6	4859	22.6	1200
510	7.3	<1	598±2	3	11497	70.8	1200
540	11.6	1	597±2	1	20752	129.7	1200
570	15.5	2	599±2	1	28079	175.8	1200
600	21.8	2	596±1	<1	30778	194.0	1200
630	25.0	3	595±1	1	23899	150.4	1200
660	31.0	4	600±1	2	13900	85.8	1200
690	37.3	4	627±1	<1	47622	283.5	1200
720	38.6	4	651±1	<1	39188	222.8	1200
750	54.4	6	697±1	<1	48779	255.8	1200
780	31.7	4	738±1	<1	36204	176.7	1200
810	15.1	2	810±1	1	26408	114.7	1320
840	28.7	3	881±1	1	27742	108.5	1200
870	28.0	3	942±2	<1	30874	111.0	1260
900	31.2	4	968±2	<1	31144	108.0	1200
950	53.0	6	977±4	<1	44928	154.6	1200
1000	63.0	7	982±2	<1	31030	105.8	1260
1050	51.4	6	977±3	1	25797	88.2	1200
1100	72.2	8	970±3	2	16539	56.7	1200
1150	99.0	11	990±9	2	15108	50.4	2580

$J = 2.49 \times 10^{-3}$ ±0.5%

GF-35K2 K-FELDSPAR (VG3600)

°C	mV39	%39	AGE(Ma)	%atmos	40/36	39/36	TIME (sec)
500	27	1	726±27	<1	242565	1086.2	1200
550	19	<1	509±9	20	1451	7.9	1200
600	27	1	607±2	<1	35895	197.5	1200
650	54	2	531±1	4	7281	45.3	1200
700	64	3	589±1	10	2994	15.5	1560
750	55	2	628±1	3	8451	43.4	1200
800	114	5	668±1	1	20228	98.7	1500
830	67	3	742±2	2	13404	57.2	1200
860	50	2	757±2	3	10115	41.8	1200
890	50	2	852±3	3	10846	38.8	1440
920	52	2	890±3	3	9482	31.9	1200
950	70	3	901±2	2	18938	63.9	1200
980	86	4	936±2	1	28025	90.5	1200
1010	154	7	908±2	1	24923	83.6	1320
1040	97	4	923±2	4	8079	25.9	1440
1070	130	6	917±1	1	27315	90.5	1380
1090	123	5	928±1	1	25604	83.6	1800
1110	123	5	942±1	1	20043	63.9	1200
1130	700	31	935±1	<1	37247	120.7	1200
1150	147	6	966±1	1	29177	90.5	1200
1180	17	<1	976±1	<1	32222	98.7	1200
1210	56	2	975±2	3	11259	33.9	420

$J = 2.22 \times 10^{-3}$ ±1.0%

CI-14K K-FELDSPAR (VG3600)

°C	mV39	%39	AGE(Ma)	%atmos	40/36	39/36	TIME (sec)
500	25	1	626±33	32	932	3.4	1800
550	25	1	506±2	39	760	3.2	1560
600	47	3	488±1	23	1303	7.2	1320
650	46	3	496±1	26	1151	6.0	1320
700	112	6	601±2	16	1899	9.0	1440
750	125	7	608±1	10	2950	14.7	1440
800	111	6	636±1	9	3294	15.7	1800
830	70	4	691±2	14	2054	8.4	1380
860	58	3	738±2	13	2306	8.8	1500
890	56	3	774±3	13	2266	8.2	1500
910	30	2	792±4	20	1506	4.9	1200
940	55	3	829±2	8	3911	13.7	1560
970	42	2	847±2	10	3062	10.2	1200
1000	68	4	877±2	10	3079	9.9	1200
1030	100	5	900±2	5	6213	20.3	1500
1060	121	7	950±2	4	7544	23.2	1200
1090	728	40	1038±2	1	26537	74.9	1200
1120	1	<1	789±68	81	365	0.3	1440
1150	1	<1	920±9	38	787	1.6	1200

$J = 2.22 \times 10^{-3}$ ±1.0%

APPENDIX D
AMPHIBOLE ELECTRON MICROPROBE DATA (AVERAGED)

Electron microprobe analyses were obtained for amphiboles on a Jeol-733™ system using four WDS spectrometers. Operating conditions were 15 kV at 10 na beam current. A Tracor-Northern ZAF matrix correction program was used for data reduction. Two to four analyses per grain of two to four grains per polished thin section were obtained. More analyses were obtained for the samples which exhibited zoning or multiple kinds of amphibole. Analyses presented below represent averages of three to six individual analyses.

Error estimates were obtained on data used to calculate Ca/K ratios. Error on Ca has been determined by replicate analyses of standard KK hornblende; for all samples, error is 2% (2σ). For K, 39 replicate analyses of KK (weight % K_2O = 2.04%) were conducted over a six-week period, during four separate sessions (R. Mackay, pers. comm. 1991). The replicates gave a mean K_2O of 1.96 with a S.D. of 0.05. Error on K is therefore about 8 - 10% (2σ). Net error on Ca/K ratios is estimated at roughly 10% (2σ).

wt. % oxides	GF-44H core	GF-44H rim	GF-44 actin[1]	GF-2 Mghb[2]	GF-2 hsthb[3]
SiO_2	47.13	43.74	51.40	45.33	43.09
TiO_2	0.36	0.78	0.21	0.92	0.21
Al_2O_3	9.33	12.22	5.07	9.23	11.56
Cr_2O_3	0.23	0.18	0.00	0.05	0.00
FeO	11.90	13.74	9.61	17.21	18.80
MnO	0.19	0.20	0.23	0.34	0.35
MgO	14.17	12.24	16.96	10.74	9.29
CaO	12.02	11.95	12.47	12.04	12.00
Na_2O	1.40	1.85	0.81	1.28	1.47
K_2O	0.07	0.18	0.00	0.76	0.77
Cl	0.05	0.11	0.03	0.14	0.17
F	0.00	0.00	0.01	0.02	0.07
TOTAL	96.85	97.19	96.80	98.06	97.78
Ca/K	153.1	56.1	-	13.3	13.0
Fe#	0.49	0.56	0.39	0.64	0.70

[1] actinolitic hornblende
[2] magnesio-hornblende (Leake and Winchell, 1978)
[3] magnesian hastingsitic hornblende (Leake and Winchell, 1978)

wt.% oxides	GF-32H	CI-37H	GF-8H TZ-19H	GF-34H	GF-35H
SiO_2	43.02	43.02	40.95	40.63	41.76
TiO_2	0.85	1.50	1.50	1.83	1.58
Al_2O_3	9.16	10.97	12.71	11.08	10.63
Cr_2O_3	0.00	0.04	0.00	0.00	0.06
FeO	20.06	17.09	19.50	18.38	17.69
MnO	0.49	0.30	0.38	0.28	0.65
MgO	8.97	9.72	7.73	9.35	9.80
CaO	11.45	11.65	11.53	11.51	11.46
Na_2O	1.73	1.95	1.58	1.69	1.62
K_2O	1.24	0.72	1.48	1.54	1.60
Cl	-	-	0.04	-	-
F	-	-	0.17	-	-
TOTAL	96.97	97.05	97.57	96.29	96.85
Ca/K	7.7	13.6	6.5	6.3	6.0
Fe#	0.71	0.67	0.74	0.69	0.67

APPENDIX E
THEORY OF K-FELDSPAR DIFFUSION EXPERIMENTS

E.1) Determination of closure temperature from step-heating experiments (Berger and York (1981) method) - (modified after Grist, 1989)

Assuming that diffusion of argon out of mineral grains in nature is a thermally activated process, the temperature at which diffusion effectively stops (denoted T_C) can be described by the following relationship (Dodson, 1973):

$$E_a/RT_c=\ln[A\tau(D_0/a^2)] \quad (1)$$

where E_a is the activation energy; R is the gas constant; T_c is the closure temperature in degrees Kelvin; τ is the time constant (the time for D to diminish by e^{-1}); A is a geometrical constant; D_0 is the diffusion coefficient as the temperature approaches infinity; and a is the effective diffusion length (also expressed as l).

Changes in concentration of argon with respect to time in a 3-dimensional system (thermally induced mass diffusion), can be described by Fick's second law:

$$\frac{\partial C}{\partial t}=D\left(\frac{\partial^2 C}{\partial x^2}+\frac{\partial^2 C}{\partial y^2}+\frac{\partial^2 C}{\partial z^2}\right) \quad (2)$$

Numerical solutions to this equation have been developed describing diffusion out of simple geometric forms. Diffusion in feldspars is best described by the equations for diffusion from either a sphere or an infinite plane-sheet:

For a sphere:

$$f\simeq 1-(6/\pi^2)\exp(-\pi Dt/a^2) \quad \text{for } 0.85\leq f\leq 1 \quad (3)$$

$$f\simeq (6/\pi^{\frac{3}{2}})(\pi^2 Dt/a^2)^{\frac{1}{2}}-(3/\pi^2)(\pi^2 Dt/a^2) \quad \text{for } 0\leq f\leq 0.85 \quad (4)$$

For a plane-sheet:

$$f\simeq 1-(8/\pi^2)\exp(-\pi^2 Dt/4l^2) \quad \text{for } 0.45\leq f\leq 1 \quad (5)$$

$$f\simeq (2/\sqrt{\pi})(Dt/l^2)^{\frac{1}{2}} \quad \text{for } 0\leq f\leq 0.60 \quad (6)$$

where f is the fraction of gas lost by diffusion in terms of the

parameter (D/l^2) (or D/a^2), l (or a) is the effective diffusion distance, and t is the time diffusion is occurring.

In laboratory step-heating experiments, f and t can be measured and can be used to calculate D/a^2, if the following stipulations hold:

1) the phase remains stable throughout the duration of the experiment;

2) the shape of the diffusion domains in the experiment conforms to the shape assumed in the solution of the diffusion equation;

3) only one mineral phase is present (e.g. no contribution of gas from sericitic alteration, perthite lamellae, etc.);

4) the initial distribution of argon is uniform;

5) heating is isothermal.

The means by which these calculations are carried out for step-heating experiments is as follows:

Refer to figure A, which is a diagrammatic representation of the method described here.

Consider gas evolving from a sphere (for $0 \leq f \leq 0.85$). This is described by equation (4). Rearranging:

$$\frac{Dt}{a^2} = \frac{2}{\pi} - \frac{f}{3} - \frac{2}{\pi}\sqrt{1 - \frac{\pi f}{3}} \qquad (7)$$

At temperature T(1) (see fig. A):

$$\frac{D(1)\,t(1)}{a^2} = \frac{2}{\pi} - \frac{f(1)}{3} - \frac{2}{\pi}\sqrt{1 - \frac{\pi f(1)}{3}} \qquad (8)$$

where $f(1)$ is the fraction of total gas released in the first heating step. (Normally the ^{39}Ar release is used to determine this). $t(1)$ is the duration of the first heating step. Both these values are known and therefore $D(1)/a^2$ can be calculated.

At $t(1)$, temperature is increased to $T(2)$, and diffusion becomes more rapid. At $T(2)$:

$$\frac{D(2)\,t(2)}{a^2} = \frac{2}{\pi} - \frac{f(1)}{3} - \frac{2}{\pi}\sqrt{1 - \frac{\pi f(1)}{3}} \qquad (9)$$

and:

$$\frac{D(2)\,t(2)'}{a^2} = \frac{2}{\pi} - \frac{f(1)+f(2)}{3} - \frac{2}{\pi}\sqrt{1 - \frac{\pi (f(1)+f(2))}{3}} \qquad (10)$$

$f(1)$ and $f(2)$ are known but $t(2)$ and $t(2)'$ are not. However:

$$t(2)' - t(2) = \Delta t(2)$$

which is the heating time for the second step. By subtraction:

$$\frac{D(2)\Delta t(2)}{a^2} = \frac{2}{\pi} - \frac{f(2)}{3} - \frac{2}{\pi}\left(\sqrt{1-\frac{\pi(f(1)+f(2))}{3}} - \sqrt{1-\frac{\pi f(1)}{3}}\right) \qquad (11)$$

Dividing by $\Delta t(2)$, D/a^2 is calculated for the second step. The calculation is repeated iteratively for subsequent heating steps.

The D/a^2 values are normally plotted on a log scale ($log_{10}D/a^2$) versus the inverse of temperature (in Kelvin). This is known as an Arrhenius plot because the Arrhenius equation plots as a straight line in the form:

$$\log\left(\frac{D}{a^2}\right) = \frac{-.4343E_a(1000)}{RT} + \log\left(\frac{D_0}{a^2}\right) \qquad (12)$$

This allows derivation of the activation energy (E_a), from the slope of the line, and of the frequency factor D_0/a^2 from the y-intercept.

Assuming a cooling rate, which defines τ by the relationship:

$$\tau = \frac{-RT_c^2}{E_a(dT/dt)} \qquad (13)$$

equation (1) can be used to calculate T_c, using the E_a and D_0/a^2 derived by the experiment.

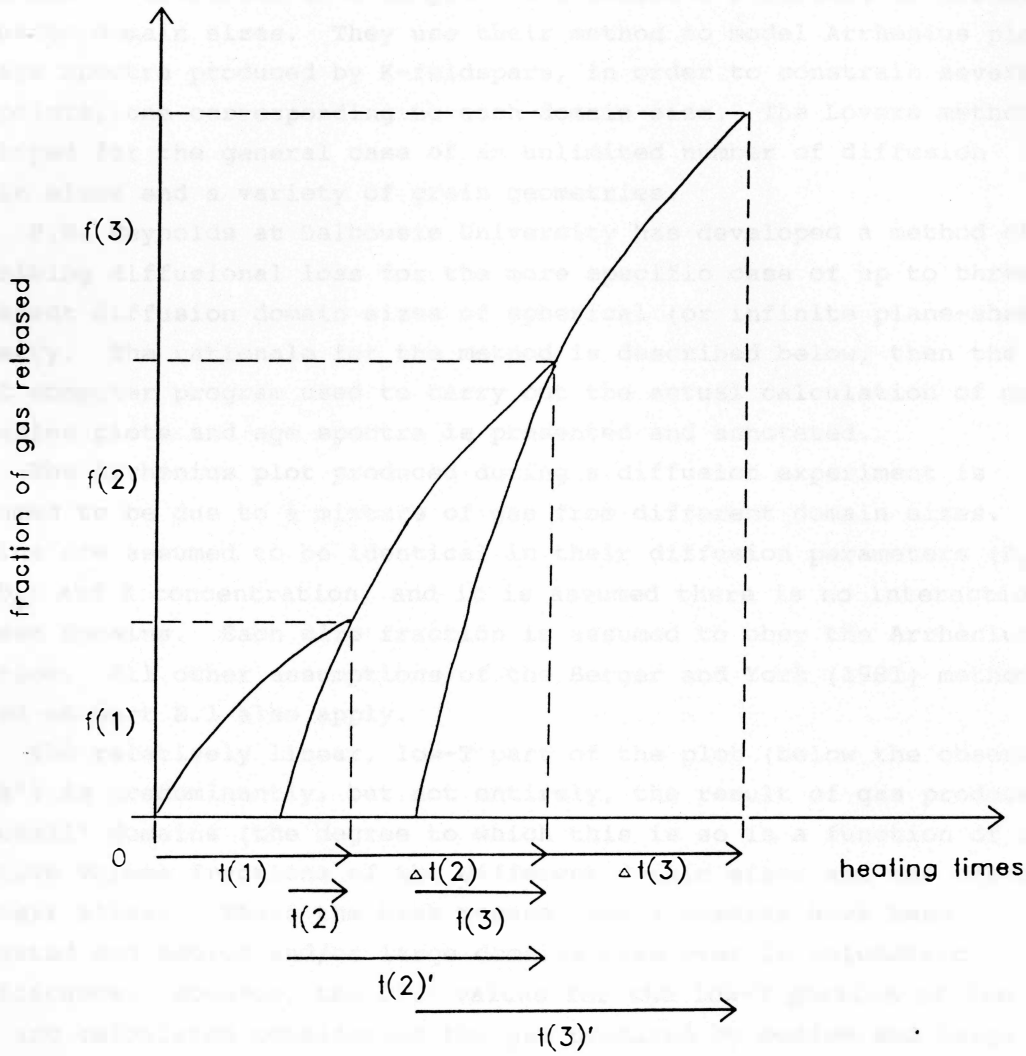

Fig. A. Diagram illustrating the Berger and York (1981) method of calculating diffusion parameters (see text for a complete description of the method). t(1), Δt(2), and Δt(3) are actual laboratory heating times. f(1), f(2),...f(n) are the fractions of gas evolved during each of the heating steps, such that f(1)+f(2)...+f(n) = 1. The times t(2) and t(2)' are the theoretical times required to obtain volumes of gas equivalent to f(1) and f(1)+f(2), respectively, had all heating been conducted at the elevated temperature T(2) rather than at the actual temperatures T(1) and T(2) respectively. The difference of t(2)' and t(2) is known, as is f(1)+f(2), and can therefore be used to calculate D/a2 for the second step using equation (11).

E.2) Determination of closure T for a distribution of diffusion domain sizes

Lovera et al. (1989) have derived a method to describe loss of argon due to diffusion in a sample which contains a mixture of effective diffusion domain sizes. They use their method to model Arrhenius plots and age spectra produced by K-feldspars, in order to constrain several T-t points, one corresponding to each domain size. The Lovera method is developed for the general case of an unlimited number of diffusion domain sizes and a variety of grain geometries.

P.H. Reynolds at Dalhousie University has developed a method of describing diffusional loss for the more specific case of up to three different diffusion domain sizes of spherical (or infinite plane-sheet) geometry. The rationale for the method is described below, then the BASIC computer program used to carry out the actual calculation of model Arrhenius plots and age spectra is presented and annotated.

The Arrhenius plot produced during a diffusion experiment is presumed to be due to a mixture of gas from different domain sizes. The domains are assumed to be identical in their diffusion parameters (E_a and D_0) and K concentration, and it is assumed there is no interaction between domains. Each size fraction is assumed to obey the Arrhenius equation. All other assumptions of the Berger and York (1981) method as stated in part E.1 also apply.

The relatively linear, low-T part of the plot (below the observed "kink") is predominantly, but not entirely, the result of gas produced by "small" domains (the degree to which this is so is a function of the relative volume fractions of the different domain sizes and the contrast in their sizes). Where the kink occurs, small domains have been exhausted and medium and/or large domains take over in volumetric significance. However, the D/a^2 values for the low-T portion of the plot are calculated considering the gas produced by medium and large domains as well, since the calculation includes terms incorporating the fraction of the total gas released (see equation (8)). Thus a calculated D_0/a^2 using the y-intercept of a line fit to the low-temperature end of the whole Arrhenius plot does not accurately represent the small domains, but is some function of the two or three domains' D_0/a^2.

If <u>only</u> the gas produced below the temperature at which the kink occurs is considered in the calculation of D/a^2 for each step, this is a closer approximation of the contribution of gas by the small domains. The calculated D_0/a^2 value is still a function of the larger domains' contribution, but this value sets a lower limit on the D_0/a^2 of small domains.

D_0/a^2 for the "medium" and/or "large" domains is initially guessed at by assessing the degree of offset of the higher-T parts of the Arrhenius curve from the low-T part. The relative proportions of the total gas contributed by each of the domain sizes is also guessed at, based in part on the shape of the age spectrum, in which local flattening of the step ages (a "plateau") may indicate the predominance of one particular domain outgassing (according to single-site diffusion theory).

The calculated E_a and assumed D_0/a^2 values for two or three domains, and the assumed volume fractions of domain sizes, are entered into a BASIC computer program (annotated below), which calculates the (D/a^2, 1000/T) pairs. These values are tested for fit to the measured Arrhenius curve. The fit is assessed on the basis of the match in (D/a^2, 1000/T) pairs and by comparison of the predicted percentage of outgassing of the sample at incongruent melting (or at the end of the experiment for 100% outgassing before melting). The latter constraint is important since it is possible to find domain distributions which fit the curve but predict either too much or too little outgassing. The relative sizes and proportions of the domains are adjusted, and the program re-run, until the best fit is obtained.

The distribution of domains (D_0/a^2, volume fraction pairs) thus calculated is then used to model the age spectrum. The method follows that of Lovera et al. (1989), which uses an age spectrum normalized to τ to calculate the age of gas for each heating step for each domain (P.H. Reynolds, pers. comm., 1991). The BASIC program annotated below includes this function but is bypassed for the initial assessment of domain distribution. In this procedure, an assumed peak age of each domain, and a time constant τ (related to cooling rate by equation (13)) applicable to this age, are input; a model age spectrum is generated and is compared for fit to the observed spectrum. The input parameters are again adjusted until a satisfactory fit is achieved.

The Arrhenius parameters obtained from the modelling of Arrhenius plots are finally used in the following modification of the Dodson equation to calculate closure temperatures for the peak age of each domain size (assuming spherical geometry):

$$T_p = \frac{E_a}{R \ln(\gamma \pi^2 \tau D_0 a^{-2})} \qquad (14)$$

where: T_p is the closure temperature applying to the peak age, and γ is Euler's constant.

E.3) Program MODSPEC (in GWBASIC), used to calculate Arrhenius parameters for model diffusion domain distributions, and model age spectra (modified after original by Dr. P.H. Reynolds)

```
10    REM PROGRAM MODSPEC TO CALCULATE SUM OF
      LOSSES FROM THREE SPHERES OF DIFFERING
      RADIUS, AND MODEL AGE SPECTRA
20    READ SAMPNUM$
30    READ N,RR
40    PRINT "For ";SAMPNUM$
50    INPUT "Enter activation energy: ", E
60    INPUT "Enter D0/a2 for three domains,
      starting with large domains.  Separate
      values with commas.", D1,D2,D3
70    INPUT "Enter fraction of total gas, in
      percent, for three domains.  Start with
      large domains.  Separate values with
      commas.  ",F1,F2,F3
80    INPUT "Enter trial tau values (in Ma)
      as a positive number for cooling, for
      three domains.  Start with large
      domains.  ",TAU1,TAU2,TAU3
90    INPUT "Enter trial ages (in Ma) of last
      gas released from each domain size.
      Start with large domains.   ",
      MAXAGE1,MAXAGE2,MAXAGE3
100   PI = 3.14159265#
110   DIM ADT(35), L1(35), AA(35), BDT(35),
      L2(35), BB(35), CC(35), TK(35), F(35),
      SIGMA(35), BELTADA2(35), DTA2(35),
      IMTK(35), TLGDDA2(35), SUM(35),
      CDT(35), L3(35), TIME(35), TEMP(35)
120   DIM M1(35), M2(35), M3(35), T1(35),
      T2(35), T3(35), AVT(35), DELAGE1(35),
      DELAGE2(35), DELAGE3(35), STEPAGE1(35),
      STEPAGE2(35), STEPAGE3(35), TOTAGE(35),
      CUPERC(35)
130   FOR I = 1 TO N: READ TIME(I): NEXT
140   FOR I = 1 TO N: READ TEMP(I): NEXT
150   R = .001987
160   LPRINT SAMPNUM$
170   LPRINT "activation energy = "; E
180   LPRINT "D0/a2 = ", D1,D2,D3
190   LPRINT "fractions = ", F1,F2,F3
200   LPRINT "tau = ", TAU1,TAU2,TAU3
210   LPRINT "Max. ages = ", MAXAGE1,
      MAXAGE2, MAXAGE3; "  Ma"
220   LPRINT
230   FOR I = 1 TO N
240   PRINT "Please wait ....."
250   TK(I) = TEMP(I) + 273
260   TADA2 = TIME(I) * D1 * (1 / EXP (E1 /
      (R * TK(I)))): TBDA2 = TIME(I) * D2 *
      (1 / EXP (E2 / (R * TK(I)))): TCDA2 =
      TIME(I) * D3 * (1 / EXP (E3 / (R *
      TK(I))))
270   ADT(I) = ADT(I - 1) + TADA2
280   DT = ADT(I)
290   IF I = 1 GOTO 310
300   IF AA(I-1) < .0001 GOTO 430
310   GOSUB 1220
```

line 30: reads number of steps and value of RR from data statement 1420;if RR > 1 then program bypasses printout of model age spectrum and prints only values for model Arrhenius plot

line 130: reads times (in seconds) of heating steps

line 140: reads temperatures (in °C) of heating steps

line 260: calculates Dt/a^2 for small (A), medium (B) and large (C) domains

```
320   L1(I) = (1 - (6 / (PI ^ 2)) * F) * F1
330   IF F1 = 0 GOTO 360
340   M1(I) = L1(I) / F1
350   GOTO 370
360   M1(I) = 0
370   AA(I) = L1(I) - L1(I - 1)
380   T1(I) = -2 * A/B
390   DELAGE1(I) = T1(I) * TAU1
400   STEPAGE1(I) =(MAXAGE1 + DELAGE1(I)) *
      AA(I)
410   GOTO 430
420   AA(I) = 0: T1(I) = 0: L1(I) = L1(I-1):
      M1(I) = 1
430   BDT(I) = BDT(I - 1) + TBDA2
440   DT = BDT(I)
450   IF I = 1 GOTO 470
460   IF BB(I-1) < .0001 GOTO 580
470   GOSUB 1220
480   L2(I) = (1 - (6 / (PI ^ 2)) * F)
      * F2
490   BB(I) = L2(I) - L2(I - 1)
500   IF F2 = 0 GOTO 530
510   M2(I) = L2(I) / F2
520   GOTO 540
530   M2(I) = 0
540   T2(I) = -2 * A/B
550   DELAGE2(I) = T2(I) * TAU2
560   STEPAGE2(I) = (MAXAGE2 + DELAGE2(I)) *
      BB(I)
570   GOTO 590
580   BB(I) = 0: T2(I) = 0: L2(I) = L2(I-1):
      M2(I) = 1
590   CDT(I) = CDT(I - 1) + TCDA2
600   DT = CDT(I)
610   IF I = 1 GOTO 630
620   IF CC(I-1) < .0001 GOTO 740
630   GOSUB 1220
640   L3(I) = (1 - (6 / (PI ^ 2)) * F)
      * F3
650   CC(I) = L3(I) - L3(I - 1)
660   IF F3 = 0 GOTO 690
670   M3(I) = L3(I) / F3
680   GOTO 700
690   M3(I) = 0
700   T3(I) = -2 /A*B
710   DELAGE3(I) = T3(I) * TAU3
720   STEPAGE3(I) = (MAXAGE3 + DELAGE3(I)) *
      CC(I)
730   GOTO 750
740   CC(I) = 0: T3(I) = 0: L4(I) = L3(I- 1):
      M3(I) = 1
750   SUM(I) = AA(I) + BB(I) + CC(I)
760   CUPERC(I) = L1(I) + L2(I) + L3(I)
770   IF SUM(I) < .001 GOTO 920
780   TOTAGE(I) = (STEPAGE1(I) + STEPAGE2(I)
      + STEPAGE3(I)) / SUM(I)
790   IF RR >1 GOTO 930
800   LPRINT "T=",TEMP(I),"DEG C"
810   LPRINT TAB(5) L1(I) TAB(20) AA(I)
      TAB(30) M1(I)
820   LPRINT "DELTA t / TAU = ",T1(I)
830   LPRINT TAB(5) L2(I) TAB(20) BB(I)
```

lines 270 - 420: for small domains: sums Dt/a^2 for present and previous steps; substitutes this into calculation of theoretical fraction of gas loss (in subroutine at line 1220 and in line 320); calculates gas fraction in present step; calculates age of gas on normalized age spectrum; calculates actual age of gas relative to peak age of domains, and weights age by volume fraction of step

lines 430 - 580: repeats as above for medium domains

lines 590 - 740: repeats as above for large domains.

line 750: sums total volume fraction of gas evolved from three domains in present step.

line 760: sums total cumulative volume fraction of gas evolved to present step.

line 780: calculates age of gas in present step by summing weighted ages of individual domains and normalising to total gas in step

```
      TAB(30) M2(I)
840   LPRINT "DELTA t / TAU = ",T2(I)
850   LPRINT TAB(5) L3(I) TAB(20)
      CC(I)TAB(30) M3(I)
860   LPRINT "DELTA t / TAU = ",T3(I)
870   LPRINT TAB(5) "SUM=",SUM(I)
880   LPRINT TAB(15) "CUMULATIVE GAS = ",
      CUPERC(I)
890   LPRINT TAB(15) "AGE OF STEP = ",
      TOTAGE(I)
900   LPRINT
910   GOTO 930
920   LPRINT "INSIGNIFICANT GAS REMAINING"
930   NEXT
940   LPRINT
950   PRINT "SPHERICAL MODEL"
960   LPRINT
970   LPRINT "Ea = ";E;"kcal/mol"
980   LPRINT "D0/a^2 = ";D1;",";D2;",";D3;"
      /sec"
990   LPRINT "proportions = ";F1;"%"; F2;"%";
      F3;"%"
1000  LPRINT
1010  LPRINT TAB(5) "1000/T(K)";"LOG10D/A^2";
      "F(I)"
1020  LPRINT
1030  TL=0
1040  FOR I = 1 TO N: TL = TL+SUM(I): NEXT
1050  FOR I = 1 TO N: F(I) = SUM(I)/TL:NEXT
1060  FOR I = 1 TO N: SIGMA(I) = SIGMA(I-1) +
      F(I)
1070  NEXT
1080  FOR I = 1 TO N: IF SIGMA(I) > .85 THEN
      GOTO 1110
1090  DTA2(I) = (2/PI) - SIGMA(I) /3) -
      (2/PI*SQR(1-PI*SIGMA(I)/3))
1100  GOTO 1130
1110  IF SIGMA(I) > .99 THEN SIGMA(I) = .99
1120  DTA2(I) = (1/(PI^2))*LOG(6/((PI^2) *
      (1-SIGMA(I))))
1130  NEXT
1140  FOR I = 1 TO N: BELTADA2(I) =
      (DTA2(I) - DTA2(I-1))/TIME(I):NEXT
1150  FOR I = 1 TO N-1: IF BELTADA2(I) < 0
      THEN GOTO 1180
1160  TLGDDA2(I) = LOG (BELTADA2(I))* .4343:
      IMTK(I) = 1000 / (TK(I))
1170  LPRINT TAB(5) IMTK(I) TAB(25)
      TLGDDA2(I) TAB (40) SIGMA(I)
1180  NEXT
1190  LPRINT
1200  LPRINT "END"
1210  END
1220  F = 0
1230  B=0: M=1
1240  DF = 1/((EXP((M^2)*(PI^2)*DT))*(M^2))
1250  DB = DF * (M^2)
1260  F = F + DF
1270  B = B + DB
1280  M = M + 1
1290  IF DF/F < .0001 GOTO 1310
1300  GOTO 1240
```

lines 1010 to 1210: For calculation of Arrhenius parameters only:

line 1040: calculates total volume of gas evolved during whole experiment

line 1050: calculates volume fraction of total for each step

line 1060: calculates cumulative volume fraction evolved after each step

lines 1090 and 1120: calculate Dt/a^2 for cumulative gas fractions < .85 and >.85, respectively

line 1140: calculates D/a^2 for step

line 1160: calculates log D/a^2, 1000/T(°K) points for Arrhenius plot

lines 1240 and 1260: summation to calculate F, is substituted into lines 320,480,640

lines 1250, 1270 to 1390: calculate terms A and B which substitute into lines 340, 580, 700 to calculate normalized age spectrum following method of Lovera et al. (1989)

```
1310  IF DB/B < .0001 GOTO 1330
1320  GOTO 1240
1330  A=0: M=2
1340  DA = LOG (M) / EXP ((M^2)*(PI^2)*DT)
1350  A = A + DA
1360  M = M + 1
1370  IF A/B < .0001 GOTO 1400
1380  IF DA/A < .0001 GOTO 1400
1390  GOTO 1340
1400  RETURN
1410  DATA "Sample GF-32K orthoclase"
1420  DATA 30,1
1430  DATA 1560, 1200, 1200, 1320, 1380,
      2100, 1200, 1200, 1680, 1380, 1380,
      1200, 1200, 1500, 1560, 1200, 1260,
      1200, 1200, 1200, 1140, 1260, 1200,
      1200, 1200, 1200, 1200, 1200, 1200,
      1200
1440  DATA 500, 550, 600, 650, 700, 750, 800,
      830, 860, 890, 920, 950, 980, 1010,
      1040, 1070, 1100, 1140, 1160, 1190,
      1220, 1250, 1350, 1400, 1500, 1600,
      1700, 1800, 1900, 2000
```

lines 1410 to 1440: example data statements for sample GF-32K.

REFERENCES

Alexander, Jr., E.C., Michelson, G.M. and Lanphere, M.A. 1978. MMhb-1: A new $^{40}Ar/^{39}Ar$ dating standard. Short Paper, 4th Int. Conf. on Geochronology, Cosmochronology and Isotope Geology. United States Geological Survey, Open-File Report, 78 -701: pp. 6 - 8.

Anderson, S.L. 1988. Interpretation of K-Ar mineral dates from the Grenville orogenic belt. American Journal of Science, 288, pp. 701 - 734.

Baldwin, S.L., Harrison, T.M., and FitzGerald, J.D. 1990. Diffusion of ^{40}Ar in metamorphic hornblende. Contributions to Mineralogy and Petrology, 105, pp. 691 - 703.

Beaumont, C., Quinlan, G.M., and Hamilton, J. 1988. Orogeny and stratigraphy: numerical models of the Paleozoic in eastern North America. Tectonics, vol. 7, no. 3, pp. 389 - 416.

Berger, G.W. and York, D. 1981. Geothermometry from $^{40}Ar/^{39}Ar$ dating experiments. Geochimica et Cosmochimica Acta, 45: pp. 795 - 811.

Berry, R.F. and McDougall, I. 1986. Interpretation of $^{40}Ar/^{39}Ar$ and K/Ar dating evidence from the Aileu Formation, East Timor, Indonesia. Chemical Geology (Isotope Geoscience Section), 59, pp. 43 - 58.

Bethune, K.M. 1989. Deformation, metamorphism, diabase dykes, and the Grenville Front southwest of Sudbury, Ontario. in Current Research, Part C, Geological Survey of Canada, Paper 89-1C, pp. 19 - 28.

Bethune, K.M. 1991. Fate of the Sudbury dykes in the Tyson Lake area south of Sudbury, Ontario; Implications for Grenville Front history and the origin of coronites of high-grade terranes. GAC/MAC Joint Annual Meeting, Prgram with Abstracts, vol. 16.

Bethune, K.M. and Davidson, A. 1988. Diabase dykes and the Grenville Front southwest of Sudbury, Ontario, in Current Research, Part C, Geological Survey of Canada, Paper 88-1C, pp. 151 - 159.

Bethune, K.M., Davidson, A. and Dudas, F.Ö. 1990. Structure and metamorphism of the Sudbury dykes; Constraints on the tectonic evolution of the Grenville Front south of Sudbury, Ontario. GAC/MAC Joint Annual Meeting, Program with Abstracts, vol. 15.

Bickford, M.E., Van Schmus, W.R., and Zietz, I. 1986. Proterozoic history of the midcontinent region of North America. Geology, 14: pp. 492 - 496.

Bowen, N.L. and Tuttle, O.F. 1950. The system $NaAlSi_3O_8$ - $KAlSi_3O_8$ - H_2O. Journal of Geology, vol. 58, no. 5, pp. 489 - 511.

Burke, M.M. 1991. Reflectivity of Highly Deformed Terranes Based on Laboratory and In Situ Velocity Measurements from the Grenville Front Tectonic Zone, Central Ontario, Canada. Unpublished Ph.D. thesis, Dalhousie University.

Card, K.D., 1978. Geology of the Sudbury Manitoulin Area, Districts of Sudbury and Manitoulin. Ontario Geological Survey Report 166, 238 pp. Accompanied by Map 2360, and 4 charts.

Cliff, R.A. 1985. Isotopic dating in metamorphic belts. Journal of the Geological Society of London, vol. 142, pp. 97 - 110.

Clifford, P.M. 1986. Petrological and structural evolution of the rocks in the vicinity of Killarney, Ontario: an interim report. in Current Research, Part B, Geological Survey of Canada, Paper 86 - 1B, pp. 147 - 155.

Corfu, F. 1988. Differential response of U-Pb systems in coexisting accessory minerals, Winnepeg River Subprovince, Canadian Shield: implications for Archean crustal growth and stabilization. Contributions to Mineralogy and Petrology, 98, pp. 312 - 325.

Corfu, F. and Andrews, A.J. 1986. A U-Pb age for mineralized Nipissing Diabase, Gowganda, Ontario. Canadian Journal of Earth Sciences, 23: pp. 107 - 109.

Corrigan, D., 1990. Geology and U-Pb geochronology of the Key Harbour area, Britt domain, SW Grenville Province. Unpublished M.Sc. thesis, Dalhousie University, 165 pp.

Cosca, M.A., Sutter, J.F., and Essene, E.J. 1988. Late metamorphic cooling and erosion history of the Ontario Grenville Province: Constraints from $^{40}Ar/^{39}Ar$ thermochronometry. Manuscript submitted to Tectonics.

Culshaw, N.G., Reynolds, P.H., and Check, G. A $^{40}Ar/^{39}Ar$ study of post-tectonic cooling and uplift in the Britt domain, Grenville Province, Ontario. Earth and Planetary Science Letters, in press.

Dallmeyer, R.D. 1987. $^{40}Ar/^{39}Ar$ mineral age record of variably superimposed Proterozoic tectonothermal events in the Grenville Orogen, central Labrador. Canadian Journal of Earth Sciences, 24, pp. 314 - 333.

Dalrymple, G.B. and Lanphere, M.A. 1969. Potassium - argon dating. Freeman, San Francisco. 258 pp.

Davidson, A., 1986. Grenville Front relationships near Killarney, Ontario, in The Grenville Province, J.M. Moore, A. Davidson, and A.J. Baer, eds., Geological Association of Canada Special Paper 31, pp. 107 - 117.

Davidson, A., 1986. New interpretations in the southwestern Grenville Province, in The Grenville Province, J.M. Moore, A. Davidson, and A.J. Baer, eds. Geological Association of Canada Special Paper 31, pp. 61 - 74.

Davidson, A. and Bethune, K.M. 1988. Geology of the north shore of Georgian Bay, Grenville Province of Ontario; in Current Research, Part C, Geological Survey of Canada, Paper 88-1C, pp. 135 - 144.

Davidson, A., Carmichael, D.M. and Pattison, D.R.M. 1990. Metamorphism and geodynamics of the southwestern Grenville Province, Ontario. IGCP Project 235 - 304, Field Trip #1 Guidebook.

Davis, D.W. 1982. Optimum linear regression and error estimation applied to U-Pb data. Canadian Journal of Earth Sciences, 19: pp. 2141 - 2149.

Deer, W.A., Howie, R.A., and Zussman, J. 1966. An Introduction to the Rock-forming Minerals. Longman Group Limited, Essex. 528 pp.

Dempster, T.J. 1986. Isotope systematics in minerals: biotite rejuvenation and exchange during Alpine metamorphism. Earth and Planetary Science Letters, 78, pp. 355 - 367.

Desmons, J., Hunziker, J.C., and Delaloye, M. 1982. Unconvincing Evidence Against the Blocking Temperature Concept: Comments on "^{40}Ar - ^{39}Ar Dating of High Pressure Metamorphic Micas from the Gran Paradiso Area (Western Alps): Evidence Against the Blocking Temperature Concept" by C. Chopin and H. Maluski. Contributions to Mineralogy and Petrology, 80, pp. 386 - 390.

Deutsch, A. and Steiger, R.H. 1985. Hornblende K-Ar ages and the climax of Tertiary metamorphism in the Lepontine Alps (south-central Switzerland): an old problem reassessed. Earth and Planetary Science Letters, 72, pp. 175 - 189.

Dewey, J.F. 1988. Extensional collapse of orogens. Tectonics, vol. 7, no. 6, pp. 1123 - 1139.

DeWitt, E., Armstrong, R.L., Sutter, J.F., and Zartman, R.E. 1984. U-Th-Pb, Rb-Sr, and Ar-Ar mineral and whole-rock isotope systematics in a metamorphosed granitic terrane, southeastern California. Geological Society of America Bulletin, 95, pp. 723 - 739.

Dodson, M.H. 1973. Closure temperatures in cooling geochronological and petrological systems. Contributions to Mineralogy and Petrology, 40: pp. 250 - 274.

England, P.C., and Thompson, A.B. 1984. Pressure - Temperature - Time Paths of Regional Metamorphism I. Heat Transfer during the Evolution of Regions of Thickened Continental Crust. Journal of Petrology, 25, part 4, pp. 894 - 928.

Fahrig, W.F., and West, T.D. 1986. Diabase dyke swarms of the Canadian Shield. Geological Survey of Canada, Map 1627A.

Faure, G. 1986. Principles of Isotope Geology, 2nd. edn. J. Wiley & Sons, 589 pp.

FitzGerald, J.D., and Harrison, T.M. 1991. Microstructures in MH-10 and their Implications for Domain Models in K-feldspars. in American Geophysical Union, Spring Meeting 1991, Program with Abstracts.

Fleck, R.D., Sutter, J.F., and D. Elliot, 1977. Interpretation of discordant $^{40}Ar/^{39}Ar$ age-spectra of Mesozoic tholeiites from Antarctica. Geochimica et Cosmochimica Acta, 41, pp. 15 - 32.

Foland, K.A. 1974. ^{40}Ar diffusion in homogeneous orthoclase and an interpretation of Ar diffusion in K-feldspar. Geochimica et Cosmochimica Acta, 38, pp. 151 - 166.

Foland, K.A. 1979. Limited mobility of argon in a metamorphic terrane. Geochimica et Cosmochimica Acta, 43, pp. 793 - 801.

Foster, D.A., Harrison, T.M., Copeland, P. and Heizler, M.T. 1990. Effects of excess argon within large diffusion domains on K-feldspar age spectra. Geochimica et Cosmochimica Acta, 54, pp. 1699 - 1708.

Fowler, C.M.R., and Nisbet, E.G. 1988. Geotherms in the continental crust and metamorphism. in Heat, Metamorphism, and Tectonics, E.G. Nisbet and C.M.R. Fowler, eds., MAC Short Course Handbook, 14, 319 pp.

Frarey, M.J. 1985. Proterozoic Geology of the Lake Panache - Collins Inlet area, Ontario. Geological Survey of Canada, Paper 83 - 22, 61 pp., accompanied by map 1593A, scale 1:50,000.

Gaber, L.J., Foland, K.A., and Corbató, C.E. 1988. On the significance of argon release from biotite and amphibole during $^{40}Ar/^{39}Ar$ vacuum heating. Geochimica et Cosmochimica Acta, 52: pp. 2457 - 2465.

Ghent, E.D., Stout, M.Z., and Parrish, R.R. 1988. Determination of Metamorphic Pressure-Temperature-Time (P-T-t) Paths. in Heat, Metamorphism, and Tectonics, E.G. Nisbet and C.M.R. Fowler, eds., MAC Short Course Handbook, 14, 319 pp.

Green, A.G., Milkereit, B., Davidson, A., Spencer, C., Hutchinson, D.R. Cannon, W.F., Lee, M.W., Agena, W.F., Behrendt, J.C., and Hinze, W.J. 1988. Crustal structures of the Grenville Front and adjacent terranes. Geology 16, pp. 788 - 792.

Grist, A.M. 1989. Provenance and Thermal History of Detrital Sandstones of the Scotian Basin, Offshore Nova Scotia, Using the Apatite Fission Track and $^{40}Ar/^{39}Ar$ Methods. Unpublished M.Sc. thesis, Dalhousie University, 196 pp.

Hanson, G.N., Catanzoro, E.J., and Anderson, D.H. 1971. U-Pb ages for sphene in a contact metamorphic zone. Earth and Planetary Science Letters, 12, pp. 231 - 237.

Harrison, T.M. 1981. Diffusion of ^{40}Ar in Hornblende. Contributions to Mineralogy and Petrology, 78, pp. 324 - 331.

Harrison, T.M. 1983. Some observations on the interpretation of $^{40}Ar/^{39}Ar$ age spectra. Isotope Geoscience, 1: pp. 319 - 338.

Harrison, T.M. 1990. Some observations on the interpretation of feldspar $^{40}Ar/^{39}Ar$ results. Chemical Geology (Isotope Geoscience Section), 80: pp. 219 - 229.

Harrison, T.M., and McDougall, I. 1980. Investigations of an intrusive contact, northwest Nelson, New Zealand. I. Thermal, chronological and isotopic constraints. Geochimica et Cosmochimica Acta, 44, pp. 1985 - 2003.

Harrison, T.M., and McDougall, I. 1981. Excess ^{40}Ar in metamorphic rocks from Broken Hill, New South Wales: Implications for $^{40}Ar/^{39}Ar$ age spectra and the thermal history of the region. Earth and Planetary Science Letters, 55, pp. 123 - 149.

Harrison, T.M., and McDougall, I. 1982. The thermal significance of potassium feldspar K-Ar ages inferred from $^{40}Ar/^{39}Ar$ age spectrum results. Geochimica et Cosmochimica Acta, 46, pp. 1811 - 1820.

Harrison, T.M., Duncan, I. and McDougall, I. 1985. Diffusion of ^{40}Ar in biotite: temperature, pressure, and compositional effects. Geochimica et Cosmochimica Acta, 49, pp. 2461 - 2468.

Harrison, T.M., Lovera, O.M., and Heizler, M.T. 1991. $^{40}Ar/^{39}Ar$ results for alkali feldspars containing diffusion domains with differing activation energy. Geochimica et Cosmochimica Acta, 55, pp. 1435 - 1448.

Harrison, T.M., Morgan, P. and Blackwell, D.D. 1986. Constraints on the age of heating at the Fenton Hill Site, Valles caldera, New Mexico. Journal of Geophysical Research, 91, pp. 1899 - 1908.

Heizler, M.T. and Harrison, T.M. 1988. Multiple trapped argon isotope components revealed by $^{40}Ar/^{39}Ar$ isochron analysis. Geochimica et Cosmochimica Acta, 52, pp. 1295 - 1303.

Heizler, M.T., Lux, D.R., and Decker, E.R. 1988. The age and cooling history of the Chain of Ponds and Big Island Ponds plutons and the Spider Lake Granite, west-central Maine and Quebec. American Journal of Science, 288, pp. 925 - 952.

Hess, J.C., and Lippolt, H.J. 1986. Kinetics of isotopes during neutron irradiation: ^{39}Ar loss from minerals a source of error in $^{40}Ar/^{39}Ar$ dating. Chemical Geology, 59, pp. 223 - 236.

Hoffman, P.F. 1988. Mantle superswell as cause of middle Proterozoic anorogenic magmatism, and implications for Grenvillian deformation, Keewanawan rift volcanism and MacKenzie dyke injection. in GAC/ MAC Joint Annual Meeting, Program with Abstracts, v. 13.

Huneke, J.C. and Smith, S.P. 1976. The realities of recoil: ^{39}Ar recoil and anomalous patterns in ^{39}Ar - ^{40}Ar dating. Geochimica et Cosmochimica Acta, Supplement 7 (Proceedings of the 7th Lunar Science Conference), pp. 1987 - 2008.

Indares, A. and Martignole, J. 1989. The Grenville Front south of Val d'Or, Quebec. Tectonophysics, 157: pp. 221 - 239.

Jamieson, R.A., and Beaumont, C. 1988. Deformation and P-T-t paths in Convergent Orogens. in Heat, Metamorphism, and Tectonics, E.G. Nisbet and C.M.R. Fowler, eds., MAC Short Course Handbook, 14, 319 pp.

Jamieson, R.A., and Beaumont, C. 1989. Deformation and Metamorphism in Convergent Orogens: A Model for Uplift and Exhumation of Metamorphic Terranes. in Evolution of Metamorphic Belts, J.S. Daly, R.A. Cliff, and B.W.D. Yardley, eds., Geological Society of London Special Publication No. 43, pp. 117 - 129.

Jamieson, R.A., Culshaw, N.G., Wodicka, N., Corrigan, D. and Ketchum, J. 1991. Timing and tectonic setting of Grenvillian metamorphism - constraints from a transect along Georgian Bay, southwestern Ontario. Manuscript submitted to Journal of Metamorphic Geology.

Koons, P. 1989. The topographical evolution of collisional mountain belts: A numerical look at the Southern Alps. American Journal of Science, 289, pp. 1041 - 1069.

Krogh, T.E., 1973. A low contamination method for the hydrothermal decomposition of zircon and extraction of U and Pb for isotopic age determinations. Geochimica et Cosmochimica Acta, 37: pp. 485 - 494.

Krogh, T.E., 1982. Improved accuracy of U-Pb zircon ages by the creation of more concordant systems using an air abrasion technique. Geochimica et Cosmochimica Acta, 46: pp. 637 - 649.

Krogh, T.E., 1989. U-Pb systematics of zircon and titanite in metasediments and gneisses near the Grenville Front, Ontario. in GAC/MAC Joint Annual Meeting, Program with Abstracts, v. 14.

Krogh, T.E. and Davis, G.L. 1970. Isotopic ages along the Grenville Front in Ontario. Carnegie Institute of Washington Yearbook 68, pp. 309 - 313.

Krogh, T.E. and Davis, G.L. 1975. The production and preparation of ^{205}Pb for use as a tracer for Isotope Dilution Analyses. Carnegie Institute of Washington Yearbook, 74: pp. 416 - 417.

Krogh, T.E., Davis, G.L., and Frarey, M.J. 1971. Isotopic ages along the Grenville Front in the Bell Lake area, southwest of Sudbury, Ontario. Carnegie Institute of Washington Yearbook 69, pp. 337 - 339.

Krogh, T.E. and Wardle, R. 1984. U-Pb isotopic ages along the Grenville Front. GAC/MAC Joint Annual Meeting, Program with Abstracts, vol. 9, p. 80.

Krogh, T.E., Corfu, F., Davis, D.W., Dunning, G.R., Heaman, L.H., Kamo, S.L., Machado, N., Greenough, J.D., and Nakamura, E. 1987. Precise U-Pb isotopic ages of diabase dykes and mafic to ultramafic rock using trace amounts of baddelyite and zircon, in Mafic Dyke Swarms, H.C. Halls and W. Fahrig, eds., Geological Association of Canada, Special Paper 34, pp. 147 - 152.

Lanphere, M.A. and Dalrymple, G.B. 1976. Identification of excess ^{40}Ar using the $^{40}Ar/^{39}Ar$ age spectrum technique. Earth and Planetary Science Letters, 32, pp. 141 - 148.

Leake, B.E. and Winchell, H. 1978. Nomenclature of amphiboles. American Mineralogist, vol. 63, pp. 1023 - 1052.

Lee, J.K.W., Onstott, T.C., Cashman, K.V., Cumbest, R.J., and Johnson, D. 1991. Argon release mechanisms during incremental heating of hornblende in vacuo: Elucidation and Enlightenment. in American Geophysical Union, Spring Meeting 1991, Program with Abstracts.

Lo, C.H. and Onstott, T.C. 1989. ^{39}Ar recoil artifacts in chloritized biotite. Geochimica et Cosmochimica Acta, 53, pp. 2697 - 2711.

Lovera, O.M., Harrison, T.M., and M.T. Heizler, 1991a. K-feldspar Thermochronometry II: - Identification of Diffusion Domains. in American Geophysical Union, Spring Meeting 1991, Program with Abstracts.

Lovera, O.M., Richter, F.M. and Harrison, T.M. 1989. The $^{40}Ar/^{39}Ar$ Thermochronometry for Slowly Cooled Samples Having a Distribution of Diffusion Domain Sizes. Journal of Geophysical Research, 94, no. B12: pp. 17,917 - 17,935.

Lovera, O.M., Richter, F.M. and Harrison, T.M. 1991b. Diffusion domains determined by ^{39}Ar release during step-heating. Journal of Geophysical Research, 96, pp. 2057 - 2069.

Lowdon, J.A., Stockwell, C.H., Tipper I.W., and Wanless, R.K. 1963. Age determinations and geological studies (including isotopic ages, Report 3). Geological Survey of Canada Paper 62-17, Part 1.

Lumbers, S.B. 1975. Geology of the Burwash Area, Districts of Nipissing, Parry Sound, and Sudbury; Ontario Division of Mines, GR116, 160 pp. Accompanied by Map 2271, scale 1 inch to 2 miles.

Maboko, M.A.H., McDougall, I., Zeitler, P.K., and FitzGerald, J.D. 1991. Discordant ^{40}Ar - ^{39}Ar ages from the Musgrave Ranges, central Australia: Implications for the significance of hornblende ^{40}Ar - ^{39}Ar age spectra. Chemical Geology (Isotope Geoscience Section), 86, pp. 139 - 160.

Maluski, H. 1978. Behaviour of biotites, amphiboles, plagioclases, and K-feldspars in response to tectonic events with the ^{40}Ar - ^{39}Ar radiometric method; Example of Corsican granite. Geochimica et Cosmochimica Acta, 42, pp. 1619 - 1633.

McDougall, I. and Harrison, T.M. 1988. Geochronology and Thermochronology by the $^{40}Ar/^{39}Ar$ method. Oxford University Press, New York, 212 pp.

Mezger, K., Rawnsley, C.M., Bohlen, S.R., and Hanson, G.N. 1991. U-Pb garnet, sphene, monazite and rutile ages: Implications for the duration of high-grade metamorphism and cooling histories, Adirondack Mts., New York. Journal of Geology, 99, pp. 415 - 428.

Mitchell, J.G. 1968. The argon-40 / argon-39 method for potassium-argon age determination. Geochimica et Cosmochimica Acta, 32: pp. 781 - 790.

Molnar, P. and Lyon-Caen, H. 1988. Some simple physical aspects of the support, structure and evolution of mountain belts. Geological Society of America Special Paper 218, pp. 179 - 207.

Molnar, P. and Tapponnier, P. 1975. Cenozoic Tectonics of Asia: Effects of a Continental Collision. Science, v. 189, no. 420, pp. 419 - 425.

Muecke, G.K., Elias, P., and Reynolds, P.H. 1988. Hercynian/ Alleghanian overprinting of an Acadian terrane: $^{40}Ar/^{39}Ar$ studies in the Meguma zone, Nova Scotia, Canada. Chemical Geology (Isotope Geoscience Section), 73: pp. 153 - 167.

Nadeau, L. 1990. Tectonic, thermal and magmatic evolution of the Central Gneiss Belt, Hunstville region, southwestern Grenville orogen. Unpublished Ph.D. thesis, Carleton University, 269 pp.

Onstott, T.C. and Peacock, M.W. 1987. Argon retentivity of hornblendes: A field experiment in a slowly cooled metamorphic terrane. Geochimica et Cosmochimica Acta, 51, pp. 2891 - 2903.

Owen, J.V., Rivers, T., and Gower, C.F. 1986. The Grenville Front on the Labrador coast. in The Grenville Province, J.M. Moore, A. Davidson, and A.J. Baer, eds. Geological Association of Canada Special Paper 31, pp. 95 - 106.

Owen, J.V., Dallmeyer, R.D., Gower, C.F., and Rivers, T. 1988. Metamorphic conditions and $^{40}Ar/^{39}Ar$ geochronologic contrasts across the Grenville Front zone, coastal Labrador, Canada. Lithos, 21, pp. 13 - 35.

Parrish, R.R. and Krogh, T.E. 1987. Synthesis and purification of ^{205}Pb for U-Pb geochronology. Chemical Geology (Isotope Geoscience Section), 66: pp. 103 - 110.

Parrish, R.R. and Roddick, J.C. 1985. Geochronology and isotope geology for the geologist and explorationist. Geological Association of Canada, Cordilleran Section, Short Course No. 4, Handbook.

Parsons, I., Rex, D.C., Guise, P. and Halliday, A.N. 1988. Argon loss by alkali feldspars. Geochimica et Cosmochimica Acta, 52, pp. 1097 - 1112.

Parsons, I., Waldron, K.A., Walker, F.D.L., Burgess, R., and Kelley, S.P. 1991. Microtextural Controls of ^{40}Ar loss and ^{18}O exchange in Alkali Feldspars. in American Geophysical Union, Spring Meeting 1991, Program with Abstracts.

Quinlan, G. and Beaumont, C. 1984. Appalachian thrusting, lithospheric flexure and the Paleozoic stratigraphy of eastern North America. Canadian Journal of Earth Sciences, 21: pp. 973 - 996.

Reynolds, P.H., Elias, P., Muecke, G.K., and Grist, A.M. 1987. Thermal history of the southwestern Meguma zone, Nova Scotia, from an $^{40}Ar/^{39}Ar$ and fission track dating study of intrusive rocks. Canadian Journal of Earth Sciences, 24, pp. 1952 - 1965.

Richter, F.M., Lovera, O.M., Harrison, T.M., and Copeland, P. 1991. Tibetan tectonics from a single feldspar sample: An application of the $^{40}Ar/^{39}Ar$ method. Earth and Planetary Science Letters, in press.

Rivers, T. 1983. The northern margin of the Grenville Province in Western Labrador - Anatomy of an ancient orogenic front. Precambrian Research, 22, pp. 41 - 73.

Rivers, T. and Chown, E.H. 1986. The Grenville orogen in eastern Quebec and western Labrador - definition, identification and tectonometamorphic relationships of autochthonous, parautochthonous and allochthonous terranes. in The Grenville Province, J.M. Moore, A. Davidson, and A.J. Baer, eds., Geological Association of Canada Special Paper 31, pp. 31 - 50.

Rivers, T., Martignole, J., Gower, C.F., and Davidson, A. 1989. New tectonic divisions of the Grenville Province, southeast Canadian Shield. Tectonics, vol. 8, no. 1, pp. 63 - 84.

Roddick, J.C. 1978. The application of isochron diagrams in $^{40}Ar-^{39}Ar$ dating: a discussion. Earth and Planetary Science Letters, 41, p. 233.

Roddick, J.C., Cliff, R.A., and Rex, D.C. 1980. The evolution of excess argon in Alpine biotites - A $^{40}Ar-^{39}Ar$ analysis. Earth and Planetary Science Letters, 48, pp. 185 - 208.

Ross, J.A. and Sharp, W.D. 1988. The effects of sub-blocking temperature metamorphism on the K/Ar systematics of hornblendes: $^{40}Ar/^{39}Ar$ dating of polymetamorphic garnet amphibolite from the Franciscan Complex, California. Contributions to Mineralogy and Petrology, 100, pp. 213 - 221.

Schärer, U., Krogh, T.E. and Gower, C.F. 1986. Age and evolution of the Grenville Province in eastern Labrador from U-Pb systematics in accessory minerals. Contributions to Mineralogy and Petrology, 94: pp. 438 - 451.

Schärer, U., Copeland, P., Harrison, T.M., and Searle, M.P. 1990. Age, cooling history, and origin of post-collisional leucogranites in the Karakorum Batholith; A multi-system isotope study. Journal of Geology, 98, pp. 233 - 251.

Schermer, E.R., Lux, D.R., and Burchfiel, D.C. 1990. Temperature - time history of subducted continental crust, Mount Olympus region, Greece. Tectonics, vol. 9, no. 5, pp. 1165 - 1195.

Snee, L.W. 1982. Emplacement and cooling of the Pioneer Batholith, southwestern Montana. Unpublished Ph.D. thesis, Ohio State University, Columbus. 320 pp.

Snelling, N.J. 1962. Potassium - argon dating of rocks north and south of the Grenville Front in the Val d'Or region, Quebec. Geological Survey of Canada Bulletin, 85, 27 pp.

Stacey, J.S. and Kramers, J.D. 1975. Approximation of terrestrial lead isotope evolution by a two-stage model. Earth and Planetary Science Letters, 26: pp. 207 - 221.

Steiger, R.H. and Jäger, E. 1977. Subcommission on Geochronology: Convention on the use of decay constants in geo- and cosmochronology. Earth and Planetary Science Letters, 36, pp. 359 - 362.

Tilton, G.R., Wetherill, G.W., Davis, G.L., and Bass, M.N. 1960. 1000 - million year old minerals from the eastern United States and Canada. Journal of Geophysical Research, 65, pp. 4173 - 4179.

Tucker, R.D., Raheim, A., Krogh, T.E., and Corfu, F. 1987. Uranium-lead zircon and titanite ages from the northern portion of the Western Norway Gneiss Region, south-central Norway. Earth and Planetary Science Letters, 81, pp. 203 - 211.

Turner, F.J. 1981. Metamorphic Petrology: Mineralogical, Fields, and Tectonic Aspects, 2nd ed. McGraw-Hill Book Company, New York. 524 pp.

Turner, G. 1968. The distribution of potassium and argon in chondrites. in Origin and Distribution of the Elements. L.H. Arhens ed., pp. 387 - 398. Pergamon, London.

van Breemen, O. and Davidson, A. 1988. Northeast extension of Proterozoic terranes of midcontinental North America. Geological Society of America Bulletin, vol. 100, pp. 630 - 638.

van Breemen, O., Davidson, A., Loveridge, W.D., and Sullivan, R.D. 1986. U-Pb zircon geochronology of Grenville tectonites, granulites and igneous precursors, Parry Sound, Ontario. in The Grenville Province, J.M. Moore, A. Davidson, and A.J. Baer, eds., Geological Association of Canada Special Paper 31, pp. 191 - 207.

van der Pluijm, B.A., and Carlson, K.A. 1989. Extension in the Central Metasedimentary Belt of the Ontarion Grenville: Timing and tectonic significance. Geology, 17, pp. 161 - 164.

Van Schmus, W.R., 1980. Chronology of igneous rocks associated with the Penokean orogeny in Wisconsin. Geological Society of America Special Paper 182: pp. 159- 168.

Villa, I. 1988. Ar diffusion in partially outgassed alkali feldspars: insights from $^{40}Ar/^{39}Ar$ analysis - Comments. Chemical Geology (Isotope Geoscience Section), 73, pp. 265 - 269.

Villa, I. 1991. Ar loss in Nature and the lab - is it Really Volume Diffusion? in American Geophysical Union, Spring Meeting 1991, Program with Abstracts.

Wagner, G.A., Reimer, G.M., and Jäger, E. 1977. Cooling ages derived by apatite fission-track, mica Rb-Sr and K-Ar dating: the uplift and cooling history of the Central Alps. Mem. Ist. Geol. Min. Univ. Padova, 30, pp. 1 - 28.

Wanless, R.K., Stevens, R.D., Lachance, G.R., and Delabio, R.N.D. 1974. Age determinations and geological studies, K-Ar isotopic ages. Report 12, Geological Survey of Canada Paper 74-2, p. 41.

Wanless, R.K., Stevens, R.D., Lachance, G.R., and Edmunds, C.M. 1968. Age determinations and geological studies, K-Ar isotopic ages, Report 8. Geological Survey of Canada, Paper 67-2, Part A, pp. 98 - 100.

Wanless, R.K., Stevens, R.D., and Loveridge, W.D. 1970. Anamolous isotopic relationships in rocks adjacent to the Grenville Front near Chibougamau, Quebec. Eclogae Geologicae Helvetiae, 63, pp. 345 - 364.

York, D., 1969. Least squares fitting of a straight line with correlated errors. Earth and Planetary Science Letters, 5: pp. 320 - 324.

Zeitler, P.K. 1988a. Argon diffusion in partially outgassed alkali feldspars: Insights from $^{40}Ar/^{39}Ar$ analysis. Chemical Geology, 65: pp. 167 - 181.

Zeitler, P.K. 1988b. Argon diffusion in partially outassed alkali feldspars: Insights from $^{40}Ar/^{39}Ar$ analysis - Reply. Chemical Geology (Isotope Geoscience Section), 73, pp. 265 - 269.

Zeitler, P.K. 1989. The geochronology of metamorphic processes. in Evolution of Metamorphic Belts, J.S. Daly, R.A. Cliff, and B.W.D. Yardley, eds., Geological Society of London Special Publication no. 43, pp. 131 - 147.

Zeitler, P.K., and FitzGerald, J.D. 1986. Saddle-shaped $^{40}Ar/^{39}Ar$ age spectra from young, microstructurally complex potassium feldspars. Geochimica et Cosmochimica Acta, 50, pp. 1185 - 1199.